

**Metal Fate Dynamics and Ecotoxicology
in Hydrologically Variable Aquatic Ecosystems**

by

Sara McCarthy Nedrich

A dissertation submitted in partial fulfillment
of the requirements for the degree of
Doctor of Philosophy
(Earth and Environmental Sciences)
at the University of Michigan
2017

Doctoral Committee:

Professor G. Allen Burton, Chair
Professor Joel D. Blum
Assistant Professor Rose Cory
Assistant Research Scientist Paul Drevnick
Professor Mike Wiley

Sara M. Nedrich

snedrich@umich.edu

ORCID iD: 0000-0001-8879-2847

© Sara M. Nedrich 2017

Dedication

In memory of

Kurt D. Weider,
Who grows in *Coleus* leaves,
And sings on *Coccinellidae* wings

000 & 000

[Secret Code Dedication for Nerds]:

Thorium-Hydrogen+Oxygen Oxygen+muinehtuR Tellurium+Americium:

Sulfur+Oxygen Sulfur+Arsenic+Sulfur+Yttrium,
Molybdenum+Rhenium Flourine+Uranium+Nitrogen,
Nitrogen+Oxygen Iron+Argon

Acknowledgements

I am grateful to the many colleagues, mentors, friends and family to whom I owe the successful pursuit and completion of my doctoral degree. I would foremost like to thank my chair and mentor, Allen Burton, for his encouragement towards academia and intellectualism, for his scientific contributions to this dissertation, and for his support making this research possible. I am proud to have had the opportunity to work with such a brilliant and considerate professor.

I would like to thank some of the colleagues I feel have made significant contributions to my work through discussion or written feedback. These colleagues include: Steve Brown, Anthony Chappaz, Matt Cooper, Dave Costello, Jen Daley, Kevin Farley, and my committee members, Joel Blum, Rose Cory, Paul Drevnick, and Mike Wiley. I would additionally like to thank the technical support I have received from various labs and personnel, including: Chad Hammerschmidt (Wright State), Stephan Holhowskyj (Central Michigan University), Martin Shafer (University of Wisconsin), and Timothy Veverica (U of M Biological Station).

To the current and past members of Burton-lab, I am extremely grateful for your friendship, expertise, and assistance through the years. This especially applies to Anna Harrison and Shelly Hudson, for initially helping me develop the technical skills need to conduct this research and troubleshooting with me along the way. Other honorable mentions are reserved for Burton-lab graduate students, Brittany Bennett, Eduardo Cervi, Kathryn Meyer, Gus Steigmeyer, and Kesiree Thiamkeelakul; Burton-lab technical assistants, Crystal Cole, Maggie Grundler, Enlylh King, Tanner Morris, Olivia Rath, Alison Rentschler, and Brianna Westmoreland; and visiting scientists, Min Xiao and Di Xu.

Lastly, I am grateful for my supportive family, without whom none of this would be worth the trouble. To Matt, thanks for sharing this crazy adventure with me and being there every day. To Kirstin and Ali, I am so grateful to have you both as friends/sisters/cousins (FSC's?). To my aunt Nancy, thanks for showing me from a young age that a PhD enhances career possibilities and critical thinking. And to mom, thanks for instilling the value of education deep and irrevocably into my cerebellum.

Table of Contents

Acknowledgements	iii
List of Tables	viii
List of Figures	xi
Abstract	xv
Chapter 1 - Introduction	1
1.1 Metal ecotoxicology in aquatic systems.....	2
1.2 Methods for predicting metal bioavailability	5
1.3 The importance of hydrodynamic variability for assessing environmental risk	6
1.4 Dissertation summary	9
Chapter 2 - Indirect effects of climate change on Zinc cycling in sediments: the role of changing water levels	11
2.1 Introduction	12
2.2 Materials and methods	14
2.2.1 Site/Sediment selection	14
2.2.2 Experimental design	16
2.2.3 Sampling and lab analysis.....	18
2.2.4 Statistical analysis	19
2.3 Results	20
2.3.1 Site comparison	20
2.3.2 Seiche experiment	22
2.3.3 Drought experiment.....	24
2.3.4 Comparison of seiche and drought.....	27
2.4 Discussion	28
2.4.1 Assessing ecological risk of seiche and drought	28
2.4.2 Effects of sediment chemistry on redox-induced Zn-pulse	31
2.4.3 Implications for climate research.....	34
Chapter 3 – Zn-release in hydrodynamic sediments: Assessing environmental risk to <i>Hyalella azteca</i> and <i>Daphnia magna</i>	36
3.1 Introduction	36
3.2 Methods	37

3.2.1 Site selection & experimental design	40
3.2.2 Toxicity testing.....	41
3.2.3 Analytical chemistry	43
3.2.4 Statistics.....	44
3.3 Results	45
3.3.1 Physicochemical water and sediment characterization	45
3.3.2 Surface water chemistry and toxicology to <i>D. magna</i>	46
3.3.3 Porewater and sediment chemistry during Zn-release.....	48
3.3.4 Toxicological effects to <i>H. azteca</i>	52
3.4 Discussion	54
3.4.1 Field applicability	54
3.4.2 Ecotoxicology of redox-sensitive systems.....	54
3.4.3 Applicability and effectiveness of predictive toxicology toolkits.....	56
3.4.4 Chemical mechanisms of Zn-release	56
3.4.5 Implications for environmental decision makers	60
3.5 Conclusion.....	62
Chapter 4 – Biogeochemical controls on the speciation and aquatic toxicity of vanadium and other metals in sediments from a river reservoir	63
4.1 Introduction	64
4.2 Methods.....	67
4.2.1 Site selection and sediment collection.....	67
4.2.2 Experimental design.....	68
4.2.3 Aqueous analyses.....	70
4.2.4 Sediment analyses.....	71
4.2.5 Toxicity testing.....	72
4.2.6 Statistical analysis and modelling	73
4.3 Results	74
4.3.1 Physicochemical sediment characterization	74
4.3.2 Vanadium speciation in sediment and porewater	75
4.3.3 Metal bioavailability in surface and porewater	77
4.3.4 Toxicity testing of <i>D. magna</i> and <i>H. azteca</i>	79
4.4 Discussion	83
4.4.1 Vanadium geochemistry	83
4.4.2 Vanadium toxicology.....	84
4.4.3 Zn toxicology.....	85
4.4.4 Implications for reservoir management	87
Chapter 5 – Biogeochemical release of sediment zinc: Assessing risk to benthic communities and periphyton	89

5.1 Introduction	90
5.2 Methods.....	92
5.2.1 Site selection.....	92
5.2.2 Experimental design.....	92
5.2.3 Water and sediment analyses	96
5.2.4 Biological analyses.....	98
5.2.5 Speciation modeling and statistics	99
5.3 Results	100
5.3.1 Controls on sediment redox.....	100
5.3.2 Metal biogeochemistry in sediment and porewater.....	103
5.3.3 Chemical speciation modeling	106
5.3.4 Benthic and periphyton community effects.....	107
5.4 Discussion	113
5.4.1 Sediment chemistry of Zn-release.....	113
5.4.2 Biological impacts from Zn-release	115
5.4.3 Comparing laboratory toxicity testing to field toxicology	117
5.4.4 General implications for aquatic systems	118
Chapter 6 - Conclusion.....	120
6.1 Summary of key findings	120
6.2 Suggestions for future work	123
References.....	125
Appendices.....	140

List of Tables

Table 2-1. Physical and chemical properties of sediment types, including sediment texture, total metal content, total Fe-oxide content, pH, loss-on-ignition (LOI), dissolved organic carbon (DOC), and [SEM-AVS]/ f_{OC} (\pm standard error, SE)..... 17

Table 3-1. Fe/Mn-oxyhydroxide content (\pm SE) in sediments prior to inundation (day-0) and after 11-days of inundation, with bound estimates for Zn. 50

Table 4-1. A summary of physicochemical properties for 4 sediment types shows SPN and WIL to have similar total metal concentrations while the two references sites (REF and CNTL) are much lower. While CNTL has lowest total metals content, REF is more similar to contaminated sites in several other parameters (texture, pH, LOI, [SEM-AVS]/ f_{OC})..... 69

Table 5-1. Physicochemical sediment properties of non-spiked sediments (using saturated and dry treatment data), including sediment texture, loss-on-ignition (LOI), simultaneously extracted metals (SEM) minus acid volatile sulfide (AVS) over the fraction of organic carbon (f_{OC}), and total metals concentrations (\pm SE). Data averaged from all sediment sampling days. 93

Table 5-2. Physicochemical properties of porewater sampled from non-spiked sediments, including (using both saturated and dry treatment sediment data), including pH, dissolved oxygen (DO), redox potential (Eh), reduced iron (Fe^{2+}), sulfide (S^{2-}), alkalinity, hardness, and dissolved metals (Fe and Mn) (\pm SE). Data averaged from all porewater sampling days. 102

Table 5-3. Summary of surface water characteristics including pH, dissolved oxygen (DO), conductivity, temperature, and dissolved Fe, Mn, and Zn. Data are averages from dry deployment and days 1, 5/6, 9, and 30 after inundation from 3 replicates per day. All data were collected in the morning (8-9 AM) except two data points collected at ~1 PM (EB). 102

Appendix A

Table A-1. Dissolved Organic Carbon (DOC) in porewater per site and experiment 140

Table A-2. Dry weight / wet weight sediment ratios per site and experiment..... 141

Table A-3. Sediment loss-on-ignition (LOI) per site and experiment 142

Table A-4. Sediment pH per site and experiment..... 142

Table A-5. Sediment Fe-oxyhydroxide content per site-rep and experiment 143

Table A-6. Sediment Mn-oxyhydroxide content per site-rep and experiment 145

Table A-7. Sediment Zn bound to amorphous, crystalline, and total Fe/Mn oxyhydroxides..... 146

Table A-8. Sediment [SEM-AVS] / f_{OC} data table	147
Table A-9. BLM output for HC5 and Toxicity Unit (TU).....	150
Table A-10. Calculated hardness corrected CCC's	150

Appendix B

Table B-1. BLM chemical input data, where constant temperature (18.35°C), pH (7.14), humic acid content (10%), and alkalinity (3.08 mgL ⁻¹ CaCO ₃) were assumed.....	151
Table B-2. Hardness corrected CCC for Zn in surface water (n=3).	152
Table B-3. BLM estimated HC5s for Zn in surface water (n=3).....	152
Table B-4. Porewater metal data in dissolved phase with standard error between replicates (n=3). Detection limits were 15 µgL ⁻¹ for Cu and 10 µgL ⁻¹ for Ni.....	153
Table B-5. Bioavailable Zn as measured using DGTs for several sediment depths.....	154
Table B-6. Porewater dissolved oxygen (DO) and reduced Fe per day and site-rep.....	155
Table B-7. Surface water and sediment pH	156
Table B-8. Porewater metal concentrations for Fe, Mn, Zn, Ca, and Mg.....	157
Table B-9. Sediment simultaneously extracted metals (SEM) minus acid volatile sulfide (AVS), loss-on-ignition (f_{OC}), and water content.	160
Table B-10. Extended Sediment [SEM-AVS] / f_{OC} data table.....	161
Table B-11. <i>Hyaella azteca</i> survival, individual growth rate, and body burden Zn.....	162
Table B-12. <i>Daphnia magna</i> survival, reproduction, growth, body burden Zn	163

Appendix C

Table C-1. Porewater chemistry including dissolved oxygen (DO), pH, reduced iron (Fe ²⁺) and redox potential (Eh).	164
Table C-2. Surface water dissolved Zn, Fe, and Mn concentrations.	165
Table C-3. Hardness corrected CCC's shown with initial data (porewater metal concentrations and Ca calculated hardness).....	166
Table C-4. Concentrations of Fe/Mn-oxyhydroxides in sediments prior to inundation (day-0) and after 12-days of inundation, with bound estimates for Zn and V.	168
Table C-5. BLM results show SPN to have highest theoretical toxicity to <i>D. magna</i> , followed by WIL. Bold numbers exceed a TU value of one.	169
Table C-6. V-speciation as calculated by extraction techniques for Fe/Mn-oxyhydroxides and V (+IV)/(+V).	169

Table C-7. Sediment simultaneously extracted metals (SEM) minus acid volatile sulfide (AVS), loss-on-ignition (f_{OC}), and water content. 171

Table C-8. Biotic Ligand Model input data, including temperature, pH, surface water dissolved Zn, DOC, humic acid (HA), Ca, Mg, Na, K, SO_4 , Cl, alkalinity (alk) and sulfide. 172

Appendix D

Table D-1. Modeling input for incremental oxidation..... 174

Table D-2. Modeling input for oxidation via surface water input. 175

Table D-3. Input code for evaporation model. Example is for EB but similar model ran for LBC and QC as well. 176

Table D-4. Acid volatile sulfide (AVS), simultaneously extracted metals (SEM) and fraction of organic carbon (f_{OC}) for all sites days and treatments..... 178

Table D-5. Abundance (N), dominant species, relative abundance of dominant species (rN), species richness, evenness and diversity (Simpson's and Shannon's). 180

Table D-6. Net primary productivity (NPP) and Chlorophyll (Chl) *a* biomass for all sites and treatments..... 182

List of Figures

Figure 2-1. Map of field sites in Michigan, USA	15
Figure 2-2. Experimental microcosms with Rhizon porewater samplers	16
Figure 2-3. Average porewater Zn, Cu, Fe, and Mn for seiche and drought (\pm SE).....	23
Figure 2-4. [SEM-AVS]/ f_{OC} (\pm SE) for seiche and drought with statistical differences between (a/b) and within (*) experiments ($p < 0.05$).....	24
Figure 2-5. Porewater hardness (\pm SE) for seiche and drought with lettering for statistical significance ($p < 0.05$).	25
Figure 2-6. Porewater reduced iron and dissolved oxygen (\pm SE) indicate oxidation at day-1 followed by reduction to day-30 (after inundation).....	26
Figure 2-7. Comparison of Zn concentrations to hardness-corrected CCC and BLM-derived chronic HC5 values for drought experiment.....	30
Figure 2-8. A schematic is provided of the chemical equations associated with Zn-release and subsequent reduction.....	32
Figure 3-1. Organism exposure bottles depicted, where vertical bottles are for surface water exposure of <i>D. magna</i> and horizontally placed bottles are for sediment exposure of <i>H. azteca</i> . 41	
Figure 3-2. Porewater dissolved Fe^{2+} , dissolved oxygen, and surface and porewater dissolved Zn (\pm standard error, SE) changed with time after inundation. All four non-control sediment types exceeded USEPA thresholds for aquatic toxicity (WQC) on days 1 and 3, but only LBC	46
Figure 3-3. Toxicological endpoints for <i>D. magna</i> and <i>H. azteca</i> , including survival, reproduction (R_0), individual growth rate (IGR), and body burden Zn (BB_{Zn}) (\pm SE) for sediment treatments.....	48
Figure 3-4. Porewater hardness (\pm SE) as $CaCO_3$ and total hardness shown for days 1 and 11 per each sediment type. Large decreases in hardness were observed for all sediment types with inundation.	49
Figure 3-5. <i>H. azteca</i> IGR is negatively correlated with Zn body burden for all sites ($p < 0.03$) and especially for LBC and QC only ($p < 0.001$).....	51
Figure 3-6. Relationship between dissolved porewater Zn for sites with elevated $>120 \mu gL^{-1}$...	52
Figure 3-7. DGT concentrations of Zn are correlated with three factors for (A) sediment/porewater, including porewater Zn, <i>H. azteca</i> body burden, and total sediment Zn, and two factors for (B) surface water exposures, including surface water Zn and <i>D. magna</i> body burden.	53

Figure 3-8. Principal components analysis for several variables which correlated with porewater Zn on day-1, including acid volatile sulfide concentration, total Zn bound to Fe-oxides, the change in reduced iron between day 1 and 11, and hardness.	60
Figure 4-1. Site map included three Lake Catherine sites and Michigan control site.	67
Figure 4-2. Sediment acidity was negatively correlated with redox (Eh) condition. Figure is based on day 7 and 11 data only. Increasing pH 7 to 11 days after inundation may be linked to decreasing metal concentrations in porewater and hydrolysis of metals.	75
Figure 4-3. Porewater (left) and sediment (right) V speciation as a function of days after inundation (\pm standard error, SE) with lettering for statistical significance within species ($p < 0.08$). For porewater, V(IV) and V(V) are dissolved concentrations and total V is particulate. ...	76
Figure 4-4. XANES spectra of samples and reference compounds.	77
Figure 4-5. Porewater metal concentrations (\pm SE) show Zn, Cd, and Al CCCs were exceeded on some days and for some sediment types. Table with extended metal concentrations is provided in Appendix C.	78
Figure 4-6. Potential toxicity estimated by (SEM-AVS)/ f_{OC}	79
Figure 4-7. Toxicity test results for <i>H. azteca</i> and <i>D. magna</i> , including survival, individual growth rate (IGR), Zn and V body burden, and reproduction (R_0) (\pm SE).	82
Figure 4-8. <i>H. azteca</i> Zn body burden was negatively correlated with IGR, indicating sublethal effects of Zn-oxidative release.	83
Figure 4-9. Schematic overview of the main findings in this chapter.	88
Figure 5-1. Mesocosm design with mesh	94
Figure 5-2. Timeline for sampling regime depicting days after (or prior to) inundation of dry treatment sediments.	95
Figure 5-3. Temporal changes in porewater redox (Eh in mV) and reduced iron (Fe^{2+}) are shown for “dry” treatments of all three sites on days 1, 5 or 6, and 9 after inundation.	100
Figure 5-4. Hydrographs show water level fluctuations (WLF) for all sites. When water elevation exceeds red line, dry deployed mesocosms became inundated.	101
Figure 5-5. Temporal changes in porewater Zn (\pm standard error, SE) for natural sediments show low Zn in porewater for non-spiked sediments.	103
Figure 5-6. Porewater Zn (\pm SE) in days after inundation for spiked sediments show relatively little evidence for Zn-oxidative release, with the exception of EB.	104
Figure 5-7. Metal binding to sulfide as predicted by the theoretical method for toxicity (SEM-AVS)/ f_{OC} for dry treatment sediments only. Statistical lettering signifies differences between sampling days for each sediment.	105
Figure 5-8. Model predicted sediment oxidation leads to decreased porewater Zn.	107
Figure 5-9. Net primary productivity (NPP) and biomass of chlorophyll (Chl) <i>a</i> (\pm SE) for each site comparing dry and saturated (sat) treatments. Asterisks indicate statistical differences between site treatments.	108

Figure 5-10. A strong negative correlation predicts the effect of porewater Zn on chlorophyll (Chl) *a* production (all sites included). This relationship was not observed for natural and reference sediment as Zn concentrations were too low to show effects. 109

Figure 5-11. Abundance, richness, and diversity (\pm SE) were statistically different between dry and saturating treatments in EB sediments ($p < 0.03$). 110

Figure 5-12. pH was strongly correlated with abundance, richness, and Shannon-Weiner diversity for all three sites. 111

Figure 5-13. Relationships between Chlorophyll (Chl) *a*, porewater dissolved oxygen (DO) and porewater pH are shown. Chl *a* was correlated with porewater pH between sites, and may be attributed to the different pH and DO relationship for EB versus QC/LBC. 112

Figure 5-14. Survival of *H. azteca* toxicity testing at EB show low survival. 113

Figure C-1. Full array of dissolved porewater metal concentrations show two temporal patterns. Cr, Al, Mn, and Fe show a day-7 peak, while Ni, Cd, Zn, and V decrease with time. 170

Figure D-1. Values for (SEM-AVS)/ f_{OC} analyses for dry and sat treatments for QC non-spiked and spiked sediments, days 0 and 9/10 (not 30). QC non-spiked statistically different ($p = 0.06$) for SEM-AVS and for AVS in spiked sediments ($p < 0.05$). 177

List of Appendices

Appendix A (Chapter 2 Data).....	140
Appendix B (Chapter 3 Data).....	151
Appendix C (Chapter 4 Data).....	164
Appendix D (Chapter 5 Data).....	174

Abstract

Predicting the environmental fate and effects of metals is nuanced, due to the diverse interplay of biogeochemical and physicochemical variables, and is vital to protecting and preserving aquatic resources. Regulatory methods for toxicity testing and ecological risk assessment often lack sufficient data to address simple and critical changes in environmental conditions, such as hydrologic extremes (drought/flood), which are predicted to become more severe with climate change. This is a particular concern, as water quality criteria (e.g., regulatory standards for metal thresholds) are defined by laboratory toxicity test methods.

In this dissertation, the effects of altered hydrology on sediment metal biogeochemistry and associated effects to aquatic organisms are investigated. Water level fluctuation experiments are conducted on high carbonate sediments collected from coastal wetlands in the Great Lakes region, showing a significant release of porewater Zinc (Zn) due to altered geochemistry following drought conditions, with sublethal effects to benthic macroinvertebrates (Chapter 2-3). In a subsequent study (Chapter 4), Zn-release and effects to organism growth is again observed in more acidic reservoir sediments with different geochemical controls. Vanadium (V) redox biogeochemistry is also investigated and oxidation had relatively little effect on V speciation due to strong complexation with iron oxyhydroxide compounds. In the final chapter (Chapter 5), field validation of Zn-release is performed at the same wetland sites used for laboratory testing and demonstrated positive benthic community responses. The effects of elevated sediment Zn are confounded by a strong positive relationship between benthic community abundance, richness, and diversity with sediment pH. The pH shift was likely driven by periphyton photosynthesis,

altering metal speciation and complexation and the periphyton served as a food source benefiting the benthic macroinvertebrate community.

General implications of this research are elucidated, including relevance to the management and restoration of aquatic systems, regulatory driven toxicology, and improving the extrapolation of laboratory to field studies. Finally, it appears that increases in hydrologic extremes, as predicted with climate change, will alter metal biogeochemistry in sediments, thereby resulting in wide-ranging effects on benthic macroinvertebrate communities.

Chapter 1 - Introduction

One footprint of the Anthropocene will be a legacy of elevated metals diagenetically imprinted into the earth's stratigraphy. During the industrial revolution (circa 1900's) and into the late-20th century, pollution went unabated, releasing metals into the environment with little awareness of impacts to environmental health (Forstner and Wittmann, 2012). While most countries have implemented laws and regulations to prevent the most blatant sources of metal contamination, legacy metals remain in surface sediments, while many non-point (or diffuse) sourced metals are still released into the environment (Mason, 2013). Three on-going goals of metal ecotoxicology are to remediate legacy sites, prevent metal pollution from non-point sources, and better predict the fate and effects of metals in the environment (Gambrell, 1994a). This dissertation focuses on the latter goal, to the end that effects of metals to aquatic organisms can be better mitigated.

This introduction will provide a brief overview of metal ecotoxicology in aquatic systems, with a specific focus on sediment and water biogeochemistry in hydrologically variable aquatic systems. The primary purpose of focusing on these hydrologically variable systems is attributed to climate change which is predicted to intensify the hydrologic cycle, leading to increased precipitation (flooding) and sequential numbers of dry days (drought) in the future (Milly et al., 2005). Increased hydrologic extremes can affect sediment chemistry such that environmental risk to organisms can be difficult to predict due to complex changes in metal

speciation and lability. These concepts will be discussed at greater depth in the introduction and following chapters.

More specifically, this dissertation will focus primarily on redox sensitive biogeochemical processes affecting metal bioavailability and environmental risk. In this dissertation, bioavailability refers to whether the metal is in a form which can be incorporated into an organism's body. The main objectives are to assess (1) sediment drying (oxidation + evaporation) and re-inundation (forced by water level variability) on metal bioavailability and speciation, (2) if increased metal bioavailability associated with water level variability alters environmental risk, (3) what actions aquatic managers can take to improve water quality and ecosystem function given increasingly hydrodynamic aquatic system, and (4) whether or how metal-specific environmental risk modelling tools can be improved to reflect systems with variable hydrology. Background information presented in the introduction will provide context to these objectives, including an overview of: Sediment metal ecotoxicology, methods for predicting metal bioavailability, the importance of water level variability in aquatic biogeochemistry, and an executive summary of each following chapter.

1.1 Metal ecotoxicology in aquatic systems

Metals are both common and ubiquitous in the environment, but often become elevated in concentration due to anthropogenic and natural (weathering or volcanism) inputs. Common sources of anthropogenic metals include mining, smelting, industrial production (metal plating, steelwork, refineries), urbanization (storm water runoff), combustion byproducts (i.e. auto, coal, etc.), and agricultural products such as fertilizer, sewage sludge application, pesticides, and algaecides (Flemming and Trevors, 1989). Sediments in aquatic systems are a major sink for

metals, which can be deposited from precipitation, runoff, sedimentation, atmospheric deposition, or direct disposal.

Most of this dissertation focuses on the fate and effects of Zinc (Zn) and Vanadium (V), which have similar sources. These metals were chosen due to known negative effects to organisms at elevated concentrations and high lability (Zn) or lack of data and novelty (V). Primary sources of Zn to the environment include mining, iron and steel production, electroplating, combustion byproducts (coal, gasoline, refuse incineration), and domestic wastewater (ATSDR, 2017). Annual production (mining) of V is much greater than Zn (77 vs. 12 million metric tons/year), with demand increasing at about 9% per year (Perles, 2012; USGS, 2016a, 2016b). The dominant sources of V to the environment are mine drainage, combustion byproducts (fossil fuels, paper mills, smelting), and as a common impurity in fertilizers (Irwin et al., 1997).

Biological impairment from these metals can occur when their concentrations exceed tolerable ranges. Metals become exposed to aquatic organisms through sediment or water exposure, including uptake of contaminated food, ingestion of metal contaminated sediment particles, or ingestion through gills (De Schamphelaere et al., 2004b; Muysen and Janssen, 2001). Regulators and researchers use toxicity testing to predict effects for surface water or porewater exposures using water quality criteria (WQC), above which impacts to organisms are likely to occur. From a multitude of toxicity tests, effects of metals have been found to be wide-ranging, including negative impacts to survival, growth, reproduction, metabolism, or immune response (DeForest and Meyer, 2014; Gough et al., 2008; Hansen et al., 2002). These individual effects can be scaled to estimate effects to the aquatic population and community level (Forbes et

al., 2001). Background information on how Zn and V specifically affect these endpoints and validity testing of WQC is discussed in more detail in chapters 3 and 4.

Where water quality criteria are used to estimate effects to surface water organisms, sediment quality guidelines (SQG's) are used to predict effects to benthic (sediment-dwelling) organisms. Total metal concentrations may fall below a given SQG, such as the threshold effect level (TEL), indicating toxicity is highly unlikely; or be in exceedance of a given SQG, like the probable effects level (PEL), indicating toxicity is likely. Vanadium aquatic toxicology information is relatively limited with no existing sediment quality guidelines while information regarding Zn is relatively abundant. One criticism of SQG's is that the total metal concentration is not always reflective of bioavailability (Simpson and Batley, 2016). As total metal concentration does not reflect the speciation or phase of a metal, detailed chemical data is often needed to accurately predict toxicity.

The bioavailability of metals in sediments is tied to the abundance of binding ligands, which are ultimately controlled by three master variables: pH, redox, and microbial activity. While all metals are cations, and many behave as cations in the environment (Zn, Ni, Cu, Cd, Fe, Mn, Ca, Mg), others form oxy-anions (V, Cr, As). The bioavailability of cationic metals generally increases with sediment acidity, while for oxy-anions, they are more bioavailable in alkaline sediments. The behavior of sediment-bound metals in response to altered redox and microbial activity is less known, and will be discussed in the following chapters (for Zn and V specifically) and effects will be compared to established SQG.

The most prevalent binding ligands affecting bioavailability include sulfide/sulfate, carbonates, Fe/Mn-oxyhydroxides, and organic matter. All of these ligands react to changes in redox and pH, and can be involved in microbial metabolism (Gambrell et al., 1991). Most

cationic (and oxy-anionic to a lesser extent) metals bind to sulfide complexes under reduction and are released during oxidation (Simpson et al., 1998). Fe/Mn-oxyhydroxide metal complexes are generally un-reactive to oxygenation, but may release metals during reduction (Kostka et al., 1995). Both organic matter and carbonate binding are more so impacted by changes in sediment acidity, where low pH decreases their binding capacity (Grybos et al., 2009; Patterson et al., 1977). Many of these chemical transformations are kinetically mediated by sediment microbes (Howell et al., 1998; Kosolapov et al., 2004). Of these ligands, most research has focused on sulfide and organic matter binding, with relatively little focus on the role of carbonates and Fe/Mn-oxyhydroxides. Predicting sediment toxicity in hydrologically dynamic watersheds is nuanced due to the complexity of formation of these compounds.

1.2 Methods for predicting metal bioavailability

In addition to single concentration WQC, more chemically rigorous methods of predicting surface water metal bioavailability are available. In the United States, the Environmental Protection Agency (U.S. EPA) recommends a correction for water hardness, as increased cation concentration in water can competitively exclude metals from biological uptake. The hardness corrected WQC are also thought to be appropriate for porewater, though some studies suggest otherwise (Carr et al., 2001). The Biotic Ligand Model (BLM) is a more rigorous bioavailability model, which implements major cation, anion, and water chemical data to predict effects of divalent cations (Cu, Ni, Zn, Cd) on aquatic organisms. This dissertation aims to test the efficacy of both models on surface and porewater data, and suggest potential improvements.

A few different models can be used to predict theoretical sediment metal toxicity where SQG's are generally just used for screening. The most well-known and established method estimates metal binding to sulfides, where if the simultaneously extracted metals (SEM) exceed

acid volatile sulfide (AVS) concentrations, toxicity may occur (Allen et al., 1993, 1991). If, however, AVS exceeds SEM, toxicity is improbable (USEPA, 2005). When metal binding to organic matter is thought to be high, this value should be divided by the fraction of organic carbon (f_{OC}) for better predictive outcomes (Campana et al., 2013). This method links metal bioavailability and predicted toxicity to the availability of sulfide metal binding sites.

Other sediment models, such as the sediment-BLM and the tableau input coupled equilibrium transport model (TICKET), are more complex requiring extensive input data and apply to specialized chemical contexts. The sediment-BLM is designed to estimate theoretical sediment-metal toxicity when organic carbon and sulfide are the dominant binding ligands (Di Toro et al., 2005). One important ligand missing from this model is iron and manganese oxyhydroxides, which are predominant ligands for several metals (Terzano et al., 2007a). Further, the sediment-BLM was designed to predict equilibrium metal partitioning, without inclusion of sediment kinetics or time series processes. The TICKET model; however, is equipped to predict changes to kinetics in a time series, with such applications as predicting metal bioavailability during sediment resuspension or redoximorphic change (Farley et al., 2008). The practicality of using either model in a regulatory context is debated, as large datasets of relatively complex chemical data are needed for accurate results.

1.3 The importance of hydrodynamic variability for assessing environmental risk

As toxicity testing and predictive models for toxicity all assume chemical equilibrium, it is vitally important to determine how these methods can be applied to non-equilibrium systems. Changing water levels can affect numerous sediment parameters, including water content, microbial activity, microbial community composition, redox, pH, bulk density, temperature, and nutrient availability (Coops et al., 2003; Leira and Cantonati, 2008; Van Der Valk, 2005). A few

relevant studies which have linked changes in these variables to increased environmental risk in aquatic systems will be discussed, particularly where increased risk was due to altered metal bioavailability.

The most redox affected aquatic systems have acid sulfate sediments, or sediments with high concentrations of metal sulfides (predominately FeS). Work spanning the globe has shown oxidation of reduced sediments can lead to a substantial decrease in pH associated with oxidation of FeS, including in Hamburg Harbor, Germany (Calmano et al., 1993), in the Lower Murray River, Australia (Creeper et al., 2015; Mosley et al., 2014), and in Billings Reservoir, Brazil (Carvalho et al., 1998). In the study from Brazil, toxicity to the zooplankton *Ceriodaphnia dubia* was increased directly with oxidation. Acid sulfate soils cover extensive areas in tropical soils (oxisols) and boreal peatlands (Caon et al., 2015). However, other sediment types are more prevalent and less studied in regards to redox changes.

Although alkaline (high-carbonate/gypsum) soils are prevalent in areas with limestone bedrock and in the increasingly arid regions of the world (Caon et al., 2015), there are relatively few studies investigating biogeochemical effects of water level variability in these systems, and none investigating metal ecotoxicology. One study of an alkaline freshwater tidal wetland in Virginia showed a direct correlation between oxidation and acidification (Seybold et al., 2002). Although the change in pH observed was a smaller magnitude than the acid-sulfate systems, the change was sufficient to alter metal bioavailability. Another study in the Mississippi River (La Crosse, Wisconsin), found an increase in porewater Zn (and other metals) during an oxidation event (Kreiling et al., 2015), which may have been due to changes in pH associated with oxidation. Other studies are more focused on nutrient availability, but show that Fe oxidizes

completely after several weeks of sediment drying, with important impacts to phosphate availability (Kinsman-Costello et al., 2014; Steinman et al., 2012).

There is only one study linking water level fluctuations to increased environmental risk in high carbonate aquatic systems. In White et al. (2008), aquatic species richness decreased in years where the magnitude of water fluctuation was the highest in high carbonate pothole lakes. Although metal analyses were not included in the study, decreased species richness was weakly correlated to water quality parameters, particularly SO_4^{2-} and pH, which would alter metal bioavailability. Various lake and reservoir studies have shown low water level conditions to be associated with increased water temperatures and conductivity, while high water levels have increased turbidity and nutrient content (Coops and Hosper, 2009; Magbanua et al., 2015). In some systems, these surface water changes lead to decreased benthic community metrics devoid of metal dynamics (Baumgärtner et al., 2008). Further complicating effects of drought and re-flooding are recolonization dynamics of organisms, which can vary between species and with sediment properties (Richardson et al., 2002).

While hydrological variability is a norm of aquatic systems, the magnitude and duration of extreme flooding and drying events is expected to be exacerbated by climate change (Kernan et al., 2010). Regional patterns in the distribution of precipitation have already been altered, and will continue to become more dynamic (Cai et al., 2014; A.D. Gronewold and Stow, 2014). This may lead to increasingly variable biogeochemical outcomes in intermittently flooded edges of wetlands, rivers, and lakes, which in turn could potentially modify organism exposure to metals in contaminated habitats. It is, therefore, important that continued investigation of the effects of hydrologic variability on the fate and effects of metals be conducted to assess potential impacts on sensitive organisms.

1.4 Dissertation summary

In the first data chapter (Chapter two), an overview of two in-lab microcosm experiments investigating the effects of water level variability on metal bioavailability will be described. The two experiments compare a short-term drying/oxidation (seiche) event to a long-term drought, with focus on physicochemical effects on Zn-cycling. The sediments used were collected from Great Lakes coastal wetlands, with alkaline sediments (~pH 6.5 – 7.5). This chapter shows that long-term sediment oxidation of even well buffered sediments, can cause Zn-oxidative release, wherein the bioavailability of porewater Zn can be increased up to 10-fold. The results of these experiments will be used to show that increased post-drought re-flooding, as predicted by climate scientists, may lead to increased environmental risk to organisms in Zn-contaminated, hydrologically variable aquatic systems.

Chapter three investigates the effects of Zn-oxidative release on organisms *Daphnia magna* and *Hyalella azteca* in a drought microcosm study, replicate of the previous chapter. Several modes of predicting toxicological effects are prescribed to this dataset and compared for effectiveness, including the U.S. EPA WQCs, BLM, and SQGs. In this chapter, the benthic amphipod, *H. azteca*, show sub-lethal effects (growth), while the zooplankton, *D. magna*, is not negatively affected. Further, strong correlations between Zn body burden, porewater Zn, and *H. azteca* growth suggest the effects are caused by Zn-oxidative release. These results suggest drought induced sediments may negatively impact benthic fauna upon reinundation, with a call for further field validation.

In chapter four, the sediment redox chemistry for vanadium (V) is investigated through hydrologically manipulated lab microcosm testing. Sediments collected from Lake Catherine (Arkansas, USA), downstream from a derelict V mine, undergo annual redox variability from

reservoir drawdowns (oxidation) and refloods (reduction). The speciation of porewater and sediment V during oxidation and reduction and the redox chemistries of several other metals (Zn, Cd, Cu) is described. Overall, the results show that V is mostly non-bioavailable, is relatively unaffected by redox variability, and bound to sediment in the +3-oxidation state; however, other more labile metals, such as Zn and Cd, become more bioavailable and potentially toxic. From these data, it is argued that reservoir management can influence sediment biogeochemistry and environmental health, and changes in metal bioavailability should not be overlooked in water resources management.

Chapter five includes a field validation study of the findings presented in chapters two and three. Sediments are deployed in a “dry-land”, oxic setting for 30 days, then moved to a “saturated”, reduced setting for 30 days. Porewater and sediment chemical analyses show Zn-oxidative release only occurred in one of the three sites in spiked sediments of approximately $310 \text{ mg-Zn kg}^{-1}$. While this chapter verifies that Zn-oxidative release may occur in high carbonate aquatic systems, with impending effects to periphyton biomass, the concentrations of Zn required to see such effects was higher than lab-observed values. This suggests that lab toxicity testing may overlook several important factors, including surface water chemical composition and biological transformations of metals.

Chapter six concludes by highlighting the most important findings of this dissertation, describing the implications of these findings, and providing suggestions for future research directions.

Chapter 2 - Indirect effects of climate change on Zinc cycling in sediments: the role of changing water levels

ABSTRACT

Increased variability in lake and river water levels associated with changing climate, could impact the fate and effects of metals in redox sensitive sediments through the alteration of microbial communities, acid-base and redox chemistry. The objective of this study is to determine the influence of water level variability on metal speciation in pore water and predict environmental risk to high carbonate systems. Using experimental microcosms with sediments collected from four metal contaminated coastal freshwater wetlands in Michigan, we conducted water level variability experiments. Porewater and sediment metals (Ca, Cu, Fe, Mg, Mn, Ni, Zn) and important metal binding phases (iron-oxide speciation, acid-volatile sulfide) were quantified. In a short-term drying (seiche) experiment, there were decreases in all porewater metals upon inundation of saturated sediments. During a drought experiment, re-inundation of oxidized sediments increased porewater Cu, Zn, Mg, Ca for most sites. Porewater Zn increased upon inundation to levels exceeding the USEPA threshold for chronic toxicity. These data show the dissolution of metal carbonates and metal sulfates contributes to metal release after re-flooding. These data show we may expect increased ecological risk to organisms present in drought sensitive regions where altered hydroperiods are likely to increase metal bioavailability.

2.1 Introduction

Climate change is affecting regional hydrology, with collateral effects on the biogeochemistry of aquatic systems (Firth and Fisher, 1992). While climate is variable in nature, the magnitude, frequency, timing, and duration of precipitation or flooding events (hydroperiod) is expected to be altered significantly on a regional basis by warming global temperatures (Milly et al., 2005). Increased water level variability affects coastal ecosystem biogeochemistry by altering sediment acid-base chemistry, redox potential and microbial community response, which can facilitate release or sorption of metal contaminants (De Jonge et al., 2012a). These processes are relevant to several hydrologic types, such as streams and wetlands.

The fate and release of metal contaminants is controlled primarily by the abundance and reactivity of ligands that bind metals, thereby reducing their ecotoxicity. Many metals of concern (Zn, Cu, and Ni) are primarily toxic to organisms in their +2-oxidation state, when dissolved. Our primary objectives were to determine the influence of water level variability on metal speciation in porewater and sediments, to identify the key binding ligands associated with metal flux, and discuss potential effects to benthic macroinvertebrate populations.

Many ligands are sensitive to redox, pH, or microbial changes associated with water level variability; including Fe/Mn oxyhydroxides, metal sulfides, and metal carbonates. Oxygen fluxes affect the formation and dissolution of Fe/Mn oxyhydroxides, which can release or bind metals (Davranche and Bollinger, 2000). Another primary fate process of these metals is binding to sulfide complexes under reduction and release upon oxidation of sediments (Simpson et al., 1998). In this reaction, sediment microbes kinetically mediate the production and oxidation of sulfide. While the formation of metal carbonates is less influenced by redox or microbial activity, it is highly a function of pH, which has been shown to increase upon reduction of oxidized

sediments (Patterson et al., 1977). A fourth primary binding phase is organic carbon, which is thought to be less affected by redox state and varies in its importance depending on the metal of interest (Mahony et al., 1996). Predicting sediment toxicity in hydrologically dynamic watersheds is nuanced due to the complexity of formation of these compounds.

Sediments with low acid neutralizing capacity (ANC, such as acid-sulfate or low carbonate systems) are very sensitive to hydrologic pulses. In one study in Hamburg Harbor, Germany, oxidation of reduced sediments led to a decrease from pH 8 to 4, leading to release of metals into the water column (Calmano et al., 1993). Recent work investigating effects of flooding on the drought-induced floodplain of Australia's Lower Murray River similarly show a sudden decrease in pH upon inundation due to release of iron sulfate, with acidity persisting in sediments for over 3 years after the initial inundation (Creepers et al., 2015; Mosley et al., 2014). Further studies of sulfide oxidation focus on treatment of acid mine drainage, more specifically using the Global Acid Rock Drainage (GARD) guide to predict geochemical behavior of waste rock (Sapsford et al., 2009).

Work investigating the role of hydroperiod on metal dynamics in medium-high ANC freshwater systems has primarily focused on nutrient availability and has not been linked to metal toxicity. Re-flooding of oxidized sediment as a part of a wetland restoration led to eventual reduction of Fe and release of phosphate into surface water (Kinsman-Costello et al., 2014). Steinman et al. (2012) showed similar results in a controlled laboratory testing of coastal Great Lakes wetland sediments, after 8 weeks of soil desiccation. These studies suggest Fe oxidation plays an important role in hydrologically dynamic sediments, which may influence the fate of other metals.

One metal-centric study of a high-ANC floodplain forest along the upper Mississippi River (La Crosse, Wisconsin), found an increase in porewater Zn and other metals during a four-month oxidation period (Kreiling et al., 2015). In a freshwater tidal wetland in Virginia, Seybold et al. (2002) showed a direct correlation of oxidation and acidification, which helps explain why metal flux is being observed in low-acid systems. Further evidence is needed to show whether metal flux associated with water level variability in high carbonate sediments are likely to induce effects to macroinvertebrate populations.

We predict that (1) inundation of oxidized sediments will lead to a release of previously sediment-bound metals, (2) long-term, drought events will produce higher porewater metal bioavailability and theoretical toxicity than short-term, seiche events, due to an increase in oxidized sediment fraction, and (3) sulfide, iron/manganese oxides, and carbonate binding ligands will be the primary controls on metal flux. These data will help predict the effect of climate induced water level variability on metal cycling and toxicity in the freshwater systems, such as the Great Lakes, and inform continued management and protection of wetland and shallow water ecosystems.

2.2 Materials and methods

2.2.1 Site/Sediment selection

We selected four coastal lacustrine wetlands of high sediment metal content, variable hydrology, and diverse sediment chemical composition and grain size (all minerotrophic). By selecting several sites, we can compare effects of sediment type and improve relatability to multiple field conditions. The sites are: (1) Quanicassee Wildlife Refuge (*QC*), (2) East Bay Park (*EB*), (3) Little Black Creek (*LBC*), (4) Lake Erie Metropark Wetlands (*DRW*). A map of

sediment collection sites is provided in [Figure 2-1](#). We also collected non-polluted sediments as a control from the River Raisin (*RAIS*) in Manchester, MI.

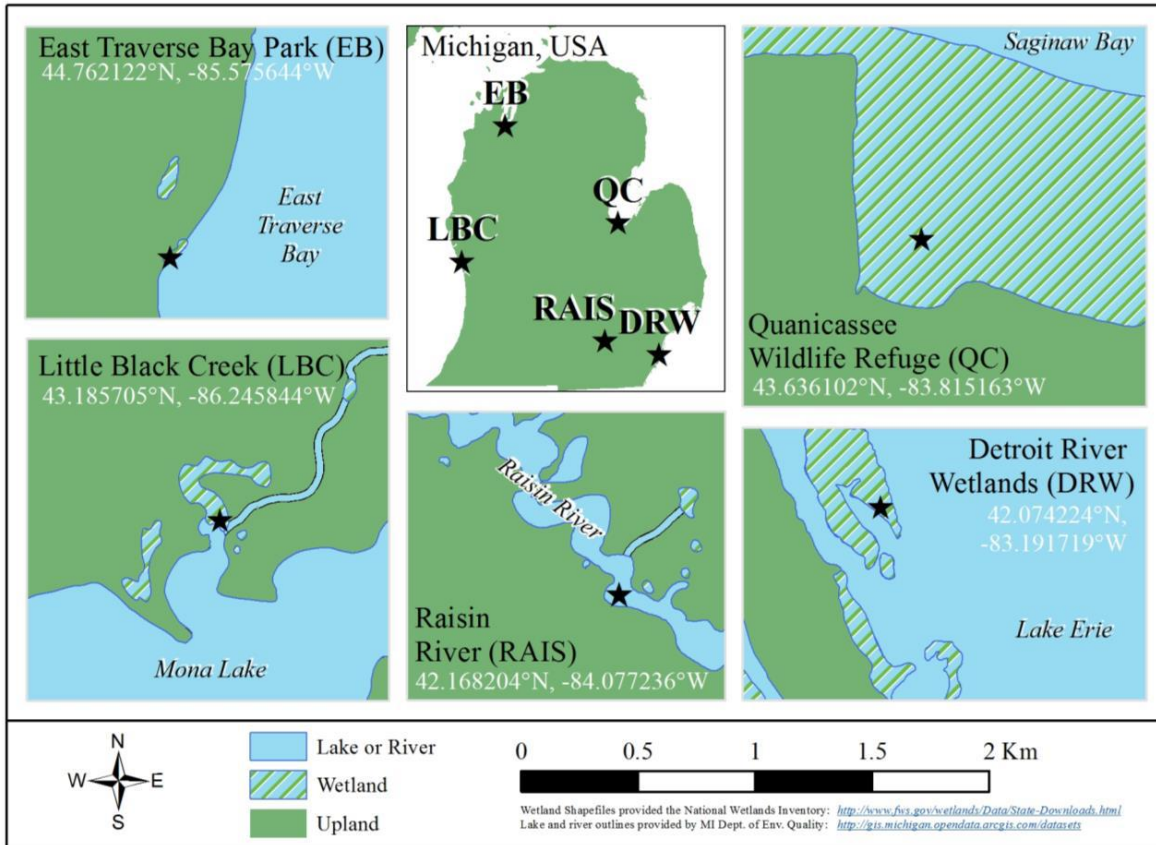


Figure 2-1. Map of field sites in Michigan, USA

Sites differ in their surrounding land-use, probable source of contaminants, and hydrology. QC is a fringing wetland to Saginaw Bay, receiving runoff from adjacent farm fields and located adjacent to the Karn-Weadock Generating Complex (a coal-fired power plant). EB is a fringing wetland to East Traverse Bay located at the output of a storm drain outlet. LBC is a riverine wetland located at the outflow of Little Black Creek into Mona Lake (Muskegon, MI) and is located downstream from a historic petroleum refinery and the Peerless Plating superfund site (Cooper et al., 2001). DRW is a riverine wetland located at the outlet of the Detroit River into Lake Erie. Riverine hydrology influences LBC and DRW to a greater degree than the

primarily lacustrine influenced EB and QC sites. A detailed comparison of site characteristics and summary table is provided in [Table 2-1](#).

2.2.2 Experimental design

Sediment columns were extracted intact with a trenching shovel from each site and placed in three replicate microcosm chambers per site (November 2014). Sediments were irrigated and remained saturated at room temperature to support microbial life until experiments began in January 2015. Microcosm design is depicted in [Figure 2-2](#). Input water chemical composition is similar to Great Lakes surface water with an average of $152.9 \pm 1.4 \text{ mgL}^{-1}$ CaCO_3 , $6.2 \pm 0.02 \text{ mgL}^{-1}$ O_2 , $7.6 \pm 0.1 \text{ pH}$, $40.7 \pm 0.4 \text{ mgL}^{-1}$ Na, $3.4 \pm 0.3 \text{ mgL}^{-1}$ K, and approximately 0.15 mgL^{-1} Cl. Concentrations of other metals in input water were below detection ($\sim 5 \text{ }\mu\text{gL}^{-1}$). The flow rate was constant at $1.55 \pm 0.5 \text{ cm}^3 \text{ s}^{-1}$ during water additions.

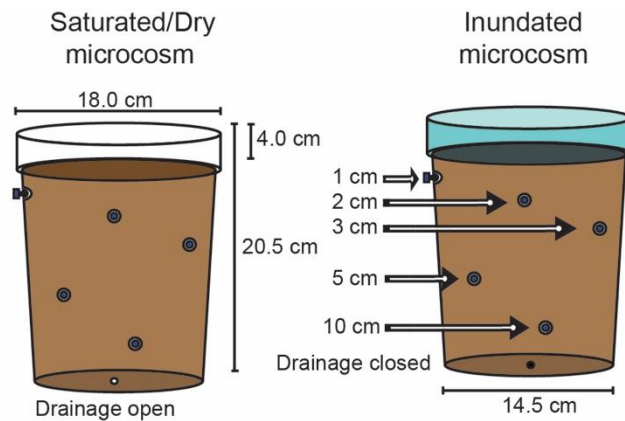


Figure 2-2. Experimental microcosms with Rhizon porewater samplers

Table 2-1. Physical and chemical properties of sediment types, including sediment texture, total metal content, total Fe-oxide content, pH, loss-on-ignition (LOI), dissolved organic carbon (DOC), and [SEM-AVS]/ f_{OC} (\pm standard error, SE).

Site	Texture	pH*	LOI (% C)	DOC (mgL ⁻¹ C)	[SEM-AVS] / f_{OC}	Total Fe- oxides (μ mol- Fe gdw ⁻¹)	Total Metals (mg kg ⁻¹)				
							Cu	Fe	Mn	Ni	Zn
QC	Sandy	7.3 ^a ± 0.03	8.0 ^a ± 1.4	0.65 ^a ± 0.20	-0.9 ^a ± 8.0	30.5 ^a ± 1.3	6.1 ^a ± 1.8	3640 ^a ± 268	68.5 ^a ± 11.9	ND	27.4 ^a ± 2.2
EB	Sandy	7.4 ^b ± 0.04	7.0 ^a ± 2.4	0.37 ^b ± 0.10	3.5 ^{a/b} ± 3.7	36.4 ^a ± 7.7	4.6 ^a ± 3.3	3010 ^a ± 720	71.9 ^a ± 20.8	ND	18.0 ^a ± 9.8
LBC	Sandy Loam	6.2 ^c ± 0.05	13.0 ^b ± 1.2	1.07 ^c ± 0.21	16.5 ^c ± 4.4	212.0 ^b ± 18.7	48.5 ^b ± 21.6	14300 ^b ± 5400	609.8 ^b ± 326.4	24.6 ^a ± 12.3	195.9 ^b ± 83.3
DRW	Sandy Clay Loam	6.8 ^d ± 0.06	25.1 ^c ± 1.0	0.21 ^b ± 0.03	11.7 ^{b/c} ± 11.2	198.0 ^b ± 10.8	66.1 ^b ± 2.8	22100 ^b ± 459	285.5 ^b ± 23.2	34.4 ^a ± 0.5	263.2 ^b ± 6.6
RAIS	Sand	7.5 ^b ± 0.05	2.0 ^d ± 0.4	-	-119.8 ^e ± 59.8	88.3 ^c ± 2.7	ND	8600 ^c ± 1370	386.0 ^b ± 105.9	ND	14.6 ^a ± 4.5

ND = No detect (detection limit for Ni: 19 μ g L⁻¹ or \approx 17.9 mg kg⁻¹; Cu: 0.5 μ g L⁻¹ or \approx 0.5 mg kg⁻¹)

a/b/c/d indicates statistical differences between sites ($p < 0.05$)

*Calculated from drought experiment data only

Two experiments mimicking a seiche (short-term drying) and a month-long drought were conducted, both with sediment drying followed by sediment re-wetting (15-hr and 32-days for seiche and drought, respectively). The seiche and drought hydroperiod were chosen due to their frequency of occurrence in Great Lakes systems. Seiches occur during storm events, when wind pushes water to one side of a lake, causing a basin-wide standing wave. The month-drought was designed to mimic seasonal low water (dry season) and high water (wet season).

Surface water was drained from microcosms with a 250- μm mesh syringe during drying with additional drainage from a small 1 cm hole in the bottom of each chamber. An over-head drip system was used to re-inundate sediments and the drainage hole in the bottom of each chamber was left open (seiche) or closed (drought). This irrigation system emulated precipitation and may have slightly different results than a groundwater fed system due to the potential for trapped air in microcosm sediments. Excess water overflowed into a drainage basin and was discarded. During the seiche and drought experiments, water was refreshed for 10 minutes every 6 hours or 4 minutes every 24 hours (complete surface water renewal after ~ 6 and ~ 72 hours), respectively.

2.2.3 Sampling and lab analysis

Porewater metals were sampled at all depths before and after 15-hours of re-flooding (for seiche), or after 1, 11, 16, 32 day(s) of re-flooding (for drought). Additional sampling for redox parameters (dissolved oxygen and reduced Fe) occurred on days 3, 9, and 24 (for drought). Water was extracted with a nitrogen-purged syringe. A maximum volume of 15-mL porewater was filtered through Rhizon samplers to 0.19- μm and surface waters were filtered with a 0.45- μm Millipore syringe-attachable filter. Dissolved oxygen in porewater was immediately measured using a 100- μm diameter oxygen microelectrode. Filtered samples were

then acidified with trace metal grade nitric acid to 2%, stored in the dark at 4° C, and analyzed within a month on an ICP-OES for metals Cu, Ni, Zn, and other important metals associated with binding (Ca, Fe, Mg, and Mn). Metal detection limits were ~5-10 μgL^{-1} (Cu, Ni, Zn) or 50 μgL^{-1} (Ca, Fe, Mg, Mn). Concentrations were corrected using a procedural blank (run for every 30 samples). Additional porewater was sampled and quickly analyzed for reduced iron (Fe^{2+}) concentration using a colorimetric (ferrozine) method (Viollier et al., 2000). Porewater dissolved organic carbon was analyzed after acidification (with 6M HCl to a pH of 2) on an OI Analytical Aurora 1030 TOC analyzer.

Dry and wet phase sediment cores were extracted from each microcosm on the day prior to re-inundation, 15 or 24 hours after inundation, and additionally (for drought experiment) 1 and 32-days after inundation. Sediment cores were sectioned with an acid-cleaned plastic spatula into 1.5 cm increments in a N_2 filled, continuous-flow purging bag. Sediment was processed for acid volatile sulfide (AVS) content and simultaneously extracted metals (SEM) (Allen et al., 1991), iron oxide crystalline and amorphous content (Kostka and Luther, 1994), dry weights, and loss-on-ignition (LOI) (6 hour combustion at 450°C) for organic carbon content. Replicate procedural blanks and reference sediments were run with digestions to verify >80% recovery between iron oxide extractions and correct for reagent associated metals. Extracted metals solutions were analyzed on an ICP-OES. Sediment pH was measured using a sediment probe.

2.2.4 Statistical analysis

Statistical significance testing was conducted on two levels: (1) multi-site level, including all microcosms as one sample and (2) single-site level, looking at individual sites (QC, EB, DRW, and LBC) separately. Most data were not normally distributed with a right skew due to natural heterogeneity (mottling of metals) in sediments. For nonparametric data Kruskal-Wallis

tests were used for multiple variable comparisons and the median or sign test was used for paired analysis. Where distributions were found to be normal, the equivalent ANOVA and paired t-tests were used. Pearson correlations between porewater metal content and chemical parameters were used when assumptions were met (normality, linearity, homoscedasticity). For non-parametric data, Spearman rank test was used to determine correlations. All statistical tests were conducted in RStudio Version 0.98.1102.

The BLM program (Ver 3.1.2.37, Windward Environmental, LLC) was used to calculate Zn-BLM chronic-HC5s for *Ceriodaphnia dubia*. Assumptions included sulfide concentrations ranging from 0.001 mg L⁻¹ on day-1 to 0.00599 mg L⁻¹ on day-32 to reflect increases in measured AVS. Alkalinity was calculated using a *p*CO₂ of 3.5 assuming an open system. Due to insufficient porewater samples sizes, unmeasured parameters (Na, K, SO₄, and Cl) needed to be estimated, and were done so per BLM recommendations with reference to Appendix C of the U.S. EPA's AWQC document for Cu (USEPA, 2007). These parameters were a lower priority for analyzing from the limited sample volume because they are less influential in predicting Zn toxicity than other inputs, such as pH and Ca (Deforest and Van Genderen, 2012).

2.3 Results

2.3.1 Site comparison

The most obvious and potentially important difference between sediments is the sediment texture, in addition to LOI (% C), sediment pH, and metal content. Important differences between sites are illustrated in Table 1. Particle size distribution indicates EB and QC are coarse sandy sediments, LBC is a sandy loam, and DRW is the most fine as a sandy clay loam. Percent by weight of carbon (from LOI) was statistically higher for DRW and LBC than for EB and QC (*p* < 0.01). Three statistical groupings for porewater DOC include high (LBC), moderate (QC),

and low (EB and DRW) ($p < 0.01$). Sediment pH is statistically different on average between all sites, where LBC is most acidic, followed by DRW, QC, and EB ($p = 0.001$).

Porewater concentrations of Cu, Fe, Mn, and Zn were statistically highest in LBC ($p < 0.004$). For Cu and Zn, there were two statistical groupings of high metal content (mean = $3.5 \pm 0.6 \mu\text{gL}^{-1}$ Cu and $159.3 \pm 16.5 \mu\text{gL}^{-1}$ Zn) in LBC, and low metal content (mean = $0.6 \pm 0.2 \mu\text{gL}^{-1}$ Cu and $7.0 \pm 4.6 \mu\text{gL}^{-1}$ Zn) in DRW, EB, and QC. For higher concentration metals, Fe and Mn, three statistical groupings existed for LBC (mean = $14.8 \pm 1.8 \text{mgL}^{-1}$ Fe and $2.2 \pm 0.2 \text{mgL}^{-1}$ Mn), DRW (mean = $6.8 \pm 0.7 \text{mgL}^{-1}$ Fe and $0.9 \pm 0.1 \text{mgL}^{-1}$ Mn), and EB/QC (mean = $1.4 \pm 0.1 \text{mgL}^{-1}$ Fe and $0.4 \pm 0.03 \text{mgL}^{-1}$ Mn). Reduced iron concentrations followed this trend as well. Porewater Ca, Mg, and Ni were similar between sites. Total metals analysis shows higher metal concentrations for LBC and DRW than QC and EB, as shown in [Table 2-1](#).

When comparing sulfide concentrations in sediments, EB has less AVS on average than the other sites (mean = 0.8 ± 0.3 vs. $3.4 \pm 0.9 \mu\text{mol-S}^{2-} \text{gdwt}^{-1}$) ($p = 0.001$). [SEM-AVS] as normalized for organic carbon was different between most sites. From highest (theoretically most toxic) to lowest (theoretically non-toxic), the three groupings were (1) LBC and DRW, (2) EB (and DRW), and (3) QC (and EB) (Table 1) ($p < 0.02$).

Higher concentrations of Mn and Fe in LBC and DRW sediments led to higher fractions of Fe-oxides, Mn-oxides, and Zn bound to Fe/Mn oxides in these sediments than QC and EB ($p < 0.001$). Average total oxidized concentration for high and low statistical groupings were 71.1 ± 3.8 and $8.6 \pm 1.4 \mu\text{mol-Fe gdwt}^{-1}$, 3.2 ± 1.7 and $0.9 \pm 0.7 \mu\text{mol-Mn gdwt}^{-1}$, and 3.0 ± 1.3 and $0.6 \pm 0.2 \mu\text{mol-Zn gdwt}^{-1}$. Many of the differences between sites are likely related to site hydrology, as LBC and DRW are low energy (depositional) riverine wetlands, whereas EB and QC are high energy (less depositional) lacustrine, fringing wetlands.

2.3.2 Seiche experiment

After the 15-hour drying period, surface sediments remained partially saturated and chemically reduced. Upon inundation, sediment moisture content increased by a range of 1-15 percent (average of $10.0 \pm 2.4\%$), from $39.1 \pm 7.5\%$ to $49.0 \pm 9.2\%$ on average. Sites with a sandy soil texture (EB and QC) had the highest change in moisture content, compared to sandy loam (LBC) and sandy clay loam (DRW) sediments. Upon inundation, pH decreased for LBC and DRW microcosms by 0.6 ± 0.05 ($p \leq 0.035$), from 6.8 to 6.3 ± 0.03 , but there was no change for QC or EB. The pH remained neutral in all microcosms (range 6.0-7.4; average 6.7 ± 0.3). A decrease in porewater Fe^{2+} concentration between saturated and inundated phases suggests sediment oxidation ($p < 0.002$). Although the Fe^{2+} decrease was observed for all microcosms, as individual sites, it was only significant for DRW ($p = 0.04$). We observed no change in porewater dissolved oxygen content (from 0-1 cm) upon inundation.

All measured porewater metals, including Ca, Cu, Fe, Mg, Mn, Ni, and Zn, decreased in concentration upon inundation of sediments, as shown in [Figure 2-3](#). A significant decrease in Zn resulted from inundation ($p = 0.00006$), largely due to decreases of Zn in sandy sediment microcosms (QC and EB). Likewise, a decrease in Ca and Mg ($p \leq 0.02$) occurred from 64.5 ± 6.5 to $47.0 \pm 4.7 \text{ mgL}^{-1}$ Ca and 188.0 ± 11.6 to $157.1 \pm 9.4 \text{ mgL}^{-1}$ Mg for all sites on average. Decreases in Ca and Mg were only significant for LBC and EB on the single-site level ($p < 0.05$). Other decreases (Cu, Fe, Mn, and Ni) were not significant on the multi-site level; however, Fe decreased in LBC from 39.5 ± 4.6 to $21.0 \pm 5.0 \text{ mgL}^{-1}$ ($p < 0.04$). Nevertheless, results for Cu and Ni may be misleading as concentrations were occasionally below detection.

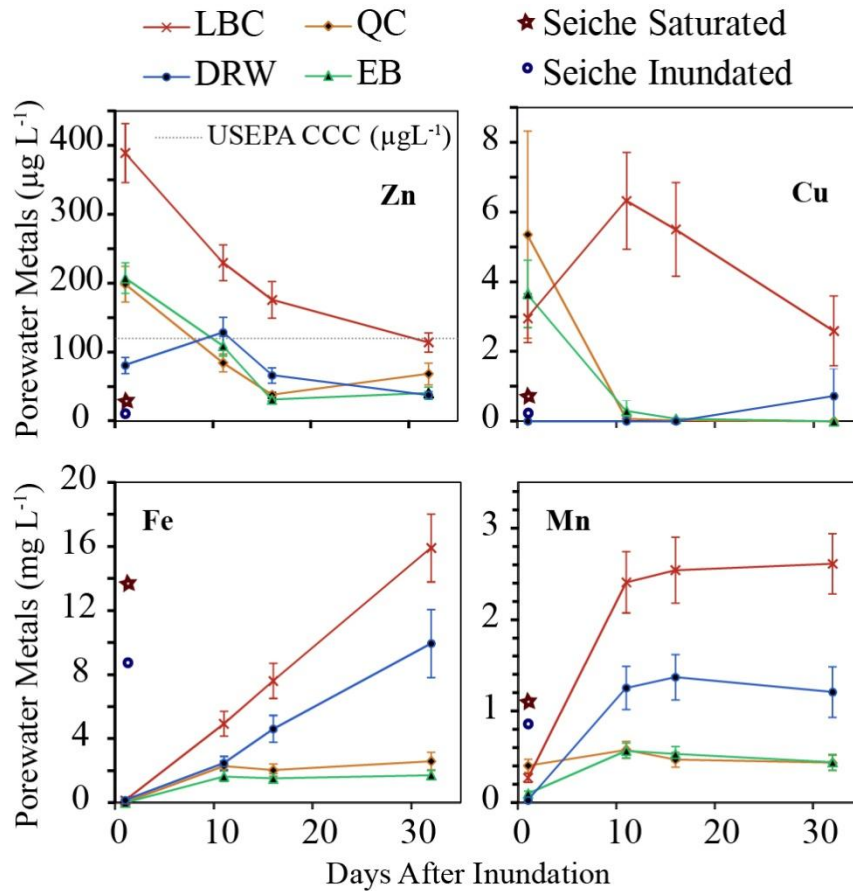


Figure 2-3. Average porewater Zn, Cu, Fe, and Mn for seiche and drought (\pm SE). Seiche inundated is sediment with 4-cm standing water and saturated is pre-inundation (wetted sediment with no standing water).

All sediments from the seiche experiment had a negative average [SEM-AVS] when normalized to organic carbon, as shown in Figure 2-4, indicating theoretically non-toxic sediments due to sulfide binding. Increased variability for DRW and QC sediments was likely due to wide ranging AVS values caused by strong vertical redox gradients. In other words, DRW and QC sediments had a strongly defined oxic (\approx 0-1.5 cm) and reduced layer (\approx 1.5-3 cm). Saturated and inundated sediments showed no differences in [SEM-AVS] on average on the single or multi-site level.

Additionally, no differences in total, amorphous, or crystalline oxidized iron content were observed between saturated and inundated sediments. Average total and amorphous oxidized

iron between all sediments were 131.8 ± 21.8 and $43.9 \pm 7.6 \mu\text{mol-Fe gdw}^{-1}$, respectively. This suggests metal binding to Fe-oxyhydroxides is unchanged during seiche events. As shown in Figure 5, porewater hardness decreased between saturated and inundated phases for EB and LBC ($p < 0.05$), suggesting formation of metal bicarbonates (Figure 2-5).

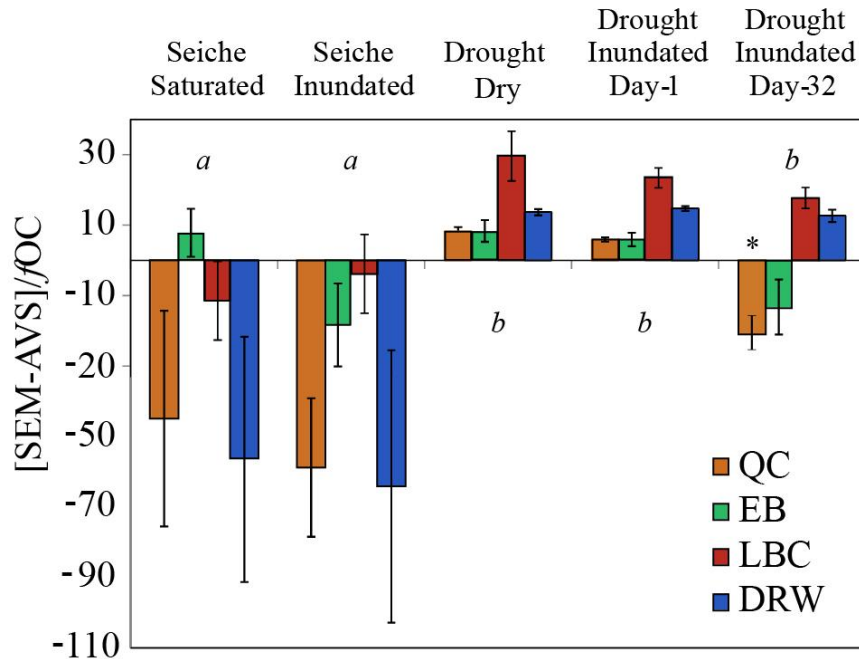


Figure 2-4. [SEM-AVS]/ f_{OC} (\pm SE) for seiche and drought with statistical differences between (*a/b*) and within (*) experiments ($p < 0.05$).

2.3.3 Drought experiment

After 32-days of drying, sediment was oxic with no extractable porewater. Sediment moisture increased upon inundation by a range of 8-32% average of $24.8 \pm 4.5\%$, from $17.7 \pm 2.5\%$ to $45.3 \pm 7.5\%$ on average. The sandy clay loam (DRW) sediments had a very small increase in water content (8.5%) compared to the sandy and sandy loam sediments. Throughout the experiment, sediment pH either increased (for LBC and DRW from 6.4 to 6.7 ± 0.06) or stayed the same (QC and EB). This suggests that QC and EB have a greater apparent acid

buffering capacity than LBC and DRW. The pH stability in QC/EB may also be due to lower concentrations of iron sulfides in these sediments. Dissolved oxygen in porewater (0-2 cm depth) decreased on average during the 32-day inundation while Fe^{2+} concentration increased, indicating sediment reduction (Figure 2-6). When considering all sites, Fe^{2+} concentrations increased between days 1, 3, 9, and 16 ($p < 0.001$).

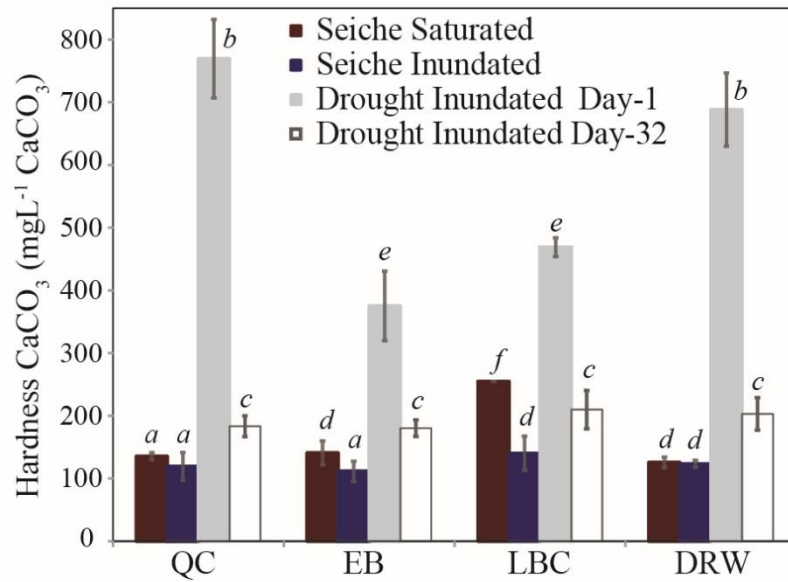


Figure 2-5. Porewater hardness (\pm SE) for seiche and drought with lettering for statistical significance ($p < 0.05$).

As predicted, inundation of oxidized sediments led to increased porewater Zn and Cu, which then decreased over 32-days (Figure 2-3). The observed increase in porewater Zn for LBC is especially notable, as it exceeded the USEPA threshold for chronic toxicity (CCC) to freshwater organisms ($120 \mu\text{g L}^{-1}$) for approximately 30-days (USEPA, 2016a). EB and QC exceeded the CCC, but only on day-1 after inundation, while DRW did not for either experiment (though it did in later trials with increased sediment drying). For Cu; however, LBC and DRW microcosms did not show a significant day 1 increase. These sediments had the highest LOI ($p < 0.05$), which suggests a greater role of organic carbon in controlling Cu partitioning.

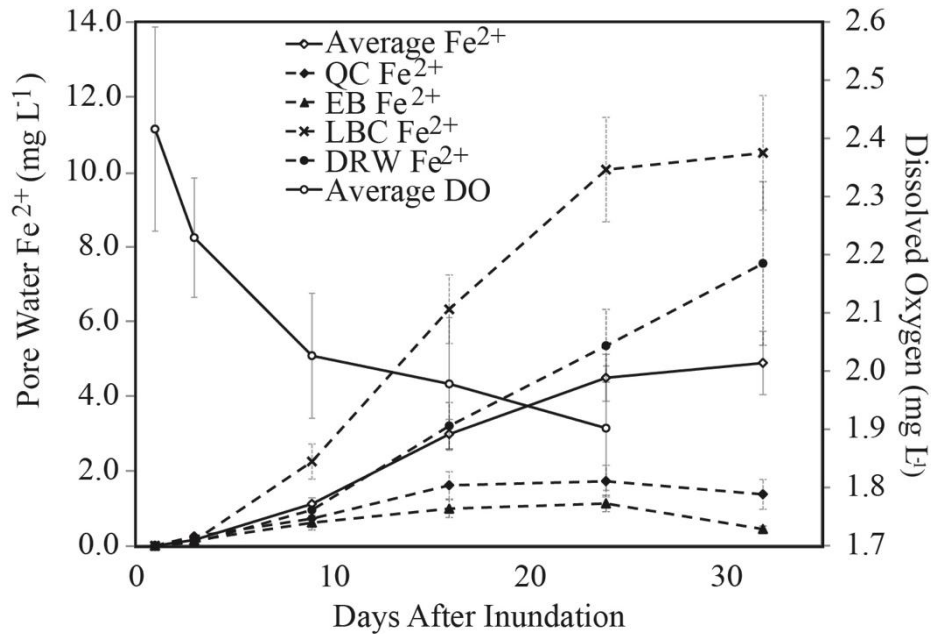


Figure 2-6. Porewater reduced iron and dissolved oxygen (\pm SE) indicate oxidation at day-1 followed by reduction to day-30 (after inundation).

We observed the opposite trend for Fe and Mn, where metals started in low concentrations and increased throughout the study (Figure 2-3). This effect is likely due to reductive dissolution of Fe/Mn in sediments as reflected in the formation of reduced Fe. Fe and Mn sampling concentrations measured on day-1 after inundation were lower than on days 11, 16, and 32 ($p < 0.00001$). The only exception to this trend was for Mn in the QC microcosms which were all similar.

Oxidized sediments pre-inundation and 24 hours after inundation had a positive average [SEM-AVS] as normalized to organic carbon of 13.6 ± 1.50 , which suggests potential sediment toxicity to benthic macroinvertebrates (Figure 2-4). [SEM-AVS] became positive because all microcosms had AVS concentrations of $0 \mu\text{mol g}^{-1}$ on day-1 after inundation. After 32-days of inundation, [SEM-AVS] decreased for all sites except DRW. On the multi-site level, decreases in

[SEM-AVS] were not significant (likely due to small sample size); however, QC's decreases were significant ($p = 0.001$).

No difference in total, amorphous, or crystalline Fe/Mn-oxyhydroxide content occurred between oxidized and inundated sediments at the experiment or site scale. Average total and amorphous oxidized iron between all sediment types was 98.5 ± 17.6 and 33.2 ± 5.8 $\mu\text{mol-Fe gdw}^{-1}$, respectively. In addition, a large fraction of total Zn ($63.5 \pm 1.4\%$) was bound to Fe/Mn-oxyhydroxide minerals between all sites. The only phase that decreased upon inundation was the amorphous Fe/Mn-oxyhydroxide bound Zn ($p = 0.055$). Carbonate in sediment and porewater may have also influenced metal flux, as porewater hardness decreased between day-1 and day-32 of inundation (from 477.8 ± 46.3 to 152.1 ± 11.3 mgL^{-1} as CaCO_3) ($p < 0.0000001$), suggesting precipitation of metal bicarbonates (Figure 2-5).

2.3.4 Comparison of seiche and drought

Our prediction that metal flux would be greater in the drought experiment than the seiche was correct for several metals. Porewater concentrations of Ca, Cu, Mg, and Zn were greater on average (all days) in the drought experiment than the seiche experiment ($p < 0.001$). Conversely, for porewater Fe (total and reduced fractions) seiche induced sediments had higher concentrations than drought sediments ($p = 0.008$). Reduced iron concentration was also greater in seiche sediment with 4.0 ± 0.4 mgL^{-1} Fe^{2+} as compared with 2.3 ± 0.2 mgL^{-1} Fe^{2+} in drought sediment. Porewater concentrations of Ni and Mn were similar between experiments.

The potential for sediment toxicity as [SEM-AVS] normalized to organic carbon was statistically different between the seiche and drought experiments ($p < 0.0001$). While this value stayed mostly negative during the seiche event (mean = -29.8 ± 8.2) it was mostly positive during the drought oxidation event (mean = 8.9 ± 1.9), suggesting that drought inducing conditions create

higher theoretical risk of toxicity. All sediment sampled during both experiments had similar oxidized iron content. Sediment pH was on average greater in the drought experiment than the seiche experiment (mean = 6.9 ± 0.03 vs. 6.6 ± 0.08 pH units) ($p < 0.000001$).

Some measured parameters, such as dissolved organic carbon (DOC) in porewater and sediment loss-on-ignition (LOI), were not affected by hydrologic manipulations. Sediment organic matter was similar throughout the seiche and drought experiments (mean = $0.13 \pm 0.04\%$ C). Porewater DOC was similar for all microcosms between all experiments; however, one exception was a statistical decrease in DOC for EB during the drought experiment (mean = 1.1 ± 0.3 to 0.5 ± 0.2 mgL^{-1} C) ($p < 0.02$).

2.4 Discussion

2.4.1 Assessing ecological risk of seiche and drought

The magnitude of chemical change observed during the simulated seiche is relatively un-concerning from a biological perspective. Metals concentrations did not exceed CCC, with $[\text{SEM-AVS}]/f_{\text{OC}}$ values remaining negative. The pH decrease observed for LBC and DRW may indicate oxidation or increased microbial production upon inundation of sediments. Several species of amphipods can be sensitive to acidification with changes to pH of >0.7 units, although this is mostly an issue in warmer temperature water with low pH (<6) (France and Stokes, 1987; Pilgrim and Burt, 1993). While the magnitude of sediment acidification in LBC and DRW during the seiche was less than 0.7, field-monitoring efforts should consider large-scale changes in sediment pH with seiche events as the magnitude may vary. Typically, porewater metal concentrations increase with acidification, but the opposite was observed. It is possible metals leached from the microcosm chambers, as some drainage occurred in attempt to emulate groundwater dynamics. Leaching of metals would not necessarily occur in natural sediments,

where re-inundation would include metal-rich groundwater inputs (which our experimental design did not include) (Taniguchi and Fukuo, 1996).

The increase in porewater Zn after inundation of drought/oxidized sediments is ecologically relevant, as it may adversely affect benthic macroinvertebrates inhabiting metal contaminated aquatic systems. While QC, EB, and LBC all exceeded the USEPA threshold for chronic toxicity, when compared to the hardness corrected criteria LBC was the only site in exceedance, as depicted in [Figure 2-7](#). However, recent studies using a biotic ligand model (BLM) for Zn show that chronic toxicity to organisms is often underestimated using the hardness corrected criteria (Deforest and Van Genderen, 2012), particularly for *Ceriodaphnia dubia*. In this study, we found the hardness corrected criteria to be somewhat underprotective as compared to the Zn-BLM for two of our sites (EB on day-1 and LBC on days 1-16). The BLM is designed to address environmental risk to surface water organisms and not benthic organisms exposed to porewater; however, it is more mechanistic and chemically descriptive than current theoretical models or screening methods for sediments such as SEM-AVS or Probable Effects Concentrations. A sediment BLM which can accurately predict metal bioavailability where organic carbon is the primary binding ligand has been produced; however, it is not yet fully applicable to field settings or designed to account for changing redox conditions (Shi et al., 2013). Future model development is needed to accurately incorporate benthic species into the BLM or similar user-friendly and mechanistically driven model.

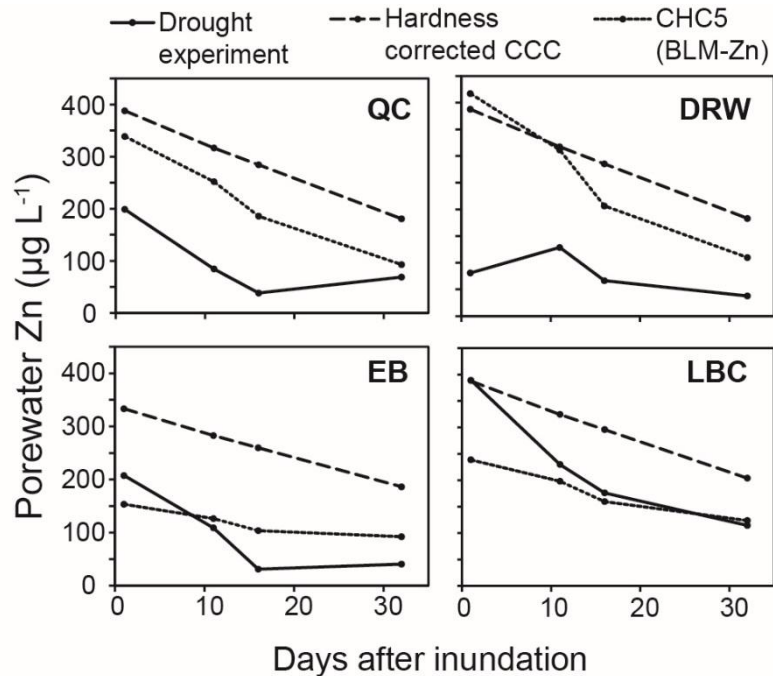


Figure 2-7. Comparison of Zn concentrations to hardness-corrected CCC and BLM-derived chronic HC5 values for drought experiment.

While the probability of toxic effects to organisms associated with Zn pulsing is debatable, one study has confirmed its occurrence during field sampling in a similar watershed. In Krieling et al. (2015), porewater ion content measured by a Plant Root Simulator (PRS) showed increasing Zn concentrations with sediment oxidation in a floodplain of the Upper Mississippi (Wisconsin). Further, in White et al. (2008), species richness in high carbonate lakes (in Great Lakes region) were found to be highest when the magnitude of water fluctuation remains unchanged year to year. The loss of species richness was weakly correlated to water quality (DOC, Ca^{2+} , Conductivity, pH, SO_4^{2-}), although metal analyses were not included in the study. These two lines of evidence, in conjunction with findings from this study, suggest that field studies should be conducted to precisely assess the magnitude, duration, and impacts of Zn oxidative release. These studies should try to control for additional ecological effects associated

with drying and subsequent inundation (organism migration, nutrient availability, turbidity, etc.) (Covich et al., 1999).

In addition to the dissolved Zn porewater concentrations, [SEM-AVS] values are another line of evidence indicating sediments oxidized during drought may have increased theoretical toxicity to organisms. Several studies using Zn spiked sediments have clearly shown that [SEM-AVS] values > 0 are strongly correlated with metal toxicity to several macroinvertebrate species (Han et al., 2005; Lee and Lee, 2005). Despite these findings, others suggest it may not be appropriate in non-equilibrium systems, due to differences in reaction kinetics of sulfide reduction between sediment types and the preference for less toxic microsites by organisms (Brown, 2000; S. Simpson et al., 2012). Regardless, it is still a useful tool to help predict metal binding to sulfide and organic matter in sediments, and metal bioavailability.

2.4.2 Effects of sediment chemistry on redox-induced Zn-pulse

During these experiments, several important metal binding phases were affected during drought conditions, including carbonates and sulfides. Sulfide (as AVS) and carbonate (in porewater) were moderately correlated with Zn in LBC porewater ($cc = -0.64$, $p < 0.01$; $cc = 0.59$, $p < 0.001$). This is strong evidence that porewater Zn increased upon inundation due to oxidation of Zn sulfides and dissolution of Zn carbonates. A theoretical schematic of these reactions is provided as [Figure 2-8](#). Zinc sulfides have been well studied and are known to be an important ligand for Zn bioavailability (de Livera et al., 2011; Simpson et al., 2000). The mechanics of Zn carbonate formation and dissolution are less studied, but are of considerable importance in high carbonate systems (Korfali and Davies, 2004). Zn carbonate precipitation may have increased during sediment drying, leading to increased dissolution upon sediment

inundation. This effect would be enhanced by the observed increase in sediment acidity on day-1.

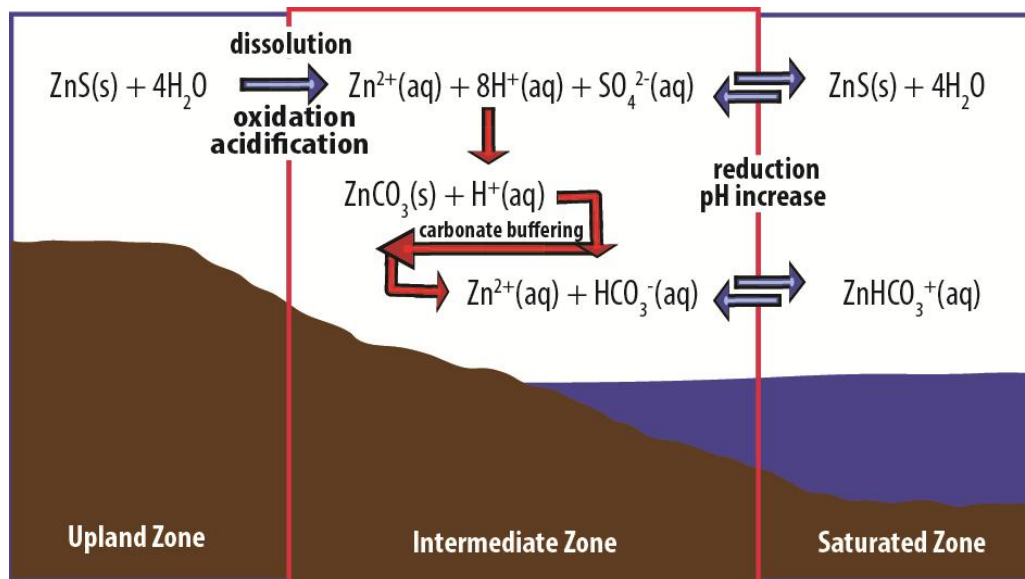


Figure 2-8. A schematic is provided of the chemical equations associated with Zn-release and subsequent reduction.

It is somewhat surprising that there was not a clear change in sediment Fe/Mn-oxyhydroxide content (crystalline, amorphous, or total), especially in sediments with high iron (DRW and LBC). Most studies show an overall decrease in sediment Fe/Mn-oxyhydroxide content with reduction, though these studies use homogenized (not heterogeneous) sediment. In more controlled studies, reductive dissolution of Fe/Mn-oxyhydroxides has been found to be important for porewater metal equilibrium (Grybos et al., 2007). Further evidence using electron microscopy techniques show the formation of Zn on and in amorphous ferrihydrite and vernadite-like minerals in oxidized sediments (Hochella et al., 2005b). For other metals (Cu and Ni), crystalline Fe/Mn oxide content increases and amorphous Fe/Mn oxide content decreases as oxic and anoxic sediment layers form with aging (David M Costello et al., 2015). Sediment heterogeneity and mottling added to the complexity of this system such that more intensive

sampling was likely needed to see effects to Fe/Mn-oxyhydroxide content. Further, sediment desiccation likely decreased microbial productivity, which would also decrease kinetic rates of Fe/Mn-oxyhydroxide transformation.

While an overall decrease in Zn bound (through complexation or adsorption) to amorphous Fe/Mn-oxyhydroxides (ferrihydrite, lepidocrocite) was observed during the inundation, it was not correlated with porewater Zn concentration ($p > 0.25$). This may indicate the amorphous Fe/Mn-oxyhydroxide-Zn is being reduced to a non-labile form, or the relationship is confounded by other ligands such as sulfide, carbonates, or particulate organic matter (POM). Our findings agree in that the amorphous Fe/Mn-oxyhydroxides seem more important to Zn bioavailability than the crystalline phases, since we observed a change in Zn binding to amorphous but not crystalline Fe/Mn-oxyhydroxides. This is likely due the large surface area of amorphous compounds which increases available binding sites (Guo et al., 2016).

As porewater DOC did not change during the experiment, it is unlikely it influenced Zn bioavailability. Our sampling design; however, did not allow sampling of porewater POM, which we would expect to become more sorptive to metals as pH increases. In future studies we hope to measure the changes in metal binding to POM with post-drought re-flooding.

Previous studies have shown inundation of oxidized sediment to cause toxicity in low acid-neutralizing capacity systems. Carvalho et al. (1998) assessed impacts of resuspension on macroinvertebrate populations in the acid-sulfate sediments of Billings Reservoir, Brazil, in which sediment oxidation caused acute toxicity to *Daphnia similis*. Their findings; however, are only tangentially applicable to high ANC systems.

This study shows that systems with relatively high pH and high buffer capacity can also release bioavailable metals into aquatic systems. Sediment pH was strongly correlated to

porewater Zn for DRW and LBC sediments only, during the drought experiment ($cc = -0.5$, $p < 0.0001$). Well-buffered QC and EB sediments did not experience a pH change, allowing Zn to be rapidly re-adsorbed to sediments after the initial inundation. In these experiments, hydrology has proved important in (at least) two aspects: 1) it shapes sediment characteristics from allotchtionous inputs, which alters grain size, nutrient inputs, and general chemical composition, and 2) it directs the chemical equilibrium of sediments and thus the bioavailability of metal contaminants.

2.4.3 Implications for climate research

Our findings suggest additional focus is needed to predict biogeochemical effects of climate variability on affected aquatic systems. Our regional focus for was the lower Great Lakes, where increased variability in water levels have occurred in recent years, ranging from record lows (2013) followed by surges of 0.6-1 meters in lake water levels (2014) (Andrew D. Gronewold and Stow, 2014). This hydrologic variability is correlated with surface water temperatures, the duration and coverage of winter lake ice, evaporation, and precipitation, all factors influenced on a regional scale by El Niño climatic events and weakening of the circumpolar vortex (A.D. Gronewold and Stow, 2014). Both of these climatic phenomena are expected to strengthen with continued climatic warming, further increasing variability in Great Lakes water levels (Cai et al., 2014). Strong evidence suggests the metal pulse we observed in our experimental microcosms is occurring in coastal sediments of the Great Lakes. If so, this could have important biogeochemical ramifications to these aquatic systems.

As a lab microcosm study, this research has a few limitations to its field applicability, including the absence of plants and autochthonous inputs. The presence of plants can add new organic carbon to sediments and plant rhizospheres can alter the oxidation of sediments, which

influences metal binding (Jacob and Otte, 2003). Water level variability influences plant community composition and type (submerged, emergent, floating) which may seasonally affect redox in the sediment or water column (Desgranges et al., 2006). Increased rates of porewater dilution or advection in response to surface and groundwater inputs may decrease the temporal duration of elevated porewater Zn. Further bioturbation by organisms may alter sediment chemistry and increase Zn uptake by benthic organisms (Remaili et al., 2016), which was not included in the experimental design of this study. With these important distinctions in mind, the data and results of this research can be broadly applied to freshwater aquatic systems.

While this research shows increased bioavailability of metals in just one aquatic system (high carbonate coastal freshwater wetlands), similar biogeochemical effects are predicted for riparian and inland freshwater aquatic systems. Our stated predictions were partially correct, in that (1) sediment oxidation led to Zn-release, (2) long-term drying (drought) had a larger effect on theoretical toxicity than short-term drying (seiche), and (3) dominant binding ligands associated with Zn-oxidative release were sulfide, carbonate, and amorphous Fe/Mn-oxyhydroxides. The redox-induced pulse of metals into sediment porewaters can lead to changes in nutrient availability, sediment chemistry, and environmental risk; therefore, site-specific hydrochemical parameters should be considered when assessing sediment quality.

Chapter 3 – Sediment Zn-release during post-drought re-flooding: Assessing environmental risk to *Hyaella azteca* and *Daphnia magna*

ABSTRACT

Hydrologic variability exacerbated by climate change affects biogeochemical cycling in sediments through changes in pH, redox, and microbial activity. These alterations affect the lability and speciation of metals, such that toxicity may be observed in otherwise non-toxic sediments. In this study, we investigate the effects of drought and reflooding on metal bioavailability in sediments with low to moderate concentrations of Zn (18 to 270 mg kg⁻¹). Sediments were collected from coastal wetlands in Michigan, dried (36-days) and re-inundated in lab microcosms. We investigated the relationships between key parameters, for surface/porewater (dissolved and particulate metals, dissolved oxygen, redox (Eh), reduced iron, and temperature) and sediment (simultaneously extracted metals (SEM), acid volatile sulfide (AVS), Fe/Mn-oxyhydroxide, organic carbon, water content analyses, and diffusive gradient in thin films (DGTs) metal concentrations). Porewater Zn increased with inundation of dried sediments for all sediment types, exceeding United States Environmental Protection Agency (U.S. EPA) chronic criteria for freshwater organisms, and decreased as sediments became reduced. Effects on *Hyaella azteca* (7-day exposure) and *Daphnia magna* (10-day exposure) were quantified. Results show decreased growth of *H. azteca* for sites with elevated Zn and increased Zn-body concentration (BC_{Zn}) in the most contaminated sediment type. Further, BC_{Zn}

was negatively correlated with *H. azteca* growth. *D. magna* survival, growth, and reproduction were not affected. DGT metal concentrations were more reflective of porewater than organism bioaccumulation. Outcomes of predictive toxicology methods are compared to toxicity test results and suggestions are provided for model improvements. This study demonstrates that post-drought re-flooding of sediments affects Zn biogeochemical cycling with potentially adverse effects on benthic organisms, even in sediments with only moderately elevated concentrations ($>150 \text{ mg kg}^{-1}$).

3.1 Introduction

The frequency and magnitude of hydrologic extremes (i.e. floods, droughts) are predicted to increase with climate change, affecting biogeochemical cycles in aquatic systems (Kernan et al., 2010). Previous work has investigated the role of fluctuating water levels on metal cycling, including the finding that Zn bioavailability (or fraction available for uptake by organisms) increases with sediment oxidation and drying (Zn-release) (Nedrich and Burton, 2017). While relatively little information is available on how variable hydrology influences metal bioavailability and effects on aquatic organisms, knowledge of potential effects is important for conservation and restoration, water management, and ecological risk assessment. This study will assess the effects of Zn-release for sediment and surface water organism exposures, to *H. azteca* and *D. magna*, respectively, in several freshwater high-carbonate sediment types.

Previous work showing biological effects from metal oxidation was conducted in acid-sulfate sediments with little attention to other sediment types. In Carvalho et al. (1998), acid-sulfate sediment resuspension caused oxidation and release of metals with acute toxicity to *Daphnia similis*. Many have investigated the effects of sediment oxidation on metal toxicity, including Simpson (Simpson et al., 2012; Simpson and Spadaro, 2016; Simpson et al., 2000,

1998), De Jonge (De Jonge et al., 2012a, 2012b), via sediment resuspension for Fetters et al. (Fetters et al., 2016), and for mine tailing oxidation (Plante et al., 2011; Sapsford et al., 2009). This study focused on high carbonate sediments types, as they are incredibly abundant (~20% of earth's surface) and are relatively unstudied (Middleton, 2003).

The dominant driver for Zn release is the oxidation of sediment sulfide (to sulfate), releasing Zn^{2+} (aq) from ZnS (s), which explains the previous focus on acid sulfate sediment. The dissolution and oxidation of metal sulfides concurrently decreases pH, thus increasing porewater Zn^{2+} via acidification of Zn-hydroxides (ie $Zn(OH)_2$ or $Zn(OH)^{-1}$) and carbonates (ie $ZnHCO_3^{-1}$ or $ZnCO_3$). Less is known about the importance of post-drought re-flooding on other metal-binding solid phases in sediments such as Fe/Mn-oxyhydroxides and organic carbon (Hochella et al., 2005a). Evidence suggests amorphous Fe/Mn oxyhydroxides content (ferrihydrite, lepidocrocite) is more effected by sediment redox and drying than crystalline phases (hematite, etc.) (Guo et al., 2016). Increased acidity (H^+) may decrease Zn-binding sites on organic carbon or Fe oxides, which would also affect Zn cycling. This study aims to verify and further investigate the chemical dynamics of Zn-release in sediments where sulfides are less prevalent.

Relevant exposures for this study are through surface water (zooplankton) and surficial sediments (benthos) and are reflected by toxicity testing of *D. magna* and *H. azteca*. Elevated Zn in surface water can lead to competitive exclusion of dietary Ca, causing hypocalcaemia in fish and *D. magna*, which decreases growth, affects organism movement, and decreases filtration rate (Muysen et al., 2006). In extreme cases, mortality is observed. For benthic organisms, such as *H. azteca*, exposure pathways include ingestion of sediment and water or filtration. Ingestion of metals can lead to cellular damage and displacement of dietary Fe and Cu in benthic organisms

causing growth inhibition, reproductive issues, and mortality (Borgmann et al., 1993; Kubitz et al., 1995). Linking Zn-release to these effects can be aided by biochemical toxicology modeling toolkits.

Modeling toolkits are used by toxicologist to predict effects of contaminants on biota and require extensive validation for assessing applicability. In this study, predicted effects of several models will be compared to toxicity test results, including metal screening levels for water (water quality criteria, WQC) and sediment (sediment quality guidelines, SQG's), the biotic ligand model (BLM) for surface water, and the theoretical model for sediment toxicity ((SEM-AVS)/ f_{OC}). WQC and SQG's are single concentration criteria, above which impacts to organisms are likely to occur (Buchman, 2008; USEPA, 2016b). While WQC for metals are often hardness-dependent, SQG's do not change despite varying sediment chemical properties. For surface water, the BLM is preferably used when data on major cation, anion, and water chemistry are available, and predicts effects of divalent metals (Cd, Cu, Ni, Zn) (Borgmann et al., 2004; Santore et al., 2002). Theoretical sediment toxicity can be estimated by measuring simultaneously extracted metal (SEM), acid volatile sulfide (AVS), and organic carbon (Allen et al., 1993, 1991; Campana et al., 2013), where an AVS > SEM is predictive of non-toxic sediments (USEPA, 2005). It is important to test these models as limited validation exists for sediments with fluctuating redox and water content (i.e. non-equilibrium systems).

Due to increasing records of high magnitude drought and flood events, determining the biogeochemical ramifications of Zn-release has never been more important. Further, no experiments have yet been conducted to determine the effects on organisms in high carbonate sediments. The main objective of the present study is to assess environmental risk from Zn-release using test organisms *H. azteca* and *D. magna*. A secondary objective is to test how well

existing ecotoxicological modeling tools, based on assumptions of chemical equilibrium, predict observed results.

3.2 Methods

3.2.1 Site selection & experimental design

Four coastal wetland sites and one reference site were selected for sediment collection. Sites were selected to represent a range of sediment types including variable organic carbon, acid volatile sulfide, Fe-oxide, and sediment metal content (Table 2-1), with hydrological connection to the Great Lakes. These sites included Quanicassee Wildlife Refuge (QC), East Bay Park in Traverse City (EB), Little Black Creek (LBC) in Mona Lake, and Detroit River Wetlands (DRW) in Lake Erie Metropark (Figure 2-1). Criteria for reference site selection included similar sediment pH and texture, but with low metal content. Reference sediments were collected from the Raisin River (RAIS) in Michigan.

Sediments were collected intact with a trenching shovel and placed in experimental laboratory microcosms constructed from polycarbonate containers and equipped with rhizon porewater samplers at 1 and 2 cm depths as shown in the previous chapter (Figure 2-2) (Seeberg-Elverfeldt et al., 2005). Surface water was removed with a fine-mesh syringe and sediment drying occurred over 36-days to emulate drought conditions. Over-head drip irrigation was implemented to re-inundate sediments with excess water discarded into an overflow basin. Input water was refreshed for 4 minutes every 24 hours at a flow rate of $1.55 \pm 0.5 \text{ cm}^3 \text{ s}^{-1}$ (complete surface water renewal after ~72 hours). Chemical composition of input water is described in the results section and is meant to emulate Great Lakes surface water.

3.2.2 Toxicity testing

Surface water toxicity tests were conducted in the first 10-days of inundation via exposure of 3-4 day old *D. magna* (USEPA, 1991). Measured endpoints included survival, growth, reproduction, and metal body concentration. Two replicate exposure bottles were placed vertically in each microcosm with 5 individuals in each (Figure 3-1) (David M. Costello et al., 2015). *D. magna* were fed 0.5mL day⁻¹ per organism a mixture of *Raphidocelis subcapitata* (green algae) (1.0×10^7 algal cells mL⁻¹) and cerophyl. The *D. magna* controls were conducted identically, with the same input water as test microcosms (but without sediment).



Figure 3-1. Organism exposure bottles depicted, where vertical bottles are for surface water exposure of *D. magna* and horizontally placed bottles are for sediment exposure of *H. azteca*.

Sediment toxicity tests with amphipod *H. azteca* were conducted on days 1-7 after inundation, with endpoints survival, growth, and metal body concentration (Borgmann and Norwood, 1995). Two replicate exposure bottles with 10 individuals (7-9 days old) each were placed with a mesh opening laid face down ~0.5 cm deep into sediment. This method directly exposes *H. azteca* to surficial sediments while increasing organism recovery. Additionally, *H.*

azteca were not fed. For *H. azteca*, we used RAIS sediments with an identical setup as the control group.

After the exposure period, organisms were counted, depurated, weighed, and digested. For *D. magna* only, reproduction (R_0) was assessed as neonates produced per adult. A 24-hour depuration in 50 μ M EDTA solution adequately removed undigested gut material so metal content reflects true tissue concentrations (Neumann et al., 1999). Organisms were then desiccated for several days and weighed for growth. Individual growth rate (IGR) was calculated for each exposure bottle as follows:

$$IGR = \frac{\left[\frac{\sum(mass_{org})_{final}}{n_{org}} - \frac{\sum(mass_{org})_{initial}}{n_{org}} \right]}{time}$$

where *mass* is in μ g, *n* is the number of organisms per bottle, and *time* is in days. Body tissue was then digested with trace metal grade HNO_3 and measured on an ICP-MS for Zn (Norwood et al., 2006). Final body concentration (BC_{Zn}) was calculated by subtracting sediment exposed organism tissue concentrations by flume water exposed control organisms (i.e. $BC_{SED} - BC_{CNTL}$). BC_{Zn} does not represent the *true body concentration* but a value corrected for control specimen concentration, which was necessary to remove any added Zn from the algae fed to *D. magna* during the study.

A replicate microcosm “mini-experiment” was conducted in November 2015 (with a variety of sediments collected from the LBC site) to further assess the relationship between porewater Zn and *H. azteca* growth rates. The only contrasting parameter between this experiment and the original design was the drying time (29 days). Survival, growth, and BC_{Zn} of *H. azteca* were all calculated as described previously.

3.2.3 Analytical chemistry

Analyses included several physicochemical parameters for surface water, porewater, and sediments. Surface water (and input water) was monitored for dissolved metal content (Ca, Fe, Mg, Mn, Zn), dissolved oxygen (DO), and pH on days 1, 4, 6, 8, and 11 after inundation. Porewater was extracted on the same time sequence, and analyzed for DO, pH, Fe^{2+} , dissolved organic carbon (DOC), and several metals (Ca, Cu, Fe, Mg, Mn, Ni, Zn). All water was extracted with a nitrogen-purged syringe. For metals, water was filtered through 0.45 μm (surface water - Millipore) or 0.19 μm (porewater – Rhizon samplers) filters, acidified to 2% with nitric acid and analyzed on an ICP-OES for metals (Ca, Cr, Cu, Fe, Mg, Mn, Ni, and Zn). Porewater DO, pH, and Fe^{2+} were measured immediately after sample extraction to prevent oxidation (Viollier et al., 2000). Porewater dissolved organic carbon was analyzed after acidification (with 6M HCl to a pH of 2) on an OI Analytical Aurora 1030 TOC analyzer.

Sediment analyses included Fe/Mn-oxide content, simultaneously extracted metals (SEM), acid volatile sulfide (AVS), organic carbon content (f_{OC}), and water content. Single 2.6-cm diameter sediment cores were collected from each microcosm on days 0, 1, and 11 (after inundation) and carefully sectioned into 1.5 cm increments in a nitrogen purged bag. Fe/Mn amorphous and crystalline oxides and the respective bound-Zn fraction were estimated by ascorbate and dithionite extractions (Kostka and Luther, 1994). (SEM-AVS)/ f_{OC} was conducted using previously established methods (Allen et al., 1991). Loss-on-ignition (LOI) was used to determine f_{OC} by combusting dry sediment at 450°C for 6 hours. Water content was determined by drying sediment for 48 hours at 100°C.

Diffusive gradients in thin films (DGT's) were used to further assess Zn bioavailability in sediments and surface water. Commercially available sediment probes for metals (model C-

LSPM, DGT Research, Lancaster, UK) were inserted in duplicate to each sediment type on day-5 after inundation for ~24 hours. For 24 hours prior to deployment, the DGTs were soaked in deoxygenated 0.01 M NaCl (Zhang et al., 1995). Exact sediment deployment and retrieval times were recorded. Upon removal, DGT's were rinsed with Milli-Q water and immediately sectioned with a Teflon coated razor from 0-2 cm above the surface water interface (SWI) and at 1 cm increments in sediment (down to 3 cm). Extracted resins were eluted in trace metal grade 1 M HNO₃ and Zn was measured on by inductively coupled plasma mass spectrometry (ICP-MS). Final Zn concentrations (C_{DGT} as ng cm⁻³) in the DGT gel were calculated according to previously established methods (Costello et al., 2012). A corresponding blank DGT, exposed to Milli-Q only, was used to correct final C_{DGT} values.

The biotic ligand model (BLM, Ver 3.1.2.37, Windward Environmental, LLC) was used to predict surface water toxicity by calculating chronic-HC5s for *Ceriodaphnia dubia*. Input data is provided in Appendix B, [Table B-1](#). Alkalinity was calculated using a pCO₂ of 3.5 assuming an open system. Assumptions included sulfide concentrations ranging from 0.001 mgL⁻¹ on day-1 to 0.002 mgL⁻¹ on day-11 (to reflect increases in measured AVS) and a humic acid content of 10% (of total organic matter in water). Unmeasured elements (Na, K, SO₄, and Cl) were estimated with reference to the USEPA *Missing Water Quality Parameters Technical Support Document* (USEPA, 2016c).

3.2.4 Statistics

All statistical analyses were conducted in RStudio Version 0.98.1102. For significance testing, the Shapiro test for normality was first used to determine if data was normal or skewed. For nonparametric variables, Kruskal-Wallis tests were used for multiple variable comparisons and the median or sign test was used for paired analysis. Posthoc Kruskal-Nemenyi tests (R

package PMCMR) were used if further significance testing between sediment types or days was needed. Any ties present in data were broken assuming averages. For normally distributed variables, the equivalent ANOVA and paired t-tests were used with posthoc Tukey tests. For determining correlations, Pearson was used when all assumptions were met (normality, linearity, homoscedasticity) and otherwise rank-type correlations such as Spearman or Kendall tests were used.

Principle components analysis (PCA) was used to compare differences between the four sediment types on day-1 of inundation. Variables which were significantly correlated ($p < 0.05$) with porewater Zn concentrations were log transformed and applied to the PCA. Standard deviations for each principle component were calculated (PC1 = 1.8; PC2 = 0.9) accounting for 81.4% of variance. The figure was plotted using the ggbiplot package.

3.3 Results

3.3.1 Physicochemical water and sediment characterization

Surface water chemistry was monitored for DO and temperature on days 3, 5, and 9 after inundation. DO never fell below 5 mgL^{-1} with an average of $5.77 \pm 0.12 \text{ mgL}^{-1}$ and temperature ranged from $17.8\text{-}19.2^\circ\text{C}$ (average = $18.4 \pm 0.1^\circ\text{C}$). Surface water pH was 7.1 ± 0.06 units measured on days 1 and 11. Input water chemistry was monitored similarly, with the following chemical composition: $7.5 \pm 0.1 \text{ mgL}^{-1} \text{ O}_2$, $7.6 \pm 0.02 \text{ pH}$, hardness $57.3 \text{ mgL}^{-1} \text{ CaCO}_3$.

Redox indicators showed oxidized sediments on day-1 which became reduced with inundation. Fe^{2+} was the most responsive redox indicator for porewater, starting at concentrations of $0 \text{ mgL}^{-1} \text{ Fe}^{2+}$ and increasing for all sites ($p < 0.00001$). Fe^{2+} increased to a greater extent for LBC than EB ($p < 0.005$), while QC and DRW were intermediate (Figure 3-2). Porewater dissolved oxygen (DO) was low throughout the experiment with high variability on

day-1, likely due to sediment/microbial heterogeneity, converging by day-11 (Figure 3-2). Sediment/porewater pH did not change for any site ($p > 0.7$); however, EB and QC were more stable (well buffered) with slight increases in pH by day-11, whereas DRW and LBC pH's slightly decreased with reduction. Average pH for each sediment type is listed in Table 2-1.

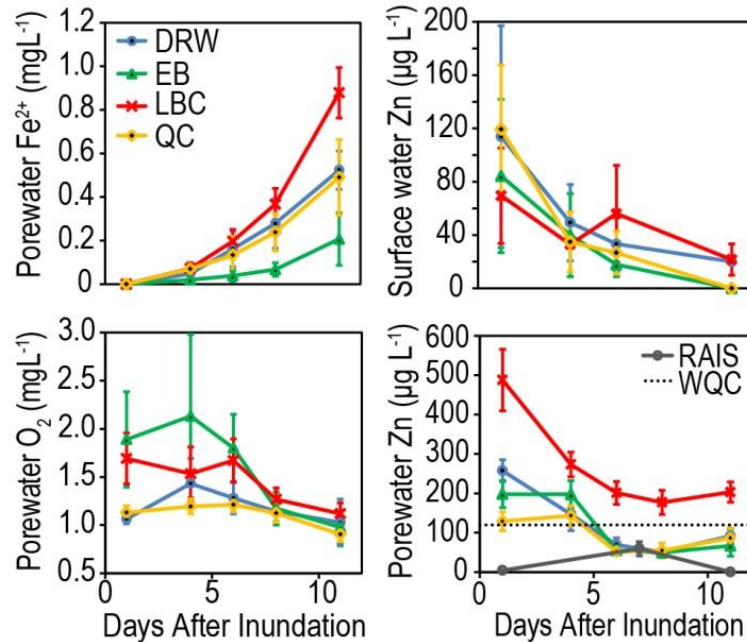


Figure 3-2. Porewater dissolved Fe²⁺, dissolved oxygen, and surface and porewater dissolved Zn (\pm standard error, SE) changed with time after inundation. All four non-control sediment types exceeded USEPA thresholds for aquatic toxicity (WQC) on days 1 and 3, but only LBC remained above this threshold through day-11.

3.3.2 Surface water chemistry and toxicology to *D. magna*

Surface water Zn did not exceed hardness corrected WQC at any time throughout the experiment (Table B-2). Zn concentrations were highest on day-1 and decreased significantly by day-11 ($p < 0.01$) (Figure 3-2). When Zn data were incorporated into the BLM for *Ceriodaphnia dubia*, all toxicity units (TU) were less than one, which suggests toxicological effects are improbable (Table B-3). Surface water C_{DGT} only exceeded the blank concentration (C_{DGT} blank = 7.7 ng-Zn cm⁻³) for DRW and LBC, with 0.5 ng-Zn cm⁻³ and 6.2 \pm 0.6 ng-Zn cm⁻³,

respectively. LBC had the highest concentration, which suggests increased Zn exposure to *D. magna* in LBC surface water.

No lethal or sublethal effects to *D. magna* were observed as compared to the control ($p > 0.1$). Average survival was $95.4 \pm 2.4\%$, IGR was $17.8 \pm 1.7 \mu\text{gday}^{-1}$, and R_0 was 2.6 ± 0.6 neonates per adult. These data are summarized in [Figure 3-3](#). The limited effect on these measured endpoints was not surprising given that Zn did not exceed thresholds predicted by the BLM or hardness corrected WQC. Though IGR did appear higher for the non-sediment control than sediment reference, it was not statistically significant ($p > 0.13$). Similarly, BC_{Zn} was higher for sediment exposed *D. magna* than the control ($p > 0.2$), with a range of 10.7 to 196.3 $\mu\text{g-Zn gdw}^{-1}$, though not statistically significant. In this case, the BLM and hardness-corrected WQC effectively predicted no effects.

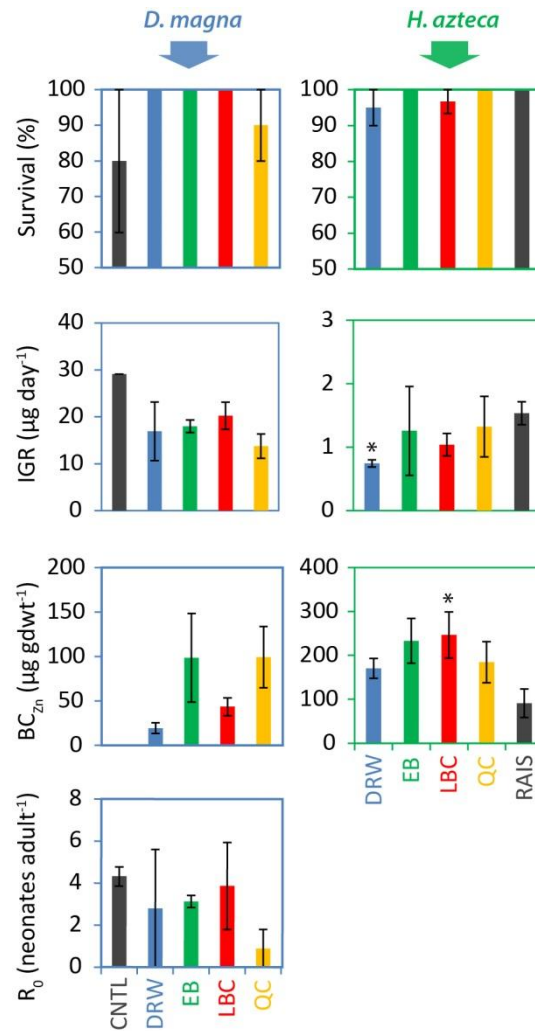


Figure 3-3. Toxicological endpoints for *D. magna* and *H. azteca*, including survival, reproduction (R_0), individual growth rate (IGR), and body concentration Zn (BC_{Zn}) (\pm SE) for sediment treatments.

3.3.3 Porewater and sediment chemistry during Zn-release

Of the several metals measured, Zn was most susceptible to oxidative release, with concentrations exceeding WQC for all sediment types (Figure 3-2). Porewater Zn in LBC was highest ($p < 0.001$), and decreased in concentration for all sediment types throughout the experiment ($p < 0.0001$). Zn exceeded WQC for LBC on all days and on days 1 and 3 for the other three sediment types. Porewater Zn in the reference sediment (RAIS) remained low

throughout the study. The other metals measured did not exceed WQC with ranges of 0-0.45 $\mu\text{g-Cu L}^{-1}$, 0-0.9 $\mu\text{g-Ni L}^{-1}$, 0-3.4 mg-Fe L^{-1} , and 0-4.2 mg-Mn L^{-1} (Table B-4).

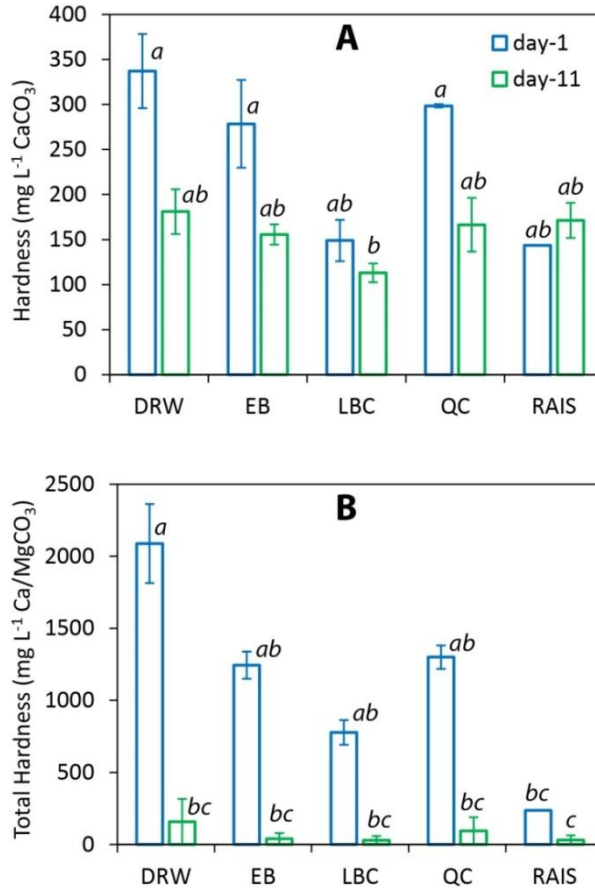


Figure 3-4. Porewater hardness (\pm SE) as CaCO_3 and total hardness shown for days 1 and 11 per each sediment type. Large decreases in hardness were observed for all sediment types with inundation.

Of the measured sediment binding ligands, $(\text{SEM-AVS})/f_{\text{OC}}$ values did not change over the 11-day study period; however, sites had statistically different values (Table 2-1). The differences between sites were influenced by AVS content moreso than organic content. Carbonate content as a function of porewater hardness was highest on day-1 and decreased significantly by day-11 ($p < 0.01$), which may have important implications for metal

bioavailability (Figure 3-4). For example, the release of Ca and Mg ions into porewater may increase cation competition for organism binding sites, potentially decreasing bioavailability.

Fe and Mn-oxyhydroxide content remained relatively stable in sediments between oxidized and reduced phases (Table 3-1). Since Fe and Mn concentrations were an order of magnitude higher in DRW and LBC sediments than EB and QC, the sediment types were analyzed separately. Total Fe/Mn-oxyhydroxide content decreased for low Fe sites ($p < 0.05$), as expected with sediment reduction. Some of the Zn released into porewater may have been due to the low amorphous Fe/Mn-oxyhydroxide bound Zn content on day-0, which increased with reduction for DRW and LBC ($p < 0.05$). Typically thought to form with oxidation (not reduction), it is possible dissolution of amorphous Fe/Mn-oxyhydroxides upon inundation may have lead to the counter-intuitive result. Further, since sediments were heterogeneous with complex mottling, it is possible additional replication may have been needed to account for high variability. The decrease of amorphous Fe/Mn-oxyhydroxide bound Zn may further help explain why the Zn-release was less apparent in EB and QC sediments.

Table 3-1. Fe/Mn-oxyhydroxide content (\pm SE) in sediments prior to inundation (day-0) and after 11-days of inundation, with bound estimates for Zn.

Sediment Type	Day	Total Metal-Oxyhydroxides			Amorphous Metal-Oxyhydroxides		
		(mg gdw ⁻¹)			(mg gdw ⁻¹)		
		Fe	Mn	Zn	Fe	Mn	Zn
High Fe	0	14.54 ± 2.12	0.23 ± 0.04	0.20 ± 0.03	4.98 ± 0.47	0.11 ± 0.02	0.05 ± 0.01
High Fe	11	12.01 ± 1.14	0.26 ± 0.04	0.17 ± 0.04	5.60 ± 0.81	0.16 ± 0.02	0.10* ± 0.02
Low Fe	0	3.06 ± 0.42	0.09 ± 0.01	0.02 ± 0.01	0.73 ± 0.15	0.04 ± 0.01	0.01 ± 0.01
Low Fe	11	1.6** ± 0.26	0.04* ± 0.01	0.02 ± 0.01	0.32 ± 0.12	0.02 ± 0.01	0.01 ± 0.00

*significant increase (green) or decrease (red) between days for sediment type, where: * $p < 0.05$, ** $p < 0.01$, *** $p < 0.001$

To assess the role of different binding fractions on Zn-release, multivariate analyses showed strong correlations between porewater Zn and AVS ($cc = 0.72, p < 0.01$), total Fe-oxides ($cc = 0.68, p < 0.01$), the change in porewater Fe^{2+} between days 1 and 11 ($cc = 0.66, p < 0.03$), and porewater hardness ($cc = -0.68, p < 0.02$). One additional note of importance is that organic carbon content of the sediment was not correlated with Zn-bioavailability ($p > 0.2$), which suggests it is not strongly influenced by changes to sediment redox or water content.

Bioavailable sediment Zn as predicted by DGT, show the highest exposure of *H. azteca* in LBC sediments. Of the three sediment depths measured, there was no difference in concentration between shallow, intermediate, and deep sediments ($p > 0.2$). The 5-day inundation was likely insufficient time to form an oxidized surface and reduced subsurface layer. Overall, LBC had higher C_{DGT} than EB ($p < 0.001$), though was statistically similar to DRW and QC. Average C_{DGT} for LBC was $49.9 \pm 6.8 \text{ ng-Zn cm}^{-3}$, and for all sites ranged from 6.9 – 74.7 ng-Zn cm^{-3} . A summary of these data are provided in Appendix B, [Table B-5](#).

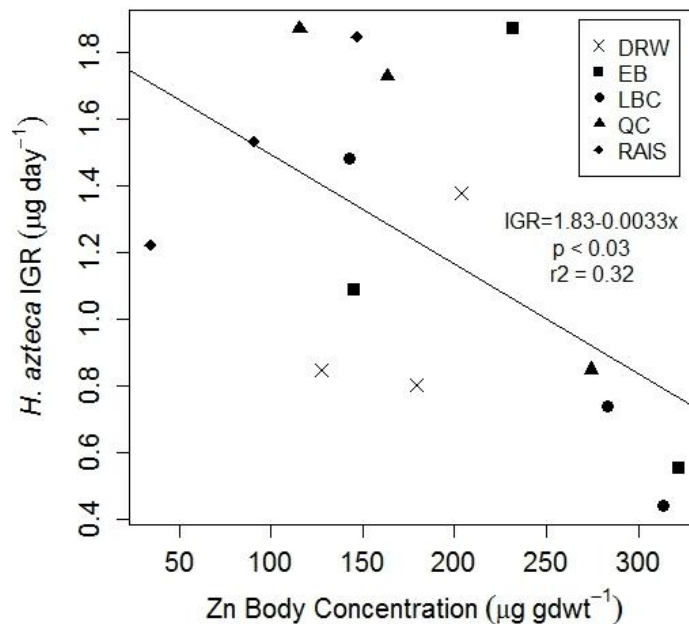


Figure 3-5. *H. azteca* IGR is negatively correlated with BC_{Zn} for all sites ($p < 0.03$) and especially for LBC and QC only ($p < 0.001$).

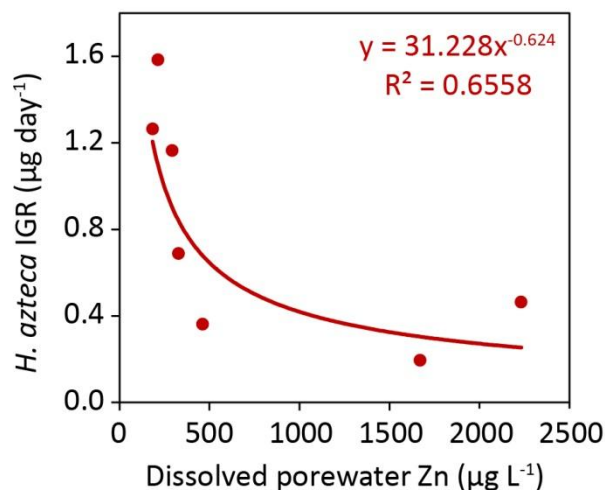


Figure 3-6. Relationship between dissolved porewater Zn for sites with elevated $>120 \mu\text{g L}^{-1}$ concentrations and *H. azteca* individual growth rates (IGR).

3.3.4 Toxicological effects to *H. azteca*

Only sub-lethal effects to *H. azteca* were observed for select sediment types. No difference in survival between reference and contaminated sediments were observed, with survival never falling below 85% (Figure 3-3). IGR was lower for *H. azteca* in DRW sediments as compared to RAIS (reference) ($p < 0.03$). BC_{Zn} was higher in contaminated sediments as compared to reference, though this was only significant for LBC ($p < 0.03$). A weak negative correlation between *H. azteca* BC_{Zn} and IGR was observed (Figure 3-5) ($p < 0.03$). This correlation was strongest for LBC and QC sediments ($p < 0.001$). Additional data collected showed a strong negative correlation between *H. azteca* IGR and porewater Zn when in exceedance of the WQC ($>120 \mu\text{g-Zn L}^{-1}$) ($p < 0.03$) (Figure 3-6). This indicates that BC_{Zn} or porewater Zn may be appropriate indicators to predict effects to growth. Although correlation does not explicitly imply causation, this is strong evidence that Zn-release affects IGR.

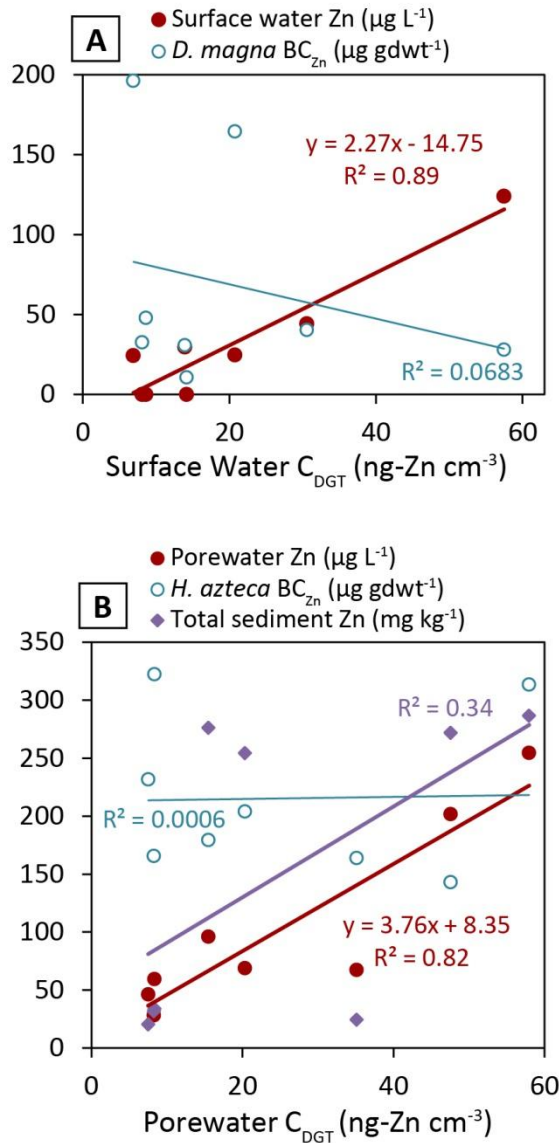


Figure 3-7. DGT concentrations of Zn are correlated with three factors for (A) sediment/porewater, including porewater Zn, *H. azteca* BC_{Zn} , and total sediment Zn, and two factors for (B) surface water exposures, including surface water Zn and *D. magna* BC_{Zn} .

DGT data were reflective of Zn concentrations, but were not predictive of biological endpoints (survival, IGR, R_0 , BC_{Zn}). A strong positive correlation between dissolved surface water Zn and $\text{C}_{\text{DGT}}\text{-Zn}$ (0-2 cm above surface water) was observed ($cc= 2.27$, $p < 0.001$) (Figure 3-7a). $\text{C}_{\text{DGT}}\text{-Zn}$ measured for surface and porewater showed no relationship with BC_{Zn} , survival, IGR, or R_0 for either *D. magna* or *H. azteca*, respectively. Porewater Zn (on day-6) was also

strongly correlated with $C_{\text{DGT-Zn}}$ (sediment exposed) as shown in [Figure 3-7b](#), which suggests DGT's were a useful chemical tool but were not appropriate indicators for biological uptake. It is possible at elevated porewater Zn-concentrations ($>120 \mu\text{g L}^{-1}$), when multiple exposure pathways show elevated Zn, C_{DGT} may be more predictive of IGR or BC_{Zn} . Unfortunately, the supplemental experiment (data shown in [Figure 3](#)) did not implement DGT testing..

3.4 Discussion

3.4.1 Field applicability

As an experimental laboratory study, some thought should be given to the applicability of these findings to field settings. Several controlled variables, such as prohibiting plant growth, static input water composition, and uniform flow rates, are not realistic for natural systems (Atkinson et al., 2007; Gambrell et al., 1991; Jacob and Otte, 2003; Korfali and Davies, 2004). Surface water renewal occurred over approximately 3-days, with similar retention times as slow flowing wetlands (DRW, QC, LBC), but not high energy sites (EB). For Zn-release to be observed in natural wetlands, sediment drying would have to lead to oxidation of the top 1-2 cm, which would likely only occur in systems with a lowered water table (in addition to drought conditions). These conditions imply that Zn-release may be relatively rare, only occurring extensively after severe drought, though further field validation is needed. After recognizing these important differences, the findings of this paper can be broadly applied to freshwater aquatic systems.

3.4.2 Ecotoxicology of redox-sensitive systems

While surface water organisms, such as *D. magna*, were not significantly affected by Zn-release, benthic organisms (i.e. *H. azteca*) may have increased environmental risk. Since the *H.*

azteca IGR was strongly correlated with porewater Zn, it is likely that the impacts to amphipod growth are related to exposure to sediment porewater. Surface water exposures alone pose little risk, especially when concentrations of Zn remain low. It is possible that other factors may have obscured effects of Zn to *D. magna* (such as turbidity), which is discussed at length in the SI, Discussion. Among benthic organisms, some of those exposed to sediment porewater and sensitive to Zn include chironomids, Ephemeroptera, and some crustaceans (including amphipods) (Brinkman and Johnston, 2008; Clernents et al., 1992). Further tests should be conducted to determine if similar effects occur to other benthic species.

It is possible that other factors may have obscured effects of Zn to *D. magna* (such as turbidity). *D. magna* IGR and R_0 were low compared to previous studies, while BC_{Zn} are slightly higher. A previous study, with similar exposures times but different sediment types, resulted in 2x the IGR and R_0 values reported in this study (unpublished data). Unsurprisingly, the range of BC_{Zn} is likewise much higher (~4x). Measured IGR, R_0 , and BC_{Zn} may have been affected by deployment and retrieval of DGTs as increased turbidity is known to affect *D. magna*, leading to decreased reproduction rates, feeding rates, and motility (Bash et al., 2001; Blankson and Klerks, 2016; Chen et al., 2012). Further, the non-sediment control had greater IGR and lower BC_{Zn} than the sediment (reference RAIS) control. The effect of increased turbidity may have obscured any effects of Zn-release on organism health, which in addition to previous reports that Zn decreases reproduction, is evidence that further tests need conducted (De Schampelaere et al., 2004a; Paulauskis and Winner, 1988).

IGR and BC_{Zn} for *H. azteca* were mostly within predicted ranges as compared to previous exposure scenarios. IGR ranged on the lower end of reported values, with the highest tissue concentrations around 1.9 versus reported maximum of $9.2 \mu\text{gday}^{-1}$ (unpublished data). Reported

BC_{Zn} ranges from about 59-180 $\mu\text{g}\text{gdwt}^{-1}$ for *H. azteca* exposed to approximately 200-500 $\mu\text{g}\text{L}^{-1}$ Zn in surface water (Borgmann et al., 1993). The range reported in this study (66 to 383 $\mu\text{g}\text{gdwt}^{-1}$) extends above this range; however, it is likely due to the diverse exposure pathways (ingestion, inhalation, and dermal exposures) inherent with sediment toxicity testing.

While this experiment largely focused on replicating the ecotoxicology of mudflats or riverbanks, similar processes are likely to occur in other redox sensitive aquatic systems, where elongated exposure is more likely to occur. Resuspension of sediments in deltas and lakes has been shown to cause oxidation of ZnS, leading to toxicity (Simpson et al., 2000). In cases where ZnS oxidation occurs throughout an aquatic system (and not just along the shoreline), organism exposure to elevated Zn is unavoidable. Where Zn-release is spatially confined to the edges of a lake/wetland/river, benthic organisms may be more able to avoid unsuitable conditions. In summary, this research is useful to understanding the effects of redox on organism exposures to Zn in a variety of aquatic systems.

3.4.3 Applicability and effectiveness of predictive toxicology toolkits

Generally speaking, in non-equilibrium systems the BLM should be a more effective predictor of surface water toxicity than the hardness corrected WQC as it is responsive to redox sensitive ions which may affect organism exposure/uptake (Santore et al., 2001). In the present study, we found both methods to be accurate in predicting “no effect” to the test species *D. magna*. For all contaminated sediments, the chronic toxicity units (TU) were higher on day-1 than day-11 after inundation, though never exceeding one. This suggests inundation of oxidized sediment increased the theoretical risk to organisms.

Predictors of sediment toxicity were generally overprotective (i.e. more conservative than necessary to protect aquatic life), except for the theoretical predictor (SEM-AVS)/ f_{OC} . Sites

DRW and LBC both exceeded threshold effects concentrations (TECs) while only DRW showed significant sublethal effects on IGR. The hardness corrected WQC for porewater were overprotective for EB and QC, with toxicity predicted on days 1-3 where no effects were observed. The WQC were likely overprotective as they did not account for increased porewater Mg^{2+} (and possibly Fe/Mn^{2+}), which functions as a competitive ion to Zn. Conversely, the strong positive correlation observed between porewater Zn and BC_{Zn} suggests that in some cases and for some sediment types, porewater WQC may be predictive of organism exposure and effects.

(SEM-AVS)/ f_{OC} values were generally low ($<35 \mu\text{mol gdw}^{-1}$) compared to reported toxicity thresholds for Zn $\sim 500 \mu\text{mol gdw}^{-1}$ (Burton et al., 2005). According to the USEPA recommended SEM-AVS model, these sediments would be considered “not toxic” (USEPA, 2005). Since sublethal effects were observed for DRW sediments, this model is therefore underprotective. It is not clear the SEM-AVS model is effective for systems with variable hydrology or where Fe/Mn-oxyhydroxides are predominant (Campana et al., 2013). Previous studies have reported similar findings (Brown, 2000; Simpson et al., 2012), and it is clear new modeling techniques, such as the recently developed sediment-BLM (Di Toro et al., 2005), are needed to address the impacts redox variability in contaminated aquatic sediments. A discussion of variables important for inclusion in future models is provided (next section).

While in this study DGT's were only predictive of metal bioavailability, others have argued they predict bioaccumulation (or body concentration). In Simpson et al. (2012), C_{DGT-Cu} and bivalve tissue Cu show a strong, positive correlation. Other bivalve studies have confirmed a similar effect for Zn and Pb (Amato et al., 2016, 2015) and for other organisms *Chironomus riparius* and *Saccostrea glomerata* for Cu and Pb (but not Cd) (Jordan et al., 2008; Roulier et al., 2008). Conversely, some studies have shown C_{DGT} to be reflective of metal bioavailability and

not bioaccumulation (Costello et al., 2012; Schintu et al., 2008). The most logical explanation for this discrepancy is that exposure is relevant in determining the effectiveness of DGTs in predicting organism bioaccumulation. In this example, the bivalve DGT studies focused predominately on surface water characterization through water uptake/filtration (not ingestion) (Simpson et al., 2012); however, for *D. magna* and *H. azteca* Zn bioaccumulation is often thought to occur through to ingestion/feeding (De Schamphelaere et al., 2004a). DGT's will not always reflect organism tissue since it does not assess various exposure pathways or diverse life histories of the organisms involved.

3.4.4 Chemical mechanisms of Zn-release

In this section, important variables to include in future predictive toxicology models and their relation to Zn-release are discussed. Of the variables correlated with porewater Zn-release, each represents different processes responsible for Zn bioavailability, where: AVS, oxidation of ZnS; total Fe-oxides, release of Zn from Fe-oxyhydroxides; and hardness, common ion effect where Ca^{2+} decreases Zn^{2+} solubility and/or improved buffering preventing Zn-release. The change in porewater Fe^{2+} could represent several important sediment characteristics, such as (1) the total Fe content in sediment, (2) microbial activity, as microbes are primarily responsible for Fe reduction, and (3) increased Zn displacement of FeS (forming $\text{ZnS} + \text{Fe}^{2+}$) during reduction.

These modes of Zn-release are (mostly) similar to those described in the previous chapter, with a few exceptions. In the previous chapter, oxidation of ZnS, dissolution of ZnHCO_3^+ , and (to a smaller extent) dissolution of amorphous Zn-Fe-oxyhydroxides were associated with Zn-release (Nedrich and Burton, 2017). A slow increase in pH occurred over 32-days of reduction in LBC and DRW, which was attributed to decreased Zn-bioavailability. We are able to reaffirm oxidation of ZnS and dissolution of Zn-Fe-oxyhydroxides was tied to Zn-

release; however, while Zn-bicarbonates do likely dissolve, cation competition actually seems to counteract release and effects of Zn. Moreover, the pH increase observed after 32-days was not observed after 11-days of inundation and therefore cannot be the explanation for decreasing Zn-bioavailability with reduction. The source of these inconsistencies may be the temporal data gap in the first study, which only measured these characteristics on days 1 and 32 after inundation.

PCA was used to conceptualize the importance of four different characteristics for each sediment type (Figure 3-8). Two components account for 81.4% of the variability and showed QC and EB more influenced by hardness while LBC and DRW are more influenced by sulfide and iron biogeochemistry. Since LBC is more influenced by AVS and Fe-oxyhydroxides, this may explain the longer period of Zn-elevation than other sediments. Formation of metal sulfides is a kinetically slow process (Douglas and Beveridge, 1998; Jensen et al., 2003), which is predominately controlled by microbial reduction. Further, in the completely oxidized and desiccated drought sediments, microbial function would be slow to regenerate (Zajic, 1969). For the hardness controlled sites (QC, EB), Zn-release recovery was rapid. These trends are also likely tied to the total Zn concentration being lower in QC/EB as coarser sediments adsorb less metal to particle surfaces. This suggests lacustrine sandy sediments are less susceptible to Zn-release than more mineral-rich and riverine influenced coastal sediment types.

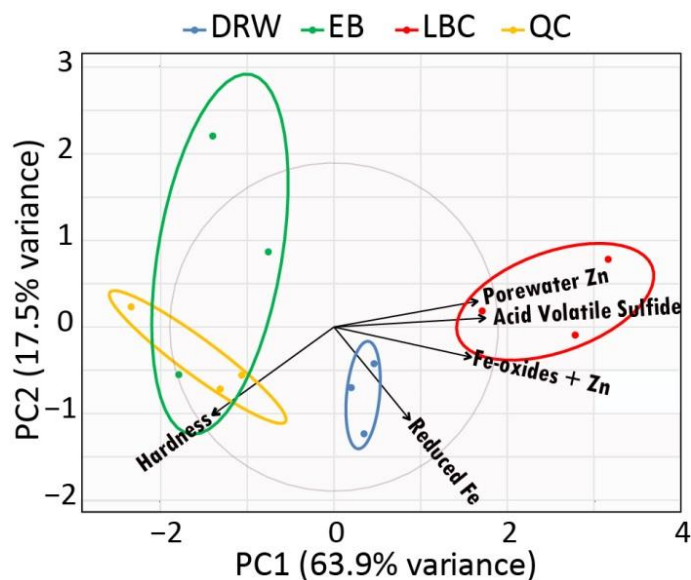


Figure 3-8. Principal components analysis for several variables which correlated with porewater Zn on day-1, including acid volatile sulfide concentration, total Zn bound to Fe-oxides, the change in reduced iron between day 1 and 11, and hardness.

It is clear that high carbonate sediments, while displaying the positive effects of increased buffering capacity for some sediment types, are still subject to Zn-release under specific conditions. Some of these conditions include a long duration (>20 days) of sediment drying/oxidation, moderate to high concentrations of total sediment Zn (>150 mgkg⁻¹), and a predominance of Fe and S as Zn-ligands. Sediment toxicology models should include these important variables. Future chemical work should aim to further assess the role of carbonates, particulate organic carbon, and microbial mediation/activity on Zn-release.

3.4.5 Implications for environmental decision makers

These findings have important implications for the risk assessment and management of aquatic systems. Site-specific hydrology and redox variability are not included in standard sediment toxicity tests conducted by the USEPA (USEPA, 2005). While environmental risk assessment using a weight-of-evidence approach does recommend considerations of site specific context dependencies (such as hydrology), data linking physicochemical variability to

toxicological endpoints in sediments are lacking (USEPA, 1998). These considerations are further complicated by climate change, which has already changed hydrologic patterns on a regional scale, including the magnitude and duration of drought, high flow and flooding events (Milly et al., 2005).

In managed aquatic systems where water level can be manipulated, improvement to water quality may be possible by applying biogeochemical principles. For example, when water levels in created/restored wetlands are maintained with water control structures. If the wetland was oligotrophic in nature, where Zn is limiting, re-flooding could be timed with biologically important periods (reproduction for invertebrates, growing season for plants, etc.) to improve nutrient availability and thus biological productivity. Or in a managed reservoir with high levels of Zn contamination, toxic metal exceedances in the surface water may be avoided by ensuring re-flooding (after a drawdown) occurs when surface sediments (of mudflat) are not oxidized or desiccated, for instance after significant precipitation (sediment saturation) or groundwater upwelling (anoxic input water). Thinking in terms of sediment biogeochemical processes can help avoid metal releases, potentially lowering water treatment costs and protecting biological integrity of the reservoir.

In cases where hydrology cannot be artificially manipulated, simple knowledge of Zn-release may be helpful in monitoring and prioritizing conservation and restoration efforts. For instance, when data is collected for environmental regulatory purposes (i.e. contaminant exceedances, chemical mitigation requirements, etc.) it may be most informative to collect and measure water during extreme climatic events (i.e. after a long drought, during times of extreme flooding). Targeted sampling can help identify the effect of hydrological variability on aquatic systems and inform management decisions. It is likely that the observed Zn-release induced by

sediment re-flooding after drought conditions will be most prominent in semi-arid regions, where groundwater tables drop significantly during the dry season leading to sediment oxidation and desiccation. While this article has focused on just one aspect of altered biogeochemistry associated with hydrological variability, it is important to maintain a broad ecological perspective to determine the best environmental management strategies.

3.5 Conclusion

Climate induced alteration of water regimes lead to biogeochemical variability, and in high carbonate systems, Zn-release is an environmental concern. As a predominately sediment driven chemical phenomenon, Zn-release is most likely to impact benthic communities. Better predictive toxicology tools are needed to address aquatic systems with hydrological variability and to be more reflective of biogeochemical disequilibrium. With biogeochemical knowledge, aquatic systems monitoring and management can be optimized.

Chapter 4 – Biogeochemical controls on the speciation and aquatic toxicity of vanadium and other metals in sediments from a river reservoir

ABSTRACT

Effects of hydrologic variability on reservoir biogeochemistry are relatively unknown, particularly for less studied metals like vanadium (V). Further, few studies have investigated the fate and effects of sediment-associated V to aquatic organisms in hydrologically variable systems. Our primary objective was to assess effects of hydrologic manipulation on speciation and toxicity of V (range: 635 to 1620 mg kg⁻¹) and other metals to *Hyalella azteca* and *Daphnia magna*. Sediments were collected from a reservoir located in a former mining area and microcosm experiments were conducted to emulate 7-day drying and inundation periods. Despite high sediment concentrations, V bioavailability remained low with no significant effects to organism survival, growth, or reproduction. The lack of V toxicity was attributed to reduced speciation (III, IV), non-labile complexation, and sorption to Al/Fe/Mn-oxyhydroxides. Zinc (Zn) increased in surface and porewater with inundation, for some sediments exceeding the U.S. EPA threshold for chronic toxicity. While no effects of Zn to organism survival or growth were observed, Zn body concentrations (BC_{Zn}) were negatively correlated with *H. azteca* growth. Results from this study indicate that V bioavailability and environmental risk is dependent on V-speciation, and V is less influenced by hydrologic variability than more labile metals such as Zn.

4.1 Introduction

Human alteration of natural aquatic ecosystems using water control structures often have collateral effects to surrounding habitats. Beneficial ecosystem services can be impacted, such as fisheries health, water quality, carbon sequestration, and stream bank stabilization (Jager and Smith, 2008; Richter et al., 2003). Hydrologic variability caused by reservoir management may lead to a redistribution of sediment and altered biogeochemical cycling at the sediment-water interface (SWI) (Carvalho et al., 1998; Ney, 1996; Skalak et al., 2016). This is particularly true for the geochemistry of redox sensitive transition metals with multiple oxidation such as vanadium (V) (De Jonge et al., 2012a).

Published studies on V ecotoxicology are limited, and consist mostly in presenting sources and surface water toxicity of V (Canada, 2010; Irwin et al., 1997; Nriagu, 1998). Vanadium is toxic to organisms at elevated concentrations due to phosphate mimicry in the V(V)-oxidation phase, leading to inhibition of various phosphohydrolases and enzymes (Chasteen, 1983). *Hyalella azteca* and *Daphnia magna* have a lethal concentration (LC₅₀) of 400 µg L⁻¹ and effects concentration (EC₁₀) of 1000 µg L⁻¹, respectively, for surface water (Canada, 2010). Recently, a new species sensitivity distribution (SSD) derived LC₅₀ of 0.64 mgL⁻¹ and HC5 of 0.05 mgL⁻¹ has been reported for midges in surface water (Schiffer and Liber, 2015). No similar values have been published for porewater or sediment. Release into the environment can occur from mine drainage, as combustion byproducts (fossil fuels, paper mills, smelting), and as a common impurity in fertilizers, with V production increasing at approximately 9% annually (Irwin et al., 1997; Perles, 2012).

Vanadium is chemically complex, influenced by a trifecta of pH, redox, and coordination chemistry. Upon introduction into the aquatic environment, V can be present in three oxidation

states. In surface and oxygenated porewater oxo- and oxyhydroxide-V compounds are the most abundant and biologically available. Some examples include (1) vanadates, $\text{H}_3\text{V(V)O}_4$, $\text{H}_2\text{V(V)O}_4^-$, HV(V)O_4^{2-} , and V(V)O_4^{3-} ; (2) oxyhydroxides, $\text{V(V)O}_2(\text{OH})_2^-$, V(IV)OOH^+ ; and vanadyl, V(IV)O^{+2} . Of these, vanadate is thought to be the most toxic and most labile species, particularly in alkaline and oxic waters due to its anionic nature. Vanadyl can also be toxic to organisms when dissolved, although lower oxidation states (V(IV), V(III)) are mostly found in sediment phases, they may be rapidly transformed to aqueous vanadate via hydrolysis or oxidation (Irwin et al., 1997). Previous studies focus on V toxicity in surface water, with relatively little focus on sediment toxicity, sediment-water interactions, or V speciation at the SWI.

Porewater V bioavailability to aquatic organisms is partially controlled by the proportion of non-labile to labile forms (i.e. Fe/Mn oxyhydroxides, sulfide, and organic matter) present in sediments (Canada, 2010). Selective extractions show the largest fraction of total V in sediments is typically non-labile, being associated with one of several mineral forms, accounting for 50-95% of total V (Abollino et al., 2006; Terzano et al., 2007b). The largest labile fraction of total V is often adsorbed on the surface of Al/Fe/Mn oxyhydroxides (2-40%) (Harita et al., 2005; Larsson et al., 2013; Mikkonen and Tummavuori, 1994; Terzano et al., 2007b). Although vanadyl sulfides and sulfates represent a minor V-fraction in most sediments (<1%), they can form in reducing conditions or through biological uptake (Wanty and Goldhaber, 1992). The fraction of V bound to organic matter is thought to be low (<10%) in most sediments as predominately reduced V(III) or V(IV) (Abollino et al., 2006). Bacteria and meso/thermophilic methanogens can also mediate reduction of vanadate (Carpentier et al., 2003; Ortiz-Bernad et al., 2004; Zhang

et al., 2014). Investigating the biogeochemistry of these V-phases is important to this study, as they are likely to influence V bioavailability.

While V-speciation and toxicity was the main focus of this study, it is important to consider the effects of co-occurring metals. At many sites metals are co-occurring and can vary in their relative bioavailability. Total chromium (Cr), nickel (Ni), and zinc (Zn) concentrations in sediments exceeded their respective probable effects concentrations (PEC) (Buchman, 2008). Dissolved Ni, and Zn species are primarily toxic to organisms as divalent cations and Cr(VI) toxicity (and carcinogenic properties) have been demonstrated for aquatic life (Gambrell et al., 1991). Within sediments, these metals are sensitive to redox changes, pH alteration, and microbial activity. When exposed to sediments, metals can be adsorbed on Fe/Mn oxyhydroxides, precipitate with sulfide or carbonate discrete phases, or react with organic matter (Gambrell, 1994b). There is currently no data on V as a multiple stressor with divalent metals, so it is unclear whether toxicological effects would be additive or antagonistic.

Our primary objective was to determine the effect(s) of sediment drying and re-inundation on V speciation and potential toxicity of elevated-metal sediments. We expected that porewater metal concentrations (including V) would increase with inundation of oxidized sediments and subsequent reduction to lower oxidation states would decrease bioavailability. Toxicity testing using *D. magna* and *H. azteca* provided an indication of bioavailable metal release associated with sediment oxidation. This study provides predictive toxicology tools for hydrologically variable systems and can inform reservoir management for improved biological health and water quality.

4.2 Methods

4.2.1 Site selection and sediment collection

A Ponar dredge was used to collect surface sediments (approximately top 8 cm) from embayments in Lake Catherine (Hot Springs, Arkansas, USA) near the outlets of two creeks [Wilson Creek (WIL) and Indian Springs Creek (SPN)] which drain a former V mine site (Supporting Information (SI), Figure S1). A reference sediment (REF) was collected from an upstream embayment within Lake Catherine with similar bathymetric and hydrologic characteristics. The sites are affected by annual reservoir drawdown exposing mudflats in October, with re-inundation in spring. A laboratory control sediment (CNTL) was collected from Raisin River in Manchester, Michigan, USA. Within 24-hours of collection, the headspace of sediment containers was nitrogen purged and stored at 4°C until experiments commenced. A map of site locations is provided (Figure 4-1).

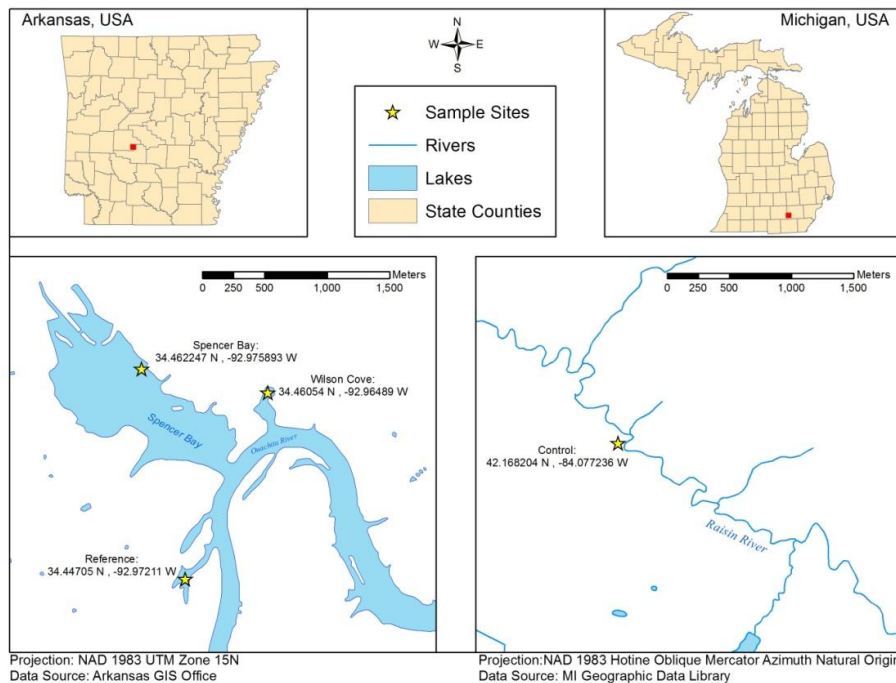


Figure 4-1. Site map included three Lake Catherine sites and Michigan control site.

Sediment physiochemical differences include sediment texture, organic content, total metal content and Fe/Mn-oxyhydroxide content. In order from finest to most coarse is SPN (clay loam, 35% clay, 33% silt), WIL (loam, 41 % silt, 51% sand), REF (sandy loam, 33% silt, 60% sand), and CONTROL (92% sand). Sediment organic content (loss-on-ignition, LOI) was higher in WIL sediments than CONTROL ($p < 0.02$), but otherwise there were no differences between sediment types (range: 0.4-10%). Total metal in sediment also remained constant. REF had lower Fe and Mn-oxyhydroxide content than SPN or WIL ($p < 0.002$), while SPN had higher Mn-oxyhydroxide content for than WIL ($p < 0.05$). Due to these differences, Fe/Mn-oxyhydroxides content were statistically analyzed for each site separately. An overview of general sediment characteristics including total metal concentrations is provided in [Table 4-1](#).

4.2.2 Experimental design

Sediment-filled microcosms were used to conduct wetting/dry experiments to test redox effects on chemical and biological endpoints. The polycarbonate microcosms were fitted with Rhizon samplers at 1 and 3 cm sediment depths to facilitate porewater sampling. Each microcosm was equipped with a small bottom drainage port with 250- μm mesh to reduce sediment loss. Three replicate microcosms for each sediment type were flooded for several days prior to starting the experiment. The experiment began with 7-days of sediment drying, followed by an 11-day inundation. To facilitate sediment drying, surface water was removed with a syringe and the bottom drainage hole was opened. During inundation, the drainage hole was closed to prevent leaching and water was introduced for 4 minutes every 12 hours at a rate of $1.55 \pm 0.5 \text{ cm}^3 \text{ s}^{-1}$ to emulate rainfall. Input water chemical composition had an average hardness of $152.9 \pm 1.4 \text{ mgL}^{-1} \text{ CaCO}_3$, dissolved oxygen (DO) of $6.4 \pm 0.2 \text{ mgL}^{-1}$, and pH of 7.5 ± 0.1 .

Table 4-1. A summary of physicochemical properties for 4 sediment types shows SPN and WIL to have similar total metal concentrations while the two references sites (REF and CNTL) are much lower. While CNTL has lowest total metals content, REF is more similar to contaminated sites in several other parameters (texture, pH, LOI, [SEM-AVS]/foc).

Site	Texture	pH	LOI (% C)	[SEM- AVS] /foc	Total Metals (mg kg ⁻¹)						
					Cd	Cr	Fe	Mn	Ni	V	Zn
SPN	Clay	6.47 ^a	4.96 ^{ab}	70.39 ^a	0.98 ^a	*129.82 ^a	63272.06 ^a	1644.55 ^a	39.72 ^a	1124.72 ^a	*178.66 ^a
	Loam	±0.07	±0.90	±23.80	±0.05	±11.76	±5692.92	±143.12	±3.21	±97.55	±11.64
WIL	Loam	6.48 ^a	7.88 ^a	72.53 ^a	1.74 ^a	70.24 ^{ab}	49393.47 ^a	633.63 ^{ab}	*104.98 ^a	807.45 ^{ab}	*274.22 ^a
		±0.05	±1.18	±22.88	±0.22	±3.97	±3452.31	±73.18	±5.88	±55.05	±17.63
REF	Sandy	6.13 ^a	4.10 ^{ab}	43.34 ^a	0.14 ^b	26.63 ^c	10490.66 ^b	174.76 ^c	8.83 ^b	118.16 ^{bc}	29.10 ^b
	Loam	±0.09	±1.03	±8.81	±0.00	±1.54	±542.29	±13.09	±0.39	±6.52	±1.47
CNTL	Sand	7.46 ^b	1.98 ^b	-9.59 ^b	0.09 ^b	24.61 ^{bc}	16628.50 ^b	458.50 ^{bc}	7.63 ^b	31.24 ^c	24.10 ^b
		±0.05	±0.40	±6.78	±0.00	±4.97	±1171.94	±61.45	±1.24	±3.16	±4.72

a/b/c/d indicates statistical differences between sites ($p < 0.05$)

*Concentration of metal exceed probable effects concentration (PEC)(Buchman, 2008)

4.2.3 Aqueous analyses

Laboratory analyses included total metal content, V-speciation, and general chemical parameters of surface water, porewater, and sediment. Surface water general chemical parameters included DO, pH, Eh, conductivity, and temperature measured on days 1, 7, and 11 for all microcosms, with the exception that Eh was not measured on day-1 due to probe malfunction. A maximum volume of 15-mL porewater filtered to 0.19- μm (Rhizon) was sampled on days 1, 7, and 11, including analyses of dissolved oxygen (DO), pH, Eh, and reduced iron (Fe^{2+} , via ferrozine method) (Stookey, 1970; Viollier et al., 2000). All parameters were measured immediately after sampling to restrict porewater oxidation.

For metal analyses, syringe-extracted surface and porewater filtered to 0.22 (or 0.19) μm was acidified with trace metal grade HNO_3 to 2% and analyzed on a HR-ICP-MS (porewater, Thermo-Finnigan Element XR) or ICP-OES (surface water). Concentrations were corrected with procedural blanks (run for every 30 samples). Surface water metals were occasionally below ICP-OES detection limits of $\sim 5\text{-}10 \mu\text{g L}^{-1}$. Additional porewater was immediately stored in N_2 -purged centrifuge tubes for V(IV) and V(V) speciation. V-speciation was estimated using an acetate extraction passed through a Chelex-resin as described by Schafer et al.(2012).

Additional testing was conducted to quantify oxidation of V-species during sampling, storage, and lab processing. In July 2016, three ponar-grabs from WIL were each split into 6 treatments, including three immediately N_2 purged samples and three non-purged sediment samples. Among these samples, two were spiked with either V(IV) or V(V) and one was left unspiked. Samples were shipped overnight and immediately processed for total V and V-speciation (IV/V) in porewater and sediment.

Results indicate that N₂ purging in the field had no effect on V-speciation as indicated from t-tests comparing purged to non-purged treatments ($p > 0.15$). Further comparison of the added V(IV) and V(V) spiked gradient showed that sediment heterogeneity outweighed the effect of spiked additions, such that no difference between spiked and non-spiked treatments was observed ($p > 0.12$). Another possibility is that spiked V quickly partitioned to Fe/Mn-oxyhydroxides and were no longer extractable for speciation analyses. Our results; however, show no clear evidence of oxidative change associated with sediment collection or handling.

4.2.4 Sediment analyses

Sediment cores (diameter = 2.6 cm, depth 0-1.5 cm) collected one day prior to inundation and again on days 1 and 12 after inundation were immediately placed in a N₂ purged, continuous-flow glove-bag. Two grams of sediment were placed in N-purged bottles to be analyzed for V(IV) and V(V) speciation (Shafer et al., 2012). Additional sediment was taken from the top of the core for Fe/Mn-oxyhydroxide analysis using a dithionite and ascorbate extraction method (Kostka and Luther, 1994). Remaining sediment was weighed for SEM/AVS analysis (Allen et al., 1991), dry weights, loss on ignition (LOI) (450°C combustion for 6 hours), and microwave digestion for total metals in a 3.2:1.6:1 matrix of metal grade concentrated HNO₃, HCl, and HF to be analyzed on a HR-ICP-MS. Replicate procedural blanks and reference sediments were run with digestions to correct for background metals and verify >80% metal recovery.

Additional sediments were collected and used for x-ray adsorption near edge structure (V-XANES) analysis, which provides information on the oxidation state, coordination chemistry, and mineral partitioning. Under nitrogen atmosphere, two reduced sediment samples (WIL) were transferred and flattened (1-mm thickness) to obtain an even surface in sample slots that were

subsequently sealed. XANES analyses were run at beamline 13-BM-D at the Advanced Photon Source (APS). A Si (111) double crystal monochromator was used in conjunction with harmonic rejection mirrors. Fluorescence X-rays were measured using a Canberra 16 element Ge detector. The incident beam intensity was detuned by ~20–30% to reject higher-order harmonic frequencies. At least three spectra per sample were merged to improve signal-to-noise ratio and energy resolution. For data interpretation, three V standards were also characterized: $V_2(III)O_{3(s)}$, $V(IV)O_{2(s)}$, $V_2(VI)O_{5(s)}$ (Wagner et al., 2017). All data were processed and analyzed using the Demeter software package containing Athena (Ravel and Newville, 2005).

4.2.5 Toxicity testing

The test organisms cultured at University of Michigan were used to elucidate two separate exposure pathways; *D. magna* for surface water and *H. azteca* for porewater/sediment exposure. *D. magna* age 3-4 days were exposed to surface water for 10-days for survival, growth, reproduction, and body concentration endpoints, according to U.S. EPA procedure (USEPA, 1991). *H. azteca* (aged 7-9 days) were exposed for 7-days for endpoints survival, growth, and body concentration (Borgmann and Norwood, 1995). Three representative groups (10 organisms each) were collected to estimate initial mass. Duplicate mesh bottles with 10 *H. azteca* and 5 *D. magna* were placed in each microcosm as pictured in [Figure 3-1](#) (David M. Costello et al., 2015). Each *D. magna* exposure bottle was fed 2.5mL of sel-cero every day for an average of 0.5mL day⁻¹ per organism. Sel-cero is a mixture of *Raphidocelis subcapitata* (green algae) and cerophyl (1.0×10^7 algal cells mL⁻¹). *H. azteca* were not fed during the test to encourage direct feeding on sediment nutrients.

At the end of the exposure period, organism bottles were removed and individuals counted. Surviving organisms were depurated in a 50 μ M EDTA solution for 24 hours, air dried

for several days, and weighed. Organism body tissues were digested with trace metal grade HNO₃ and 30% H₂O₂ as described in previous studies (Norwood et al., 2006). Individual growth rate (IGR) was calculated for each bottle as follows

$$IGR = \frac{\left[\frac{\sum(mass_{org})_{final}}{n_{org}} - \frac{\sum(mass_{org})_{initial}}{n_{org}} \right]}{time}$$

where *mass* is in µg, *n* is the number of organisms per bottle, and *time* is days. All body concentration (BC_M) metals (M = V, Zn) were measured on an ICP-MS and corrected for metals using a procedural blank (*H. azteca*) or input water control group (*D. magna*) to account for metals associated with Sel-cero feeding. Reproduction (R₀) was calculated as the number of neonates produced per adult.

4.2.6 Statistical analysis and modelling

Significance testing included comparisons of the lab control versus Lake Catherine sites and as individual sites (SPN, WIL, REF, CNTL) separately. Most data were normally distributed and thus ANOVA and paired t-tests were used. For nonparametric data, Kruskal-Wallis tests were used for multiple variable comparisons (all sites comparison) and the median or sign test was used for paired analysis (control vs. Lake Catherine sites). Pearson correlations between metal body concentration, porewater/surface water metal content and toxicological endpoints were used when assumptions were met (normality, linearity, homoscedasticity). For non-parametric data, Spearman rank tests were used to estimate correlation. All statistical tests were conducted in RStudio Version 0.98.1102.

The Biotic Ligand Model (BLM) program (Ver 3.1.2.37, Windward Environmental, LLC) was used to calculate Zn-BLM chronic hazard concentration for 5% of the population (CHC5s) for *Ceriodaphnia dubia*. Calculated input water chemistry which remained static from

day-1 to 11, include sulfide (0.1 ngL^{-1}), chlorine (0.15 mgL^{-1}), and DOC concentrations (0.08 mg-C L^{-1}). Alkalinity was calculated using a $p\text{CO}_2$ of 3.5 assuming an open system. Sulfate (SO_4) had to be estimated with reference to the USEPA *Missing Water Quality Parameters Technical Support Document* (USEPA, 2016c). All other inputs, including temperature, pH, Zn, Ca, Mg, Na, and K were measured on days 1, 7, and 11 (Deforest and Van Genderen, 2012).

4.3 Results

4.3.1 Physicochemical sediment characterization

At the end of the 7-day oxidation period, sediments in the experimental microcosms were relatively oxidized, becoming more reduced during the inundation. Chemical characteristics observed in the microcosms during the inundation period (from day-1 to day-11) are summarized in Appendix C, [Table C-1](#). Redox indicators changed significantly on average for all sediment types during the experiment, including a decrease in porewater DO ($p < 0.05$, from 4.7 ± 0.2 to $3.0 \pm 0.2 \text{ mgL}^{-1}$), an increase in Fe^{2+} ($p < 0.02$, from 0.9 ± 0.4 to $4.3 \pm 0.6 \text{ mgL}^{-1}$), and a decrease in sediment Eh ($p < 0.07$). Sediment acidity (pH) remained stable for CNTL but increased slightly for other sediments. A strong, negative correlation between Eh and pH was observed, showing that oxidation increased acidity in these sediments (correlation coefficient, $cc = -0.643$; $p < 0.001$) ([Figure 4-2](#)).

Water quality conditions met acceptability standards for toxicity testing (USEPA, 1991). More specifically, DO remained above 5 mgL^{-1} , except on day-7 where two microcosms (SPN-rep3 and WIL-rep2) fell below $4.5 \pm 0.5 \text{ mgL}^{-1}$ 1 hour before the twice-daily water change. Surface water pH ranged from 6.6 to 7.15 and temperature was constant at $20 \pm 1^\circ\text{C}$. Conductivity ranged from 300-350 μS throughout the experiment.

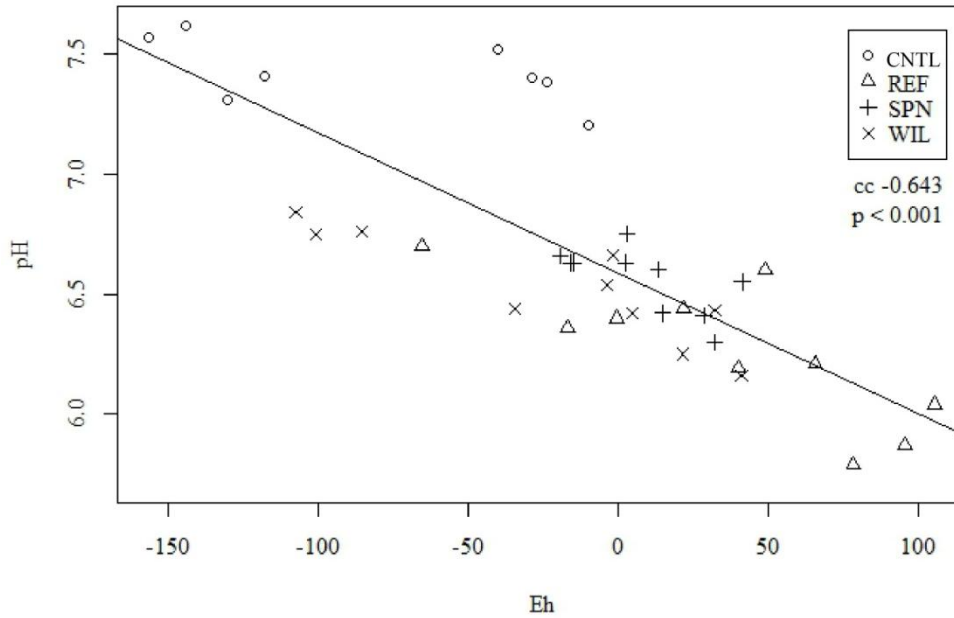


Figure 4-2. Sediment acidity was negatively correlated with redox (Eh) condition. Figure is based on day 7 and 11 data only. Increasing pH 7 to 11 days after inundation may be linked to decreasing metal concentrations in porewater and hydrolysis of metals.

4.3.2 Vanadium speciation in sediment and porewater

Sediment speciation (derived from the acetate extraction method) showed V-species to be relatively unaffected by redox changes, with low concentrations of sediment V(V) and V(IV) (~0.01-0.7% of total V) (Figure 4-3). Total sediment V was higher in SPN and WIL than REF ($p < 0.001$), with some loss in total V from the SPN microcosms between days 1 and 11. While there were no differences in V(IV) or V(V) concentrations between sediment types, an increase in V(V) was observed for SPN between days 1 and 11. With these few exceptions, V species remained stable within sediment despite hydrologic variability.

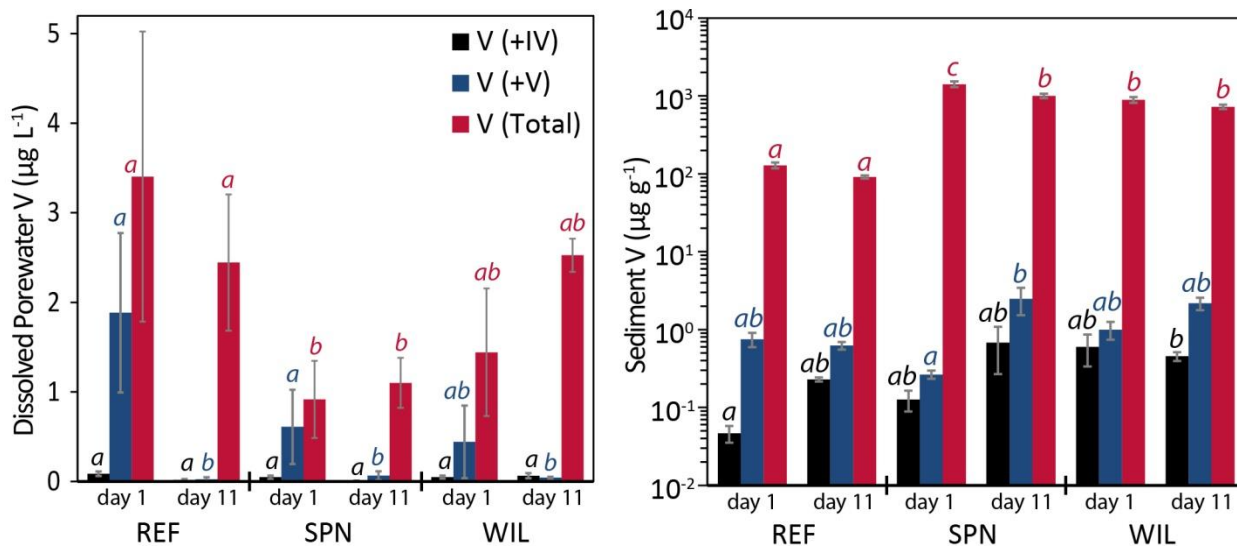


Figure 4-3. Porewater (left) and sediment (right) V speciation as a function of days after inundation (\pm standard error, SE) with lettering for statistical significance within species ($p < 0.08$). For porewater, V(IV) and V(V) are dissolved concentrations and total V is particulate.

XANES results showed a weakly-pronounced pre-edge feature for both samples (Figure 4-4) suggesting V is mostly present as V(III) in WIL sediment. Linear combination fitting (LCF) findings confirm this result. Different combinations of V standards were tested (4). For both samples, the best fits were obtained for a mix of $V_2(III)O_{3(s)}$ ($74 \pm 2\%$) and $V(IV)O_{2(s)}$ ($26 \pm 2\%$).

Concentrations of V in porewater were low throughout the experiment and surprisingly non-labile given the high sediment concentrations (~ 800 - 1150 mg kg^{-1}) (Figure 4-3). While total porewater V (particulate) remained stable from days 1-11, filtered total concentrations decreased substantially from an average of 1.1 ± 0.4 (day-1) to $0.1 \pm 0.02 \text{ } \mu\text{g L}^{-1}$ (day-11) ($p < 0.001$). This suggests V in porewater transformed by day-11 into a non-bioavailable (particulate) form(s). A decrease in porewater V(V) was observed between day-1 and day-11 as depicted in Figure 4-3 ($p < 0.01$). The V(IV) also decreased, though the change was not statistically significant.

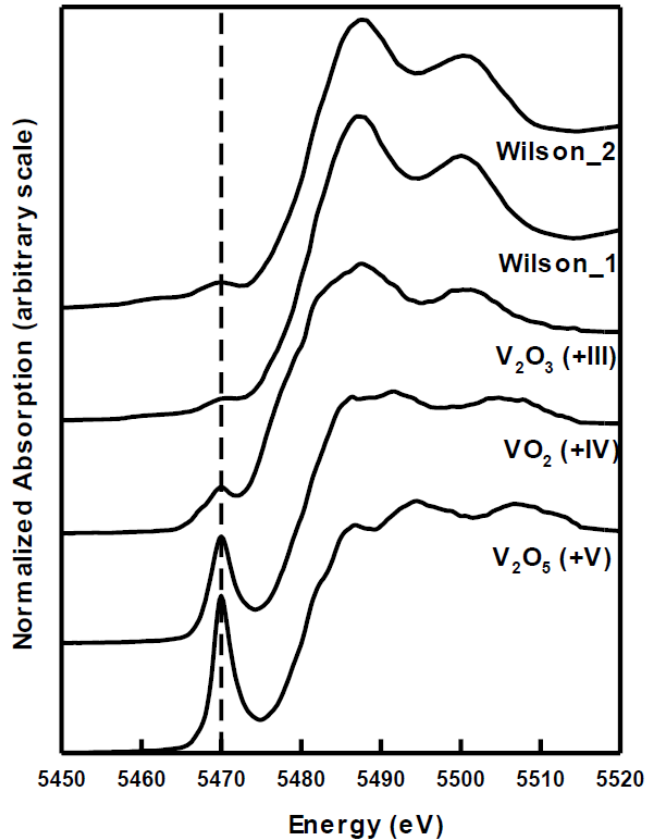


Figure 4-4. XANES spectra of samples and reference compounds.

4.3.3 Metal bioavailability in surface and porewater

Microcosm surface water overlying three of the four sediments (except REF) exceeded the U.S. EPA threshold for chronic toxicity of Zn (CCC). Surface water Zn did not change over 11-days ($p > 0.7$) and was not different between sites ($p > 0.09$), with a concentration of $130.2 \pm 11.7 \mu\text{g-Zn L}^{-1}$. Surface water Mn was higher in WIL and SPN than in REF and CNTL ($p < 0.03$). Surface water concentrations for many metals (V, Ni, Cu, Fe) were below detection limits (DL $\sim 20 \mu\text{gL}^{-1}$) (Table C-2).

Porewater concentrations for Al, Cd, and Zn exceeded their CCC for 4 or more sampling points (including hardness correction for Cd and Zn) (Figure 4-5). Of all porewater concentrations, Al CCC were exceeded for 28% of observations, while Zn and Cd were 18% and

6%, respectively. Zn and Cd exceeded CCC most often in WIL sediments, while all four sediment types (including REF) had exceedances for Al (Table C-3). These metals depicted different temporal trends, where Al concentrations peaked on day-7 ($p < 0.05$) Cd and Zn were highest on day-1 and decreased with sediment reduction ($p < 0.05$).

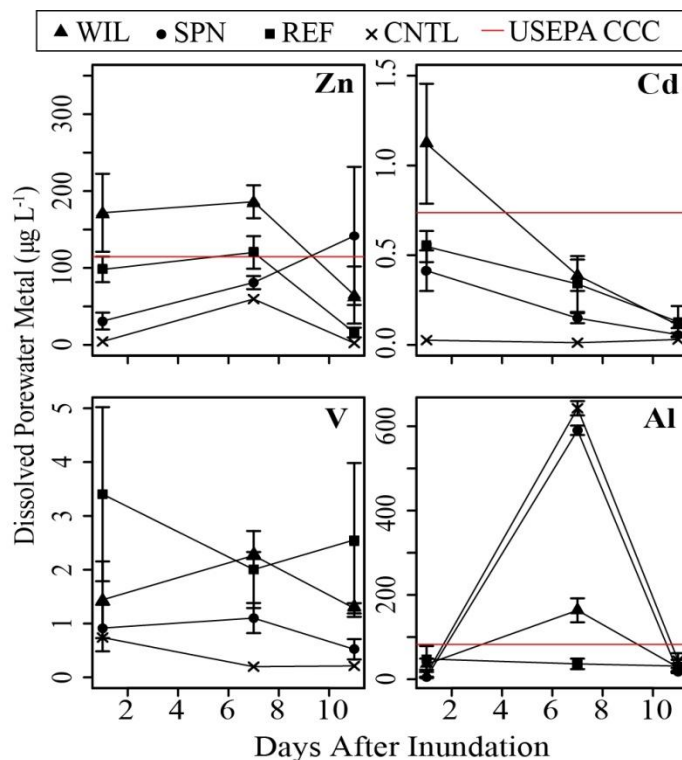


Figure 4-5. Porewater metal concentrations (\pm SE) show Zn, Cd, and Al CCCs were exceeded on some days and for some sediment types. Table with extended metal concentrations is provided in Appendix C.

The U.S. EPA theoretical model used to assess metal bioavailability in sediments ($(SEM-AVS)/f_{OC}$) resulted in positive values, suggesting the potential for toxicity. Values were highest on day-1, decreasing with reduction to day-12 ($p < 0.04$) (Figure 4-6). Further, the Lake Catherine (WIL, SPN) and onsite reference (REF) had higher $(SEM-AVS)/f_{OC}$ values than the offsite reference (CNTL) ($p < 0.02$). Metal binding to sulfide appears to be an important biogeochemical process affecting bioavailability in these sediments.

Sediment Fe/Mn-oxyhydroxide content was also altered with reduction (Table C-4).V binding to amorphous metal hydroxides decreased with reduction for all sites, which may have implications for metal bioavailability ($p < 0.04$). Additionally, some sites had decreases in amorphous Fe/Mn-oxyhydroxide content (SPN, WIL, REF), with additional decreases in total Fe/Mn-oxyhydroxides for REF ($p < 0.05$). Apparent Zn binding to total Fe/Mn-oxyhydroxides increased with reduction ($p < 0.04$), though it may be more reflective of formation of $Zn(OH)_2$ with hydrolysis. These findings emphasize the importance of Fe/Mn-oxyhydroxides as ligands affecting metal bioavailability.

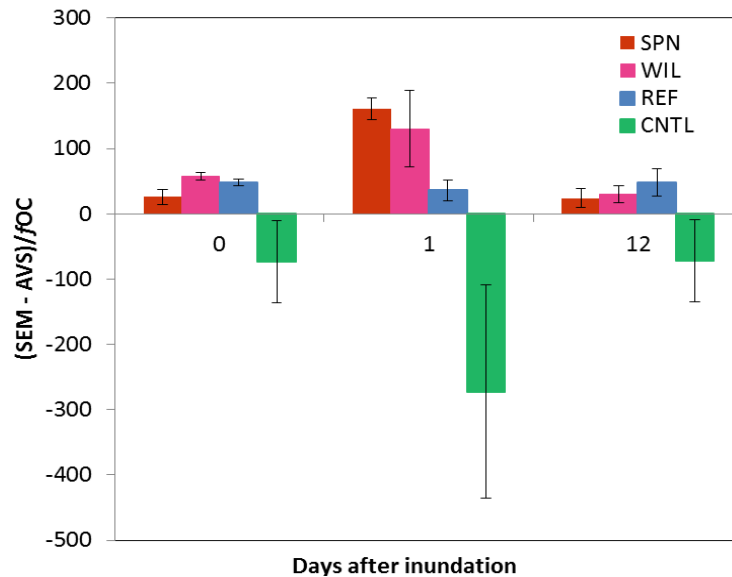


Figure 4-6. Potential toxicity estimated by $(SEM - AVS)/foc$.

4.3.4 Toxicity testing of *D. magna* and *H. azteca*

Survival and individual growth rate (IGR) of *H. azteca* met or exceeded minimum acceptable control performance criteria. *H. azteca* survival was $> 80\%$ in all laboratory control, reference, and elevated metal sediment exposures. Compared to controls and reference site data, exposure to sediments from Lake Catherine stations WIL and SPN produced no adverse effects

on *H. azteca* survival or IGR (Figure 4-7). *H. azteca* survival and IGR were not correlated with concentrations of Zn, Cd, Al, or V (or other metals) in either solid phase sediments or porewater ($p > 0.4$).

No differences were observed between tissue concentrations of Zn in *H. azteca* exposed to sediments from the reference site and those exposed to sediments from the WIL and SPN stations in Lake Catherine; however, BC_{Zn} and IGR were negatively correlated ($r^2 = 0.85$; $p < 0.0002$) (Figure 4-8). High variability in BC_{Zn} between replicates confounded the overall effects to *H. azteca* growth between sediment types. V was higher in Lake Catherine sediments ($p < 0.02$), but did not show adverse growth effects ($p > 0.4$) (Figure 4-7). Neither sediment nor porewater Zn concentrations were correlated with body concentration ($p > 0.25$), suggesting that (1) these parameters may not be sufficient for predicting exposure or (2) additional replicates were needed. BC_V was positively correlated with sediment concentrations of total V ($p < 0.03$), V(IV) ($p < 0.03$), and V(V) ($p < 0.05$), but not porewater V ($p > 0.2$). *H. azteca* IGR and BC_V were not correlated ($p < 0.6$).

IGR and survival for *D. magna* met or exceeded minimum acceptable control performance criteria. Compared to control and reference sediments, exposure to sediments from Lake Catherine sites WIL and SPN produced no adverse effects on IGR and survival in *D. magna* ($p > 0.4$) (Figure 4-7). Reproduction (R_0) in *D. magna* exposed to SPN sediments was 51% lower compared to REF ($p < 0.03$), but was not different from that observed for CNTL and WIL. *D. magna* V and Zn tissue concentrations were higher than those observed for the reference or control sites ($p < 0.03$ and $p < 0.02$, respectively) (Figure 4-7), however, *D. magna* V and Zn body concentrations were not correlated with survival or IGR ($p > 0.2$). A weak

negative correlation between R_0 and BC_V was observed ($cc = -0.6$, $p = 0.06$), but no such relationship was observed for Zn ($p > 0.19$).

The Zn-BLM results used for predicting surface water toxicity, predicted chronic toxicity in *D. magna* exposed to SPN sediments (Table C-5), and, as noted above, effects on R_0 were observed in *D. magna* exposed to SPN sediments compared to REF. Zn-BLM model results indicated sediments from WIL and SPN produced a chronic toxicity unit (TU) for *D. magna* exceeding one. However, the TU-based prediction was shown to be overprotective given that no adverse effects were observed in *D. magna* exposed to sediments from WIL. An increase in dissolved Mg between days 7 and 11 ($p < 0.005$), led to lower BLM-predicted TUs, since Mg functions as a competitive ion to Zn decreasing biological uptake.

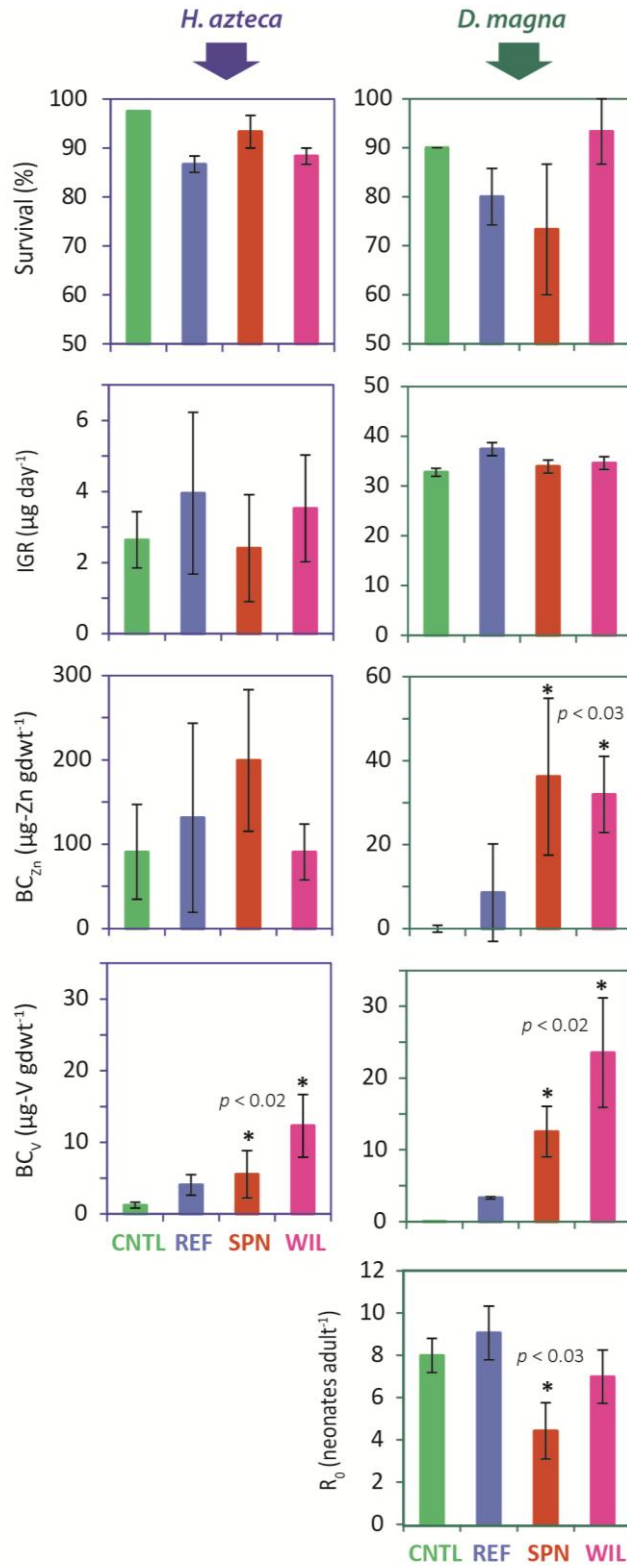


Figure 4-7. Toxicity test results for *H. azteca* and *D. magna*, including survival, individual growth rate (IGR), Zn and V body concentration, and reproduction (R_0) (\pm SE).

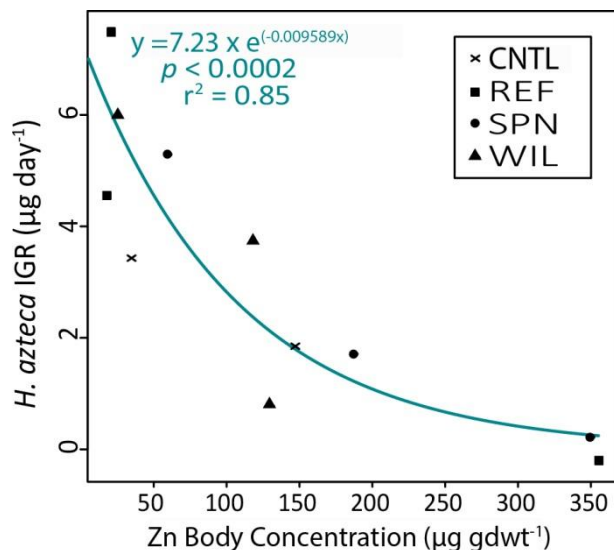


Figure 4-8. *H. azteca* BC_{Zn} was negatively correlated with IGR, indicating sublethal effects of Zn-oxidative release.

4.4 Discussion

4.4.1 Vanadium geochemistry

Although total V concentrations were elevated in sediments at two stations (WIL and SPN) down-gradient from a former mine site, remobilization into the overlying water and porewater remains low with variable hydrology. Several factors may contribute to the low remobilization of V; including, (1) the short oxidation period (7-days) used in this experiment, (2) neutral/low pH sediments which increase binding to OC, (3) low solubility of V(III) and V(IV) oxides in natural water, and (4) the dominance of mineral (non-labile) forms of V (Nriagu, 1998). Longer drying periods may lead to higher remobilization of V within the sediment through oxidation of V(III) to labile V(V). Also, as an oxyanion, V binds more strongly to sediment organic compounds when pH is neutral to acidic (Canada, 2010). Thus, the sediments in this study may be well-buffered against redoximorphic variation. Further validation of these findings is needed to address applicability to longer oxidation durations or higher alkalinity sediments.

The third rationale for low remobilization of V is supported by leaching experiments from soil and mine tailings that showed less than 1% of total V amount present in these samples was extracted (Yang et al., 2014). XANES results show the majority of sediment ~75% as V(III) (V_2O_3) and ~25% as V(IV) (VO_2), confirming that V(III/IV) oxides are not easily remobilized when being exposed to oxygen. And lastly, previous studies, including this study, have shown the dominance of non-labile V as a fraction of total V (Abollino et al., 2006).

Combined analyses of V-XANES, acetate extraction (V-speciation), and the ascorbate/dithionite extractions suggest most V is present in a relatively non-labile V (+III) phase (~75%), with an additional fraction bound to Fe/Mn-oxyhydroxides (~0-9%) (Table C-6). The differences observed, between the chemical extraction (0-0.25%) and the XANES measurements (25-27%), for the portion of V(IV) could be explained by (1) a low efficiency of the acetate extraction to dissolve some V(IV) species, and (2) an overestimation of the LCF method related to the very few V(IV) standards available (only VO_2) that were tested. The bound fraction of V to Fe/Mn-oxyhydroxides is on the low end of previous findings of 2-40% (Abollino et al., 2006), which may be due to lower sediment pH favoring reductive dissolution of Fe and Mn.

4.4.2 Vanadium toxicology

V was predominately found in non-bioavailable phases in the sediment, porewater, and surface water, and no adverse effects from V were observed in *H. azteca* or *D. magna*. V concentrations in porewater fell well below the reported (surface water) 21-day LC_{50} of $400 \mu\text{gL}^{-1}$ and ambient water criteria of $120 \mu\text{gL}^{-1}$ (Canada, 2010; Environment Canada, 2016). The fact that BC_V in *H. azteca* was higher in sediments with elevated V and yet no adverse effects were observed, suggests that V is present in a form that is not harmful to organism growth or survival.

Toxicity tests used in this study were relatively short duration (7-10 days) and focused on test organism survival, growth and reproduction. Other studies utilizing longer duration exposures and higher concentrations of V may produce different results (Environment Canada, 2016) .

H. azteca BC_V observed in this study are high compared to previous work, and highlight the need for continued investigation of sediment V exposures. In a similar 7-day *H. azteca* toxicity test, BC_V values were slightly lower (maximum of ~9 µg gdwt⁻¹) for a surface water exposure of 1 mgL⁻¹ as compared to this study (average of 21.1 µg gdwt⁻¹) (Jensen-Fontaine et al., 2014). The lower values reported in the previous study were likely a result of feeding with Tetramin instead of direct sediment exposure/feeding as conducted in this study (Jensen-Fontaine et al., 2014). Further, there are currently no published studies specifically investigating sediment V exposure.

van Leeuwen et al. (1987) observed effects on *D. magna* survival and growth (carapace length), with a decrease in carapace length of ~90% at LC₅₀ concentration of 1.7 mgL⁻¹ (van Leeuwen et al., 1987). The weak negative correlation observed between *D. magna* R₀ and body concentration does not suggest causation, as V concentrations in surface water remained below detection limits (<5 µg-V L⁻¹) and well below the reported EC₁₀ of 1 mgL⁻¹. Further, surface water modeling using the BLM showed Zn is likely responsible for any effects to R₀ in the sediment.

4.4.3 Zn toxicology

Elevated surface water Zn concentrations likely affected the decreased R₀ for *D. magna* observed in SPN sediments, as concentrations often exceeded CCC (120 µgL⁻¹). The effect of Zn on reproduction (when concentrations exceed CCC) has been clearly demonstrated by Paulauskis et al. (1988) who found increased Zn in porewater decreased *D. magna* brood size with the most

pronounced effects in soft waters with low humic content. The observed decrease in reproduction is thought to have a lower bound, such that the organisms are not rendered sterile (De Schamphelaere et al., 2004a). In the present study, test organisms and the algae fed to them were not acclimated to Zn, which may be important to achieving ecologically relevant results (De Schamphelaere et al., 2004b; Muysen and Janssen, 2001).

The BLM for Zn predicted adverse effects to *D. magna* reproduction for SPN and WIL exposures (Table C-5), and a significant decrease in R_0 (as compared to REF) was observed for SPN. Chronic hazard concentrations (CHC5's) were calculated with *Ceriodaphnia dubia* data, which are slightly more sensitive to Zn than *D. magna*. Given this information, the BLM was an adequate predictor of surface water effects of Zn to *D. magna*.

The hardness corrected CCC were overprotective to *D. magna* for Zn. While Ca hardness ranged from 61-101 mg L⁻¹ as CaCO₃ in surface water, Mg was the predominant ion contributing to cation competition, which ranged from 336-546 mg L⁻¹ as MgCO₃. When CCC were calculated using Ca hardness, they were overprotective, but with Mg hardness they were underprotective (Table C-3). It is clear from these data that Mg are important for competitive exclusion of Zn as a toxicant and should not be overlooked when predicting effects to organisms. Further, the BLM predicted the effects of Mg quite well. Daily TU's predicted decreased toxicity to *D. magna* on day 11, which corresponded to increased surface water Mg on that day (1.20 vs. 0.88, $p = 0.07$, not including CNTL). The BLM as a predictor of Zn toxicity proved to be robust to chemical variability, and therefore more effective overall.

The theoretical model for sediment toxicity (SEM-AVS) accurately predicted no effects to biological endpoints on average for any sediment type (growth and survival). Previous work suggests chronic effects from Zn are likely to be observed if (SEM-AVS)/ f_{OC} values exceed

approximately $583 \mu\text{mol g}^{-1}$, which the values in this study fell well below (Burton et al., 2005). A table including $[\text{SEM-AVS}]/f_{\text{OC}}$ values is provided in Appendix C.

The three metals exceeding porewater CCC (Zn, Cd, Al) were not correlated with survival or growth, but there was a strong relationship between BC_{Zn} and IGR. While the population-level implications of the relationship between BC_{Zn} and IGR are unknown, these results suggest sublethal Zn toxicity. BC_{Zn} data for *H. azteca* from the present study are comparable to previously reported values, where $45\text{-}70 \mu\text{g-Zn gdw}^{-1}$ was reported for control specimens and $59\text{-}180 \mu\text{g gdw}^{-1}$ was reported for organisms exposed to approximately $200\text{-}500 \mu\text{g L}^{-1}$ Zn (Borgmann et al., 1993; Borgmann and Norwood, 1995; Neumann et al., 1999). In the present study, BC_{Zn} in *H. azteca* was $25\text{-}129 \mu\text{g gdw}^{-1}$ for the reference sediments and $75\text{-}173 \mu\text{g gdw}^{-1}$ for WIL and SPN. Previous studies have found divalent metal cations to inhibit *H. azteca* growth (Kubitz et al., 1995; Milani et al., 2003); however, this is the first study to show a strong relationship between BC_{Zn} and IGR. An overview figure is provided (Figure 4-9).

4.4.4 Implications for reservoir management

Water level management can lead to an altered chemical (redox, pH) and physical (temperature, TDS, conductivity) environment controlling the fate and bioavailability of metals. The outlook for improved reservoir management is promising as new high frequency monitoring systems become more widely used and available (Marce et al., 2016). Additionally, modeling tools incorporating both ecological and anthropogenic goals for improved reservoir management have been developed (Saito et al., 2001). It is recommended that sediment metal concentrations be screened seasonally, particularly in systems with dynamic water levels.

Most biological monitoring programs in reservoirs focus predominately on primary producers (algae), and fisheries, with little to no focus on benthic communities, although

reservoirs are large sediment sinks (Marce et al., 2016). While studies focusing on fisheries provide adequate assessment of overall system function, solving issues of limited productivity often require data on lower-trophic organisms (i.e. benthic). Further, benthic organisms provide important ecosystem services, such as improving water quality, enhancing nutrient cycling, and sustaining commercial fisheries (Covich et al., 1999; Prather et al., 2013). With literature focusing mostly on fish, water quality, and not benthic organisms, data is lacking on how to preserve, restore, and maintain benthic community function in reservoirs.

The redoximorphic effects observed in this study should be applicable to hydrologic variability in other systems such as, river floodplains, wetlands, and lakes. This study shows that V is highly complexed to sediment and not bioavailable in Lake Catherine, though further experimentation is needed to test the bioavailability of V for other aquatic systems with alkaline sediment types. Additional research is needed to develop new methods for determining V speciation in reducing environments. For aquatic systems with elevated levels of Zn in sediments, potential for oxidative release and effects on benthic organisms should be a management consideration. Increased site-specific knowledge of hydrology and biogeochemistry will undoubtedly improve water management to protect natural resources.

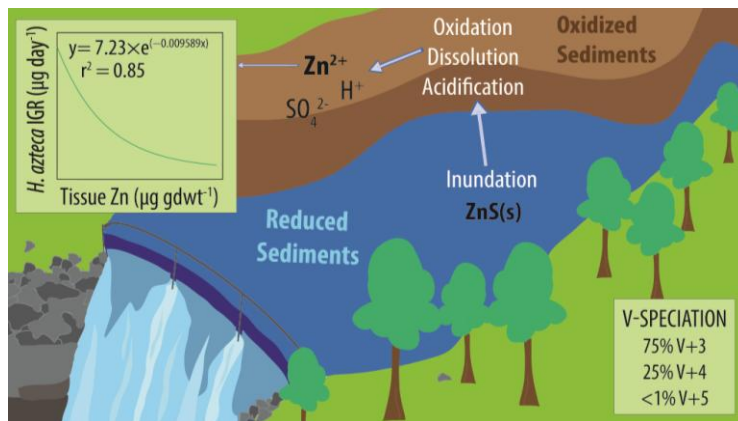


Figure 4-9. Schematic overview of the main findings in this chapter.

Chapter 5 – Biogeochemical release of sediment zinc: Assessing risk to benthic communities and periphyton

ABSTRACT

The fate and effects of zinc in aquatic systems are well known; however, most information is from laboratory studies, with little focus on hydrologic-biogeochemical interactions. We investigated Zn biogeochemistry in freshwater sediments during re-flooding after a 30-day sediment drying and the resulting responses of periphyton and macroinvertebrate communities. Mesocosms in three coastal Great Lakes wetlands in Michigan, USA showed Zn sediment release occurs at elevated concentrations ($> 310 \text{ mgkg}^{-1}$) in Zn-spiked sediments as compared to laboratory testing ($\geq 18 \text{ mgkg}^{-1}$) of non-spiked sediments. Where Zn-release occurred, benthic community abundance, richness, and diversity were enhanced whereas in the laboratory study, sub-lethal toxicity was observed. Important variables likely causing these differences included surface water chemical composition, magnitude and duration of re-inundation, groundwater inputs, and periphyton biomass (as Chlorophyll (Chl) *a*). Benthic community indicators were strongly influenced by pH ($p < 0.005$), where more alkaline sediment porewaters led to greater abundance, richness, and diversity. Evidence suggests more alkaline conditions were enhanced (at least partially) by periphyton, though the relationship varied between sites. Further, elevated porewater-Zn led to decreased periphyton Chl *a* biomass ($p < 0.08$). This has important implications for the relevance of laboratory toxicity testing which excludes important biogeochemical pathways and biota, such as the role of periphyton. The fate of Zn in sediments

is dynamic, changing with redox and speciation, and thereby cycling between sediment particles, porewater, surface water, periphyton and benthic macroinvertebrates.

5.1 Introduction

Zinc is naturally ubiquitous and relatively abundant in most environments. It is also released to aquatic ecosystems from anthropogenic sources, such as metal manufacturing, domestic waste water, fertilizers, galvanized metals, car tires and atmospheric fallout from combustion processes (ATSDR, 2017; Councell et al., 2004). Zn can become elevated in sediments and surface waters in human-dominated areas leading to biotic impairments (USEPA, 1987). The bioavailability (or fraction available for uptake by organisms) of Zn is controlled by binding to a number of ligands, such as carbonates, organic carbon, sulfides, and metal oxides that alter its fate and effects. (Gambrell, 1994b). Drying and flooding of Zn-elevated sediments in laboratory exposures showed release of bioavailable Zn into surface water and porewater associated with sediment oxidation/drying (Nedrich and Burton, 2017). Based on these findings, we conducted a field investigation to assess the role of Zn-release in shallow aquatic systems to more accurately predict environmental risk.

Several factors influence the occurrence of Zn-release in sediments, including the total concentration of sediment Zn, the abundance and speciation of binding ligands (S^{2-} , CO_3^{2-} , amorphous Fe/Mn-oxyhydroxides), site chemistry (pH, redox), microbial activity, prevalence of competing cations (Ca^{2+} , Fe^{2+} , Mg^{2+} , etc.), and magnitude and duration of sediment drying/oxidation (Guo et al., 2016; Nedrich and Burton, 2017). Sediments with total Zn >190 $mgkg^{-1}$ and a drying time of 32-days showed a 10x increase in porewater Zn. Increasing drying time and Zn concentrations increased Zn release (Nedrich and Burton, 2017). The influence of sediment pH and redox on Zn bioavailability is more nuanced, where Zn binding is enhanced in

oxic sediments by Fe/Mn-oxides, in reduced sediments by sulfide, and in alkaline sediment by carbonates (Chapman et al., 1998; Korfali and Davies, 2004). Further, sediment oxidation can alter microbial communities, leading to decreases in anaerobic populations and cell lysing (Steinman et al., 2014). While this study is conducted in high carbonate sediments, more extreme releases of Zn likely occur in acid-sulfate sediments (low pH / high sulfide) (Carvalho et al., 1998; Simpson and Spadaro, 2016).

Primary exposure pathways for Zn-uptake by benthic macroinvertebrates include ingestion of organic/inorganic matter and filtration of surface or porewater (USEPA, 2005). Elevated Zn can lead to cellular damage, hypocalcaemia, and dietary displacement of Fe and Cu causing growth inhibition, reproductive issues, and mortality to individuals (Muysen et al., 2006; Muysen and Janssen, 2001). Effects to benthic community composition may include decreased abundance, richness, and diversity (Cooper et al., 2001; Watzin and Roscigno, 1997). Organism sensitivity to Zn has additionally been linked to dietary uptake from periphyton (i.e. biofilms or aufwuchs) (Brinkman and Johnston, 2008; Kashian et al., 2004). Periphyton is an effective indicator of bioavailable Zn, as it accumulates in and adsorbs to algal cells (Meylan et al., 2003). Periphyton can also incur metal toxicity, with impacts to chlorophyll *a* production, algal community structure/composition, and growth (Genter et al., 1987).

Current environmental quality regulations for aquatic ecosystems focus on surface and porewater (dissolved Zn), sediment (total) Zn concentrations, and sediment acid volatile sulfide (AVS) – simultaneously extracted metal (SEM) relationships for predicting Zn toxicity (USEPA, 2005). Sediment screening compares total metals concentrations to USEPA developed sediment quality guidelines (SQG's), using standardized toxicity testing or AVS/SEM analyses when needed (Buchman, 2008; USEPA, 1996a, 1996b). Benthic toxicity tests generally do not

consider site specific parameters, such as surface or porewater composition, temporal changes to site chemistry (pH, redox), microbial activity, or hydrologic variability (ASTM, 2005), which may lead to oversimplified or incorrect conclusions about sediment toxicity.

The primary objectives of this paper are to (1) determine if Zn-release occurs in alkaline sediments of the Great Lakes; (2) compare field to recent laboratory tests; (3) investigate the use of periphyton as an indicator of Zn toxicity; and (4) compare the effectiveness of existing sediment toxicology approaches at predicting environmentally relevant outcomes.

5.2 Methods

5.2.1 Site selection

Three sites were selected based on accessibility, ability to camouflage experiments from the public, medium to high sediment metal content, hydrologic connection to the Laurentian Great Lakes, and diverse sediment chemical properties (sulfide content, redox, iron/manganese concentration). All sites were in Michigan, USA, and included East Bay Park (EB) on East Traverse Bay, Traverse City, Little Black Creek (LBC) on Mona Lake, Muskegon, and Quanicassee Wildlife Refuge (QC) on Saginaw Bay, Bay City ([Figure 2-1](#)). A reference site with similar sediment texture, but lower metal content was selected along the Raisin River (REF) (in Manchester). A table including physicochemical sediment properties is provided ([Table 5-1](#)). An extended description of site characteristics is provided in the supplemental information (SI), *Methods: Site Selection*.

5.2.2 Experimental design

Mesocosms were designed from polycarbonate containers with mesh openings and ports equipped with Rhizon porewater samplers (0.19- μm) ([Figure 5-1](#)). Mesh (250- μm) openings

were placed along the sides and bottom of the container to allow groundwater/porewater interchange but prevent benthic colonization. Mesocosms had two or three (reference-only) porewater sampling ports located 1-cm below the sediment-water interface (SWI). When deployed, the sediment surface of the mesocosm was level with the surrounding sediment and holes above the sediment allowed surface water inundation and drainage with water levels.

Table 5-1. Physiochemical sediment properties of non-spiked sediments (using saturated and dry treatment data), including sediment texture, loss-on-ignition (LOI), simultaneously extracted metals (SEM) minus acid volatile sulfide (AVS) over the fraction of organic carbon (f_{OC}), and total metals concentrations (\pm SE). Data averaged from all sediment sampling days.

Site	Texture	LOI (% C)	[SEM- AVS] $/f_{OC}$	Total Metals (mg kg ⁻¹)						Spiked Total Metals (mg kg ⁻¹)	
				Cr	Cu	Fe	Mn	Ni	Zn	Medium Zn	High Zn
QC	Sandy	2.3 \pm 0.4	-13.0* \pm 5.5	1.1 \pm 0.3	2.2 \pm 0.4	1674 ^a \pm 60	31.4 ^a \pm 2.2	2.2 ^a \pm 0.8	9.1 ^a \pm 1.2	280.6 ^a \pm 19.0	879.5 \pm 50.1
EB	Sandy	3.6 \pm 0.8	-53.8 \pm 24.2	3.3 \pm 1.6	8.9 \pm 5.9	2374 ^{ab} \pm 247	62.7 ^b \pm 6.0	0.8 ^{ab} \pm 0.4	0.2 ^b \pm 0.2	310.3 ^a \pm 47.2	843.3 \pm 94.8
LBC	Sandy	4.0 \pm 1.0	-4.9 \pm 12.7	16.4 \pm 5.1	27.6 \pm 9.1	2667 ^b \pm 271	180.5 ^c \pm 18.5	ND	50.0 ^a \pm 15.9	417.9 ^b \pm 29.9	740.4 \pm 78.0
REF	Sandy	3.18 \pm 0.67	-36.12 \pm 14.74	10.1 \pm 3.5	38.7 \pm 10.1	6475 ^c \pm 222	225.1 ^d \pm 9.0	3.5 ^a \pm 1.2	17.7 ^a \pm 7.9	-	-

ND = No detect (detection limit for Ni: 0.5 μ g L⁻¹ or \approx 0.5 mg kg⁻¹)

a/b/c/d indicates where statistical differences exist between sites ($p < 0.05$)

*Statistical difference between dry and saturated treatments

Four sediment Zn concentrations were deployed including non-spiked, medium-Zn, and high-Zn with a reference (REF) sediment. Non-spiked sediments were collected with a Teflon coated shovel at the test site the day of mesocosm deployment and homogenized by hand in buckets. Medium and high Zn-treatments were collected from their respective sites in July, 2015, initially superspiked in August and diluted to final concentrations (May, 2016), prior to field deployment in June/July, 2016. Reference and spiked sediments were initially gently

homogenized in buckets, nitrogen purged and sealed, then stored in the dark at 4°C prior to the experiment.

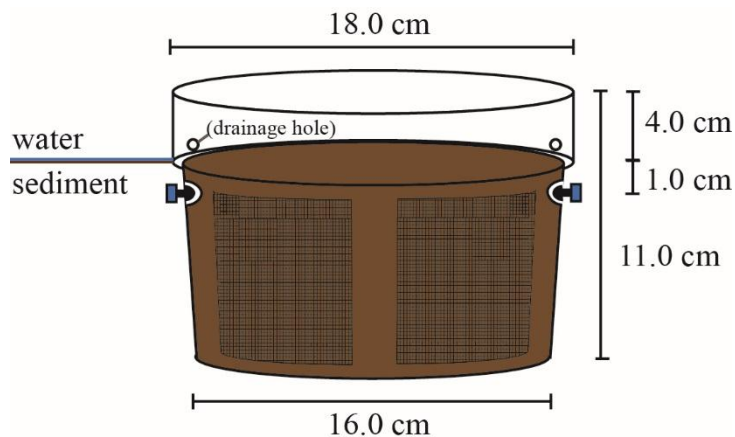


Figure 5-1. Mesocosm design with mesh

A small amount of sediment was spiked with ZnCl_2 to $10,000 \text{ mgkg}^{-1}$ as a super-spike, pH adjusted with NaOH, then diluted to medium ($\sim 600 \text{ mgkg}^{-1}$) and high ($\sim 1500 \text{ mgkg}^{-1}$) Zn (Costello et al., 2011). This approach decreases alteration of pH and other chemical properties for spiked sediments (Brumbaugh et al., 2013). Target Zn concentrations were calculated assuming complete binding to available ligands (S^{2-} , Fe/Mn-oxyhydroxides, organic matter) and with reference to Probable Effects Levels (PEL) for Zn (Buchman, 2008). The super-spike was rolled one-hour biweekly, and slowly monitored for pH variability over 3 months with routine nitrogen purging (Simpson et al., 2004). Upon dilution, medium and high Zn sediments were processed similarly over 1 month until the pH was within 0.4 units of site sediments, which allowed for maximum Zn sediment equilibration.

Sediment mesocosms underwent either a dry or saturating deployment to assess the effects of oxidation on metal bioavailability. Dry treatment sediments were initially deployed on a dry-mudflat at the wetland/upland boundary for 30-days then moved to an inundated area for ~ 30 -days. Simultaneously, saturated treatment sediments were deployed to the inundated

wetland area for all 60-days of the experiment. An example timeline is provided (Figure 5-2). Deployment was near the ordinary high water mark (OHWM) for dry sites or at a water level depth of <0.5m for saturated sites. At one site (QC), areas with *Phragmites* were purposefully avoided due to mesocosm deployment obstruction due to their extensive root mats.

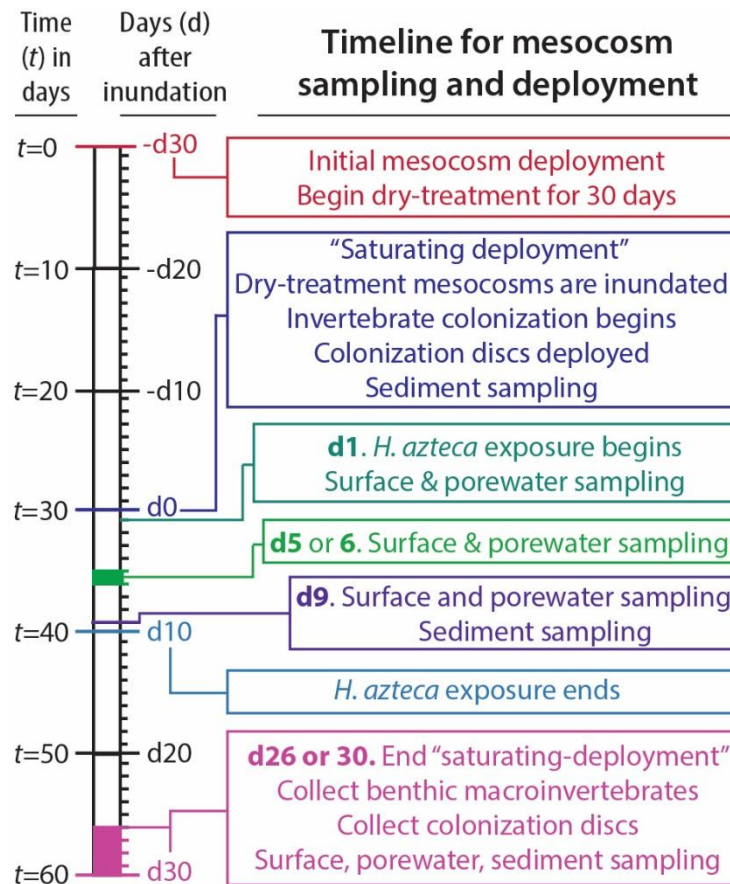


Figure 5-2. Timeline for sampling regime depicting days after (or prior to) inundation of dry treatment sediments.

Water levels were monitored over 60-days using HOB0 water level meters deployed in stilling wells at each site. Water level meters were placed in proximity to saturating-deployment sites and recorded at 10 second intervals. Data was corrected for atmospheric pressure using the barometric compensation assistant (Onset Computer Corporation, 2012). Dry deployment site

elevation above water level was estimated by measuring water table depth during initial mesocosm deployment.

5.2.3 Water and sediment analyses

Surface water sampling occurred during initial deployment, days 1, 5 or 6, 9, and ~28 after dry-sediment inundation (Figure 5-2), and included measurement of pH, redox potential (Eh), dissolved oxygen (DO), conductivity, alkalinity, hardness, temperature, and dissolved and particulate metals. All surface water samples were collected in the morning (~9 AM) with the exception of two days at EB collected around 1PM. Most parameters were measured with a multi-parameter YSI Professional Plus probe at three locations for each site. Alkalinity was analyzed using the inflection point titration method (USGS, 2012). Replicate surface water samples were collected and immediately stored at 4°C in the dark. A small quantity of water was syringe-filtered to 0.45-µm (MiliPore) within 48 hours for dissolved content, then dissolved and particulate samples were acidified with trace metal grade HNO₃ to 2% for analysis of Ca, Fe, Mg, Mn, and Zn on an ICP-OES.

A maximum volume of 15-mL porewater was collected via vacutainers from Rhizon samplers on days 1, 5 or 6, 9, and ~28 after dry-treatment sediment inundation (Figure 5-2) and immediately analyzed for DO, Eh, pH, and reduced iron (Fe²⁺). Porewater was added to a 50-mL centrifuge tube and measured for DO, pH, and Eh using a YSI Professional Plus water quality meter. Reduced iron was measured using a colorimetric reaction with ferrozine (Stookey, 1970). All samples were immediately reacted with ferrozine, stored in the dark at 4°C, and measured sequentially with Fe²⁺ standards on a spectrophotometer within 48 hours of sampling (Viollier et al., 2000).

Additional porewater was collected for analysis of dissolved metals and organic carbon (DOC). Porewater was acidified to 2% with trace metal grade HNO₃ and analyzed for Ca, Cr, Cu, Fe, Mg, Mn, Ni and Zn on an ICP-OES. Some metals concentrations were generally below detection limits, such as Cr, Cu, and Ni. Detection limits were around 3 mgL⁻¹ for Mg and Ca, 50 µgL⁻¹ for Fe, 25 µgL⁻¹ for Zn, and 10 µgL⁻¹ for Cr, Cu, Mn, and Ni. For DOC, porewater was acidified (with 6M HCl to pH=2) and diluted to 25-mL with MiliQ. DOC samples were stored in pre-combusted amber vials in the dark at 4°C and analyzed on an OI Analytical Aurora 1030 TOC analyzer.

Small, 2.5-cm diameter, sediment cores were collected to a depth of 2-cm from representative mesocosms on the initial deployment, and days 0 and 9 after dry-sediment inundation (Figure 5-2). Cores were immediately waterproofed (wrapped in parafilm) and stored vertically in a cooler at 4°C until laboratory processing (within 24 hours). Where sedimentation was visibly apparent (i.e. a dark organic layer), sedimentation depth was recorded and the organic layer was sectioned into a 50-mL centrifuge tube. Underlying sediments were stored in a separate tube. All sediments tubes were N₂ purged and frozen until further processing.

Thawed sediments were analyzed for simultaneously extracted metals (SEM) and acid volatile sulfide (AVS) (Allen et al., 1991), organic carbon content via loss-on-ignition (LOI) (6 hour combustion at 450°C), water content, total metals, and Fe/Mn-oxyhydroxides (Kostka and Luther, 1994). For total metals, dried sediment (~1g) was digested in 50-mL trace metal grade HNO₃ in a hot block (Environmental Express) at 112°C degrees for 100 minutes, in accordance with EPA method 5050B (USEPA, 1996c). For all digestions, replicate procedural blanks and reference sediments were corrected for background metals and verified >80% recovery. Extracted solutions were analyzed on an ICP-OES.

5.2.4 Biological analyses

Sediment colonization trays (Burton et al., 2005; Nguyen et al., 2011) which included all 4-sediment levels, were deployed adjacent to the mesocosms and allowed for benthic colonization during the saturating-phase only (Figure 5-2). After 28-days, sediment baskets were sieved (595 μm) and colonized organisms collected and preserved in 70% ethanol. Laboratory sorted organisms were then identified to family. Invertebrate community composition was characterized by total abundance, relative abundance (rN) of dominant taxa, total richness, Simpson diversity, Shannon-Weiner diversity, and evenness.

Periphyton colonization discs (fritted glass) were deployed on surface sediments on day-0 of the dry-treatment inundation to estimate surface sediment net primary productivity (NPP), periphyton biomass (Chlorophyll *a*), and metal uptake by periphyton. After ~28 days, disc sediment depth was measured, discs were removed, gently rinsed with site water, placed in translucent 60-mL specimen cups, and incubated for approximately 4 hours in direct sunlight. The difference in DO from beginning to end of incubation was adjusted for a background DO change (using site water) to estimate NPP. Chlorophyll (Chl) *a* was measured by extracting biofilm discs in 90% ethanol and measuring absorbance on a spectrometer (Steinman et al., 2006).

In situ toxicity testing was conducted on field mesocosms by placing ten *H. azteca* individuals in exposure bottles on the sediment surface (Borgmann and Norwood, 1995). *H. azteca* were 7 to 14 days old, collected from the University of Michigan culture. Bottles were equipped with 250-micron mesh screens so *H. azteca* were directly exposed to sediments (David M. Costello et al., 2015). Each replicate mesocosm (n=3) received two bottles (n=2) deployed on day-1 of the dry-treatment inundation, with the exception of reference sediments (where

mesocosms, n=1; bottles, n=3). At the end of a 10-day exposure, surviving organisms were carefully collected, counted, and depurated in 0.50 μM EDTA for 24 hours (Neumann et al., 1999). Air-dried weights were measured on a microbalance.

5.2.5 Speciation modeling and statistics

Model simulated oxidation and drying/reflooding was performed with chemical speciation software PHREEQC (version 2.18). Theoretical oxidation included (1) an incremental addition of O_2 (g) to equilibrated porewater and sediment and (2) the addition of oxidized surface water to sediment. For drying, simulated evaporation of water from sediment was followed by subsequent precipitation events to emulate flooding. Model input code is available in the supplemental information ([Table D-1-3](#)). Primary sediment minerals of interest included smithsonite (ZnCO_3), sphalerite (ZnS), and $\text{Zn}(\text{OH})_2$.

Significance testing included comparisons between dry and saturated treatments, site sediment types (QC v. EB v. LBC), and between days after inundation. Most biological data were normally distributed while much of the chemical data (sediment and water) were skewed, requiring non-parametric analyses. Normally distributed data underwent ANOVA and posthoc (Tukey HSD) testing. Non-parametric data underwent Kruskal-Wallis testing with posthoc (Kruskal-Nemenyi) testing. Pearson correlations were used when all assumptions were met (normality, linearity, homoscedasticity), and otherwise Spearman rank tests were used. All statistical tests were conducted in RStudio Version 0.98.1102, including use of the following packages: PMCMR, PASWR, and plyr.

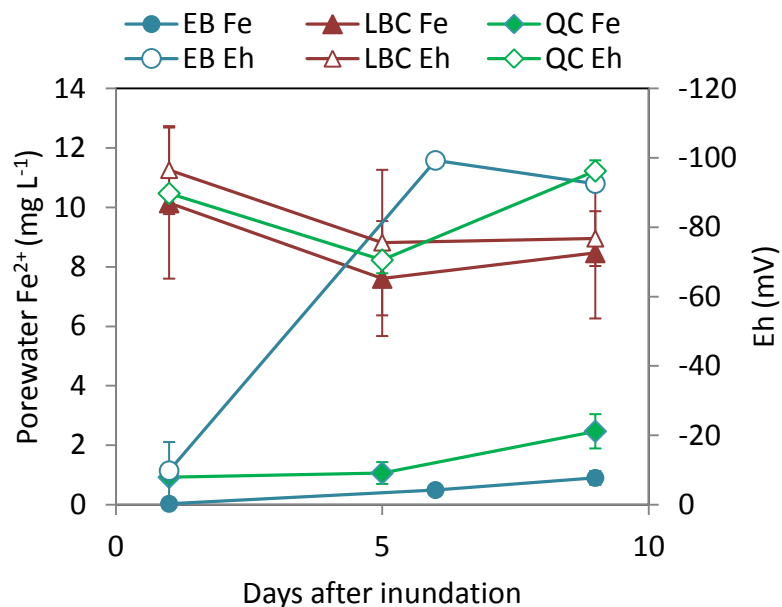


Figure 5-3. Temporal changes in porewater redox (Eh in mV) and reduced iron (Fe^{2+}) are shown for “dry” treatments of all three sites on days 1, 5 or 6, and 9 after inundation.

5.3 Results

5.3.1 Controls on sediment redox

Porewater chemistry indicates sediment oxidation in EB during the dry-deployment, but not in QC or LBC (Figure 5-3). Reduced Fe in porewater was low ($0\text{-}1\text{ mgL}^{-1}$) on day-1 of the saturating-deployment, increasing over 9-days for QC and EB, but stayed constant ($\sim 9\text{ mgL}^{-1}$) for LBC. Porewater Eh and DO were generally stable for LBC and QC, but decreased from day-1 to 9 in EB sediments, indicating oxidized sediments became reduced with inundation. Despite changes in redox for EB, porewater pH was stable between days in all sediment types ($p > 0.05$). A summary table of porewater chemical properties is provided (Table 5-2).

Dissimilar effects of drying are likely due to a combination of water levels during the study and surface water chemistry. Hydrographs indicate all sediments were (unintentionally) inundated during the dry-deployment at varying frequencies with LBC being most frequently

inundated, followed by QC, then EB (Figure 5-4). Duration of dry-deployment inundation was approximately 6, 20, and 88 minutes for EB, QC, and LBC, respectively. LBC had the highest number of days (7-days) where dry-deployment sediments were inundated, followed by QC (5-days), then EB (2-days).

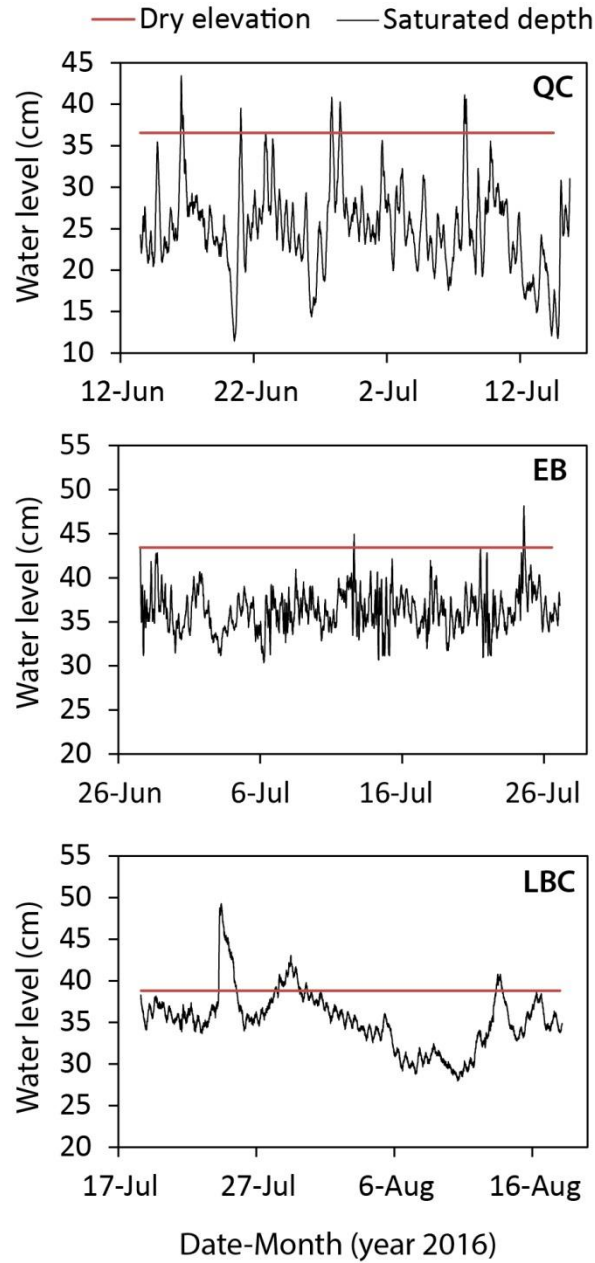


Figure 5-4. Hydrographs show water levels for all sites. When water elevation exceeds red line, dry deployed mesocosms became inundated.

Table 5-2. Physicochemical properties of porewater sampled from non-spiked sediments, including (using both saturated and dry treatment sediment data), including pH, dissolved oxygen (DO), redox potential (Eh), reduced iron (Fe²⁺), sulfide (S²⁻), alkalinity, hardness, and dissolved metals (Fe and Mn) (\pm SE). Data averaged from all porewater sampling days.

Site	pH	DO (mg L ⁻¹)	Eh (mV)	Fe ²⁺ (mg L ⁻¹)	S ²⁻ (μ mol L ⁻¹)	Alkalinity (mgL ⁻¹ CaCO ₃)	Hardness (mgL ⁻¹ CaCO ₃)	Fe (mg L ⁻¹)	Mn (mg L ⁻¹)
EB	6.9 ^a \pm 0.04	2.8 ^a \pm 0.2	-91.7 ^{ab} \pm 7.3	3.0 ^a \pm 0.6	1.7 ^a \pm 0.3	0.2 ^a \pm 0.01	208.4 ^a \pm 41.5	23.4 ^a \pm 2.4	0.8 ^a \pm 0.05
LBC	6.6 ^{ab} \pm 0.03	2.6 ^a \pm 0.1	-66.5 ^{ab} \pm 30.6	9.6 ^b \pm 1.2	1.5 ^a \pm 0.8	0.2 ^a \pm 0.01	271.4 ^a \pm 17.9	54.6 ^b \pm 2.7	4.0 ^b \pm 0.2
QC	6.5 ^b \pm 0.04	*4.1 ^b \pm 0.2	-69.8 ^a \pm 4.1	2.0 ^a \pm 0.8	3.2 ^a \pm 0.34	0.4 ^b \pm 0.02	356.1 ^b \pm 18.6	14.3 ^c \pm 0.9	1.1 ^a \pm 0.06
REF	6.8 ^{ab} \pm 0.06	2.1 ^a \pm 0.4	-123.9 ^b \pm 9.2	6.8 ^{ab} \pm 1.9	1.4 ^a \pm 0.5	0.3 ^a \pm 0.03	290.5 ^c \pm 40.7	50.4 ^b \pm 3.9	6.7 ^b \pm 0.4

*Value higher than expected likely from slow porewater sampling (surface water DO for QC was \sim 0.75 mg L⁻¹)
a/b/c/d indicates statistical differences between sites ($p < 0.05$)

Table 5-3. Summary of surface water characteristics including pH, dissolved oxygen (DO), conductivity, temperature, and dissolved Fe, Mn, and Zn. Data are averages from dry deployment and days 1, 5/6, 9, and 30 after inundation from 3 replicates per day. All data were collected in the morning (8-9 AM) except two data points collected at \sim 1 PM (EB).

Site	pH	Alkalinity (mgL ⁻¹ CaCO ₃)	DO (mg/L)	Hardness (mgL ⁻¹ CaCO ₃)	Conductivity (μ S/cm)	Temp ($^{\circ}$ C)	Fe (mgL ⁻¹)	Mn (mgL ⁻¹)	Zn (mgL ⁻¹)
QC	7.30 ^a \pm 0.05	0.25 ^a \pm 0.003	0.75 ^a \pm 0.16	222 ^a \pm 1.1	782.08 ^a \pm 12.76	22.21 ^a \pm 1.16	0.11 ^a \pm 0.02	0.09 ^{ab} \pm 0.04	0.01 ^a \pm 0.002
EB	8.3 ^b \pm 0.20	0.09 ^b \pm 0.002	9.50 ^b \pm 1.27	89.2 ^b \pm 2.6	318.43 ^b \pm 3.05	25.49 ^a \pm 1.66	0.01 ^b \pm 0.004	0.01 ^a \pm 0.002	0.01 ^a \pm 0.003
LBC	7.20 ^a \pm 0.09	0.15 ^b \pm 0.02	3.65 ^{ab} \pm 0.37	160 ^c \pm 3.6	753.83 ^a \pm 30.02	16.67 ^b \pm 0.47	0.04 ^b \pm 0.01	0.13 ^b \pm 0.01	0.01 ^a \pm 0.004

^{ab} Lettering indicates statistical differences $p < 0.05$

Surface water chemistry was highly variable between sites and likely contributed to sediment redox status. Surface water at EB had higher pH and DO, and lower conductivity than QC and LBC (Table 5-3) ($p < 0.02$). Surface water dissolved Fe and Mn concentrations were slightly higher for QC and LBC than EB, though often below detection limits (5-20 μgL^{-1}). LBC surface water temperatures are lower than QC and EB, likely due to water inputs from a shaded creek and flowing water ($p < 0.003$). Further, QC had excessively low surface water DO (0.75 $\text{mg-O}_2 \text{L}^{-1}$). In summary, sediment oxidation only occurred in EB sediments, which was likely controlled by site hydrology and surface water chemistry.

5.3.2 Metal biogeochemistry in sediment and porewater

For non-spiked sediments, porewater Zn was relatively low and not released (Figure 5-5). Non-spiked sediment porewater Zn concentrations did not exceed 50 μgL^{-1} and were similar between saturated and dry treatments ($p > 0.2$). Further, porewater Zn concentration was constant for dry, non-spiked sediments between day-1 and 30 ($p > 0.05$). While LBC and QC were not fully oxidized, the lack of Zn-release for EB suggests this may be due to the low total Zn (<65 mg kg^{-1}).

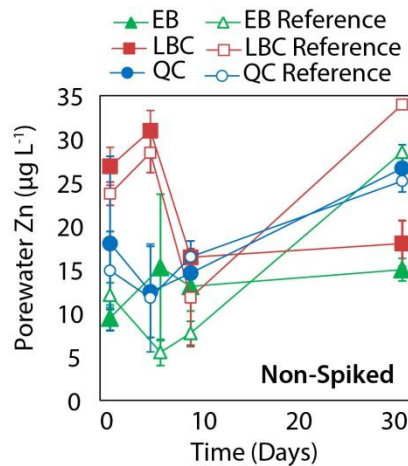


Figure 5-5. Temporal changes in porewater Zn (\pm standard error, SE) for natural sediments show low Zn in porewater for non-spiked sediments.

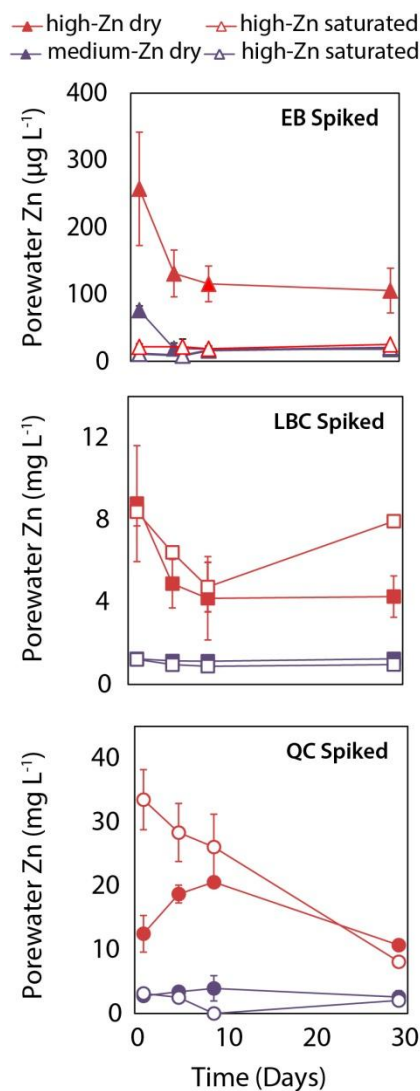


Figure 5-6. Porewater Zn (\pm SE) in days after inundation for spiked sediments show relatively little evidence for Zn-oxidative release, with the exception of EB.

Comparatively, porewater Zn was high in spiked sediments with Zn-release occurring for EB only (Figure 5-6). Porewater Zn in dry-treatment EB sediments were 5-10x higher than the saturated-treatment sediments on day-1. In both the medium and high spiked sediments, porewater concentrations decreased by day-5. The high-spike remained above the U.S. EPA Water Quality Criteria (WQC) for Zn until day-9. Although QC and LBC did not show evidence of Zn-release, porewater Zn was substantially higher than EB sediments, with an average of 12.0

$\pm 1.7 \text{ mgL}^{-1}$ for QC, $3.6 \pm 0.5 \text{ mgL}^{-1}$ for LBC, and $59.2 \pm 12.1 \text{ }\mu\text{gL}^{-1}$ for EB ($p < 0.00001$). With the exception of the medium-Zn treatment for EB ($p = 0.05$), no significant decrease in total-Zn was observed between days-1 and 30 for any site or Zn-spiked treatment ($p > 0.1$). Additionally, there were no statistical differences between total Zn in saturated versus dry treatments ($p > 0.1$).

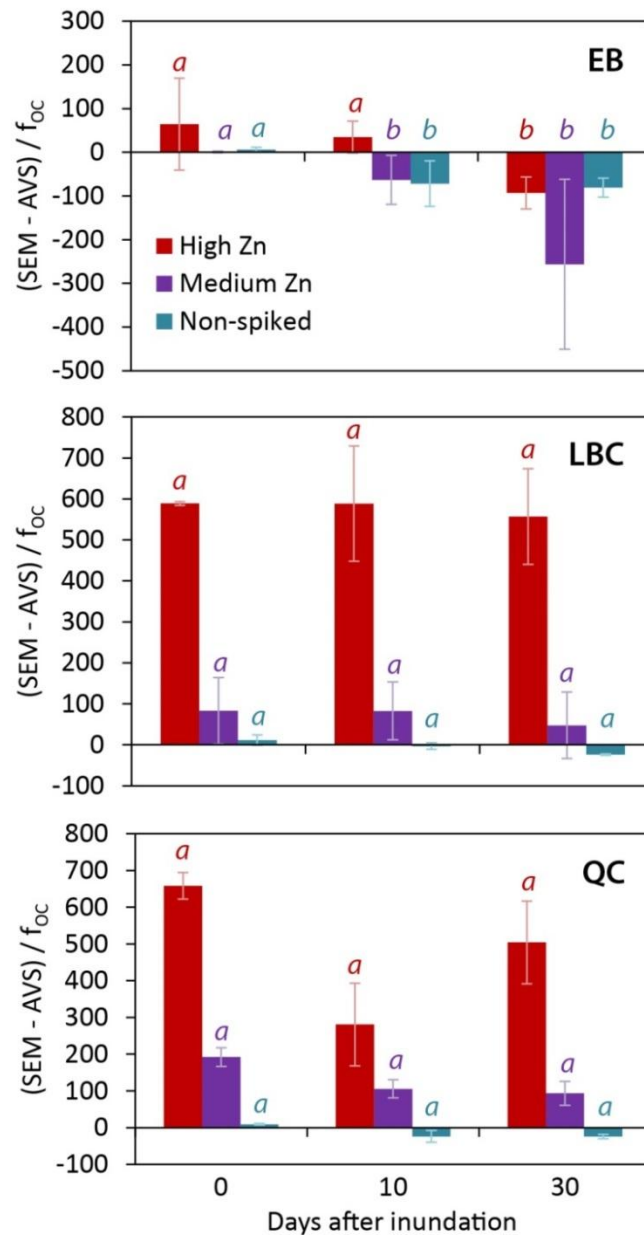


Figure 5-7. Metal binding to sulfide as predicted by the theoretical method for toxicity $(SEM - AVS) / f_{oc}$ for dry treatment sediments only. Statistical lettering signifies differences between sampling days for each sediment.

Metal binding to sulfide and theoretical toxicity was estimated using the $(SEM-AVS)/f_{OC}$ model. Non-spiked sediments had mostly negative values, with a range of -202.9 to 96.01, indicating sediments are likely not-toxic to benthic organisms. Spiked sediments generally had high positive values, suggesting possible toxicity to benthic organisms (Figure 5-7). Time series analyses show metal binding to sulfide increased with inundation time for EB ($p < 0.03$). Sediment oxidation generally decreases sulfide content; however, the only significant difference between dry and saturated treatments was for QC (not EB) ($p < 0.06$) (Figure D-2). Acid volatile sulfide was highest in EB and LBC, lowest in QC sediments ($p < 0.01$). Overall, QC had the highest theoretical toxicity as estimated by the $(SEM-AVS)/f_{OC}$ model. A summary of additional sediment chemical parameters, including total metals, is provided in Table 5-1.

5.3.3 Chemical speciation modeling

Since only one sediment type was completely oxidized, chemical modeling was needed to predict effects of oxidation and sediment drying to LBC and QC. Modeling of three chemical fate scenarios in sediment was conducted, including two different routes of sediment oxidation and one form of sediment desiccation. In the first oxidation model, incremental addition of $O_2(g)$ to the SWI predicted a decrease in dissolved porewater Zn inconsistent with field observations for EB spiked sediments (Figure 5-8). In the second oxidation model, where oxidized surface water was equilibrated with sediment (i.e. Zn-containing minerals), dissolution of smithsonite, sphalerite, and $Zn(OH)_2$ were predicted. Similar to the first oxidation model, the concentration of Zn^{+2} actually decreased with oxidation, transforming to other partially dissolved phases ($ZnHCO_3$, $ZnCO_3$).

The evaporation model predicts a 10x increase in porewater Zn associated with evaporation at EB, similar to what was observed for EB at medium to high Zn content. This

increase in Zn is concurrent with the dissolution of $Zn(OH)_2$ and smithsonite, which is mostly tied to a calculated decrease in porewater pH with evaporation, from 6.9 to 5.56. Concurrently, precipitation of amorphous and crystalline iron oxides is predicted while carbonates dissolve to buffer decreasing pH. When porewater values for spiked LBC and QC sediments were run through the model, similar results were found, suggesting similar effects would have occurred if sediments fully dried.

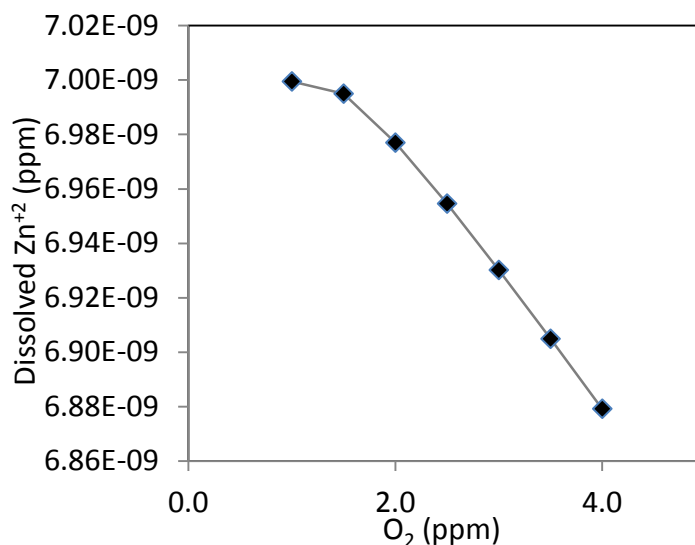


Figure 5-8. Model predicted sediment oxidation leads to decreased porewater Zn.

5.3.4 Benthic and periphyton community effects

Periphyton net primary productivity (NPP) was generally low and not affected by elevated sediment Zn or sediment drying/wetting. Visual observations confirmed periphyton abundance was low as a number of glass colonization discs were buried by sediment deposition. NPP was often low and sometimes negative (especially at EB), which indicates respiration exceeds photosynthesis in these surface sediments. Dry and saturating treatment NPP were statistically similar ($p > 0.5$) for all sites except LBC (Figure 5-9a). For LBC, the two spiked

sediments had higher NPP in the dry treatment than saturated and non-spiked dry-treatments ($p < 0.05$). These findings are not affected when buried disks are removed from the analysis.

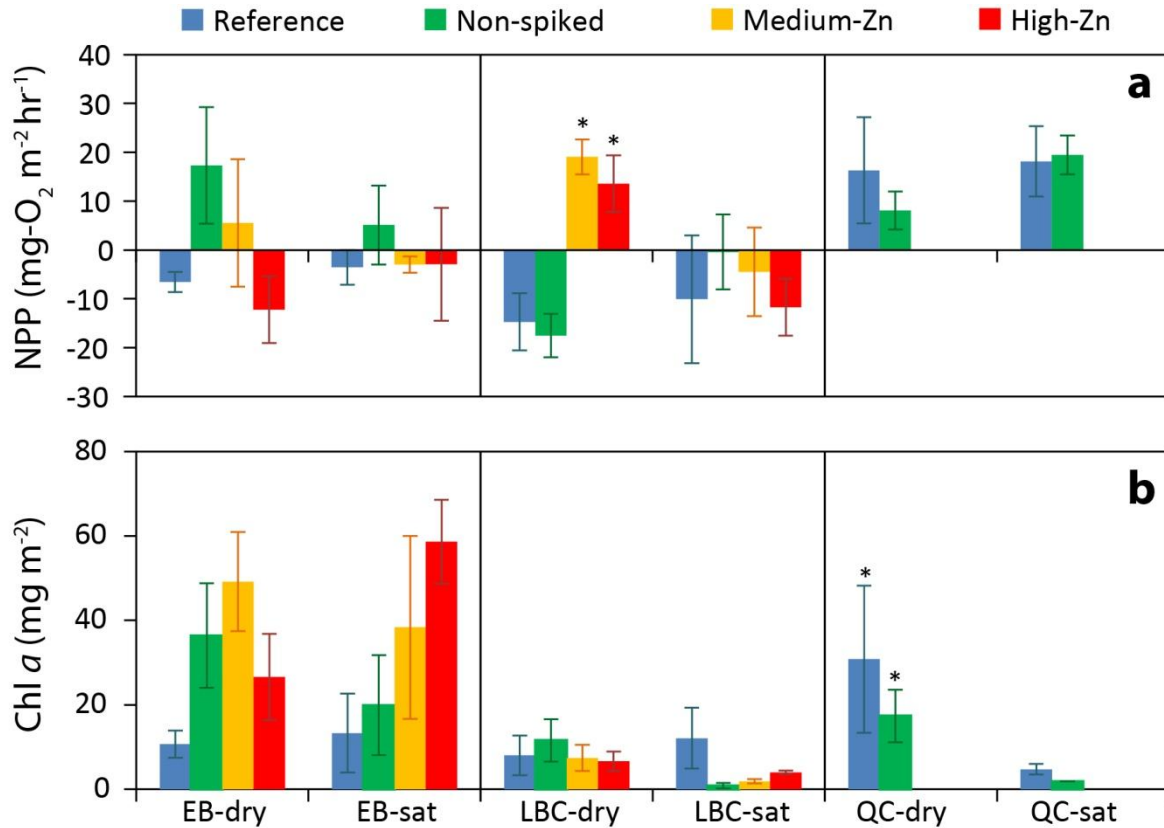


Figure 5-9. Net primary productivity (NPP) and biomass of chlorophyll (Chl) *a* (\pm SE) for each site comparing dry and saturated (sat) treatments. Asterisks indicate statistical differences between site treatments.

Periphyton Chl *a* biomass was a more sensitive endpoint to Zn than NPP. Chl *a* showed higher productivity for EB than LBC and QC sediments ($p < 0.002$) (Figure 5-9b). While the reference sediment usually had higher Chl *a* for QC and LBC deployments, it had the lowest Chl *a* for EB. There were no differences in Chl *a* content between dry and saturating-treatments, except for QC, which had higher Chl *a* in dry-treatment sediments ($p < 0.03$). No apparent effects to Chl *a* from Zn-release were observed; however, there was a strong negative correlation between porewater Zn and Chl *a* for spiked sediment types ($p < 0.08$, $r^2 = 0.75$) (Figure 5-10).

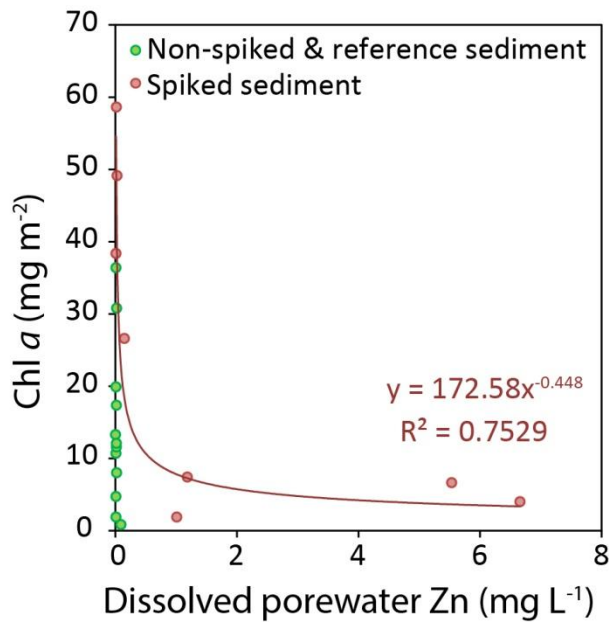


Figure 5-10. A strong negative correlation predicts the effect of porewater Zn on chlorophyll (Chl) *a* production (all sites included). This relationship was not observed for natural and reference sediment as Zn concentrations were too low to show effects.

Contrary to expectations, sediment drying increased benthic macroinvertebrate abundance, richness, and diversity for EB sediments ($p < 0.03$) (Figure 5-11). No effects on benthic communities were observed for QC or LBC between dry and saturating treatments ($p > 0.2$). Further, no significant differences between spiked and natural sediments were observed for EB, QC, or LBC ($p < 0.12$). Abundance and richness were statistically higher in LBC and EB than QC ($p < 0.02$) though no difference in species diversity was observed. *Chironomidae* (midge larvae) were dominant in 100% of mesocosms for QC ($rN = 0.6 \pm 0.07$), *Oligochaeta* (aquatic worms) in 74% of mesocosms for EB ($rN = 0.5 \pm 0.05$), and *Asellidae* (isopod crustaceans) in 52% of mesocosms for LBC ($rN = 0.5 \pm 0.04$).

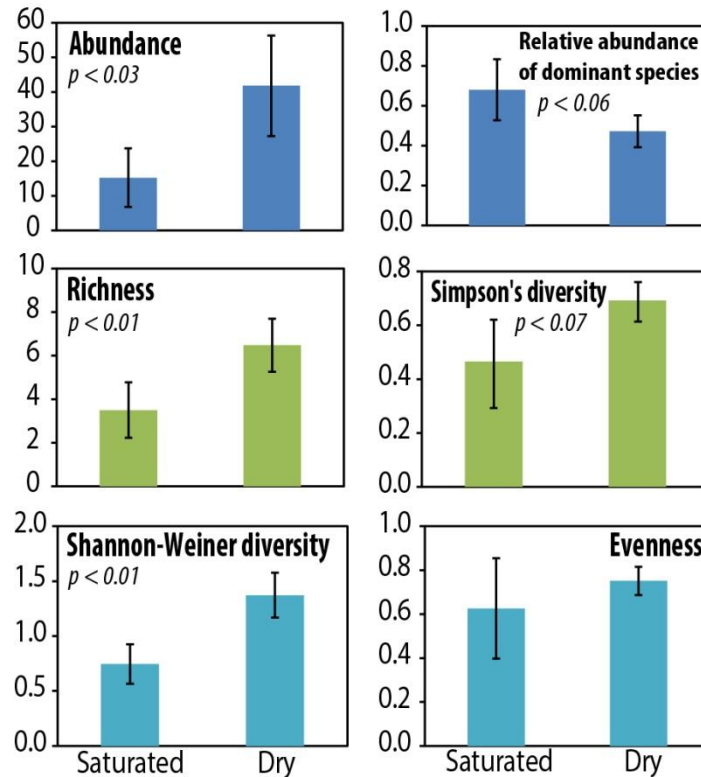


Figure 5-11. Abundance, richness, and diversity (\pm SE) were statistically different between dry and saturating treatments in EB sediments ($p < 0.03$).

A strong positive correlation between porewater pH and benthic community metrics (abundance, richness, diversity) was observed for all three sites ($p < 0.005$), as shown in [Figure 5-12](#). While no significant or direct effect of porewater Zn on benthic community metrics was observed ($p > 0.25$), Chl *a* biomass (which was affected by porewater Zn) was correlated with pH when all sites are included ($p < 0.02$) ([Figure 5-13a](#)). When analyzed as individual sites; however, a relationship between Chl *a* and pH is not observed. Porewater pH was strongly influenced by DO, with a positive correlation for EB ($p < 0.02$, $r^2 = 0.4$) and negative correlation for QC and LBC ($p < 0.01$, $r^2 = 0.5$) ([Figure 5-13b](#)). The effect of DO on pH appears stronger than Chl *a* biomass for all three sites ([Figure 5-13c&d](#)). No significant correlations between Chl *a* and invert metrics was observed ($p > 0.1$), but it is not surprising given the organisms sampled consume periphyton when present. A negative linear relationship between porewater DO and Fe

is also observed for all three sites ($p < 0.00001$, $r^2 = 0.6$), likely due to reductive dissolution of Fe-oxyhydroxides.

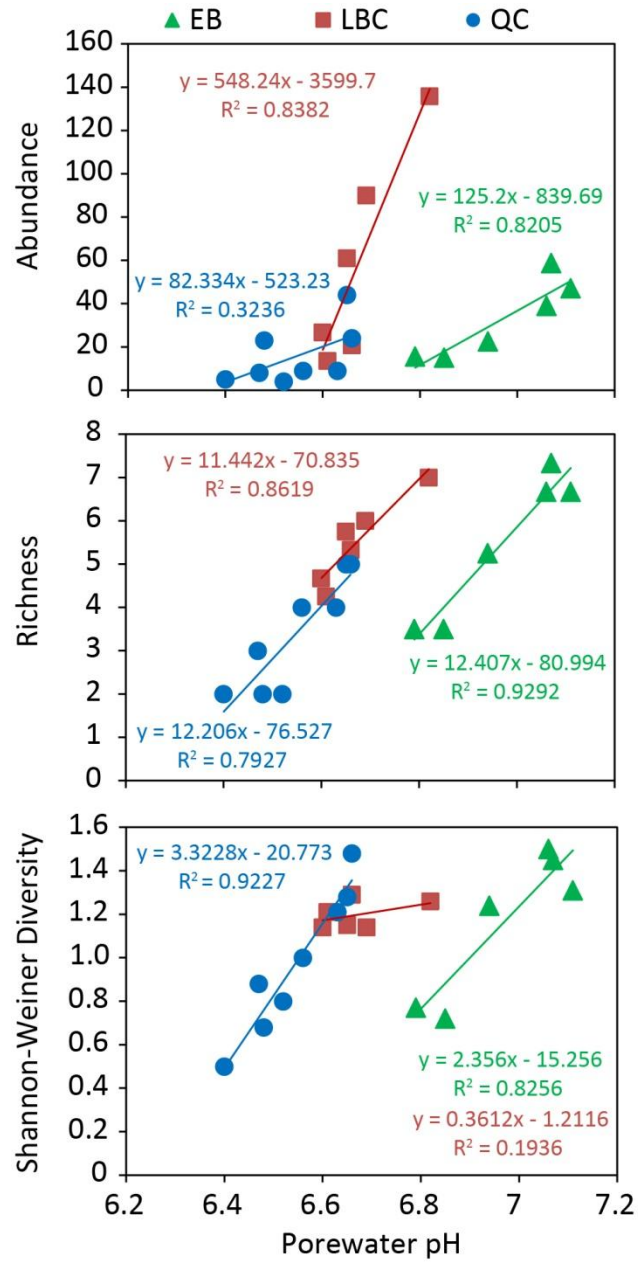


Figure 5-12. pH was strongly correlated with abundance, richness, and Shannon-Weiner diversity for all three sites.

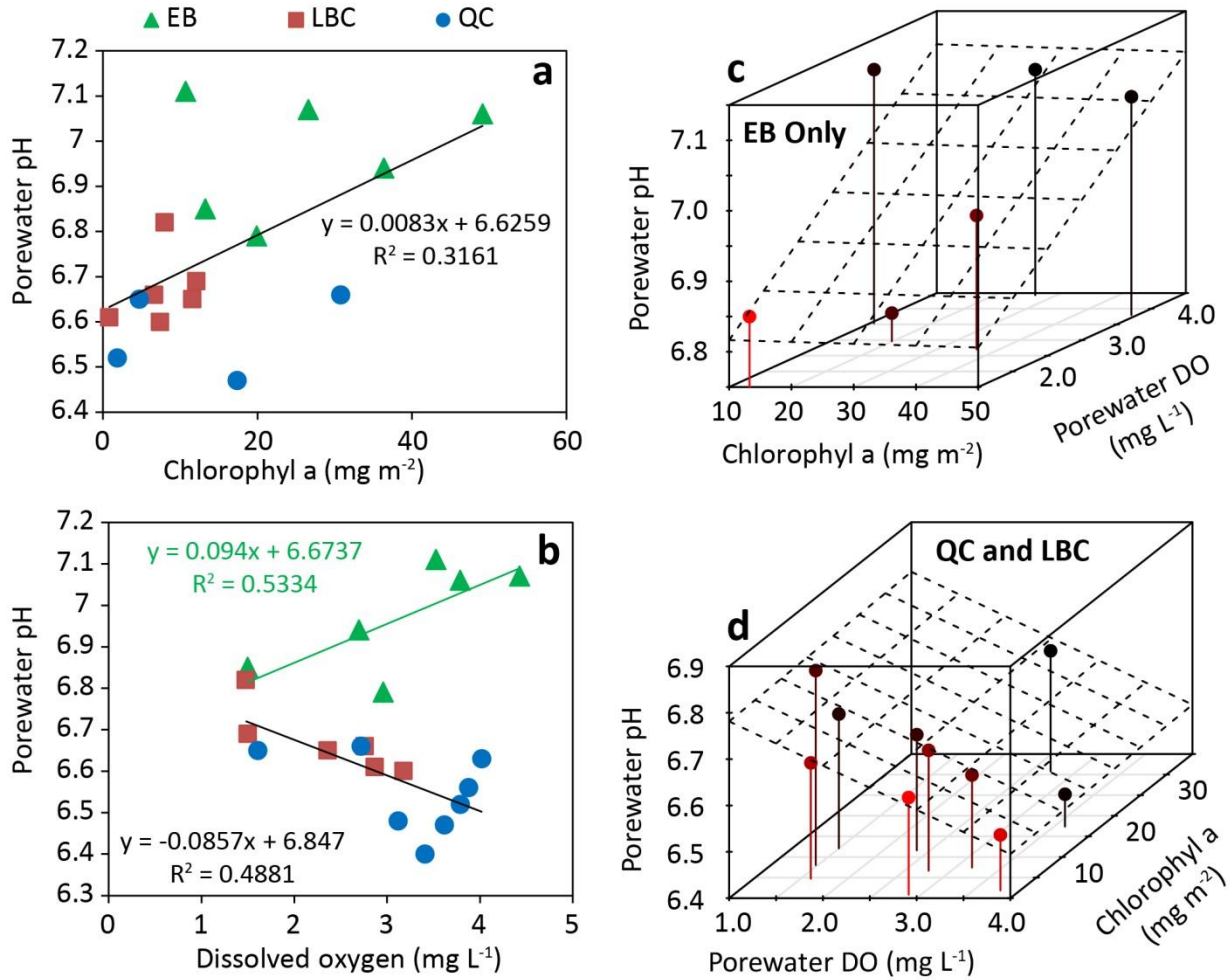


Figure 5-13. Relationships between Chlorophyll (Chl) *a*, porewater dissolved oxygen (DO) and porewater pH are shown. Chl *a* was correlated with porewater pH between sites, and may be attributed to the different pH and DO relationship for EB versus QC/LBC.

Toxicity testing with *H. azteca* was unsuccessful with complete or near-complete mortality in QC and EB (did not do exposure for LBC). At QC, DO was low at the SWI around 0.5 mg L^{-1} , which likely led to mortality. At EB, no specific water quality issues were observed, so it is unclear why mortality was high (Figure 5-14). Mortality was likely caused by burial as lower sedimentation mesocosms (generally) showed higher survival. Other (less likely) possibilities include predation by leeches or loose exposure bottle lids allowing organism escape.

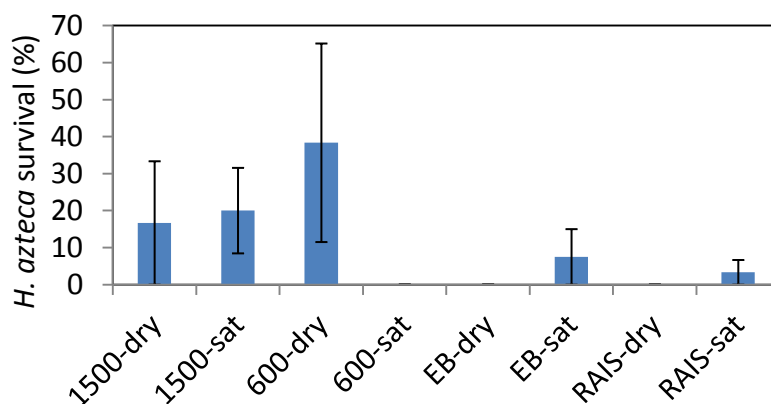


Figure 5-14. Survival of *H. azteca* toxicity testing at EB show low survival.

5.4 Discussion

5.4.1 Sediment chemistry of Zn-release

The release of bioavailable porewater Zn observed for EB high-Zn spiked sediments cannot be attributed to surface water dilution or erosional-loss, and therefore likely results from changes in sediment chemistry. This argument is supported by the lack of total sediment Zn decrease in high-Zn treatment, although it was observed for the medium-Zn spike. Further, given the Zn-spiking method, Zn should be bound to sediment phases after just ~40 days, which is well within the 9 month equilibration used in this study (Simpson et al., 2004). The acid neutralization with NaOH likely promoted Zn-hydroxide formation while oxygen deprivation encouraged formation of ZnS. The Zn-release observed at EB on day-1 of the inundation is similar to results observed in laboratory testing, although occurring at higher total-Zn concentrations (~310 mgkg⁻¹ field versus 18 mgkg⁻¹ laboratory) (Nedrich and Burton, 2017).

Although the purpose of this study was to determine if Zn-release associated with sediment drying is occurring in the environment, this chemical phenomenon seems less important compared to elevated porewater Zn in QC and LBC (as compared to EB). Since Zn was similar for medium (EB/QC same) and high-Zn treatments between sites, Zn-

binding/speciation is likely affecting bioavailability. This relationship may be influenced by site hydrology. Surface water at EB had significantly higher DO and pH, encouraging Zn binding to hydroxides, carbonates, and Fe/Mn-oxyhydroxides. LBC and QC were more acidic and reduced, leading to dissolution of these Zn and formation of Zn-sulfides. Site hydrology would promote EB sediment oxidation, since inundation time was lowest in EB. Further, QC DO (0.75 mg L^{-1}) is below ideal O_2 -criteria for benthic organisms, thus preventing oxidation during drying for QC sediments. This implies surface water composition should include site-specific physicochemical characteristics when conducting toxicity testing.

Modeling results suggest evaporation is an important pathway for Zn-release in sediments, attributable to a decrease in $\text{Zn}(\text{OH})_2$ and smithsonite being associated with pH decreases. Also, though the oxidation models were effective at predicting porewater pH from surface water and mineral exchange, they were not effective indicators of bioavailable Zn. This suggests that evaporation may be a more important driver of Zn-release than oxidation in these sediment types through precipitation/dissolution of metal salts. Interestingly, a pH decrease was not experimentally observed in EB porewater during the Zn-release in spiked sediments. This suggests other processes are on-going. It is possible that pH buffering is resulting from periphyton metabolism which is not accounted for in chemical models. In previous laboratory studies without periphyton, a decrease in pH with sediment drying was observed, as predicted by the chemical model (Nedrich and Burton, 2017). This is another example where traditional laboratory toxicity test conclusions may not reflect *in-situ* conditions.

It is interesting that the oxidation model did not effectively predict bioavailable Zn in porewater. Evidence from previous studies has suggested oxidation alters metal chemistry through oxidation of metal sulfides (Simpson et al., 2012). It is likely that chemical modeling

would be more realistic if additional data on major anions (and not just cations) were added inputs. Also, since the models are being compared to results for EB, one difference that would likely be observed is oxidation of greater quantities of FeS (and subsequent pH decreases) for QC and LBC sediments as Fe^{2+} concentrations are significantly higher in those sediments.

The evaporation model predicts that when oxidized, QC and LBC sediments should behave similarly to EB. In instances of extreme drought, when groundwater connectivity is disturbed and wetland mudflats oxidize, Zn-release is expected. Since evaporation is temperature dependent, this effect is probably more prominent in areas with higher heat indices or low moisture. However, with increasing hydrologic regime shift predicted by climate models, regions of high heat and drought will expand (Milly et al., 2005).

5.4.2 Biological impacts from Zn-release

Using USEPA approved methods for predicting Zn-toxicity to benthic organisms, the non-spiked sediments were predicted to be non-toxic while spiked (medium and high treatments) predicted toxicity (USEPA, 2005). Using three methods, including porewater water quality criteria (WQC), sediment quality guidelines (SQG's) for total metals, and SEM-AVS, non-spiked sediments were non-toxic (with $<50 \mu\text{g-Zn L}^{-1}$, $<50 \text{ mg kg}^{-1}$, and $< 96 \mu\text{mol g}^{-1}$, respectively) (Buchman, 2008; Burton et al., 2005; USEPA, 2016a). For spiked EB sediments, one of three indicators predicted toxicity, with a total sediment concentration exceeding threshold effects levels ($\text{TEL}_{\text{Zn}} = 123 \text{ mg kg}^{-1}$). Both SEM-AVS and porewater metal concentrations; however, predicted non-toxic sediments. For QC and LBC spiked sediments, all three indicators predicted toxicity, with high porewater Zn (average 3.6 and 12 mg L^{-1}), high SEM-AVS values (range 100-600), and total metals exceeding the TEL. From these analyses, we would expect significant effects to biotic indices in QC and LBC sediments.

In accordance with predicted effects by USEPA methods (WQC, SQG's, SEM-AVS), benthic community richness and abundance were significantly higher for EB as compared to QC (but not LBC), while Chl *a* was highest overall for EB. For EB dry-treatment sediments, community composition indices were actually higher than saturated treatments. This is opposite of the expected relationship, as Zn-release elevated porewater concentrations to a lethal threshold for the first 5 days of the inundation. This suggests short temporal releases of Zn may be effective at increasing nutrient availability. Another possibility is the dried sediments had characteristics promoting benthic health, such as higher oxygen content for biological uptake or increased nutrient availability (NO_3^- or PO_4^{2-}). Overall, predictive toxicology methods likely overestimated toxicity in LBC, but were effective for QC and EB.

The strong negative relationship between porewater Zn and Chl *a* production, while based on only a few high Zn data points, has been verified in a previous study and is biologically relevant (Morris et al., 2005). Periphyton likely increases benthic community indices through optimization of sediment pH (more alkaline) and providing a food source for grazers. The positive relationship observed between Chl *a* and porewater pH (Figure 5-13) could be explained by photosynthesis, which increases the pH by consuming dissolved CO_2 . Photosynthesis increases dissolved oxygen, which was seen to increase with pH for EB, but not for LBC and QC. In LBC and QC sediments, the negative correlation between DO and pH may be attributed to FeS oxidation (producing acidity). As porewater Zn was not correlated with any benthic community index, Zn likely has an indirect effect by limiting growth of periphyton (Paulsson et al., 2000).

While it may seem the NPP results contradict the photosynthesis theory (i.e., the relationship between pH and benthic community health), there are many reasons to not consider

the NPP data. For example, NPP and primary productivity are not always correlated if microbial respiration is variable. In this study respiration was not measured, so it is impossible to determine gross primary productivity from NPP. Studies have shown that rates of photosynthesis vary disproportionately to Chl *a* biomass based on bioavailability of nutrients, which may also confound a NPP to Chl *a* relationship (Guasch et al., 2003). Additionally, many colonization discs (which NPP was estimated from) became buried (up to 2-cm). While this is not surprising given the high rates of sedimentation in freshwater marshes (Mitsch et al., 2014), perhaps a better method for estimating NPP and GPP in high sedimentation systems is needed.

5.4.3 Comparing laboratory toxicity testing to field toxicology

Previously, laboratory testing of the same sediment types resulted in 10-fold increases in porewater Zn-release, at relatively low total metal contents (Zn~18 mg kg⁻¹) (Nedrich and Burton, 2017); however, the laboratory results were not predictive of field results for a few reasons. First, the surface water at QC and LBC had lower DO compared to the laboratory, which made sediment oxidation unlikely. Second, total Zn in non-spiked sediments was much lower than the laboratory study, making changes to porewater-Zn less significant for biota. Third, the laboratory study did not include potential impacts of periphyton on benthic organism responses to metal exposure. Fourth, this study was conducted during especially high Great Lakes water levels, and groundwater and precipitation may have prevented dry-treatment sediments from drying. Fifth, surface water renewal times may have been underestimated in the laboratory study (after ~72 hours) as compared to field sites, particularly for EB and LBC. This implies advection and diffusion of metals from porewater and sediment was likely greater in field conditions. Finally, bioturbation by organisms may alter sediment chemistry and increase

Zn uptake by benthic organisms (Remaili et al., 2016), a variable which was not included in the laboratory experiments.

Differences observed between the laboratory and field studies provide useful lessons for conducting realistic and context-dependent toxicity tests. Previous studies suggested the importance of periphyton on Zn-exposure and effects to organisms, where pre-exposing algae to metals prior to toxicity testing increases Zn exposure (De Schamphelaere et al., 2004a). Input water used in sediment toxicity testing is standardized (reconstituted deionized), not varying between sample sites; however, in this set of experiments surface water composition was important in predicting the bioavailability and effects of Zn (USEPA, 1991). While collecting large quantities of site water for testing is often unrealistic, it is recommended that a site-specific range of reconstituted water types be used to estimate the “best” and “worst” case-scenarios with appropriate surface water renewal times to assess metal bioavailability.

5.4.4 General implications for aquatic systems

Zn-release from sediment drying and oxidation is occurring in the Great Lakes and appears to be proportional to drought duration, sediment metal content and influenced by sediment/water chemical composition. It is important to consider the effects of water level variability on metal bioavailability in sediments, particularly in aquatic systems with long periods of drought which are hydrologically isolated with limited baseflow. Zn-release may grow in importance as hydrologic extremes (flood/drought) are expected to increase as an effect of climate change (Milly et al., 2005).

Improved environmental regulation for metals in aquatic systems would include more realistic toxicity testing, to set standards based on the ecological context for a wider range of water chemistries and also include periphyton in shallow water systems. Laboratory testing

overestimated sediment Zn-release and the important effects to periphyton were not recorded. While field surveys for periphyton are recommended in the USEPA-approved Rapid Biological Assessment methods for benthic health, this practice is not extended to predictive models or toxicity testing (USEPA, 1999). This study showed periphyton is an important vector for Zn in the environment, which should be included in predictive toxicology models and included as a variable in standardized toxicity testing.

Chapter 6 - Conclusion

Predicting the fate and effects of metal contaminants is complex due to the interactive effects of pH, redox, and biological transformations on metal speciation and bioavailability. In this dissertation, the interplay of physical, chemical, and biological factors associated with water level variability were elucidated as to their effects on metal biogeochemistry. Through laboratory and field testing, results showed that post-drought sediment re-flooding affected metal bioavailability in freshwater sediments.

To address the effects of water level variability on sediment metal bioavailability, a series of laboratory microcosm experiments with Great Lakes (alkaline) sediments and elevated metal (slightly acidic) sediments were conducted (Chapters 2-4). Then, findings from the laboratory studies were verified in a field mesocosm study (Chapter 5). An overview of the key findings from these experiments, implications of this research, and suggestions for future research are outlined in the following sections.

6.1 Summary of key findings

Zn-release from sediments to porewater can occur upon inundation after prolonged drought, with impending effects to benthic organisms. In chapters 2-3, this was shown in laboratory microcosm studies, where releases of Zn were attributed to chemical oxidation of ZnS and dissolution of Zn-bicarbonates. This effect is most likely when sediments are thoroughly dried (>15-days) and oxidized where total Zn concentrations in sediment are in exceedance of 18

mg kg⁻¹. Observed sub-lethal effects to *H. azteca* indicate Zn-release is most threatening to benthic invertebrates as they are more exposed to elevated porewater Zn than epibenthic and planktonic species.

The occurrence and effects of hydrological Zn-release has important implications from a water management and restoration perspective. For example, to protect organisms from Zn-release in Zn contaminated areas, water level management can be practiced (when possible) to avoid re-inundation of dried areas during biologically important periods, e.g., reproduction. In cases where water levels cannot be manipulated, water and sediment sampling for metals should make sure to include periods that reflect hydrologic variability. Reconnecting restored wetlands to the watershed, in some cases, could be delayed, until released Zn and nutrients have been transformed to non-bioavailable phases. In semi-arid wetlands where long periods of sediment oxidation and desiccation followed by extreme flooding is common, monitoring for biogeochemical metal-release and adaptive management techniques may be needed.

This dissertation also presented important findings on the biogeochemical cycling and bioavailability of V in sediments. In chapter 4, laboratory microcosm studies showed V to be relatively unaffected by changes to redox associated with re-inundation of dried sediment. Although sediment V content was substantially elevated (>800 mg kg⁻¹), V remained bound as V(III/IV) oxides and showed no significant effects to *D. magna* or *H. azteca* during toxicity testing. However, co-occurring Zn-release associated with post-drought re-flooding did lead to sublethal effects to growth of *H. azteca*.

The differential effects of post-drought re-flooding on Zn versus V highlights the importance of metal speciation on our ability to predict bioavailability and toxicity. Total metal concentrations alone were insufficient to predict effects of these two metals. While post-drought

re-flooding had significant impacts on the toxicity and bioavailability of Zn to benthic organisms, V is less so. Further, it is important to consider benthic community health in metal-contaminated reservoirs, to better preserve important ecosystem services, such as water quality, enhanced nutrient cycling, and productive commercial fisheries

In the final chapter, Zn-release was observed in a field study, although with seemingly beneficial effects to benthic organisms. The differential effects of Zn-release to organisms in laboratory versus field exposures is likely linked to differences in a number of variables, including surface water chemical composition, variable sediment drying times, hydrologic connectivity, vertical and horizontal water mixing, bioturbation, and total sediment Zn. High pH in sediments was positively correlated with benthic community abundance, richness, and diversity. Further, increased pH was attributed to the biomass (Chl *a*) and primary productivity of sediment-bound periphyton. While post-drying re-inundation was beneficial to benthic communities, elevated Zn in reduced porewater led to decreased growth of algae. Elevated sediment Zn can affect benthic organisms in (at least) three ways, by decreasing growth of periphyton and therefore (1) decreasing sediment pH, and (2) potentially decreasing organism food supply(e.g., periphyton), and also by (3) toxic effects due to adsorption or intake of bioavailable Zn through direct exposure.

In comparing the field study to laboratory microcosm testing, a few important lessons on the efficacy of laboratory toxicity testing were learned. First, whenever possible, a variety of surface water types representative of a field site should be tested, as the chemical composition will invariably affect the bioavailability of metals in the sediment. Second, uptake and effects of contaminants on periphyton and soil microbes is an important vector for understanding benthic toxicology. Finally, physicochemical variables, such as water level alteration, should not be

ignored as a variable impacting metal bioavailability. It is very important to consider and include the effects of biological and physicochemical variables in toxicity testing and predictive toxicology models for benthic community health.

6.2 Suggestions for future work

Further work is needed to appropriately model the interactions between periphyton, metals, and other types of contaminants. Growth and prevalence of periphyton can be highly complex, being dependent on several variables (sunlight, nutrients, substrate quality, etc.); however, periphyton effects to metal bioavailability and benthic community metrics are significant. Modeling this chemical-biological linkage would likely improve the field-realism of predictive toxicology models.

Although this dissertation shows V is relatively non-labile in circumneutral to acidic sediment types, additional testing of V redox-dynamics is needed in more alkaline systems where mobility is likely increased (Canada, 2010). Since V is an oxy-anion, its mobility is increased in anionic surface waters, where possible exposure and uptake to water column species would be possible. Increasing experimental drying time to 30+ days may indirectly decrease V bioavailability in sediments if acidity is produced from FeS oxidation. It is also important to test a range of sediment types to better develop accurate models of bioavailability and toxicity. Periphyton uptake and effects to V bioavailability should additionally be quantified to further determine biogeochemical cycling and exposure pathways.

The overall mechanisms of metal toxicity in sediments during transitions from dry to saturated to flooded phases must be addressed at a multitude of scales. To address specific chemical mechanisms of metal dynamics, a micro-scale or micro-habitat focus was necessary for this study. Value can be added to this topic by including a larger scale focus (aerially) or by

including multiple stressors effects to sediment quality and benthic community health. For instance, other studies have focused on the effects of water levels on plant diversity and richness, which has important implications for overall environmental health (Isbell et al., 2011; Keddy and Reznicek, 1986). Future effort should be applied to weaving ecological, toxicological, and biogeochemical knowledge into a digestible paradigm on the role of water level variability in aquatic environments.

References

- Abollino, O., Giacomino, A., Malandrino, M., Mentasti, E., Aceto, M., Barberis, R., 2006. Assessment of metal availability in a contaminated soil by sequential extraction. *Water. Air. Soil Pollut.* 173, 315–338. doi:10.1007/s11270-005-9006-9
- Allen, H.E., Fu, G., Boothman, W., DiToro, D.M., Mahoney, J.D., 1991. Determination of acid volatile sulfide and selected simultaneously extractable metals in sediment. Washington, DC.
- Allen, H.E., Fu, G., Deng, B., 1993. Analysis of acid-volatile sulfide (AVS) and simultaneously extracted metals (SEM) for the estimation of potential toxicity in aquatic sediments. *Environ. Toxicol. Chem.* 12, 1441–1453.
- Amato, E.D., Simpson, S.L., Belzunce-Segarra, M.J., Jarolimek, C. V., Jolley, D.F., 2015. Metal fluxes from porewaters and labile sediment phases for predicting metal exposure and bioaccumulation in benthic invertebrates. *Environ. Sci. Technol.* 49, 14204–14212. doi:10.1021/acs.est.5b03655
- Amato, E.D., Simpson, S.L., Remaili, T.M., Spadaro, D.A., Jarolimek, C. V., Jolley, D.F., 2016. Assessing the effects of bioturbation on metal bioavailability in contaminated sediments by diffusive gradients in thin films (DGT). *Environ. Sci. Technol.* 50, 3055–3064. doi:10.1021/acs.est.5b04995
- ASTM, 2005. E1706-05. Standard test method for measuring the toxicity of sediment-associated contaminants with freshwater invertebrates. ASTM International, West Conshohocken, PA.
- Atkinson, C.A., Jolley, D.F., Simpson, S.L., 2007. Effect of overlying water pH, dissolved oxygen, salinity and sediment disturbances on metal release and sequestration from metal contaminated marine sediments. *Chemosphere* 9, 1428–1437.
- ATSDR, 2017. Toxicity profile for Zn, Exposure.
- Bash, J., Berman, C., Bolton, S., 2001. Effects of turbidity and suspended solids on salmonids, Final Research Report. Seattle, Washington.
- Baumgärtner, D., Mörtl, M., Rothhaupt, K.O., 2008. Effects of water-depth and water-level fluctuations on the macroinvertebrate community structure in the littoral zone of Lake Constance. *Hydrobiologia* 613, 97–107. doi:10.1007/s10750-008-9475-0

- Blankson, E.R., Klerks, P.L., 2016. The effect of bioturbation by *Lumbriculus variegatus* on transport and distribution of lead in a freshwater microcosm. *Environ. Toxicol. Chem.* 35, 1123–1129. doi:10.1002/etc.3248
- Borgmann, U., Norwood, W.P., 1995. Kinetics of excess background copper and zinc in *Hyalella azteca* and their relationship to chronic toxicity. *Can. J. Fish. Aquat. Sci.* 52, 864–874.
- Borgmann, U., Norwood, W.P., Clarke, C., 1993. Accumulation, regulation and toxicity of copper, zinc, lead and mercury in *Hyalella azteca*. *Hydrobiologia* 259, 79–89. doi:10.1007/BF00008374
- Borgmann, U., Norwood, W.P., Dixon, D.G., 2004. Re-evaluation of metal bioaccumulation and chronic toxicity in *Hyalella azteca* using saturation curves and the biotic ligand model. *Environ. Pollut.* 131, 469–484. doi:10.1016/j.envpol.2004.02.010
- Brinkman, S.F., Johnston, W.D., 2008. Acute toxicity of aqueous copper, cadmium, and zinc to the mayfly *Rhithrogena hageni*. *Arch. Environ. Contam. Toxicol.* 54, 466–472. doi:10.1007/s00244-007-9043-z
- Brown, C.L., 2000. Influence of acid volatile sulfides and metal concentrations on metal partitioning in contaminated sediments. *Environ. Sci. Technol.* 34, 4511–4516.
- Brumbaugh, W.G., Besser, J.M., Ingersoll, C.G., May, T.W., Ivey, C.D., Schlekot, C.E., Garman, E.R., 2013. Preparation and characterization of nickel-spiked freshwater sediments for toxicity tests: Toward more environmentally realistic nickel partitioning. *Environ. Toxicol. Chem.* 32, 2482–94.
- Buchman, M.F., 2008. NOAA Screening Quick Reference Tables, NOAA OR&R Report 08-1.
- Burton, G.A.J., Nguyen, L.T.H., Janssen, C., Baudo, R., McWilliam, R., Bossuyt, B., Beltrami, M., Green, A., 2005. Field validation of sediment zinc toxicity. *Environ. Toxicol.* 24, 541–553.
- Cai, W., Borlace, S., Lengaigne, M., van Rensch, P., Collins, M., Vecchi, G., Timmermann, A., Santoso, A., McPhaden, M.J., Wu, L., England, M.H., Wang, G., Guilyardi, E., Jin, F.-F., 2014. Increasing frequency of extreme El Niño events due to greenhouse warming. *Nat. Clim. Chang.* 5, 1–6. doi:10.1038/nclimate2100
- Calmano, W., Hong, J., Forstner, U., 1993. Binding and mobilization of heavy metals in contaminated sediments affected by pH and redox potential. *Water Sci. Technol.* 28, 223–235.
- Campana, O., Blasco, J., Simpson, S.L., 2013. Demonstrating the appropriateness of developing sediment quality guidelines based on sediment geochemical properties. *Environ. Sci. Technol.* 47, 7483–7489. doi:10.1021/es4009272
- Canada, E., 2010. Screening Assessment for the Challenge Vanadium oxide (Vanadium pentoxide).

- Caon, L., Forlano, N., Keene, C., Sala, M., Sorokin, A., Verbeke, I., Ward, C., 2015. The Status of the World's Soil Resources. Rome, Italy. doi:ISBN 978-92-5-109004-6
- Carpentier, W., Sandra, K., De Smet, I., Brigé, A., De Smet, L., Van Beeumen, J., 2003. Microbial reduction and precipitation of vanadium by *Shewanella oneidensis*. Appl. Environ. Microbiol. 69, 3636–3639. doi:10.1128/AEM.69.6.3636
- Carr, R., Nipper, M., Adams, W., Berry, W., Burton, G., Ho, K., MacDonald, D., Scroggins, R., Winger, P., 2001. Porewater toxicity test: Biological, chemical, and ecological considerations with a review of methods and applications, and recommendations for future areas of research. SETAC, Pensacola, FL, USA.
- Carvalho, P.S.M., Zanardi, E., Buratini, S. V., Lamparelli, M.C., Martins, Magali, C., 1998. Oxidizing effect on metal remobilization and *Daphnia Similis* toxicity from a Brazilian reservoir sediment suspension. Water Res. 32, 193–199.
- Chapman, P.M., Wang, F., Janssen, C., Persoone, G., Allen, H.E., 1998. Ecotoxicology of metals in aquatic sediments: binding and release, bioavailability, risk assessment, and remediation. Can. J. Fish. Aquat. Sci. 55, 2221–2243. doi:10.1139/f98-145
- Chasteen, N.D., 1983. The Biochemistry of Vanadium. Copper, Molybdenum, Vanadium Biol. Syst. 105–138. doi:10.1007/BFb0111304
- Chen, L., Fu, X., Zhang, G., Zeng, Y., Ren, Z., 2012. Influences of temperature, pH and turbidity on the behavioral responses of *Daphnia magna* and Japanese Medaka (*Oryzias latipes*) in the biomonitor. Procedia Environ. Sci. 13, 80–86. doi:10.1016/j.proenv.2012.01.007
- Clerments, W.H., Cherry, D.S., Van Hasse, J.H., 1992. Assessment of the impact of heavy metals on benthic communities at the Clinch River (Virginia): Evaluation of an index of community sensitivity. Can. J. Fish. Aquat. Sci. 49, 1686–1694.
- Cooper, M.J., Rediske, R.R., Uzarski, D.G., Burton, T.M., 2001. Sediment contamination and faunal communities in two subwatersheds of Mona Lake, Michigan. J. Environ. Qual. 38, 1255–65. doi:10.2134/jeq2008.0429
- Coops, H., Beklioglu, M., Crisman, T.L., 2003. The role of water-level fluctuations in shallow lake ecosystems - Workshop conclusions. Hydrobiologia 506–509, 23–27. doi:10.1023/B:HYDR.0000008595.14393.77
- Coops, H., Hosper, S.H., 2009. Lake and Reservoir Management Water-level Management as a Tool for the Restoration of Shallow Lakes in the Netherlands. Lake Reserv. Manag. 18, 37–41. doi:10.1080/07438140209353935
- Costello, D.M., Burton, G.A., Hammerschmidt, C.R., Rogevich, E.C., Schlekot, C.E., 2011. Nickel phase partitioning and toxicity in field-deployed sediments. Environ. Sci. Technol. 45, 5798. doi:10.1021/es104373h
- Costello, D.M., Burton, G.A., Hammerschmidt, C.R., Taulbee, W.K., 2012. Evaluating the

- performance of diffusive gradients in thin films for predicting Ni sediment toxicity. *Environ. Sci. Technol.* 46, 10239–46. doi:10.1021/es302390m
- Costello, D.M., Hammerschmidt, C.R., Burton, G.A., 2015. Copper sediment toxicity and partitioning during oxidation in a flow-through flume. *Environ. Sci. Technol.*
- Costello, D.M., Hammerschmidt, C.R., Burton, G.A., 2015. Copper sediment toxicity and partitioning during oxidation in a flow-through flume. *Environ. Sci. Technol.* 49, 6926–6933. doi:10.1021/acs.est.5b00147
- Councell, T.B., Duckenfield, K.U., Landa, E.R., Callender, E., 2004. Tire-wear particles as a source of zinc to the environment. *Environ. Sci. Technol.* 38, 4206–4214. doi:10.1021/es034631f
- Covich, A., Palmer, M., Crowl, T., 1999. The role of benthic invertebrate species in freshwater ecosystems: Zoobenthic species influence energy flows and nutrient cycling. *Bioscience* 49, 119–127.
- Creep, N.L., Shand, P., Hicks, W., Fitzpatrick, R.W., 2015. Porewater geochemistry of inland acid sulfate soils with sulfuric horizons following postdrought reflooding with freshwater. *J. Environ. Qual.* 44, 989–1000. doi:10.2134/jeq2014.09.0372
- Davranche, M., Bollinger, J.C., 2000. Release of metals from iron oxyhydroxides under reductive conditions: Effect of metal/solid interactions. *J. Colloid Interface Sci.* 232, 165–173.
- De Jonge, M., Teuchies, J., Meire, P., Blust, R., Bervoets, L., 2012a. The impact of increased oxygen conditions on metal-contaminated sediments part I: Effects on redox status, sediment geochemistry and metal bioavailability. *Water Res.* 46, 2205–14. doi:10.1016/j.watres.2012.01.052
- De Jonge, M., Teuchies, J., Meire, P., Blust, R., Bervoets, L., 2012b. The impact of increased oxygen conditions on metal-contaminated sediments part II: effects on metal accumulation and toxicity in aquatic invertebrates. *Water Res.* 46, 3387–97. doi:10.1016/j.watres.2012.03.035
- de Livera, J., McLaughlin, M.J., Hettiarachchi, G.M., Kirby, J.K., Beak, D.G., 2011. Cadmium solubility in paddy soils: Effects of soil oxidation, metal sulfides and competitive ions. *Sci. Total Environ.* 409, 1489–97. doi:10.1016/j.scitotenv.2010.12.028
- De Schamphelaere, K.A.C., Canli, M., Van Lierde, V., Forrez, I., Vanhaecke, F., Janssen, C.R., 2004a. Reproductive toxicity of dietary zinc to *Daphnia magna*. *Aquat. Toxicol.* 70, 233–244. doi:10.1016/j.aquatox.2004.09.008
- De Schamphelaere, K.A.C., Heijerick, D.G., Janssen, C.R., 2004b. Comparison of the effect of different pH buffering techniques on the toxicity of copper and zinc to *Daphnia Magna* and *Pseudokirchneriella Subcapitata*. *Ecotoxicology* 13, 697–705. doi:10.1007/s10646-003-4429-9

- DeForest, D.K., Meyer, J.S., 2014. Critical review: Toxicity of dietborne metals to aquatic organisms. *Crit. Rev. Environ. Sci. Technol.* 45, 1176–1241. doi:10.1080/10643389.2014.955626
- Deforest, D.K., Van Genderen, E.J., 2012. Application of U.S. EPA guidelines in a bioavailability-based assessment of ambient water quality criteria for zinc in freshwater. *Environ. Toxicol. Chem.* 31, 1264–1272. doi:10.1002/etc.1810
- Desgranges, J.-L., Ingram, J., Drolet, B., Morin, J., Savage, C., Borcard, D., 2006. Modelling wetland bird response to water level changes in the Lake Ontario - St. Lawrence River hydrosystem. *Environ. Monit. Assess.* 113, 329–65. doi:10.1007/s10661-005-9087-3
- Di Toro, D.M., McGrath, J. a, Hansen, D.J., Berry, W.J., Paquin, P.R., Mathew, R., Wu, K.B., Santore, R.C., 2005. Predicting sediment metal toxicity using a sediment biotic ligand model: Methodology and initial application. *Environ. Toxicol. Chem.* 24, 2410–27.
- Douglas, S., Beveridge, T.J., 1998. Mineral formation by bacteria in natural microbial communities. *FEMS Microbiol. Ecol.* 26, 79–88. doi:10.1111/j.1574-6941.1998.tb00494.x
- Environment Canada, 2016. Federal environmental quality guidelines: Vanadium.
- Farley, K.J., Rader, K.J., Miller, B.E., 2008. Tableau input coupled kinetic equilibrium transport (TICKET) model. *Environ. Sci. Technol.* 42, 838–844. doi:10.1021/es0625071
- Fetters, K.J., Costello, D.M., Hammerschmidt, C.R., Burton, G.A., 2016. Toxicological effects of short-term resuspension of metal-contaminated freshwater and marine sediments. *Environ. Toxicol. Chem.* 35, 676–686. doi:10.1002/etc.3225
- Firth, P., Fisher, S.G., 1992. *Global Climate Change and Freshwater Ecosystems*. Springer-Verlag, New York.
- Flemming, C.A., Trevors, J.T., 1989. Copper toxicity and chemistry in the environment: A review. *Water. Air. Soil Pollut.* 44, 143–158.
- Forbes, V.E., Calow, P., Sibly, R.M., 2001. Are current species extrapolation models a good basis for ecological risk assessment? *Environ. Toxicol. Chem.* 20, 442–447. doi:10.1002/etc.5620200227
- Forstner, U., Wittmann, G., 2012. *Metal pollution in the aquatic environment*. Springer Science & Business Media.
- France, R.L., Stokes, P.M., 1987. Life stage and population variation in resistance and tolerance of *Hyalla azteca* (amphipoda) to low pH. *Canada J. Fish Aquat. Sci.* 44, 1102–1111.
- Gambrell, R.P., 1994. Trace and toxic metals in wetlands - A review. *J. Environ. Qual.* 23, 883–891.
- Gambrell, R.P., Wiesepape, J.B., Patrick, W.H., Duff, M.C., 1991. The effects of pH, redox, and

- salinity on metal release from a contaminated sediment. *Water. Air. Soil Pollut.* 57–58, 359–367. doi:10.1017/CBO9781107415324.004
- Genter, R.B., Cherry, D.S., Smith, E.P., Cairns, J., 1987. Algal-periphyton population and community changes from zinc stress in stream mesocosms. *Hydrobiologia* 153, 261–275. doi:10.1007/BF00007213
- Gough, H.L., Dahl, A.L., Nolan, M. a., Gaillard, J.-F., Stahl, D. a., 2008. Metal impacts on microbial biomass in the anoxic sediments of a contaminated lake. *J. Geophys. Res.* 113, G02017. doi:10.1029/2007JG000566
- Gronewold, A.D., Stow, C.A., 2014. Water loss from the Great Lakes. *Science* (80-.). 343, 1084–1085. doi:10.1126/science.1249978
- Gronewold, A.D., Stow, C. a., 2014. Unprecedented seasonal water level dynamics on one of the earth's largest lakes. *Bull. Am. Meteorol. Soc.* 95, 15–17. doi:10.1175/BAMS-D-12-00194.1
- Grybos, M., Davranche, M., Gruau, G., Petitjean, P., 2007. Is trace metal release in wetland soils controlled by organic matter mobility or Fe-oxyhydroxides reduction? *J. Colloid Interface Sci.* 314, 490–501. doi:10.1016/j.jcis.2007.04.062
- Grybos, M., Davranche, M., Gruau, G., Petitjean, P., Pédrot, M., 2009. Increasing pH drives organic matter solubilization from wetland soils under reducing conditions. *Geoderma* 154, 13–19. doi:10.1016/j.geoderma.2009.09.001
- Guasch, H., Admiraal, W., Sabater, S., 2003. Contrasting effects of organic and inorganic toxicants on freshwater periphyton. *Aquat. Toxicol.* 64, 165–175. doi:10.1016/S0166-445X(03)00043-2
- Guo, S., Liu, Z., Li, Q., Yang, P., Wang, L., He, B., Xu, Z., Ye, J., Yeng, E., 2016. Leaching heavy metals from the surface soil of reclaimed tidal flat by alternating seawater inundation and air drying. *Chemosphere* 157, 262–270.
- Han, J., Ma, D., Quan, X., Wang, J., Yan, Q., 2005. Bioavailability of zinc in the sediment to the estuarine amphipod *Grandidierella japonica*. *Hydrobiologia* 541, 149–154. doi:10.1007/s10750-004-5289-x
- Hansen, J. a, Welsh, P.G., Lipton, J., Cacela, D., Dailey, A.D., 2002. Relative sensitivity of bull trout (*Salvelinus confluentus*) and rainbow trout (*Oncorhynchus mykiss*) to acute exposures of cadmium and zinc. *Environ. Toxicol. Chem.* 21, 67–75.
- Harita, Y., Hori, T., Sugiyama, M., 2005. Release of trace oxyanions from littoral sediments and suspended particles induced by pH increase in the epilimnion of lakes. *Limnol. Oceanogr.* 50, 636–645.
- Hochella, M.F., Kasama, T., Putnis, A., Putnis, C. V., Moore, J.N., 2005a. Environmentally important, poorly crystalline Fe/Mn hydrous oxides: Ferrihydrite and a possibly new

- vernadite-like mineral from the Clark Fork River Superfund Complex. *Am. Mineral.* 90, 718–724. doi:10.2138/am.2005.1591
- Hochella, M.F., Moore, J.N., Putnis, C. V., Putnis, A., Kasama, T., Eberl, D.D., 2005b. Direct observation of heavy metal-mineral association from the Clark Fork River Superfund Complex: Implications for metal transport and bioavailability. *Geochim. Cosmochim. Acta* 69, 1651–1663. doi:10.1016/j.gca.2004.07.038
- Howell, J.R., Donahoe, R.J., Roden, E.E., Ferris, F.G., 1998. Effects of microbial iron oxide reduction on pH and alkalinity in anaerobic bicarbonate-buffered media: implications for metal mobility. *Mineral. Mag.* 657–658.
- Irwin, R.J., VanMouwerik, L.S., Seese, M.D., Basham, W., 1997. Vanadium Entry, *Environmental Contaminants Encyclopedia*. Fort Collins, Colorado.
- Isbell, F., Calcagno, V., Hector, A., Connolly, J., Harpole, W.S., Reich, P.B., Scherer-Lorenzen, M., Schmid, B., Tilman, D., van Ruijven, J., Weigelt, A., Wilsey, B.J., Zavaleta, E.S., Loreau, M., 2011. High plant diversity is needed to maintain ecosystem services. *Nature* 477, 199–202. doi:10.1038/nature10282
- Jacob, D.L., Otte, M.L., 2003. Conflicting processes in the wetland plant rhizosphere: Metal retention or mobilization? *Water, Air, Soil Pollut.* 3, 91–104.
- Jager, H.I., Smith, B.T., 2008. Sustainable reservoir operation: Can we generate hydropower and preserve ecosystem values. *River Res. Appl.* 24, 340–352. doi:10.1002/rra
- Jensen-Fontaine, M., Norwood, W.P., Brown, M., Dixon, D.G., Le, X.C., 2014. Uptake and speciation of vanadium in the benthic invertebrate *Hyalella azteca*. *Environ. Sci. Technol.* 48, 731–738. doi:10.1021/es403252k
- Jensen, M.M., Thamdrup, B., Rysgaard, S., Holmer, M., Fossing, H., 2003. Rates and regulation of microbial iron reduction in sediments of the Baltic-North Sea transition. *Biogeochemistry* 65, 295–317. doi:10.1023/A:1026261303494
- Jordan, M.A., Teasdale, P.R., Dunn, R.J.K., Lee, S.Y., 2008. Modelling copper uptake by *Saccostrea glomerata* with diffusive gradients in a thin film measurements. *Environ. Chem.* 5, 274–280. doi:10.1071/EN07092
- Kashian, D.R., Prusha, B.A., Clements, W.H., 2004. Influence of total organic carbon and UV-B radiation on zinc toxicity and bioaccumulation in aquatic communities. *Environ. Sci. Technol.* 38, 6371–6376. doi:10.1021/es049756e
- Keddy, P.A., Reznicek, A.A., 1986. Great Lakes vegetation dynamics: The role of fluctuating water levels and buried seeds. *J. Great Lakes Res.* 12, 25–36.
- Kernan, M., Battarbee, R.W., Moss, B., 2010. *Climate Change Impacts on Freshwater Ecosystems*. Wiley-Blackwell, Oxford, UK.

- Kinsman-Costello, L.E., O'Brien, J., Hamilton, S.K., 2014. Re-flooding a historically drained wetland leads to rapid sediment phosphorus release. *Ecosystems*. doi:10.1007/s10021-014-9748-6
- Korfali, S.I., Davies, B.E., 2004. Speciation of metals in sediment and water in a river underlain by limestone: Role of carbonate species for purification capacity of rivers. *Adv. Environ. Res.* 8, 599–612. doi:10.1016/S1093-0191(03)00033-9
- Kosolapov, D.B., Kuschik, P., Vainshtein, M.B., Vatsourina, A.V., Wießner, A., Kästner, M., Müller, R. a., 2004. Microbial processes of heavy metal removal from carbon-deficient effluents in constructed wetlands. *Eng. Life Sci.* 4, 403–411. doi:10.1002/elsc.200420048
- Kostka, J.E., Luther, G., Iii, G.W.L., 1995. Seasonal cycling of Fe in saltmarsh sediments. *Biogeochemistry* 29, 159–181. doi:10.1007/BF00000230
- Kostka, J.E., Luther, G.W., 1994. Partitioning and speciation of solid phase iron in saltmarsh sediments. *Geochim. Cosmochim. Acta* 58, 1701–1710.
- Kreiling, R.M., De Jager, N.R., Swanson, W., Strauss, E. a., Thomsen, M., 2015. Effects of flooding on ion exchange rates in annual Upper Mississippi River floodplain forest impacted by herbivory, invasion, and restoration. *Wetlands* 35, 1005–1012. doi:10.1007/s13157-015-0675-x
- Kubitz, J.A., Lewek, E.C., Besser, J.M., Drake, J.B., Giesy, J.P., 1995. Effects of copper-contaminated sediments on *Hyaella azteca*, *Daphnia magna*, and *Ceriodaphnia dubia*: Survival, growth, and enzyme inhibition. *Arch. Environ. Contam. Toxicol.* 29, 97–103. doi:10.1007/BF00213093
- Larsson, M.A., Baken, S., Gustafsson, J.P., Hadialhejazi, G., Smolders, E., 2013. Vanadium bioavailability and toxicity to soil microorganisms and plants. *Environ. Toxicol. Chem.* 32, 2266–2273. doi:10.1002/etc.2322
- Lee, J.-S., Lee, J.-H., 2005. Influence of acid volatile sulfides and simultaneously extracted metals on the bioavailability and toxicity of a mixture of sediment-associated Cd, Ni, and Zn to polychaetes *Neanthes arenaceodentata*. *Sci. Total Environ.* 338, 229–41. doi:10.1016/j.scitotenv.2004.06.023
- Leira, M., Cantonati, M., 2008. Effects of water-level fluctuations on lakes: An annotated bibliography. *Hydrobiologia* 613, 171–184. doi:10.1007/s10750-008-9465-2
- Magbanua, F.S., Yvette, N., Mendoza, B., Jewel, C., Uy, C., Matthaei, C.D., Ong, P.S., 2015. Water physicochemistry and benthic macroinvertebrate communities in a tropical reservoir: The role of water level fluctuations and water depth. *Limnologia* 55, 13–20. doi:10.1016/j.limno.2015.10.002
- Mahony, J.D., Ditoro, D.M., Gonzalez, a M., Curto, M., Dilg, M., Derosa, L.D., Sparrow, L. a., 1996. Partitioning of metals to sediment organic carbon. *Environ. Toxicol. Chem.* 15, 2187–2197. doi:10.1897/1551-5028(1996)015<2187:POMTSO>2.3.CO;2

- Marce, R., George, G., Buscarinu, P., Deidda, M., Dunalska, J., De Eyto, E., Flaim, G., Grossart, H.P., Istvanovics, V., Lenhardt, M., Moreno-Ostos, E., Obrador, B., Ostrovsky, I., Pierson, D.C., Potuzak, J., Poikane, S., Rinke, K., RodriguezMozaz, S., Staehr, P.A., Sumberova, K., Waajen, G., Weyhenmeyer, G.A., Weathers, K.C., Zion, M., Ibelings, B.W., Jennings, E., 2016. Automatic high frequency monitoring for improved lake and reservoir management. *Environ. Sci. Technol.* 50, 10780–10794. doi:10.1021/acs.est.6b01604
- Mason, R., 2013. Trace metals in aquatic systems. John Wiley & Sons, Inc.
- Meylan, S., Behra, R., Sigg, L., 2003. Accumulation of copper and zinc in periphyton in response to dynamic variations of metal speciation in freshwater. *Environ. Sci. Technol.* 37, 5204–5212. doi:10.1021/es034566+
- Middleton, G. V., 2003. Encyclopedia of sediments and sedimentary rocks. Kluwer Academic, Boston, MA.
- Mikkonen, A., Tummavuori, J., 1994. Retention of vanadium (V) by three Finnish mineral soils. *Eur. J. Soil Sci.* 45, 361–368. doi:10.1111/j.1365-2389.1994.tb00520.x
- Milani, D., Reynoldson, T.B., Borgmann, U., Kolasa, J., 2003. The relative sensitivity of four benthic invertebrates to metals in spiked-sediment exposures and application to contaminated field sediment. *Environ. Toxicol. Chem.* 22, 845–854. doi:10.1002/etc.5620220424
- Milly, P.C.D., Dunne, K. a, Vecchia, a V, 2005. Global pattern of trends in streamflow and water availability in a changing climate. *Nature* 438, 347–350. doi:10.1038/nature04312
- Mitsch, W.J., Nedrich, S.M., Harter, S.K., Anderson, C., Nahlik, A.M., Bernal, B., 2014. Sedimentation in created freshwater riverine wetlands: 15 years of succession and contrast of methods. *Ecol. Eng.* 72, 25–34. doi:10.1016/j.ecoleng.2014.09.116
- Morris, J.M., Nimick, D.A., Farag, A.M., Meyer, J.S., 2005. Does biofilm contribute to diel cycling of Zn in High Ore Creek , Montana. *Biogeochemistry* 76, 233–259. doi:10.1007/s10533-005-4774-2
- Mosley, L.M., Fitzpatrick, R.W., Palmer, D., Leyden, E., Shand, P., 2014. Changes in acidity and metal geochemistry in soils, groundwater, drain and river water in the Lower Murray River after a severe drought. *Sci. Total Environ.* 485–486, 281–91. doi:10.1016/j.scitotenv.2014.03.063
- Muyssen, B.T.A., De Schampelaere, K.A.C., Janssen, C.R., 2006. Mechanisms of chronic waterborne Zn toxicity in *Daphnia magna*. *Aquat. Toxicol.* 77, 393–401. doi:10.1016/j.aquatox.2006.01.006
- Muyssen, B.T.A., Janssen, C.R., 2001. Multigeneration zinc acclimation and tolerance in *Daphnia magna*: Implications for water-quality guidelines and ecological risk assessment. *Environ. Toxicol. Chem.* 20, 2053–2060. doi:10.1897/1551-5028(2001)020<2053:MZAATI>2.0.CO;2

- Nedrich, S.M., Burton, G.A., 2017. Indirect effects of climate change on zinc cycling in sediments: The role of changing water levels. *Environ. Toxicol. Chem.* 36, 1–9. doi:10.1002/etc.3783
- Neumann, P.T.M., Borgmann, U., Norwood, W., 1999. Effect of gut clearance on metal body concentrations in *Hyaella azteca*. *Environ. Toxicol. Chem.* 18, 976–984. doi:10.1002/etc.5620180524
- Ney, J.J., 1996. Oligotrophication and its discontents: effects of reduced nutrient loading on reservoir fisheries. *Am. Fish. Soc. Symp.* 16, 285–295.
- Nguyen, L.T.H., Burton, G.A., Schlekot, C.E., Janssen, C.R., 2011. Field measurement of nickel sediment toxicity: Role of acid volatile sulfide. *Environ. Toxicol. Chem.* 30, 162–172. doi:10.1002/etc.358
- Norwood, W.P., Borgmann, U., Dixon, D.G., 2006. Saturation models of arsenic, cobalt, chromium and manganese bioaccumulation by *Hyaella azteca*. *Environ. Pollut.* 143, 519–528. doi:10.1016/j.envpol.2005.11.041
- Nriagu, J.O. (Ed.), 1998. *Vanadium in the Environment*. John Wiley & Sons, Inc., New York, NY.
- Onset Computer Corporation, 2012. *HOBO U20 water level logger manual*.
- Ortiz-Bernad, I., Anderson, R.T., Vrionis, H.A., Lovley, D.R., 2004. Vanadium respiration by *Geobacter metallireducens*: Novel strategy for in situ removal of vanadium from groundwater. *Appl. Environ. Microbiol.* 70, 3091–3095. doi:10.1128/AEM.70.5.3091-3095.2004
- Patterson, J.W., Allen, H.E., Scala, J.J., 1977. Carbonate precipitation for heavy metals pollutants. *J. water Pollut. Control Fed.* 49, 2397–2410.
- Paulauskis, J.D., Winner, R.W., 1988. Effects of water hardness and humic acid on zinc toxicity to *Daphnia magna Straus*. *Aquat. Toxicol.* 12, 273–290. doi:10.1016/0166-445X(88)90027-6
- Paulsson, M., Nyström, B., Blanck, H., 2000. Long-term toxicity of zinc to bacteria and algae in periphyton communities from the river Gota Alv, based on a microcosm study. *Aquat. Toxicol.* 47, 243–257. doi:10.1016/S0166-445X(99)00013-2
- Perles, T., 2012. *Vanadium Market Fundamentals and Implications*. Berlin, Germany.
- Pilgrim, W., Burt, M.D.B., 1993. Effect of acute pH depression on the survival of the freshwater amphipod *Hyaella azteca* at variable temperatures: field and laboratory studies. *Hydrobiologia* 254, 91–98.
- Plante, B., Benzaazoua, M., Bussière, B., 2011. Predicting geochemical behaviour of waste rock with low acid generating potential using laboratory kinetic tests. *Mine Water Environ.* 30,

2–21. doi:10.1007/s10230-010-0127-z

- Prather, C.M., Pelini, S.L., Laws, A., Rivest, E., Woltz, M., Bloch, C.P., Del Toro, I., Ho, C.K., Kominoski, J., Newbold, T.A.S., Parsons, S., Joern, A., 2013. Invertebrates, ecosystem services and climate change. *Biol. Rev.* 88, 327–348. doi:10.1111/brv.12002
- Ravel, B., Newville, M., 2005. ATHENA, ARTEMIS, HEPHAESTUS: Data analysis for X-ray absorption spectroscopy using IFEFFIT. *J. Synchrotron Radiat.* 12, 537–541. doi:10.1107/S0909049505012719
- Remaili, T.M., Simpson, S.L., Amato, E.D., Spadaro, D.A., Jarolimek, C. V., Jolley, D.F., 2016. The impact of sediment bioturbation by secondary organisms on metal bioavailability, bioaccumulation and toxicity to target organisms in benthic bioassays: Implications for sediment quality assessment. *Environ. Pollut.* 208, 590–599. doi:10.1016/j.envpol.2015.10.033
- Richardson, S.M., Hanson, J.M., Locke, A., 2002. Effects of impoundment and water-level fluctuations on macrophyte and macroinvertebrate communities of a dammed tidal river. *Aquat. Ecol.* 36, 493–510. doi:10.1023/A:1021137630654
- Richter, B.D., Mathews, R., Harrison, D.L., Wigington, R., 2003. Ecologically sustainable water management: Managing river flows for ecological integrity. *Ecol. Appl.* 13, 206–224.
- Roulier, J.L., Tusseau-Vuillemin, M.H., Coquery, M., Geffard, O., Garric, J., 2008. Measurement of dynamic mobilization of trace metals in sediments using DGT and comparison with bioaccumulation in *Chironomus riparius*: First results of an experimental study. *Chemosphere* 70, 925–932. doi:10.1016/j.chemosphere.2007.06.061
- Saito, L., Johnson, B.M., Bartholow, J., Hanna, R.B., Hann, R.B., 2001. Assessing ecosystem effects of reservoir operations using food web-energy transfer and water quality models. *Ecosystems* 4, 105–125.
- Santore, R.C., Di Toro, D.T.M., Paquin, P.R., Allen, H.E., Meyer, J.S., 2001. Biotic ligand model of the acute toxicity of metals. 2. Application to acute copper toxicity in freshwater fish and *Daphnia*. *Environ. Toxicol. Chem.* 20, 2397–402.
- Santore, R.C., Mathew, R., Paquin, P.R., DiToro, D., 2002. Application of the biotic ligand model to predicting zinc toxicity to rainbow trout, fathead minnow, and *Daphnia magna*. *Comp. Biochem. Physiol. Part C* 133, 271–85.
- Sapsford, D.J., Howell, R.J., Dey, M., Williams, K.P., 2009. Humidity cell tests for the prediction of acid rock drainage. *Miner. Eng.* 22, 25–36. doi:10.1016/j.mineng.2008.03.008
- Schiffer, S., Liber, K., 2015. Estimation of vanadium guidelines for the protection of aquatic life relevant to the Canadian Oil Sands region, in: Society of Environmental Toxicology. Salt Lake City, UT.
- Schintu, M., Durante, L., Maccioni, A., Meloni, P., Degetto, S., Contu, A., 2008. Measurement

- of environmental trace-metal levels in Mediterranean coastal areas with transplanted mussels and DGT techniques. *Mar. Pollut. Bull.* 57, 832–837.
doi:10.1016/j.marpolbul.2008.02.038
- Seeberg-Elverfeldt, J., Schluter, M., Feseker, T., Kolling, M., 2005. Rhizon sampling of porewaters near the sediment-water interface of aquatic systems. *Limnol. Oceanogr.* 3, 361–371. doi:Pii S0012-821x(02)01064-6 Doi 10.1016/S0012-821x(02)01064-6
- Seybold, C.A., Mersie, W., Huang, J., Mcnamee, C., 2002. Soil redox, pH, temperature, and water-table patterns of a freshwater tidal wetland. *Wetlands* 22, 149–158.
- Shafer, M.M., Toner, B.M., Overdier, J.T., Schauer, J.J., Fakra, S.C., Hu, S., Herner, J.D., Ayala, A., 2012. Chemical speciation of vanadium in particulate matter emitted from diesel vehicles and urban atmospheric aerosols. *Environ. Sci. Technol.* 46, 189–195.
doi:10.1021/es200463c
- Shi, Z., Di Toro, D.M., Allen, H.E., Sparks, D.L., 2013. A general model for kinetics of heavy metal adsorption and desorption on soils. *Environ. Sci. Technol.* 47, 3761–7.
doi:10.1021/es304524p
- Simpson, S., Ward, D., Strom, D., Jolley, D.F., 2012. Oxidation of acid-volatile sulfide in surface sediments increases the release and toxicity of copper to the benthic amphipod *Melita plumulosa*. *Chemosphere* 88, 953–61. doi:10.1016/j.chemosphere.2012.03.026
- Simpson, S.L., Angel, B.M., Jolley, D.F., 2004. Metal equilibration in laboratory-contaminated (spiked) sediments used for the development of whole-sediment toxicity tests. *Chemosphere* 54, 597–609. doi:10.1016/j.chemosphere.2003.08.007
- Simpson, S.L., Apte, S.C., Batley, G.E., 1998. Effect of short-term resuspension events on trace metal speciation in polluted anoxic sediments. *Environ. Sci. Technol.* 32, 620–625.
doi:10.1021/es970568g
- Simpson, S.L., Apte, S.G., Batley, G.E., 2000. Effect of short-term resuspension events on the oxidation of cadmium, lead, and zinc sulfide phases in anoxic estuarine sediments. *Environ. Sci. Technol.* 34, 4533–4537. doi:10.1021/es991440x
- Simpson, S.L., Batley, G.E., 2016. Sediment quality assessment. CSIRO Publishing.
- Simpson, S.L., Spadaro, D.A., 2016. Bioavailability and chronic toxicity of metal sulfide minerals to benthic marine invertebrates: implications for deep sea exploration, mining and tailings disposal. *Environ. Sci. Technol.* 50, 4061–4070. doi:10.1021/acs.est.6b00203
- Simpson, S.L., Yverneau, H., Cremazy, A., Jarolimek, C. V., Price, H.L., Jolley, D.F., 2012. DGT-induced copper flux predicts bioaccumulation and toxicity to bivalves in sediments with varying properties. *Environ. Sci. Technol.* 46, 9038–9046. doi:10.1021/es301225d
- Skalak, K., Benthem, A., Hupp, C., Schenk, E., Galloway, J., Nustad, R., 2016. Hydrogeomorphology- Ecology Interactions in River Systems. *River Res. Appl.* 22, 1085–

1095. doi:10.1002/rra

Steinman, A.D., Lamberti, G.A., Leavitt, P.R., 2006. *Methods in Stream Ecology*, 2nd ed. Elsevier, London, UK.

Steinman, A.D., Ogdahl, M.E., Weinert, M., Thompson, K., Cooper, M.J., Uzarski, D.G., 2012. Water level fluctuation and sediment – water nutrient exchange in Great Lakes coastal wetlands. *J. Great Lakes Res.* 38, 766–775.

Steinman, A.D., Ogdahl, M.E., Weinert, M., Uzarski, D.G., 2014. Influence of water-level fluctuation duration and magnitude on sediment - water nutrient exchange in coastal wetlands. *Aquat. Ecol.* 48, 143-159.

Stookey, L.L., 1970. Ferrozine-A new spectrophotometric reagent for iron. *Anal. Chem.* 42, 779–781.

Taniguchi, M., Fukuo, Y., 1996. An effect of seiche on groundwater seepage rate into Lake Biwa, Japan. *Water Resour. Res.* 32, 333–338.

Terzano, R., Spagnuolo, M., Vekemans, B., De Nolf, W., Janssens, K., Falkenberg, G., Fiore, S., Ruggiero, P., 2007a. Assessing the origin and fate of Cr, Ni, Cu, Zn, Pb, and V in industrial polluted soil by combined microspectroscopic techniques and bulk extraction methods. *Environ. Sci. Technol.* 41, 6762–6769. doi:10.1021/es070260h

Terzano, R., Spagnuolo, M., Vekemans, B., De Nolf, W., Janssens, K., Falkenberg, G., Fiore, S., Ruggiero, P., 2007b. Assessing the origin and fate of Cr, Ni, Cu, Zn, Pb, and V in industrial polluted soil by combined microspectroscopic techniques and bulk extraction methods. *Environ. Sci. Technol.* 41, 6762–6769. doi:10.1021/es070260h

USEPA, 2016a. National Recommended Water Quality Criteria - Aquatic Life Criteria [WWW Document]. URL <http://www.epa.gov/wqc/national-recommended-water-quality-criteria-aquatic-life-criteria-table> (accessed 2.7.16).

USEPA, 2016b. National Recommended Water Quality Criteria - Aquatic Life Criteria [WWW Document].

USEPA, 2016c. Draft technical support document: Recommended estimates for missing water quality parameters for application in EPA ' s biotic ligand model.

USEPA, 2007. Aquatic life ambient freshwater quality criteria-Copper. 2007 Revision.

USEPA, 2005. Procedures for the derivation of equilibrium partitioning sediment benchmarks (ESBs) for the protection of benthic organisms: metal mixtures (cadmium, copper, lead, nickel, silver, and zinc). Washington, DC.

USEPA, 1999. Rapid biological assessment protocols: An introduction.

USEPA, 1998. A framework for ecological risk assessment at the EPA, USEPA. Washington,

DC. doi:10.1002/etc.5620111202

- USEPA, 1996a. Field sample processing, transport, and storage of sediments.
- USEPA, 1996b. Ecological effects test guidelines: Aquatic invertebrate acute toxicity test, freshwater daphnids. Washington, DC.
- USEPA, 1996c. Method 3050B - Acid digestion of sediments, sludges, and soils., 1996. doi:10.1117/12.528651
- USEPA, 1991. Compendium of ERT Toxicity Testing Procedures. Washington DC.
- USEPA, 1987. Ambient Water Quality Criteria for Zinc. United States Environ. Prot. Agency.
- USGS, 2016a. Zinc - minerals information.
- USGS, 2016b. Vanadium - minerals information.
- USGS, 2012. Alkalinity and acid neutralizing capacity, USGS TWRI Book 9 Chapter A6.
- Van Der Valk, A.G., 2005. Water-level fluctuations in North American prairie wetlands. *Hydrobiologia* 539, 171–188. doi:10.1007/s10750-004-4866-3
- van Leeuwen, C.J., Niebeek, G., Rijkeboer, M., 1987. Effects of chemical stress on the population dynamics of *Daphnia magna*: a comparison of two test procedures. *Ecotoxicol. Environ. Saf.* 14, 1–11. doi:10.1016/0147-6513(87)90077-7
- Viollier, E., Inglett, P.W., Hunter, K., Roychoudhury, A.N., Cappellen, P. Van, 2000. The ferrozine method revisited : Fe (II)/Fe (III) determination in natural waters. *Appl. Geochemistry* 15, 785–790.
- Wagner, M., Chappaz, A., Lyons, T.W., 2017. Molybdenum speciation and burial pathway in weakly sulfidic environments: Insights from XAFS. *Geochim. Cosmochim. Acta* 206, 18–29. doi:10.1016/j.gca.2017.02.018
- Wanty, R.B., Goldhaber, M.B., 1992. Thermodynamics and kinetics of reactions involving vanadium in natural systems: Accumulation of vanadium in sedimentary rocks. *Geochim. Cosmochim. Acta* 56, 1471–1483. doi:10.1016/0016-7037(92)90217-7
- Watzin, M.C., Roscigno, P.R., 1997. The effects of zinc contamination on the recruitment and early survival of benthic invertebrates in an estuary. *Mar. Pollut. Bull.* 34, 443–455. doi:10.1016/S0025-326X(96)00132-4
- White, M.S., Xenopoulos, M. a., Hogsden, K., Metcalfe, R. a., Dillon, P.J., 2008. Natural lake level fluctuation and associated concordance with water quality and aquatic communities within small lakes of the Laurentian Great Lakes region. *Hydrobiologia* 613, 21–31. doi:10.1007/s10750-008-9469-y

- Yang, J., Tang, Y., Yang, K., Rouff, A.A., Elzinga, E.J., Huang, J.H., 2014. Leaching characteristics of vanadium in mine tailings and soils near a vanadium titanomagnetite mining site. *J. Hazard. Mater.* 264, 498–504. doi:10.1016/j.jhazmat.2013.09.063
- Zajic, J.E., 1969. *Microbial biogeochemistry*.
- Zhang, H., Davison, W., Miller, S., Tych, W., 1995. In situ high resolution measurements of fluxes of Ni, Cu, Fe, and Mn and concentrations of Zn and Cd in porewaters by DGT. *Geochim. Cosmochim. Acta* 59, 4181–4192. doi:10.1016/0016-7037(95)00293-9
- Zhang, J., Dong, H., Zhao, L., McCarrick, R., Agrawal, A., 2014. Microbial reduction and precipitation of vanadium by mesophilic and thermophilic methanogens. *Chem. Geol.* 370, 29–39. doi:10.1016/j.chemgeo.2014.01.014

Appendix A (Chapter 2 Data)

Notes: Experiment abbreviations are seiche saturated (1a), seiche inundated (1b), drought oxidized/dry (2a), drought day-1 inundation (2b), and drought day-30 inundation (2c). The seiche experiment is experiment “1” and drought is experiment “2”.

Table A-1. Dissolved Organic Carbon (DOC) in porewater per site and experiment

Site	Experiment	DOC (mg L ⁻¹)
DRW	1a	0.188167
DRW	1b	0.230667
DRW	2b	0.136667
DRW	2c	0.359333
EB	1a	0.1355
EB	1b	0.7175
EB	2b	1.142667
EB	2c	0.512167
LBC	1a	1.687333
LBC	1b	0.693167
LBC	2b	0.265167
LBC	2c	0.7615
QC	1a	0.255667
QC	1b	0.1795
QC	2b	1.693833
QC	2c	0.581

Table A-2. Dry weight / wet weight sediment ratios per site and experiment

Site	Experiment	Dry weight / wet weight	Standard Error
DRW	1a	0.219167	0.016098
DRW	1b	0.209167	0.012308
DRW	2a	0.3755	0.007302
DRW	2b	0.290833	0.007821
DRW	2c	0.262333	0.016208
EB	1a	0.770833	0.022675
EB	1b	0.619667	0.032484
EB	2a	1.008833	0.021309
EB	2b	0.702667	0.046156
EB	2c	0.679333	0.028046
LBC	1a	0.545	0.075226
LBC	1b	0.449167	0.033002
LBC	2a	0.826667	0.138524
LBC	2b	0.504167	0.022176
LBC	2c	0.4605	0.016091
QC	1b	0.481833	0.042277
QC	2a	0.903333	0.016946
QC	2b	0.590333	0.043891
QC	2c	0.545167	0.051523

Table A-3. Sediment loss-on-ignition (LOI) per site and experiment

Site	Experiment	Mean LOI	Standard error
DRW	1a	0.27	0.018619
DRW	1b	0.23	0.009309
DRW	2a	0.258333	0.004773
DRW	2b	0.25	0.011547
DRW	2c	0.246667	0.008028
LBC	1a	0.136667	0.010541
LBC	1b	0.105	0.010247
LBC	2a	0.145	0.015438
LBC	2b	0.133333	0.018012
LBC	2c	0.128333	0.007032
EB	1a	0.046667	0.011155
EB	1b	0.056667	0.011155
EB	2a	0.138333	0.074896
EB	2b	0.045	0.009916
EB	2c	0.065	0.011762
QC	1b	0.085	0.008466
QC	2b	0.073333	0.017448
QC	2c	0.08	0.017127

Table A-4. Sediment pH per site and experiment

Site	Experiment	Mean pH	Standard error
DRW	2-d03	6.657333	0.059574
DRW	2-d09	6.662	0.073603
DRW	2-d16	6.873333	0.06247
DRW	2-d24	6.938	0.060192
EB	2-d03	7.424286	0.030862
EB	2-d09	7.419286	0.033074
EB	2-d16	7.393333	0.057913
EB	2-d24	7.426667	0.037463
LBC	2-d03	6.130667	0.056841
LBC	2-d09	6.166	0.042278
LBC	2-d16	6.239333	0.050384
LBC	2-d24	6.428	0.04484
QC	2-d03	7.274	0.025162
QC	2-d09	7.276	0.029854
QC	2-d16	7.281333	0.054115
QC	2-d24	7.307333	0.025884

Table A-5. Sediment Fe-oxyhydroxide content per site-rep and experiment

Site-Rep	Experiment	Amorphous FeO ($\mu\text{mol gdw}^{-1}$)	Crystalline FeO ($\mu\text{mol gdw}^{-1}$)	Total FeO ($\mu\text{mol gdw}^{-1}$)
DRW1	1a	75.7525	132.0955	207.848
DRW1	1b	41.435	91.1145	132.5493
DRW1	2a	54.76	118.145	172.9
DRW1	2b	55.755	95.39	151.135
DRW1	2c	38.14	81.59	119.73
DRW2	1a	106.3085	191.8735	298.182
DRW2	1b	61.582	93.388	154.9701
DRW2	2a	75.9	172.36	248.26
DRW2	2b	70.66	104.61	175.27
DRW2	2c	77.025	122.265	199.28
DRW3	1a	68.5205	158.2275	226.747
DRW3	1b	101.888	206.3505	308.2385
DRW3	2a	71.485	152.115	223.6
DRW3	2b	62.69	116.245	178.935
DRW3	2c	81.835	83.425	165.255
EB1	1a	4.371	17.9135	22.2845
EB1	1b	3.0575	5.8325	8.89
EB1	2a	2.505	7.9	10.405
EB1	2b	2.615	12.43	15.05
EB1	2c	2.755	9.42	12.175
EB2	1a	4.4715	31.4655	35.9375
EB2	1b	59.2345	121.987	181.2215
EB2	2a	5.835	36.47	42.315
EB2	2b	6.105	25.62	31.725
EB2	2c	8.635	28.585	37.22
EB3	1a	11.0255	27.888	38.914
EB3	1b	7.542	21.112	28.6541
EB3	2a	7.585	21.995	29.58
EB3	2b	6.645	15.305	21.95
EB3	2c	6.95	22.585	29.53
LBC1	1a	86.745	257.9895	344.7345
LBC1	1b	67.1285	78.616	145.7445
LBC1	2a	98.1	153.45	251.545
LBC1	2b	78.19	67.88	146.075
LBC1	2c	53.61	129.745	183.36
LBC2	1a	85.8155	89.9475	175.763
LBC2	1b	71.3475	102.4885	173.8361
LBC2	2a	112.86	356.3	469.16
LBC2	2b	54.31	92.63	146.94
LBC2	2c	57.615	57.37	114.985

Site-Rep	Experiment	Amorphous FeO ($\mu\text{mol gdw}^{-1}$)	Crystalline FeO ($\mu\text{mol gdw}^{-1}$)	Total FeO ($\mu\text{mol gdw}^{-1}$)
LBC3	1a	95.2415	197.5995	292.841
LBC3	1b	49.827	115.131	164.9578
LBC3	2a	57.655	136.945	194.6
LBC3	2b	56.575	116.63	173.205
LBC3	2c	65.415	138.425	203.84
QC1	1a	12.269	26.663	38.932
QC1	1b	6.909	24.4955	31.40425
QC1	2a	7.525	11.845	19.375
QC1	2b	6.525	16.19	22.715
QC1	2c	7.145	19.69	26.835
QC2	1a	4.917	35.075	39.9925
QC2	1b	0.341	20.779	21.1199
QC2	2a	5.575	20.595	26.17
QC2	2b	5.44	20.475	25.915
QC2	2c	10.73	20.765	31.495
QC3	1a	13.759	36.4595	50.2185
QC3	1b	13.7055	25.7335	39.43895
QC3	2a	8.96	24.455	33.41
QC3	2b	8.585	17.875	26.46
QC3	2c	8.685	19.76	28.45

Table A-6. Sediment Mn-oxyhydroxide content per site-rep and experiment

Site	Experiment	Amorphous MnO ($\mu\text{mol gdw}^{-1}$)	Crystalline MnO ($\mu\text{mol gdw}^{-1}$)	Total MnO ($\mu\text{mol gdw}^{-1}$)
DRW1	2a	1.2325	0.61	1.8425
DRW1	2b	1.5825	0.5735	2.1565
DRW1	2c	1.035	0.613	1.648
DRW2	2a	1.814	1.951	3.765
DRW2	2b	1.836	1.18	3.016
DRW2	2c	2.1375	0.8695	3.007
DRW3	2a	1.081	1.8685	2.95
DRW3	2b	1.6065	1.027	2.6335
DRW3	2c	1.3555	0.4935	1.8495
EB1	2a	0.2095	0.15	0.359
EB1	2b	0.2195	0.132	0.3515
EB1	2c	0.232	0.0925	0.3245
EB2	2a	0.6695	2.212	2.8815
EB2	2b	0.857	0.219	1.076
EB2	2c	1.118	0.846	1.964
EB3	2a	0.4645	0.2895	0.754
EB3	2b	0.437	0.129	0.5655
EB3	2c	0.5705	0.2795	0.85
LBC1	2a	2.2585	3.3895	5.648
LBC1	2b	2.5455	0.2355	2.607
LBC1	2c	1.7745	2.3795	4.1545
LBC2	2a	3.563	4.9195	8.4825
LBC2	2b	1.091	1.09	2.181
LBC2	2c	1.8685	0.3155	2.184
LBC3	2a	1.468	2.049	3.517
LBC3	2b	1.6135	0.223	1.837
LBC3	2c	2.3715	0.9785	3.35
QC1	2a	0.3875	0.0645	0.452
QC1	2b	0.2345	0.2545	0.489
QC1	2c	0.6315	0.406	1.0375
QC2	2a	0.3085	0.2315	0.54
QC2	2b	0.309	0.0925	0.4015
QC2	2c	1.2405	0.114	1.355
QC3	2a	0.424	0.34	0.764
QC3	2b	0.363	0.3295	0.6925
QC3	2c	0.416	0.201	0.617

Table A-7. Sediment Zn bound to amorphous, crystalline, and total Fe/Mn oxyhydroxides

Site-Rep	Experiment	Amorphous Zn ($\mu\text{mol gdwt}^{-1}$)	Crystalline Zn ($\mu\text{mol gdwt}^{-1}$)	Total Zn ($\mu\text{mol gdwt}^{-1}$)
DRW1	2a	1.2445	2.1405	3.3845
DRW1	2b	1.164	1.5385	2.702
DRW1	2c	0.42	2.4345	2.8545
DRW2	2a	1.057	2.6115	3.6685
DRW2	2b	1.283	1.54	2.824
DRW2	2c	1.105	2.88	3.9855
DRW3	2a	1.38	3.044	4.424
DRW3	2b	1.2915	1.4205	2.7115
DRW3	2c	0.769	2.133	2.9025
EB1	2a	0.277	0.126	0.403
EB1	2b	0.2075	0.4	0.608
EB1	2c	0.2405	0.09	0.331
EB2	2a	0.3545	0.47	0.8115
EB2	2b	0.127	0.233	0.3605
EB2	2c	0.253	0.2265	0.479
EB3	2a	0.493	0.038	0.4145
EB3	2b	0.4845	0.226	0.5735
EB3	2c	0.1705	0.358	0.5285
LBC1	2a	1.8385	2.9055	4.744
LBC1	2b	1.3855	0.9025	2.287
LBC1	2c	0.8845	2.0835	2.968
LBC2	2a	2.1455	4.3215	6.467
LBC2	2b	0.7395	1.105	1.8445
LBC2	2c	0.4785	1.0585	1.5365
LBC3	2a	0.899	0.906	1.805
LBC3	2b	0.904	0.6445	1.5485
LBC3	2c	0.574	0.9195	1.494
QC1	2a	0.6815	0	0.419
QC1	2b	0.1645	0.4065	0.571
QC1	2c	0.2655	0.1325	0.398
QC2	2a	0.7395	0.086	0.7445
QC2	2b	0.3815	0.428	0.8095
QC2	2c	0.4425	0.2265	0.669
QC3	2a	0.5215	0.25	0.7715
QC3	2b	0.4765	0.3045	0.781
QC3	2c	0.2735	0.143	0.417

Table A-8. Sediment [SEM-AVS] / f_{oc} data table

Site-Rep	Depth (cm)	Experiment	$\mu\text{mol g}^{-1}$								SEM-AVS / (f_{oc})
			S^{2-}	Cu	Ni	Zn	Cd	Cr	Pb	SEM	
QC3	1	1a	0.63	0.16	0.08	0.46	0.04	0.20	0.06	0.99	4.39
QC3	2	1a	5.38	0.08	0.04	0.24	0.00	0.07	0.04	0.47	-77.42
QC2	1	1a	0.92	0.16	0.09	0.36	0.00	0.23	0.00	0.84	-0.86
QC2	2	1a	0.57	0.10	0.08	0.20	0.00	0.21	0.00	0.59	0.40
QC1	1	1a	15.91	0.00	0.03	0.41	0.00	0.11	0.00	0.56	-150.98
EB3	1	1a	0.10	0.14	0.00	0.26	0.00	0.01	0.48	0.90	25.66
EB3	2	1a	1.34	0.06	0.00	0.14	0.00	0.04	0.25	0.50	-20.44
EB2	1	1a	0.01	0.06	0.00	0.16	0.00	0.02	0.14	0.38	14.43
EB2	2	1a	0.02	0.08	0.00	0.14	0.00	0.03	0.25	0.51	21.32
EB1	1	1a	0.05	0.05	0.00	0.20	0.00	0.00	0.16	0.41	4.28
EB1	2	1a	0.15	0.00	0.00	0.20	0.00	0.05	0.02	0.27	1.78
LBC3	1	1a	4.95	0.29	0.08	1.70	0.01	0.23	0.41	2.73	-20.86
LBC3	2	1a	1.38	0.29	0.13	1.18	0.02	0.35	0.38	2.34	9.29
LBC2	1	1a	12.23	0.94	0.36	3.09	0.07	1.45	1.11	7.03	-32.28
LBC2	2	1a	2.59	0.44	0.20	1.44	0.03	0.71	0.50	3.33	4.67
LBC1	1	1a	12.84	0.73	0.36	2.74	0.05	1.07	0.92	5.87	-50.12
LBC1	2	1a	2.92	0.76	0.45	2.76	0.05	0.99	0.97	5.97	20.66
DRW3	1	1a	2.54	0.75	0.53	2.60	0.01	0.06	0.32	4.27	7.12
DRW3	2	1a	37.43	0.41	0.32	2.83	0.01	0.37	0.43	4.38	-111.26
DRW1	1	1a	3.49	0.69	0.15	2.24	0.01	0.09	0.37	3.54	0.22
DRW1	2	1a	31.31	0.12	0.21	2.44	0.00	0.23	0.37	3.37	-121.93
SAND	1	1a	0.00	0.00	0.45	0.05	0.07	0.00	0.00	0.57	571.00
QC3	1	1b	1.46	0.18	0.16	0.36	0.00	0.40	0.00	1.11	-3.31
QC3	2	1b	8.43	0.11	0.05	0.29	0.00	0.14	0.00	0.59	-105.20
QC2	1	1b	3.00	0.10	0.00	0.26	0.00	0.00	0.00	0.36	-33.76
QC2	2	1b	3.97	0.00	0.03	0.14	0.00	0.09	0.00	0.26	-64.85
QC1	1	1b	17.05	1.28	0.00	2.69	0.00	0.00	0.00	3.97	-124.22
QC1	2	1b	1.96	0.08	0.02	0.16	0.00	0.08	0.00	0.34	-21.34
EB3	1	1b	0.54	0.08	0.02	0.15	0.00	0.09	0.22	0.57	0.92
EB3	2	1b	4.29	0.06	0.02	0.19	0.01	0.13	0.33	0.74	-60.51
EB2	1	1b	6.18	0.26	0.08	1.14	0.01	0.34	0.38	2.21	-42.15
EB2	2	1b	1.85	0.26	0.13	1.21	0.01	0.42	0.40	2.45	7.24
EB1	1	1b	0.07	0.07	0.11	0.14	0.00	0.28	0.00	0.60	9.14
EB1	2	1b	0.80	0.00	0.02	0.08	0.00	0.11	0.00	0.21	-24.64
LBC3	1	1b	3.74	0.29	0.11	1.25	0.01	0.36	0.35	2.38	-16.58
LBC3	2	1b	1.86	0.26	0.28	1.18	0.01	0.75	0.35	2.84	12.98
LBC2	1	1b	4.21	0.65	0.23	1.98	0.04	0.72	0.62	4.24	0.31
LBC2	2	1b	9.12	0.54	0.22	1.75	0.03	0.76	0.58	3.89	-53.17
LBC1	1	1b	4.62	0.79	0.73	2.60	0.04	2.01	0.81	6.99	16.88

Site-Rep	Depth (cm)	Experiment	$\mu\text{mol g}^{-1}$								SEM- AVS /(foc)
			S ²⁻	Cu	Ni	Zn	Cd	Cr	Pb	SEM	
DRW3	1	1b	52.79	0.40	0.21	2.55	0.01	0.25	0.34	3.76	-220.00
DRW3	2	1b	34.44	0.32	0.36	2.48	0.01	0.53	0.33	4.03	-143.16
DRW2	1	1b	3.07	0.70	0.12	2.17	0.00	0.07	0.38	3.44	1.78
DRW2	2	1b	10.93	0.63	0.38	2.75	0.01	0.49	0.35	4.62	-23.38
DRW1	1	1b	4.29	0.98	0.57	2.92	0.01	0.87	0.45	5.78	6.57
DRW1	2	1b	5.79	0.49	0.32	2.66	0.01	0.39	0.34	4.21	-6.58
SAND	1	1b	0.00	0.00	0.00	0.00	0.00	0.13	0.00	0.13	88.88
QC3	1	2a	0.04	0.10	0.01	0.43	0.16	0.00	0.04	0.74	10.2
QC3	2	2a	0.02	0.10	0.00	0.29	0.01	0.00	0.03	0.43	5.9
QC2	1	2a	0.05	0.15	0.00	0.74	0.00	0.00	0.02	0.91	13.4
QC2	2	2a	0.04	0.08	0.00	0.31	0.00	0.00	0.03	0.42	5.8
QC1	1	2a	0.10	0.14	0.00	0.65	0.00	0.00	0.03	0.82	7.2
QC1	2	2a	0.03	0.06	0.00	0.30	0.00	0.00	0.00	0.36	6.9
EB3	1	2a	0.04	0.07	0.00	0.59	0.00	0.00	0.25	0.91	19.8
EB3	2	2a	0.02	0.05	0.00	0.19	0.00	0.00	0.20	0.44	7.9
EB2	1	2a	0.03	0.11	0.00	0.48	0.00	0.00	0.28	0.87	1.7
EB2	2	2a	0.03	0.08	0.00	0.40	0.00	0.00	0.28	0.77	15.2
EB1	1	2a	0.02	0.03	0.00	0.24	0.08	0.00	0.00	0.35	3.4
EB1	2	2a	0.03	0.01	0.01	0.16	0.01	0.00	0.00	0.19	2.1
LBC3	1	2a	0.44	0.39	0.02	1.33	0.02	0.17	0.46	2.39	19.5
LBC3	2	2a	1.75	0.26	0.00	0.99	0.01	0.45	0.30	2.01	2.8
LBC2	1	2a	0.62	1.24	0.29	4.09	0.06	1.80	1.04	8.51	27.5
LBC2	2	2a	0.46	1.65	0.35	5.39	0.11	1.63	1.56	10.7	34.6
LBC1	1	2a	0.61	1.16	0.16	3.87	0.03	0.29	0.56	6.08	27.6
LBC1	2	2a	1.26	0.88	0.14	2.91	0.05	0.77	1.03	5.78	26.9
DRW3	1	2a	0.08	0.78	0.39	2.48	0.00	0.00	0.33	3.98	15.5
DRW3	2	2a	0.19	0.83	0.12	2.72	0.00	0.00	0.41	4.07	14.8
DRW2	1	2a	0.06	0.85	0.07	2.44	0.00	0.15	0.41	3.91	14.2
DRW2	2	2a	0.10	0.90	0.06	2.74	0.04	0.05	0.43	4.23	15.5
DRW1	1	2a	0.08	0.79	0.01	2.05	0.00	0.00	0.31	3.16	11.9
DRW1	2	2a	1.10	0.75	0.08	2.30	0.01	0.00	0.36	3.50	10.2
SAND	1	2a	0.01	0.00	0.01	0.05	0.00	0.03	0.00	0.08	2.6
QC3	1	2b	0.06	0.12	0.07	0.26	0.00	0.29	0.05	0.79	5.1
QC3	2	2b	0.08	0.09	0.05	0.16	0.00	0.20	0.00	0.51	7.4
QC2	1	2b	0.04	0.13	0.02	0.25	0.00	0.07	0.04	0.51	4.2
QC2	2	2b	0.03	0.08	0.03	0.13	0.00	0.13	0.03	0.39	6.5
QC1	1	2b	0.15	0.06	0.00	0.13	0.00	0.00	0.24	0.44	7.7
QC1	2	2b	0.07	0.04	0.00	0.06	0.00	0.00	0.13	0.22	4.7
EB3	1	2b	0.08	0.10	0.01	0.28	0.02	0.00	0.05	0.46	5.2
EB3	2	2b	0.02	0.04	0.00	0.08	0.00	0.06	0.02	0.21	3.1

Site-Rep	Depth (cm)	Experiment	$\mu\text{mol g}^{-1}$								SEM-AVS /(foc)
			S ²⁻	Cu	Ni	Zn	Cd	Cr	Pb	SEM	
EB2	1	2b	0.02	0.05	0.01	0.07	0.00	0.05	0.12	0.29	10.1
EB1	1	2b	0.05	0.02	0.00	0.05	0.00	0.00	0.03	0.09	0.6
EB1	2	2b	0.04	0.02	0.00	0.08	0.00	0.00	0.02	0.12	3.6
LBC3	1	2b	0.76	0.36	0.06	1.31	0.02	0.35	0.45	2.55	13.1
LBC3	2	2b	0.63	0.31	0.06	1.05	0.01	0.43	0.37	2.24	16.4
LBC2	1	2b	0.36	0.65	0.11	1.18	0.02	0.62	0.54	3.13	26.2
LBC2	2	2b	0.55	0.67	0.12	1.26	0.02	0.70	0.54	3.31	29.3
LBC1	1	2b	0.53	0.97	0.20	2.79	0.06	1.06	1.02	6.09	26.1
LBC1	2	2b	0.92	0.81	0.17	2.23	0.05	1.14	0.87	5.27	29.4
DRW3	1	2b	0.17	0.84	0.14	2.18	0.00	0.19	0.41	3.74	13.6
DRW3	2	2b	0.17	0.89	0.14	2.10	0.00	0.16	0.39	3.69	13.6
DRW2	1	2b	0.12	0.80	0.16	2.06	0.00	0.40	0.39	3.80	17.4
DRW2	2	2b	0.12	0.95	0.14	2.08	0.00	0.28	0.41	3.85	13.7
DRW1	1	2b	0.06	0.75	0.12	1.87	0.00	0.09	0.34	3.18	13.9
DRW1	2	2b	0.12	0.98	0.22	2.70	0.01	0.22	0.44	4.58	16.1
SAND	1	2b	0.02	0.00	0.00	0.03	0.00	0.00	0.00	0.03	17.6
QC3	1	2c	2.48	0.07	0.01	0.29	0.00	0.02	0.04	0.44	-24.7
QC3	2	2c	0.82	0.13	0.03	0.36	0.00	0.10	0.07	0.70	-1.9
QC2	1	2c	3.30	0.09	0.02	0.36	0.03	0.04	0.03	0.57	-17.3
QC2	2	2c	2.19	0.05	0.01	0.14	0.00	0.02	0.06	0.28	-30.9
QC1	1	2c	2.85	0.07	0.00	0.25	0.00	0.00	0.04	0.36	-30.3
QC1	2	2c	1.07	0.04	0.00	0.16	0.00	0.00	0.03	0.24	-19.9
EB3	1	2c	2.83	0.06	0.00	0.26	0.00	0.00	0.25	0.57	-40.9
EB3	2	2c	2.48	0.02	0.00	0.22	0.00	0.00	0.05	0.29	-24.8
EB2	1	2c	0.29	0.06	0.00	0.20	0.00	0.01	0.29	0.57	5.3
EB2	2	2c	0.19	0.05	0.00	0.20	0.00	0.03	0.30	0.58	10.3
EB1	1	2c	2.39	0.02	0.00	0.33	0.00	0.00	0.05	0.40	-18.4
EB1	2	2c	0.53	0.01	0.01	0.09	0.00	0.02	0.00	0.13	-10.9
LBC3	1	2c	0.44	0.23	0.06	1.03	0.01	0.21	0.31	1.85	10.0
LBC3	2	2c	0.66	0.20	0.07	0.95	0.01	0.30	0.28	1.81	9.6
LBC2	1	2c	1.13	0.55	0.09	1.42	0.05	0.64	0.57	3.32	20.5
LBC2	2	2c	1.25	0.42	0.11	1.45	0.03	0.49	0.49	2.98	15.1
LBC1	1	2c	1.07	0.64	0.12	2.46	0.05	0.72	0.74	4.72	24.4
LBC1	2	2c	1.18	0.74	0.18	2.21	0.04	0.92	0.73	4.82	26.7
DRW3	1	2c	1.31	0.83	0.18	2.81	0.01	0.09	0.48	4.40	13.4
DRW3	2	2c	2.40	0.78	0.19	3.11	0.01	0.21	1.42	5.72	15.1
DRW2	1	2c	1.42	0.59	0.09	2.00	0.00	0.06	0.31	3.06	6.2
DRW2	2	2c	0.58	0.75	0.12	2.21	0.00	0.14	0.42	3.65	11.4
DRW1	1	2c	0.76	0.64	0.11	2.22	0.00	0.07	0.32	3.35	10.9
DRW1	2	2c	0.33	1.13	0.14	3.34	0.00	0.05	0.58	5.25	18.9

Table A-9. BLM output for HC5 and Toxicity Unit (TU)

Site	Experiment	Mean CHC5	Standard error CHC5	mean.TU	Standard error.TU
DRW	2b	417.1517	85.86548	0.16	0.00866
DRW	2b-d11	311.4817	58.88702	0.238333	0.060713
DRW	2b-d16	206.4667	20.15205	0.273333	0.115662
DRW	2c	109.705	17.44404	0.341667	0.032447
EB	2b	153.5733	31.16826	1.536667	0.267416
EB	2b-d11	126.505	25.54345	1.035	0.388887
EB	2b-d16	103.7783	17.97847	0.325	0.064291
EB	2c	92.35833	4.052589	0.321667	0.134794
LBC	2b	238.6183	5.092424	1.64	0.270201
LBC	2b-d11	197.8833	7.915036	1.21	0.162096
LBC	2b-d16	159.5017	4.623564	0.903333	0.367337
LBC	2c	123.6267	17.41992	0.831667	0.306245
QC	2b	338.73	81.95738	0.728333	0.415796
QC	2b-d11	251.955	55.20035	0.31	0.039686
QC	2b-d16	185.7267	18.30911	0.181667	0.024552
QC	2c	92.82167	5.046616	0.543333	0.178916

Table A-10. Calculated hardness corrected CCC's

Site	Experiment	Zn CCC ($\mu\text{g L}^{-1}$)
DRW	2b	387.830
DRW	2b-d11	317.431
DRW	2b-d16	285.432
DRW	2c	183.033
EB	2b	333.527
EB	2b-d11	282.924
EB	2b-d16	259.923
EB	2c	186.320
LBC	2b	387.830
LBC	2b-d11	324.597
LBC	2b-d16	295.855
LBC	2c	203.879
QC	2b	387.830
QC	2b-d11	316.617
QC	2b-d16	284.247
QC	2c	180.663

Appendix B (Chapter 3 Data)

Table B-1. BLM chemical input data, where constant temperature (18.35°C), pH (7.14), humic acid content (10%), and alkalinity (3.08 mgL⁻¹ CaCO₃) were assumed.

Site	Day	Zn (µgL ⁻¹)	DOC (mg-C L ⁻¹)	Concentration (mgL ⁻¹)						
				Ca	Mg	Na	K	SO ₄	Cl	S
DRW	1	113.87	0.14	134.81	420.75	124.83	11.27	228.64	148.04	0.001
DRW	11	20.06	0.14	72.43	233.49	67.06	6.06	122.11	79.06	0.002
EB	1	84.36	0.72	111.37	232.10	103.12	9.31	188.60	122.12	0.001
EB	11	0.00	0.72	62.31	130.69	57.69	5.21	104.83	67.87	0.002
LBC	1	69.61	0.27	59.61	151.18	55.19	4.98	100.22	64.89	0.001
LBC	11	21.56	0.27	45.22	111.19	41.87	3.78	75.65	48.98	0.002
QC	1	119.45	1.69	119.39	240.77	110.54	9.98	202.30	130.98	0.001
QC	11	0.00	1.69	66.58	137.05	61.64	5.57	112.11	72.59	0.002
RAIS	1	0.00	0.70	57.49	22.32	53.23	4.81	96.59	62.54	0.001
RAIS	11	8.69	0.70	68.52	20.89	63.45	5.73	115.44	74.75	0.002

Table B-2. Hardness corrected CCC for Zn in surface water (n=3).

Site	Day	Surface Water ($\mu\text{g-Zn L}^{-1}$)	\pm	Hardness ($\text{mgL}^{-1} \text{CaCO}_3$)	Hardness Corrected CCC	Zn exceedance?
DRW	1	113.87	83.25	337.03	335.44	No
DRW	11	20.06	1.10	181.07	198.14	No
EB	1	84.36	57.49	278.42	285.31	No
EB	11	0.00	0.00	155.77	174.43	No
LBC	1	69.61	35.72	149.02	168.00	No
LBC	11	21.56	11.69	113.06	132.95	No
QC	1	119.45	48.08	298.47	302.62	No
QC	11	0.00	0.00	166.44	184.49	No
RAIS	1	0.00	0.00	143.71	162.91	No
RAIS	11	8.69	8.69	171.31	189.06	No

Table B-3. BLM estimated HC5s for Zn in surface water (n=3).

Site	Day	Chronic HC5 (CHC5), μgL^{-1}	Zn μgL^{-1}	Chronic Toxic Units (Chronic TU=Zn/CHC5)
DRW	1	166.55	113.87	0.68
DRW	11	96.07	20.06	0.21
EB	1	121.13	84.36	0.70
EB	11	75.08	0.65	0.01
LBC	1	71.17	69.61	0.98
LBC	11	57.15	21.56	0.38
QC	1	139.79	119.45	0.85
QC	11	89.53	0.65	0.01
RAIS	1	46.82	0.65	0.01
RAIS	11	54.51	8.69	0.16

Table B-4. Porewater metal data in dissolved phase with standard error between replicates (n=3). Detection limits were 15 $\mu\text{g L}^{-1}$ for Cu and 10 $\mu\text{g L}^{-1}$ for Ni.

Site	Day	Cu ($\mu\text{g L}^{-1}$)	\pm	Fe (mg L^{-1})	\pm	Mn (mg L^{-1})	\pm	Ni ($\mu\text{g L}^{-1}$)	\pm	Zn ($\mu\text{g L}^{-1}$)	\pm
DRW	1	ND	ND	1.32	0.34	0.04	ND	ND	ND	257.54	27.85
DRW	4	ND	ND	0.35	0.07	0.23	0.07	ND	ND	146.81	41.51
DRW	6	ND	ND	0.53	0.15	0.37	0.12	ND	ND	69.21	17.72
DRW	8	0.01	ND	0.55	0.12	0.42	0.14	ND	ND	50.89	7.19
DRW	11	ND	ND	0.87	0.23	0.39	0.13	ND	ND	91.57	17.75
EB	1	ND	ND	0.05	0.02	0.02	0.01	ND	ND	198.10	34.50
EB	4	ND	ND	0.18	0.07	0.18	0.06	ND	ND	197.48	34.30
EB	6	ND	ND	0.24	0.07	0.21	0.05	ND	ND	55.32	7.75
EB	8	ND	ND	0.39	0.13	0.27	0.04	ND	ND	49.60	9.68
EB	11	ND	ND	0.49	0.17	0.28	0.05	ND	ND	66.81	26.18
LBC	1	0.01	ND	2.23	1.00	0.10	0.02	ND	ND	487.63	78.13
LBC	4	ND	ND	0.40	0.04	0.59	0.07	ND	ND	273.33	31.30
LBC	6	0.01	ND	0.83	0.21	0.73	0.10	ND	ND	201.07	28.82
LBC	8	0.01	ND	1.01	0.10	0.90	0.12	ND	ND	176.99	30.57
LBC	11	ND	ND	1.62	0.12	0.97	0.16	ND	ND	203.07	25.88
QC	1	ND	ND	0.05	0.02	0.03	0.01	ND	ND	129.17	24.03
QC	4	0.01	0.01	0.23	0.05	0.21	0.06	ND	ND	143.11	26.03
QC	6	ND	ND	0.36	0.09	0.23	0.07	ND	ND	51.62	7.84
QC	8	ND	ND	0.50	0.14	0.24	0.08	ND	ND	54.96	18.74
QC	11	ND	ND	0.76	0.27	0.28	0.11	ND	ND	86.57	25.89
RAIS	1	0.46	0.03	0.03	0.01	1.65	0.81	0.88	0.06	4.35	0.45
RAIS	7	0.39	0.09	1.55	0.75	2.76	0.16	0.20	0.09	59.57	17.77
RAIS	11	0.11	0.06	3.45	1.17	4.23	1.05	0.28	0.07	0.38	0.23

Table B-5. Bioavailable Zn as measured using DGTs for several sediment depths

Site	Replicate	Depth (cm)	C _{DGT} (ng-Zn cm ⁻³)
LBC	1	0-1	57.48
LBC	1	1-2	41.19
LBC	1	2-3	74.72
LBC	2	0-1	30.58
LBC	2	1-2	36.09
LBC	2	2-3	59.07
EB	1	0-1	8.08
EB	1	1-2	7.71
EB	1	2-3	8.97
EB	2	0-1	6.90
EB	2	1-2	6.96
EB	2	2-3	8.05
QC	1	0-1	8.63
QC	1	1-2	44.90
QC	1	2-3	25.32
QC	2	0-1	20.77
QC	2	1-2	9.27
QC	2	2-3	7.29
DRW	1	0-1	14.15
DRW	1	1-2	20.32
DRW	1	2-3	20.33
DRW	2	0-1	13.94
DRW	2	1-2	13.60
DRW	2	2-3	17.33

Table B-6. Porewater dissolved oxygen (DO) and reduced Fe per day and site-rep

Site-Rep	DO (mg L ⁻¹)					[Fe ²⁺] (mg L ⁻¹)				
	Day1	Day4	Day6	Day8	Day11	Day1	Day4	Day6	Day8	Day11
QC3-1	1.50	1.57	1.60	1.60	0.79	0.00	0.01	0.01	0.02	0.02
QC3-2	1.02	1.12	1.11	1.01	0.94	0.00	0.13	0.16	0.17	0.28
QC2-2	1.12	1.11	1.10	1.00	0.80	0.00	0.10	0.30	0.39	0.72
QC1-1	1.02	1.13	1.26	1.13	0.76	0.00	0.07	0.02	0.04	1.16
QC1-2	1.01	1.13	1.11	1.01	1.35	0.00	0.01	0.01	0.42	0.04
EB3-1	1.44	3.60	1.16	1.01	1.77	0.00	0.05	0.17	0.09	0.50
EB3-2	2.43	4.05	2.96	2.02	0.84	0.00	0.03	0.00	0.14	0.37
EB2-1	3.13	1.12	1.11	1.00	0.88	0.00	0.00	0.00	0.00	0.00
EB2-2	2.32	1.46	1.11	1.00	0.79	0.00	0.01	0.00	0.02	0.06
EB1-1	1.01	1.44	1.11	1.01	0.80	0.00	0.00	0.02	0.04	0.06
EB1-2	1.01	1.12	3.36	1.00	0.79	0.00	0.03	0.04	0.11	0.25
LBC3-1	1.63	1.20	1.24	1.09	0.95	0.00	0.06	0.13	0.31	0.75
LBC3-2	2.52	1.37	1.67	1.36	1.40	0.00	0.03	0.06	0.14	0.60
LBC2-1	2.62	3.06	3.14	1.98	0.76	0.00	0.04	0.14	0.26	0.78
LBC2-2	1.01	1.12	1.10	1.00	1.05	0.00	0.05	0.29	0.56	0.99
LBC1-1	1.02	1.32	1.47	1.17	1.02	0.00	0.11	0.24	0.41	0.96
LBC1-2	1.35	1.13	1.41	1.01	1.54	0.00	0.14	0.32	0.52	1.19
DRW3-1	1.02	1.35	1.12	1.17	1.66	0.00	0.04	0.32	0.44	0.50
DRW3-2	1.02	1.12	1.11	1.00	1.37	0.00	0.15	0.30	0.54	0.90
DRW2-1	1.31	2.77	2.11	1.68	0.76	0.00	0.00	0.01	0.06	0.12
DRW2-2	1.02	1.13	1.11	1.01	0.80	0.00	0.00	0.04	0.15	0.74
DRW1-2	1.01	1.11	1.12	1.00	0.79	0.00	0.05	0.15	0.24	0.44
SAND-1	6.19	3.42	3.05	1.95	2.98	0.00	0.00	0.00	0.00	0.00
SAND-2	8.45	2.99	2.86	-	2.83	0.00	0.00	0.00	0.00	0.00
BEAKER	7.59	7.68	-	-	7.22	0.00	0.00	0.00	0.00	0.00

Table B-7. Surface water and sediment pH

Site-Rep	Day	surface water	1-cm sediment depth	2-cm sediment depth
QC3	1	6.94	7.05	7.17
QC2	1	7.08	7.15	7.31
QC1	1	7.08	6.92	6.84
EB3	1	7.33	7.15	7.22
EB2	1	7.29	7.27	7.33
EB1	1	6.25	7	7.12
LBC3	1	7.05	7.12	7.1
LBC2	1	6.9	6.95	6.87
LBC1	1	6.67	6.7	6.74
DRW3	1	7.19	6.9	6.65
DRW2	1	7.17	6.85	6.72
DRW1	1	7.21	6.83	6.74
SAND	1	7.58	7.68	7.75
BEAKER	1	7.63	7.63	7.63
QC3	11	7.33	7.33	7.21
QC2	11	7.31	7.18	7.1
QC1	11	7.27	7.15	7.15
EB3	11	7.43	7.24	7.23
EB2	11	7.44	7.4	7.29
EB1	11	7.33	7.31	7.2
LBC3	11	6.76	6.37	5.97
LBC2	11	6.66	6.21	6.02
LBC1	11	6.74	6.39	6.13
DRW3	11	7.18	6.74	6.58
DRW2	11	7.09	6.69	6.62
DRW1	11	7.01	6.61	6.46
SAND	11	7.5	7.44	7.29
BEAKER	11	7.6	-	-

Table B-8. Porewater metal concentrations for Fe, Mn, Zn, Ca, and Mg

Site-Rep	Depth (cm)	Day	Fe (mg L ⁻¹)	Mn (mg L ⁻¹)	Zn (µg L ⁻¹)	Ca (mg L ⁻¹)	Mg (mg L ⁻¹)
QC3	1	1	0.02	0.02	46.35	10.58	20.38
QC3	2	1	0.04	0.06	69.85	13.36	23.63
QC2	1	1	0.05	0.02	171.71	11.81	28.06
QC2	2	1	0.12	0.02	147.69	NA	NA
QC1	1	1	0.02	0.01	142.28	11.14	17.84
QC1	2	1	0.03	0.02	197.11	12.94	26.49
EB3	1	1	0.06	0.05	107.50	13.34	21.37
EB3	2	1	0.03	0.00	190.41	16.65	28.18
EB2	1	1	0.01	0.00	236.39	6.90	20.31
EB2	2	1	0.15	0.01	337.86	12.44	19.88
EB1	1	1	0.02	0.05	117.79	7.87	19.94
EB1	2	1	0.02	0.01	198.63	9.62	29.58
LBC3	1	1	0.25	0.05	124.24	2.75	9.19
LBC3	2	1	4.28	0.08	526.97	11.28	24.35
LBC2	1	1	2.32	0.09	696.79	4.67	13.72
LBC2	2	1	0.18	0.08	504.28	3.59	10.47
LBC1	1	1	6.01	0.12	554.97	6.12	15.14
LBC1	2	1	0.35	0.17	518.57	8.37	20.86
DRW3	1	1	1.23	0.03	246.96	12.62	41.47
DRW3	2	1	2.51	0.03	223.53	19.51	63.32
DRW2	1	1	2.05	0.04	244.75	13.08	38.95
DRW2	2	1	1.25	0.05	390.35	14.84	42.76
DRW1	1	1	0.43	0.03	193.90	5.85	18.28
DRW1	2	1	0.44	0.03	245.77	14.99	47.66
QC3	1	4	0.08	0.06	92.84	NA	NA
QC3	2	4	0.31	0.26	146.90	NA	NA
QC2	1	4	0.14	0.11	200.92	NA	NA
QC2	2	4	0.29	0.26	108.25	NA	NA
QC1	1	4	0.13	0.15	235.36	NA	NA
QC1	2	4	0.40	0.45	74.41	NA	NA
EB3	1	4	0.49	0.43	90.75	NA	NA
EB3	2	4	0.19	0.24	197.97	NA	NA
EB2	1	4	0.02	0.04	296.68	NA	NA
EB2	2	4	0.06	0.02	111.05	NA	NA
EB1	1	4	0.12	0.17	210.83	NA	NA
EB1	2	4	0.18	0.17	277.57	NA	NA
LBC3	1	4	0.35	0.37	169.24	NA	NA
LBC3	2	4	0.35	0.68	260.97	NA	NA

Site-Rep	Depth (cm)	Day	Fe (mg L ⁻¹)	Mn (mg L ⁻¹)	Zn (µg L ⁻¹)	Ca (mg L ⁻¹)	Mg (mg L ⁻¹)
LBC2	1	4	0.49	0.38	219.73	NA	NA
LBC2	2	4	0.27	0.61	316.31	NA	NA
LBC1	1	4	0.47	0.68	283.93	NA	NA
LBC1	2	4	0.46	0.82	389.80	NA	NA
DRW3	1	4	0.59	0.16	160.74	NA	NA
DRW3	2	4	0.52	0.42	60.43	NA	NA
DRW2	1	4	0.26	0.05	83.39	NA	NA
DRW2	2	4	0.23	0.39	326.59	NA	NA
DRW1	1	4	0.32	0.03	182.83	NA	NA
DRW1	2	4	0.19	0.34	66.85	NA	NA
QC3	1	6	0.10	0.05	54.35	NA	NA
QC3	2	6	0.37	0.23	64.84	NA	NA
QC2	1	6	0.24	0.09	22.68	NA	NA
QC2	2	6	0.58	0.31	33.56	NA	NA
QC1	1	6	0.17	0.17	69.96	NA	NA
QC1	2	6	0.68	0.55	64.35	NA	NA
EB3	1	6	0.51	0.40	67.65	NA	NA
EB3	2	6	0.36	0.28	53.34	NA	NA
EB2	1	6	0.04	0.09	31.94	NA	NA
EB2	2	6	0.05	0.13	60.51	NA	NA
EB1	1	6	0.17	0.18	82.07	NA	NA
EB1	2	6	0.29	0.18	36.41	NA	NA
LBC3	1	6	0.59	0.45	112.76	NA	NA
LBC3	2	6	0.50	0.82	181.43	NA	NA
LBC2	1	6	0.41	0.40	128.81	NA	NA
LBC2	2	6	0.87	0.97	274.29	NA	NA
LBC1	1	6	1.82	0.79	239.91	NA	NA
LBC1	2	6	0.78	0.93	269.23	NA	NA
DRW3	1	6	0.61	0.23	36.94	NA	NA
DRW3	2	6	1.24	0.64	49.08	NA	NA
DRW2	1	6	0.27	0.06	40.55	NA	NA
DRW2	2	6	0.36	0.62	151.10	NA	NA
DRW1	1	6	0.21	0.02	83.77	NA	NA
DRW1	2	6	0.48	0.64	53.80	NA	NA
QC3	1	8	0.13	0.04	27.69	NA	NA
QC3	2	8	0.50	0.24	76.54	NA	NA
QC2	1	8	0.30	0.07	132.99	NA	NA
QC2	2	8	0.85	0.29	51.87	NA	NA
QC1	1	8	0.23	0.18	ND	NA	NA
QC1	2	8	0.98	0.61	40.68	NA	NA

Site-Rep	Depth (cm)	Day	Fe (mg L ⁻¹)	Mn (mg L ⁻¹)	Zn (µg L ⁻¹)	Ca (mg L ⁻¹)	Mg (mg L ⁻¹)
EB3	1	8	0.91	0.45	57.01	NA	NA
EB3	2	8	0.53	0.34	90.34	NA	NA
EB2	1	8	0.08	0.16	28.46	NA	NA
EB2	2	8	0.12	0.24	26.04	NA	NA
EB1	1	8	0.26	0.20	41.33	NA	NA
EB1	2	8	0.43	0.21	54.42	NA	NA
LBC3	1	8	1.01	0.61	59.28	NA	NA
LBC3	2	8	0.75	1.01	138.51	NA	NA
LBC2	1	8	0.74	0.49	161.75	NA	NA
LBC2	2	8	1.12	1.29	207.68	NA	NA
LBC1	1	8	1.03	0.87	218.88	NA	NA
LBC1	2	8	1.41	1.12	275.86	NA	NA
DRW3	1	8	0.75	0.27	57.78	NA	NA
DRW3	2	8	0.96	0.73	80.67	NA	NA
DRW2	1	8	0.28	0.09	48.05	NA	NA
DRW2	2	8	0.63	0.67	41.68	NA	NA
DRW1	1	8	0.17	0.02	49.07	NA	NA
DRW1	2	8	0.50	0.76	28.07	NA	NA
QC3	1	11	0.16	0.03	736.52	5.58	11.59
QC3	2	11	0.55	0.18	62.61	6.50	12.27
QC2	1	11	0.22	0.04	179.37	4.97	12.33
QC2	2	11	1.30	0.37	58.66	NA	NA
QC1	1	11	0.23	0.14	30.06	9.00	15.54
QC1	2	11	1.49	0.66	102.15	8.92	18.16
EB3	1	11	1.16	0.43	170.07	7.88	12.79
EB3	2	11	0.73	0.36	118.71	4.97	9.29
EB2	1	11	0.00	0.15	0.00	4.17	12.36
EB2	2	11	0.22	0.33	43.15	9.62	14.57
EB1	1	11	0.22	0.18	27.96	4.19	10.58
EB1	2	11	0.62	0.20	40.93	6.55	18.82
LBC3	1	11	1.76	0.65	125.02	3.82	9.29
LBC3	2	11	1.59	1.25	140.10	6.67	14.76
LBC2	1	11	1.16	0.49	235.81	3.78	11.01
LBC2	2	11	1.53	1.56	185.72	3.82	9.99
LBC1	1	11	1.60	0.84	285.41	3.27	8.08
LBC1	2	11	2.08	1.02	246.39	6.83	16.73
DRW3	1	11	0.90	0.19	109.73	6.84	22.24
DRW3	2	11	1.49	0.70	94.66	11.22	36.55
DRW2	1	11	0.42	0.12	24.14	5.39	16.76
DRW2	2	11	1.57	0.69	57.65	8.80	27.50

Site-Rep	Depth (cm)	Day	Fe (mg L ⁻¹)	Mn (mg L ⁻¹)	Zn (µg L ⁻¹)	Ca (mg L ⁻¹)	Mg (mg L ⁻¹)
DRW1	1	11	0.13	0.03	141.65	3.43	11.38
DRW1	2	11	0.73	0.64	121.62	7.77	25.68

Table B-9. Sediment simultaneously extracted metals (SEM) minus acid volatile sulfide (AVS), loss-on-ignition (f_{oc}), and water content.

Site	Experiment	(SEM-AVS)		AVS (µmol gdw ⁻¹)		f_{oc}		Water content (%)
		f_{oc}	±	±	±	±	±	
DRW	3-d1	19.52	1.33	0.06	0.03	0.21	0.00	78.33
DRW	3-d11	16.72	0.35	0.06	0.02	0.22	0.01	79.33
DRW	3A	14.04	0.57	0.24	0.10	0.24	0.01	60
EB	3-d1	11.64	4.61	0.03	0.01	0.05	0.02	43.33
EB	3-d11	16.35	6.47	0.04	0.00	0.03	0.01	33.67
EB	3A	11.06	1.30	0.02	0.00	0.06	0.02	17.67
LBC	3-d1	32.47	5.26	0.33	0.05	0.13	0.02	58
LBC	3-d11	30.89	4.80	0.23	0.03	0.14	0.04	61
LBC	3A	25.75	4.22	0.31	0.04	0.14	0.03	36
QC	3-d1	6.06	0.89	0.02	0.00	0.08	0.00	59.33
QC	3-d11	6.43	0.77	0.08	0.04	0.08	0.01	55.67
QC	3A	5.75	0.79	0.01	0.00	0.15	0.02	31
RAIS	3-d1	-109.67	NA	1.878	NA	0.02	NA	NA
RAIS	3-d11	-9.95	NA	0.818	NA	0.02	NA	NA
RAIS	3A	-11.24	NA	0.424	NA	0.03	NA	NA

Table B-10. Extended Sediment [SEM-AVS] / f_{OC} data table

Site	Day	$\mu\text{mol g}^{-1}$								SEM:AVS/ (f_{OC})
		S ²⁻	Cu	Ni	Zn	Cd	Cr	Pb	SEM	
QC3	0	0.022	0.45	0.00	1.75	0.00	0.00	0.35	2.55	13.79
QC2	0	0.009	0.61	0.00	1.98	0.00	0.00	0.00	2.58	15.21
QC1	0	0.010	0.65	0.00	2.02	0.00	0.00	0.51	3.18	30.18
EB3	0	0.024	1.00	0.00	3.27	0.00	0.00	3.16	7.44	71.29
EB2	0	0.012	0.33	0.00	1.64	0.00	0.00	0.00	1.98	64.70
EB1	0	0.017	0.64	0.00	1.61	0.00	0.00	2.06	4.31	67.93
LBC3	0	0.235	1.29	0.00	5.07	0.06	0.99	1.79	9.22	96.34
LBC2	0	0.325	3.64	0.00	10.51	0.23	3.75	3.56	21.69	122.90
LBC1	0	0.358	3.14	0.00	8.98	0.17	3.55	3.47	19.31	121.12
DRW3	0	0.037	2.38	0.00	6.14	0.00	0.44	1.25	10.21	42.56
DRW2	0	0.324	2.38	0.00	6.07	0.00	0.40	1.43	10.28	39.11
DRW1	0	0.365	2.16	0.00	5.66	0.00	0.34	0.85	9.00	38.57
QC3	1	0.024	0.47	0.00	1.45	0.00	0.00	0.00	1.92	21.17
QC2	1	0.011	0.68	0.00	1.94	0.00	0.00	0.00	2.62	31.26
QC1	1	0.019	0.65	0.00	2.29	0.00	0.00	0.37	3.31	39.49
EB3	1	0.022	0.52	0.00	1.63	0.00	0.00	2.14	4.28	133.96
EB2	1	0.021	0.65	0.00	2.02	0.00	0.00	0.00	2.66	78.77
EB1	1	0.044	0.00	0.00	1.67	0.00	0.00	0.00	1.67	17.57
LBC3	1	0.284	1.67	0.00	6.37	0.09	1.65	2.33	12.11	130.15
LBC2	1	0.287	3.41	0.00	9.13	0.20	3.08	3.38	19.19	125.80
LBC1	1	0.426	4.18	2.11	12.47	0.21	4.07	4.30	27.34	174.93
DRW3	1	0.109	1.56	0.00	4.94	0.00	0.33	0.83	7.66	35.97
DRW2	1	0.027	1.64	0.00	4.31	0.00	0.39	1.10	7.44	35.70
DRW1	1	0.040	1.75	0.00	5.11	0.00	0.00	0.98	7.83	35.50
QC3	11	0.032	0.48	0.00	1.63	0.00	0.00	0.00	2.11	28.63
QC2	11	0.033	0.00	0.00	0.93	0.00	0.00	0.00	0.93	11.58
QC1	11	0.164	0.65	0.00	2.30	0.00	0.00	0.40	3.35	33.18
EB3	11	0.036	0.56	0.00	1.69	0.00	0.00	2.23	4.48	93.15
EB2	11	0.040	0.57	0.00	1.94	0.00	0.00	2.16	4.67	219.60
EB1	11	0.050	0.00	0.00	0.81	0.00	0.00	0.00	0.81	23.89
LBC3	11	0.244	1.40	0.00	5.22	0.07	1.08	1.57	9.34	97.44
LBC2	11	0.260	2.87	0.00	7.51	0.18	2.80	2.95	16.31	126.01
LBC1	11	0.178	2.67	0.00	7.72	0.16	2.08	2.91	15.55	72.58
DRW3	11	0.048	1.32	0.00	3.95	0.00	0.00	0.70	5.98	28.23
DRW2	11	0.043	1.28	0.00	3.42	0.00	0.00	0.66	5.36	21.84
DRW1	11	0.092	1.35	0.00	4.18	0.00	0.00	0.56	6.08	29.26

Table B-11. *Hyalella azteca* survival, individual growth rate, and body concentration Zn

Site-Rep	Survival (%)	IGR ($\mu\text{g day}^{-1}$)	Zn body concentration ($\mu\text{g gdw}^{-1}$)
QC3	100	0.848	274.28
QC3	NA	NA	NA
QC2	100	2.657	66.02
QC2	100	1.086	165.45
QC1	100	1.800	138.73
QC1	100	1.657	188.73
EB3	100	1.324	145.27
EB3	100	0.848	NA
EB2	100	1.800	254.95
EB2	100	1.943	208.32
EB1	100	0.014	383.13
EB1	70	1.086	261.39
LBC3	100	1.264	324.34
LBC3	90	0.213	242.75
LBC2	100	1.165	207.33
LBC2	100	1.800	78.52
LBC1	90	0.689	362.75
LBC1	90	0.193	263.87
DRW3	90	0.689	NA
DRW3	100	1.006	127.57
DRW2	100	0.800	170.10
DRW2	100	0.800	188.36
DRW1	100	0.000	182.36
DRW1	90	2.752	225.65
SAND	70	0.000	344.65
SAND	100	0.550	197.99
CONTROL	90	4.498	0.00
CONTROL	100	4.514	0.00

Table B-12. *Daphnia magna* (DM) survival, reproduction, growth (IGR), and body concentration Zn.

Site-Rep	Survival (%)	Reproduction (neonates/adult)	DM IGR ($\mu\text{g day}^{-1}$)	DM Zn body concentration ($\mu\text{g gdw}^{-1}$)
QC3	100	1.80	16.38	85.20
QC3	100	0.00	NA	NA
QC2	NA	0.00	NA	NA
QC2	80	0.00	6.59	164.64
QC1	80	0.00	11.17	47.92
QC1	80	0.00	NA	NA
EB3	100	3.60	17.05	66.75
EB3	100	2.20	NA	NA
EB2	100	3.20	16.30	196.29
EB2	100	1.60	NA	NA
EB1	100	2.60	20.62	32.52
EB1	100	3.40	NA	NA
LBC3	100	1.60	15.95	62.31
LBC3	100	1.40	NA	NA
LBC2	100	2.00	25.69	40.30
LBC2	100	4.60	NA	NA
LBC1	100	8.00	19.09	27.96
LBC1	100	6.40	NA	NA
DRW3	100	5.60	23.18	16.68
DRW3	100	1.20	NA	NA
DRW2	100	0.00	10.67	30.79
DRW2	100	0.00	NA	NA
DRW1	100	5.20	19.30	10.65
DRW1	100	5.00	NA	NA
CONTROL	60	4.33	29.11	0.00
CONTROL	100	2.80	NA	NA

Appendix C (Chapter 4 Data)

Table C-1. Porewater chemistry including dissolved oxygen (DO), pH, reduced iron (Fe^{2+}) and redox potential (Eh).

Site	Day	DO (mgL^{-1})	\pm	pH	\pm	Fe^{2+} (mgL^{-1})	\pm	Eh (mV)	\pm
CNTL	1	5.2	0.4	7.6	-	0.3	-	-	-
	7	2.0	0.2	7.4	0.1	1.6	1.1	-25.7	6.3
	11	2.4	0.2	7.5	0.0	3.2	0.3	-137.3	6.2
REF	1	4.5	0.3	6.0	0.1	0.2	0.1	-	-
	7	2.7	0.4	6.0	0.1	3.1	1.7	67.9	14.4
	11	2.7	0.1	6.4	0.1	5.1	2.3	14.3	18.6
SPN	1	4.8	0.4	6.3	0.1	0.8	0.3	-	-
	7	4.1	0.2	6.5	0.1	6.3	2.1	28.7	7.9
	11	3.6	0.4	6.7	0.0	3.1	1.3	-6.9	5.9
WIL	1	4.6	0.4	6.4	0.0	1.7	1.2	-	-
	7	3.0	0.7	6.4	0.1	6.8	1.1	-1.3	20.9
	11	2.9	0.5	6.6	0.0	3.7	1.3	-32.5	16.0

Table C-2. Surface water dissolved Zn, Fe, and Mn concentrations.

Site	Day	Fe (mgL ⁻¹)	±	Mn (mgL ⁻¹)	±	Zn (µgL ⁻¹)	±
CNTL	1	ND		ND		89.03	9.89
CNTL	7	0.01	0.01	ND		148.42	2.08
CNTL	11	ND		0.01	0.01	137.52	25.45
REF	1	ND		ND		110.69	9.70
REF	7	ND		0.01	0.01	31.84	0.32
REF	11	ND		ND		118.40	14.54
SPN	1	ND		1.59	0.18	171.23	6.26
SPN	7	ND		0.59	0.11	160.24	10.66
SPN	11	0.06	0.04	0.27	0.09	137.91	8.34
WIL	1	ND		0.44	0.14	141.55	39.72
WIL	7	ND		0.29	0.08	184.35	19.17
WIL	11	ND		0.07	0.03	131.60	14.02

*Detection limit $\approx 10 \mu\text{g L}^{-1}$

Table C-3. Hardness corrected CCC's shown with initial data (porewater metal concentrations and Ca calculated hardness).

Day	Site-Rep	Porewater metal ($\mu\text{g L}^{-1}$)			Hardness CaCO_3 (mg L^{-1})	Hardness Corrected CCC ($\mu\text{g L}^{-1}$)		CCC Exceedance?		
		Cd	Zn	Al		Cd	Zn	Cd	Zn	Al
1	WIL1	0.94	434.01	15.00	108.58	0.84	128.47	Yes	Yes	
1	WIL1	0.17	82.73	5.10	101.03	0.80	120.86			
1	WIL2	0.42	262.30	3.37	105.42	0.82	125.30		Yes	
1	WIL2	1.76	86.14	82.30	110.30	0.85	130.19	Yes		
1	WIL3	1.72	82.80	54.20	129.23	0.97	148.89	Yes		
1	REF1	0.50	43.80	49.20	105.36	0.82	125.24			
1	REF1	0.29	161.80	5.91	108.62	0.84	128.51		Yes	
1	REF2	0.41	26.50	11.08	129.89	0.97	149.54			
1	REF2	0.70	108.10	5.42	155.77	1.13	174.43			
1	REF3	0.69	124.20	108.60	153.27	1.11	172.05			Yes
1	SPN1	0.23	11.60	1.50	128.01	0.96	147.70			
1	SPN1	0.54	16.20	7.06	174.86	1.23	192.37			
1	SPN2	0.59	35.60	2.84	126.69	0.95	146.41			
1	SPN2	0.65	19.30	2.03	124.91	0.94	144.67			
1	SPN3	0.23	51.40	6.83	112.93	0.87	132.82			
1	CNTL1	0.03	4.80	15.30	280.52	1.80	287.13			
1	CNTL1	0.02	3.90	9.16	192.60	1.33	208.79			
7	CNTL1	0.01	77.34	602.27	178.54	1.25	195.80			Yes
7	CNTL1	0.01	41.80	649.40	234.42	1.56	246.62			Yes
7	CNTL2	0.01	103.86	610.72	263.11	1.71	271.96			Yes
7	CNTL2	0.02	144.13	708.90	407.97	2.43	394.36			Yes
7	REF1	0.16	83.89	22.77	101.38	0.80	121.21			
7	REF1	0.16	90.62	4.43	149.47	1.09	168.43			
7	REF2	0.16	91.68	38.22	96.41	0.77	116.17			
7	REF2	0.26	227.60	40.89	112.23	0.87	132.12		Yes	
7	REF3	0.65	113.61	56.40	136.83	1.01	156.28			
7	SPN1	0.09	60.57	579.48	121.22	0.92	141.04			Yes
7	SPN1	0.12	67.50	585.09	145.17	1.06	164.32			Yes
7	SPN2	0.18	87.12	572.53	117.89	0.90	137.74			Yes
7	SPN2	0.22	88.65	580.79	133.65	1.00	153.19			Yes
7	SPN3	0.14	91.06	612.50	119.56	0.91	139.40			Yes
7	WIL1	0.36	362.84	101.79	131.94	0.99	151.53		Yes	Yes
7	WIL1	0.12	88.09	111.74	153.31	1.11	172.09			Yes
7	WIL2	0.91	197.06	200.33	116.55	0.89	136.42	Yes	Yes	Yes
7	WIL2	0.18	165.40	187.10	121.97	0.93	141.78		Yes	Yes

Day	Site-Rep	Porewater metal ($\mu\text{g L}^{-1}$)			Hardness CaCO_3 (mg L^{-1})	Hardness Corrected CCC ($\mu\text{g L}^{-1}$)		CCC Exceedance?		
		Cd	Zn	Al		Cd	Zn	Cd	Zn	Al
7	WIL3	0.38	151.72	190.35	115.55	0.89	135.42	Yes	Yes	
11	WIL1	0.18	178.86	10.87	107.71	0.84	127.60	Yes		
11	WIL1	0.10	351.74	3.81	98.44	0.78	118.24	Yes		
11	WIL1	0.04	9.67	14.50	137.87	1.02	157.28			
11	WIL1	0.01	13.59	9.74	115.39	0.89	135.27			
11	WIL2	0.36	60.03	101.64	109.02	0.85	128.91			Yes
11	WIL2	0.14	13.11	3.60	90.66	0.73	110.26			
11	WIL2	0.05	66.90	51.33	117.22	0.90	137.08			
11	WIL2	0.01	3.28	5.73	94.62	0.76	114.33			
11	WIL3	0.15	31.88	63.62	113.17	0.87	133.06			
11	WIL3	0.07	8.14	5.11	101.62	0.80	121.46			
11	REF1	0.04	5.66	22.91	134.88	1.00	154.39			
11	REF1	0.01	1.26	6.33	107.39	0.84	127.28			
11	REF2	0.05	2.86	38.59	123.05	0.93	142.84			
11	REF2	0.03	0.65	12.02	98.32	0.78	118.10			
11	REF2	0.10	56.56	17.04	103.36	0.81	123.22			
11	REF2	0.06	25.69	5.99	85.45	0.70	104.87			
11	REF3	0.35	30.81	118.24	126.26	0.95	145.99			Yes
11	REF3	0.26	15.66	3.83	114.27	0.88	134.15			
11	SPN1	0.09	12.49	50.86	122.16	0.93	141.96			
11	SPN1	0.04	3.77	4.39	102.63	0.81	122.48			
11	SPN1	0.06	4.70	16.57	141.94	1.04	161.21			
11	SPN1	0.03	5.59	6.31	115.45	0.89	135.32			
11	SPN2	0.12	8.76	37.26	111.78	0.86	131.67			
11	SPN2	0.04	2.89	3.90	98.90	0.78	118.70			
11	SPN2	0.07	307.71	33.40	112.71	0.87	132.60	Yes		
11	SPN3	0.04	311.87	12.47	94.90	0.76	114.62	Yes		
11	CNTL1	0.03	6.13	60.99	200.75	1.38	216.25			
11	CNTL1	0.03	0.61	4.74	146.59	1.07	165.67			
11	CNTL1	0.03	0.15	2.22	195.54	1.35	211.49			
11	CNTL2	0.02	1.96	90.57	254.06	1.66	264.01			Yes
11	CNTL2	0.01	4.95	13.08	162.11	1.16	180.42			
11	CNTL2	0.02	3.14	30.07	435.64	2.56	416.92			

Table C-4. Concentrations of Fe/Mn-oxyhydroxides in sediments prior to inundation (day-0) and after 12-days of inundation, with bound estimates for Zn and V.

Site	Day	Total Metal-Oxyhydroxides				Amorphous Metal-Oxyhydroxides			
		(mg gdw ⁻¹)		(µg gdw ⁻¹)		(mg gdw ⁻¹)		(µg gdw ⁻¹)	
		Fe	Mn	Zn	V	Fe	Mn	Zn	V
REF	0	5.75 ±0.11	0.17 ±0.02	0.31 ±0.31	52.20 ±1.37	2.32 ±0.17	0.17 ±0.01	8.74 ±0.20	52.20 ±1.37
REF	12	5.17* ±0.13	0.15 ±0.05	20.27* ±1.53	32.84 ±2.84	1.21* ±0.11	0.09* ±0.02	0.89* ±0.54	32.84* ±2.84
SPN	0	26.05 ±0.86	0.85 ±0.06	47.30 ±2.80	183.13 ±15.25	11.49 ±0.58	0.71 ±0.03	0.62 ±0.09	109.70 ±15.63
SPN	12	26.61 ±1.21	0.90 ±0.06	74.71 ±11.80	210.33 ±8.55	5.66* ±0.62	0.47* ±0.04	1.08 ±0.67	56.86* ±9.74
WIL	0	28.07 ±1.14	0.45 ±0.02	143.13 ±11.45	322.53 ±6.40	11.17 ±0.66	0.37 ±0.01	4.48 ±3.35	283.92 ±8.17
WIL	12	24.32 ±1.19	0.35* ±0.02	178.27* ±6.55	302.31 ±12.89	5.58* ±0.28	0.19* ±0.03	2.09 ±0.15	164.85* ±7.89

*significant difference between days for an individual site, $p < 0.04$

Table C-5. BLM results show SPN to have highest theoretical toxicity to *D. magna*, followed by WIL. Bold numbers exceed a TU value of one.

Site	Day	Chronic HC5 ($\mu\text{g L}^{-1}$)	Zn ($\mu\text{g L}^{-1}$)	Mg (mg L^{-1})	Chronic Toxic Units ($\text{CTU}=\text{Zn}/\text{CHC5}$)
SPN	1	113.57	175.30	349.28	1.54
	7	116.85	164.31	365.95	1.41
	11	132.35	141.98	446.11	1.07
WIL	1	123.20	145.62	336.13	1.19
	7	116.85	164.31	358.93	1.41
	11	162.03	135.67	486.43	0.84
REF	1	119.83	114.76	371.84	0.96
	7	130.57	35.91	401.91	0.27
	11	152.47	122.47	507.07	0.80
CNTL	1	136.15	93.10	416.48	0.68
	7	151.99	152.48	473.06	1.00
	11	164.08	141.59	546.74	0.86

Table C-6. V-speciation as calculated by extraction techniques for Fe/Mn-oxyhydroxides and V (+IV)/(+V).

Site	Day	% Species Fraction				TOTAL V ($\mu\text{g g}^{-1}$)
		Fe/Mn-oxyhydroxide-V	V (+V)	V (+IV)	Other	
CNTL	1	0.00	0.03	0.01	99.89	36.11
REF	1	3.21	0.59	0.04	97.02	128.43
SPN	1	2.34	0.02	0.01	99.83	1414.64
WIL	1	8.54	0.11	0.07	99.02	890.60
CNTL	11	0.00	0.04	0.02	99.76	26.36
REF	11	0.00	0.69	0.25	98.97	90.90
SPN	11	4.20	0.25	0.07	99.55	1001.64
WIL	11	8.35	0.30	0.06	98.80	724.29

Figure C-2. Full array of dissolved porewater metal concentrations show two temporal patterns. Cr, Al, Mn, and Fe show a day-7 peak, while Ni, Cd, Zn, and V decrease with time.

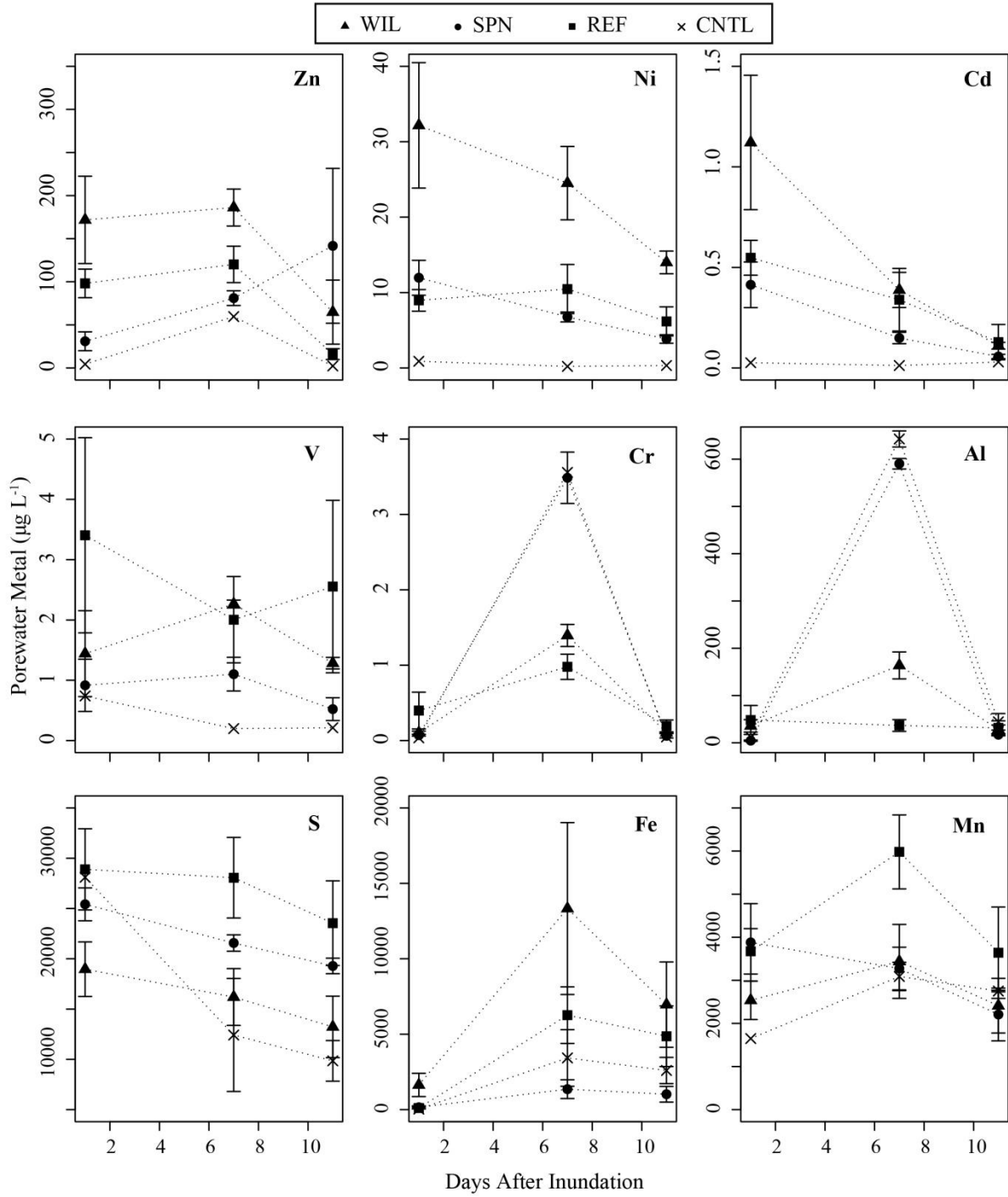


Table C-7. Sediment simultaneously extracted metals (SEM) minus acid volatile sulfide (AVS), loss-on-ignition (f_{OC}), and water content.

Site	Day	AVS (μmol gdwt^{-1})	\pm	f_{OC}	\pm	(SEM- AVS)/ f_{OC}	\pm	Water Content (%)	\pm
RAIS	0	2.39	1.96	0.03	0	-73.35	62.95	23.04	2.71
RAIS	1	1.92	0.04	0.01	0.01	-272.28	163.96	25.75	1.45
RAIS	12	1.83	1.01	0.02	0	-71.84	63.01	26.29	0.31
REF	0	0.03	0.01	0.03	0	47.51	5.05	24.19	1.14
REF	1	0.03	0.02	0.04	0.02	36.16	15.7	31.07	1.43
REF	12	1.07	1.06	0.05	0.02	47.61	20.66	32.23	0.24
SPN	0	3.41	0.93	0.07	0	26.08	11.73	40.49	0.67
SPN	1	3.19	0.38	0.01	0	160.36	16.85	44.55	1.52
SPN	12	3.94	0.82	0.07	0.01	23.87	14.62	48.12	1.15
WIL	0	3.89	1.01	0.1	0	57.38	5.91	43.06	0.90
WIL	1	4.52	2.01	0.03	0.01	130.27	58.17	48.55	1.56
WIL	12	3.26	2.08	0.1	0	29.75	12.53	50.95	1.60

Table C-8. Biotic Ligand Model input data, including temperature, pH, surface water dissolved Zn, DOC, humic acid (HA), Ca, Mg, Na, K, SO₄, Cl, alkalinity (alk) and sulfide.

Day	Site-Rep	Temp (°C)	pH	Zn (µg L ⁻¹)	DOC (mg-C L ⁻¹)	HA (%)	Ca (mg L ⁻¹)	Mg (mg L ⁻¹)	Na (mg L ⁻¹)	K (mg L ⁻¹)	SO ₄ (mg L ⁻¹)	Cl (mg L ⁻¹)	Alk (mg L ⁻¹ CaCO ₃)	Sulfide (mg L ⁻¹)
d1	REF1	20.5	7.00	95.64	0.08	10	60.51	362.54	289.30	25.79	10	0.15	2.23	1.00E-10
d1	REF2	20.5	7.00	127.17	0.08	10	61.78	378.51	289.30	25.79	10	0.15	2.23	1.00E-10
d1	REF3	20.5	7.00	121.46	0.08	10	61.95	374.47	289.30	25.79	10	0.15	2.23	1.00E-10
d1	WIL1	20.5	6.60	98.01	0.08	10	65.58	342.48	330.69	28.43	10	0.15	0.88	1.00E-10
d1	WIL2	20.5	6.60	224.50	0.08	10	63.53	326.17	330.69	28.43	10	0.15	0.88	1.00E-10
d1	WIL3	20.5	6.60	114.36	0.08	10	61.74	339.75	43.87	3.45	10	0.15	0.88	1.00E-10
d1	SPN1	19.5	7.15	187.70	0.08	10	70.13	363.14	373.04	33.21	10	0.15	3.15	1.00E-10
d1	SPN2	19.5	7.15	167.62	0.08	10	68.82	329.66	373.04	33.21	10	0.15	3.15	1.00E-10
d1	SPN3	19.5	7.15	170.60	0.08	10	71.71	355.05	373.04	33.21	10	0.15	3.15	1.00E-10
d1	RAIS1	19.5	7.15	102.98	0.08	10	88.24	418.47	200.38	14.58	10	0.15	3.15	1.00E-10
d1	RAIS2	19.5	7.15	83.21	0.08	10	86.18	414.48	200.38	14.58	10	0.15	3.15	1.00E-10
d7	REF1	20.5	7.00	35.71	0.08	10	68.28	400.42	28.09	2.62	10	0.15	2.23	1.00E-10
d7	REF2	20.5	7.00	36.53	0.08	10	69.77	406.29	28.09	2.62	10	0.15	2.23	1.00E-10
d7	REF3	20.5	7.00	35.48	0.08	10	69.62	399.01	28.09	2.62	10	0.15	2.23	1.00E-10
d7	WIL1	20.5	6.60	156.03	0.08	10	74.32	358.93	67.97	6.18	10	0.15	0.88	1.00E-10
d7	WIL2	20.5	6.60	186.87	0.08	10	75.34	343.39	67.97	6.18	10	0.15	0.88	1.00E-10
d7	WIL3	20.5	6.60	222.37	0.08	10	73.29	374.47	67.97	6.18	10	0.15	0.88	1.00E-10
d7	SPN1	19.5	7.15	160.22	0.08	10	69.16	372.24	47.48	4.15	10	0.15	3.15	1.00E-10
d7	SPN2	19.5	7.15	148.23	0.08	10	71.09	362.62	47.48	4.15	10	0.15	3.15	1.00E-10
d7	SPN3	19.5	7.15	184.48	0.08	10	68.84	362.98	47.48	4.15	10	0.15	3.15	1.00E-10
d7	RAIS1	19.5	7.15	154.56	0.08	10	88.23	488.22	43.87	3.45	10	0.15	3.15	1.00E-10
d7	RAIS2	19.5	7.15	150.41	0.08	10	101.78	457.89	43.87	3.45	10	0.15	3.15	1.00E-10
d11	REF1	20.5	7.00	144.14	0.08	10	65.04	498.24	45.81	3.23	10	0.15	2.23	1.00E-10
d11	REF2	20.5	7.00	94.84	0.08	10	63.22	513.59	45.81	3.23	10	0.15	2.23	1.00E-10
d11	REF3	20.5	7.00	128.42	0.08	10	69.55	509.37	45.81	3.23	10	0.15	2.23	1.00E-10
d11	WIL1	20.5	6.60	112.53	0.08	10	67.30	480.17	63.19	5.09	10	0.15	0.88	1.00E-10

Day	Site-Rep	Temp (°C)	pH	Zn (µg L ⁻¹)	DOC (mg-C L ⁻¹)	HA (%)	Ca (mg L ⁻¹)	Mg (mg L ⁻¹)	Na (mg L ⁻¹)	K (mg L ⁻¹)	SO ₄ (mg L ⁻¹)	Cl (mg L ⁻¹)	Alk (mg L ⁻¹ CaCO ₃)	S (mg L ⁻¹)
d11	WIL2	20.5	6.60	160.95	0.08	10	68.03	479.81	63.19	5.09	10	0.15	0.88	1.00E-10
d11	WIL3	20.5	6.60	133.54	0.08	10	67.88	499.30	63.19	5.09	10	0.15	0.88	1.00E-10
d11	SPN1	19.5	7.15	149.31	0.08	10	64.72	448.93	70.72	5.68	10	0.15	3.15	1.00E-10
d11	SPN2	19.5	7.15	151.29	0.08	10	69.22	447.40	70.72	5.68	10	0.15	3.15	1.00E-10
d11	SPN3	19.5	7.15	125.34	0.08	10	65.00	442.00	70.72	5.68	10	0.15	3.15	1.00E-10
d11	RAIS1	19.5	7.15	167.03	0.08	10	88.22	557.98	24.51	1.71	10	0.15	3.15	1.00E-10
d11	RAIS2	19.5	7.15	116.15	0.08	10	86.50	535.51	24.51	1.71	10	0.15	3.15	1.00E-10

Appendix D (Chapter 5 Data)

Table D-1. Modeling input for incremental oxidation.

```

TITLE Defining porewater and sediment composition
SOLUTION 2 PORE_WATER
    pH      7
    temp    19.0
    units   mg/L
    Ca      10
    Mg      20
    Zn      0.5
    Fe      4.0
    Mn      0.5
    Alkalinity 0.5
    Cl      2
EQUILIBRIUM_PHASES 2
    Smithsonite  0.0 2
    Sphalerite   0.0 1
    Willemite    0.0 3

    FeS(ppt)    0.0 50
    Pyrite       0.0 10
    Hematite     0.0 15
    Fe(OH)3(a)  0.0 4

    Dolomite     0.0 15
    Aragonite    0.0 15
    Siderite     0.0 10
    Rhodochrosite 0.0 20
    Calcite      0.0 15
    CO2(g)      -3.5
SAVE solution 2
END

TITLE REDOX.VARIABILITY.REACTION&GRAPH
USE solution 2
REACTION 1
    O2  1.0
    4.0 3.5 3.0 2.5 2.0 1.5 1.0 0.5
SELECTED_OUTPUT
    -file WeMBA.Exp3_Oxidation3.sel
    -reaction true
    -si Smithsonite Sphalerite Willemite Zn(OH)2(e) Pyrite Goethite Hematite
    -m Fe+2 Zn+2 Ca+2 Mg+2
END

```

Table D-2. Modeling input for oxidation via surface water input.

```

TITLE Example 1 -- Equilibrate surface water with minerals (oxidized)
EQUILIBRIUM_PHASES 1
    CO2(g) -2
    O2(g) 5
SOLUTION 1 EB Surface water (oxidized)
    pH 8.3
    temp 25.5
    units ppm
    Ca 5
    Mg 5
    K 1
    Na 5
    Cl 0.5
    Zn 0.01
    Mn 0.01
    Fe 0.01
EQUILIBRIUM_PHASES 1
    Smithsonite 0.0 2
    Sphalerite 0.0 10
    Willemite 0.0 1
    Zn(OH)2(e) 0.0 2

    FeS(ppt) 0.0 30
    Pyrite 0.0 5
    Hematite 0.0 10
    Fe(OH)3(a) 0.0 4

    Dolomite 0.0 10
    Aragonite 0.0 10
    Siderite 0.0 10
    Rhodochrosite 0.0 10
    Calcite 0.0 10
END

```

Table D-3. Input code for evaporation model. Example is for EB but similar model ran for LBC and QC as well.

```

TITLE Example 4a.--Water evaporation/loss from field sediment EB spiked
EQUILIBRIUM_PHASES 1
    CO2(g) -2
SOLUTION 2 EB Spiked Sediment Porewater
    pH 6.9
    temp 21
    units ppm
    Ca 5
    Mg 5
    K 1
    Na 5
    Cl 0.5
    Zn 3
    Mn 0.01
    Fe 0.01
EQUILIBRIUM_PHASES 2
    Smithsonite 0.0 2
    Sphalerite 0.0 10
    Willemite 0.0 1
    Zn(OH)2(e) 0.0 2

    FeS(ppt) 0.0 30
    Pyrite 0.0 5
    Hematite 0.0 10
    Fe(OH)3(a) 0.0 4

    Dolomite 0.0 10
    Aragonite 0.0 10
    Siderite 0.0 10
    Rhodochrosite 0.0 10
    Calcite 0.0 10
SAVE solution 2
TITLE evaporate some liquid
REACTION 1
    H2O -1.0
    52.73 moles
END

TITLE add some solution 2 back in -- Factor of 20 more solution
MIX
    2 100.
SAVE solution 3
END

```

Figure D-2. Values for $(SEM-AVS)/f_{oc}$ analyses for dry and sat treatments for QC non-spiked and spiked sediments, days 0 and 9/10 (not 30). QC non-spiked statistically different ($p = 0.06$) for SEM-AVS and for AVS in spiked sediments ($p < 0.05$).

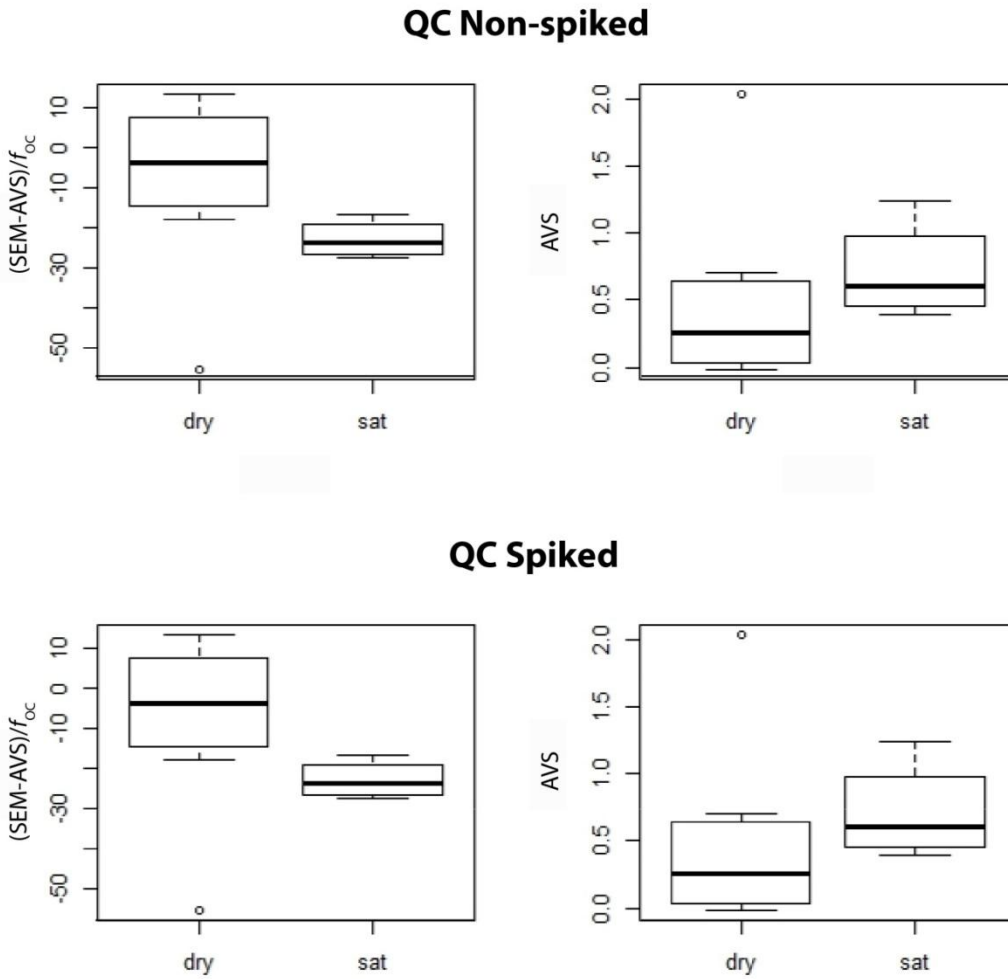


Table D-4. Acid volatile sulfide (AVS), simultaneously extracted metals (SEM) and fraction of organic carbon (f_{OC}) for all sites days and treatments.

Site	Day	Treatment			AVS ($\mu\text{mol g}^{-1}$)	SEM ($\mu\text{mol g}^{-1}$)	f_{oc}	(SEM- AVS)/ f_{oc}
		1	2	3				
QC	0	open	dry	nat	0.038	0.11	0.01	5.79
QC	0	open	dry	nat	0.038	0.17	0.02	8.91
QC	0	open	dry	nat	-0.012	0.12	0.01	12.96
QC	0	open	sat	nat	0.398	0.07	0.01	-25.48
QC	0	open	dry	nat	0.149	0.13	0.01	-3.12
QC	0	open	sat	nat	0.514	0.07	0.02	-21.86
EB	0	open	dry	nat	0.015	0.08	0.02	4.13
EB	0	open	dry	nat	0.005	0.33	0.02	16.53
EB	0	open	dry	nat	0.014	0	0.01	-1.64
EB	0	open	sat	nat	2.097	0.13	0.02	-108.56
EB	0	open	dry	nat	0.058	0.15	0.02	4.28
EB	0	open	sat	nat	1.239	0.12	0.03	-44.24
LBC	0	open	dry	nat	0.483	1.31	0.04	23.5
LBC	0	open	dry	nat	0.313	1.44	0.05	24.49
LBC	0	open	dry	nat	1.357	1.06	0.02	-13.42
LBC	0	open	sat	nat	6.348	2.01	0.03	-126.68
LBC	0	open	dry	nat	0.196	0.13	0.02	-3.61
LBC	0	open	sat	nat	0.523	0.17	0.01	-25.58
LBC	9	open	dry	nat	2.053	1.61	0.03	-13.09
LBC	9	open	dry	nat	3.25	4.77	0.12	13.1
LBC	9	open	dry	nat	1.761	1.42	0.04	-9.49
LBC	9	open	sat	nat	7.867	8.83	0.09	10.15
LBC	9	open	dry	nat	0.384	0.49	0.01	7.41
LBC	9	open	sat	nat	0.706	1.82	0.02	54.41
QC	10	open	dry	nat	2.031	0.29	0.03	-55.1
QC	10	open	dry	nat	0.377	0.13	0.02	-11.3
QC	10	open	dry	nat	0.703	0.5	0.05	-4.25
QC	10	open	sat	nat	0.706	0.24	0.03	-16.58
QC	10	open	dry	nat	0.58	0.08	0.03	-18.07
QC	10	open	sat	nat	1.241	0.12	0.04	-27.65
EB	10	open	dry	nat	14.447	0.43	0.08	-175.33
EB	10	open	dry	nat	0.816	0.34	0.06	-8.11
EB	10	open	dry	nat	0.678	0	0.02	-31.93
EB	10	open	sat	nat	10.44	13.72	0.03	96.01
EB	10	open	sat	nat	2.209	0.19	0.02	-89.18
EB	10	open	dry	nat	15.654	0.56	0.1	-155.52
EB	10	open	sat	nat	7.747	0.29	0.04	-202.94

Site	Day	Treatment			AVS ($\mu\text{mol g}^{-1}$)	SEM ($\mu\text{mol g}^{-1}$)	f_{oc}	(SEM- AVS)/ f_{oc}
		1	2	3				
QC	0	open	dry	spk	0.483	4.3	0.02	195.19
QC	0	open	dry	spk	0.525	3.62	0.02	147.07
QC	0	open	dry	spk	0.758	4.78	0.02	234.05
QC	0	open	sat	spk	1.505	4.75	0.02	141.84
QC	0	open	dry	spk	0.751	15.5	0.02	612.47
QC	0	open	dry	spk	0.423	14.64	0.02	729.64
QC	0	open	dry	spk	0.557	15.05	0.02	632.72
EB	0	open	dry	spk	3.003	2.96	0.04	-0.94
EB	0	open	dry	spk	7.176	7.34	0.06	2.64
EB	0	open	sat	spk	9.544	6.08	0.07	-49.37
EB	0	open	dry	spk	1.828	0.27	0.04	-40.88
EB	0	open	dry	spk	9.446	19.41	0.06	169.42
EB	0	open	sat	spk	10.352	11.9	0.06	24.73
LBC	0	open	dry	spk	2.795	8.67	0.04	163.98
LBC	0	open	dry	spk	1.64	5.25	1.96	1.84
LBC	0	open	dry	spk	1.89	12.92	0.02	584.5
LBC	0	open	dry	spk	4.958	19.5	0.02	593.51
LBC	9	open	dry	spk	3.588	8.11	0.38	11.89
LBC	9	open	dry	spk	2.854	8.19	0.03	153.52
LBC	9	open	sat	spk	3.967	6.87	0.02	119.27
LBC	9	open	dry	spk	2.187	15.64	0.03	447.72
LBC	9	open	dry	spk	2.393	16.98	0.02	729.26
LBC	9	open	sat	spk	3.092	18	0.02	631.03
QC	10	open	dry	spk	0.997	3.07	0.03	81.28
QC	10	open	dry	spk	1.136	5.03	0.03	130.33
QC	10	open	sat	spk	2.623	2.65	0.04	0.62
QC	10	open	dry	spk	1.153	12.69	0.03	393.27
QC	10	open	dry	spk	1.35	9.58	0.05	168.45
QC	10	open	sat	spk	1.08	18.14	0.05	341.95
EB	10	open	dry	spk	2.539	2.03	0.07	-6.94
EB	10	open	dry	spk	10.569	4.75	0.05	-119.3
EB	10	open	sat	spk	13.165	4.73	0.08	-112.15
EB	10	open	dry	spk	7.432	9.22	0.03	71.13
EB	10	open	dry	spk	14.553	14.32	0.13	-1.76
EB	10	open	sat	spk	9.65	9.55	0.05	-2.09

Table D-5. Abundance (N), dominant species, relative abundance of dominant species (rN), species richness, evenness and diversity (Simpson's and Shannon's).

Sample ID	N	Dominant Species	rN	Rich-ness	Simpson's Diversity	Shannon's Diversity	Even-ness
QC_1500_dry	9	<i>Chironomidae</i>	0.67	4	0.42	1.00	0.72
QC_1500r_sat	5	<i>Chironomidae</i>	0.8	2	0.60	0.50	0.72
QC_600_dry	9	<i>Chironomidae</i>	0.44	4	0.25	1.21	0.88
QC_600r_sat	23	<i>Chironomidae</i>	0.57	2	0.49	0.68	0.99
QC_nat_dry	4	<i>Chironomidae</i>	0.75	2	0.50	0.56	0.81
QC_nat_dry	12	<i>Chironomidae</i>	0.5	4	0.29	1.20	0.86
QC_nat_sat	4	<i>Chironomidae</i>	1	1	0.50	0.56	0.00
QC_nat_sat	4	<i>Chironomidae</i>	0.5	3	0.17	1.04	0.95
QC_ref_dry	24	<i>Chironomidae</i>	0.29	5	0.21	1.48	0.92
QC_ref_sat	44	<i>Chironomidae</i>	0.43	5	0.30	1.28	0.80
EB_1500_dry	18	<i>Chironomidae</i>	0.44	5	0.27	1.34	0.83
EB_1500_dry	53	<i>Gammaridae</i>	0.38	9	0.22	1.72	0.78
EB_1500_dry	105	<i>Oligochaeta</i>	0.47	8	0.36	1.28	0.62
EB_600_dry	35	<i>Gammaridae</i>	0.37	5	0.26	1.37	0.85
EB_600_dry	25	<i>Planorbidae</i>	0.36	9	0.16	1.89	0.86
EB_nat_dry	17	<i>Oligochaeta</i>	0.29	5	0.19	1.50	0.93
EB_nat_dry	46	<i>Oligochaeta</i>	0.43	8	0.28	1.48	0.71
EB_nat_dry	13	<i>Oligochaeta</i>	0.46	5	0.27	1.31	0.81
EB_nat_dry	14	<i>Oligochaeta</i>	0.79	3	0.62	0.66	0.60
EB_nat_sat	17	<i>Chironomidae</i>	0.29	6	0.18	1.61	0.90
EB_nat_sat	31	<i>Oligochaeta</i>	0.71	4	0.52	0.87	0.63
EB_nat_sat	11	<i>Oligochaeta</i>	0.82	3	0.65	0.60	0.55
EB_nat_sat	3	<i>Oligochaeta</i>	1	1	1.00	0.00	0.00
EB_ref_dry	78	<i>Oligochaeta</i>	0.63	7	0.42	1.23	0.63
EB_ref_dry	35	<i>Oligochaeta</i>	0.71	4	0.53	0.87	0.63
EB_ref_dry	28	<i>Oligochaeta</i>	0.29	9	0.17	1.83	0.83
EB_ref_sat	4	<i>Oligochaeta</i>	0.5	2	0.33	0.69	1.00
EB_ref_sat	26	<i>Oligochaeta</i>	0.81	5	0.65	0.75	0.46
EB_600_dry	57	<i>Oligochaeta</i>	0.54	6	0.36	1.25	0.70
LBC_1500_dry	23	<i>Tanypodinae</i>	0.48	7	0.25	1.57	0.81
LBC_1500_dry	12	<i>Oligochaeta</i>	0.58	2	0.47	0.68	0.98
LBC_1500_dry	27	<i>Asellidae</i>	0.37	7	0.21	1.63	0.84
LBC_600_dry	50	<i>Oligochaeta</i>	0.38	6	0.29	1.34	0.75
LBC_600_dry	8	<i>Chironomidae</i>	0.5	3	0.32	0.97	0.89
LBC_600_dry	22	<i>Oligochaeta</i>	0.64	5	0.42	1.10	0.68

Sample ID	N	Dominant Species	rN	Rich-ness	Simpson's Diversity	Shannon's Diversity	Even-ness
LBC_nat_dry	12	<i>Chironomidae</i>	0.33	5	0.17	1.52	0.94
LBC_nat_dry	62	<i>Asellidae</i>	0.66	6	0.47	1.05	0.58
LBC_nat_dry	89	<i>Asellidae</i>	0.46	6	0.38	1.15	0.64
LBC_nat_dry	81	<i>Asellidae</i>	0.73	6	0.55	0.90	0.50
LBC_nat_sat	19	<i>Oligochaeta</i>	0.47	6	0.27	1.41	0.79
LBC_nat_sat	14	<i>Chironomidae</i>	0.29	5	0.20	1.45	0.90
LBC_nat_sat	13	<i>Asellidae</i>	0.46	3	0.38	0.91	0.83
LBC_nat_sat	8	<i>Chironomidae</i>	0.38	3	0.25	1.08	0.99
LBC_ref_dry	116	<i>Asellidae</i>	0.84	9	0.70	0.75	0.34
LBC_ref_dry	372	<i>Asellidae</i>	0.7	8	0.27	1.59	0.77
LBC_ref_dry	39	<i>Asellidae</i>	0.28	6	0.22	1.53	0.85
LBC_ref_dry	16	<i>Asellidae</i>	0.56	5	0.35	1.19	0.74
LBC_ref_sat	15	<i>Sphaeriidae</i>	0.33	6	0.15	1.67	0.93
LBC_ref_sat	123	<i>Asellidae</i>	0.68	6	0.52	0.90	0.50
LBC_ref_sat	132	<i>Asellidae</i>	0.75	6	0.59	0.85	0.47

Table D-6. Net primary productivity (NPP) and Chlorophyll (Chl) *a* biomass for all sites and treatments.

Sample Name	Treat 1	Treat 2	Depth (cm)	NPP (mg-O ₂ m ⁻² hr ⁻¹)	Chl <i>a</i> (mg m ⁻²)
EB-EB-Open-Dry-4	dry	nat	0.5	-1.77	14.12
EB-EB-Open-Dry-2	dry	nat	0.2	51.60	78.74
EB-EB-Open-Dry-5	dry	nat	0.8	-11.51	15.82
EB-EB-Open-Dry-3	dry	nat	0.1	10.31	23.47
EB-EB-Open-Dry-1	dry	nat	0.1	37.84	49.83
EB-EB-Open-Sat-2	sat	nat	0.5	0.33	14.97
EB-EB-Open-Sat-3	sat	nat	0.2	0.32	13.26
EB-EB-Open-Sat-1	sat	nat	0.1	36.00	65.98
EB-EB-Open-Sat-4	sat	nat	1.5	-11.93	3.91
EB-EB-Open-Sat-5	sat	nat	1	0.90	1.36
EB-Rais-Open-Dry-1	dry	nat	1.5	-2.46	4.76
EB-Rais-Open-Dry-2	dry	nat	0.9	-7.95	15.82
EB-Rais-Open-Dry-3	dry	nat	0.5	-9.29	11.56
EB-Rais-Open-Sat-1	sat	nat	1	-0.01	22.62
EB-Rais-Open-Sat-2	sat	nat	0.5	-7.11	3.91
LBC-LBC-Open-Dry-3	dry	nat	0.05	-11.91	29.08
LBC-LBC-Open-Dry-2	dry	nat	0.1	-6.41	1.87
LBC-LBC-Open-Dry-5	dry	nat	0.1	-13.51	10.37
LBC-LBC-Open-Dry-4	dry	nat	0	-30.69	14.63
LBC-LBC-Open-Dry-1	dry	nat	0.1	-25.15	1.87
LBC-LBC-Open-Sat-4	sat	nat		2.55	0.17
LBC-LBC-Open-Sat-3	sat	nat	0.7	7.32	0.17
LBC-LBC-Open-Sat-1	sat	nat	0.5	11.39	2.72
LBC-LBC-Open-Sat-2	sat	nat	0.6	-22.86	0.17
LBC-Rais-Open-Dry-3	dry	nat	0.3	-4.37	4.42
LBC-Rais-Open-Dry-2	dry	nat	0	-22.76	4.42
LBC-Rais-Open-Dry-1	dry	nat	0	-33.12	26.53
LBC-Rais-Open-Dry-5	dry	nat	0.05	-2.08	3.57
LBC-Rais-Open-Dry-4	dry	nat	1	-11.34	1.02
LBC-Rais-Open-Sat-1	sat	nat	0.3	-17.17	1.02
LBC-Rais-Open-Sat-2	sat	nat	0	-28.34	9.52
LBC-Rais-Open-Sat-3	sat	nat	0	15.24	25.68
QC-QC-Open-Dry-4	dry	nat	0.3	5.57	20.58
QC-QC-Open-Dry-3	dry	nat	0.2	17.89	39.28
QC-QC-Open-Dry-5	dry	nat	0	1.57	7.82
QC-QC-Open-Dry-2	dry	nat	0	16.54	3.57
QC-QC-Open-Dry-1	dry	nat	0	-1.10	15.48

Sample Name	Treat 1	Treat 2	Depth (cm)	NPP	Chl <i>a</i>
QC-QC-Open-Sat-3	sat	nat	1.5	20.21	1.87
QC-QC-Open-sat-2	sat	nat	2	12.28	1.87
QC-QC-Open-Sat-1	sat	nat	1.5	25.94	1.87
QC-Rais-Open-Dry-2	dry	nat	0	34.04	62.24
QC-Rais-Open-Dry-1	dry	nat	0	18.37	28.23
QC-Rais-Open-Dry-3	dry	nat	0	-3.47	1.87
QC-Rais-Open-Sat-1	sat	nat	0	7.64	2.72
QC-Rais-Open-Sat-2	sat	nat	0.2	14.82	4.42
QC-Rais-Open-Sat-3	sat	nat	0.5	31.95	6.97
EB-600-Open-Dry-1	dry	spk	0.1	24.49	76.19
EB-600-Open-Dry-2	dry	spk	0.1	41.20	44.73
EB-600-Open-Dry-3	dry	spk	1.5	10.06	76.19
EB-600-Open-Dry-5	dry	spk		-25.04	28.57
EB-600-Open-Dry-4	dry	spk	1.5	-23.14	20.07
EB-600-Open-Sat-2	sat	spk		-4.66	16.67
EB-600-Open-Sat-1	sat	spk	1.5	-1.32	60.03
EB-1500-Open-Dry-1	dry	spk	0.5	-0.17	23.47
EB-1500-Open-Dry-2	dry	spk	0.5	-13.08	22.62
EB-1500-Open-Dry-3	dry	spk	1.5	-22.49	9.01
EB-1500-Open-Dry-4	dry	spk	1.5	-28.54	18.37
EB-1500-Open-Dry-6	dry	spk		15.08	76.19
EB-1500-Open-Dry-5	dry	spk	1.5	-23.91	9.86
EB-1500-Open-Sat-1	sat	spk		-0.17	38.77
EB-1500-Open-Sat-2	sat	spk		-24.21	67.69
EB-1500-Open-Sat-3	sat	spk		15.63	69.39
LBC-600-Open-Dry-2	dry	spk	0.7	15.01	1.87
LBC-600-Open-Dry-1	dry	spk	0.3	12.23	2.72
LBC-600-Open-Dry-4	dry	spk	0.25	28.40	14.63
LBC-600-Open-Dry-3	dry	spk	0.25	20.56	10.37
LBC-600-Open-Sat-2	sat	spk	0	-17.45	1.02
LBC-600-Open-Sat-1	sat	spk	0	12.98	1.87
LBC-600-Open-Sat-3	sat	spk	0.5	-8.89	2.72
LBC-1500-Open-Dry-5	dry	spk	0	27.24	6.12
LBC-1500-Open-Dry-4	dry	spk	0	17.24	5.27
LBC-1500-Open-Dry-1	dry	spk	0.5	8.18	4.42
LBC-1500-Open-Dry-2	dry	spk	0.7	-6.11	1.87
LBC-1500-Open-Dry-3	dry	spk	0	21.22	15.48
LBC-1500-Open-Sat-1	sat	spk	0.75	-5.94	3.57
LBC-1500-Open-Sat-2	sat	spk	0.75	-17.50	4.42